

Dissertation zur Erlangung des Doktorgrades
der Fakultät für Chemie und Pharmazie
der Ludwig-Maximilians-Universität München

**The synthesis and characterisation of
halogen and nitro phenyl azide derivatives
as highly energetic materials.**

von

David Adam

aus

Glasgow , Schottland

2001

Index

Acknowledgements	1
Abstract	3
1. Introduction	4
1.1 Azides	4
1.2 Nitro compounds	13
1.3 Nitrocarbons	16
1.4 Explosives	18
1.5 Theoretical Calculations	20
1.6 Pentazoles	23
2 Halogen substituted phenyl azides	27
2.1 2,4,6-tribromophenyl azide	27
2.2 2,4,6-trichlorophenyl azide	35
2.3 2,5,6-trichlorophenyl azide	42
2.4 2,4-dibromophenyl azide	43
2.5 2,4-dichlorophenyl azide	44
2.6 2,4,6-trifluorophenyl azide	44
2.7 2,3,4,5,6-pentafluorophenyl azide	47
2.8 2,6-diiodo-4-nitrophenyl azide	50
2.9 2,3,4,5,6-pentachlorophenyl azide	59

3. Nitro compounds	65
3.1 <i>o</i> -nitrophenyl azide	65
3.2 <i>m</i> -nitrophenyl azide	68
3.3 2,4-dinitrophenyl azide	70
3.4 2,4,6-trinitrophenyl azide	72
3.5 1,3,5-triazido-2,4-dinitrobenzene	94
3.6 1,3,5-triazido-2,4,6-trinitrobenzene	100
3.7 hexakis (azidomethyl) benzene.	106
3.8 hexakis (methylnitrate) benzene	108
4. Decomposition and explosion experiments	111
4.1 Thermal decomposition of TNMA , DNTA and TNTA	111
4.2 Computational Aspects	118
4.3 Thermal decomposition of halogen substituted phenyl azides	121
4.4 Thermal decomposition of hexakis (azidomethyl) benzene	122
4.5 Drophammer Tests of TNMA, DNTA and TNTA	125
4.6 Calculation of the detonation velocity from molecular formula and structure for TNMA , DNTA and TNTA	133
4.7 Calculation of the detonation velocity from molecular formula and structure for a series of azido and nitro substituted benzenes	135
5 Calculation of compounds of the type $C_6(NO_2)_{6-n}(N_3)_n$	138
5.1 Structural discussion	144
5.2 Molecular structures	145

6. Pentazoles	152
6.1 Decomposition of phenylpentazoles	153
6.2 Raman spectra	156
6.3 ¹⁴ N NMR spectra	158
6.4 <i>ab initio</i> calculations	163
7. Experimental	167
7.1 Symbols and abbreviations	167
7.2 SI and non SI units	168
7.3 Analytical techniques and instruments	169
7.4 Chemicals and solvents	170
7.5 Preparations	174
7.6 Crystallographic data	194
8. Summary	197
9. References	202

Erklärung

Diese Dissertation wurde im Sinne von § 13 Abs. 3 bzw 4 der Promotionsordnung vom 29th January 1998 von Herrn Prof. Dr. Thomas M. Klapötke betreut.

Ehrenwörtliche Versicherung

Diese Dissertation wurde selbständig, ohne unerlaubte Hilfe erarbeitet.

München, den 1. August 2001

.....
(Unterschrift der Autors)

Dissertation eingereicht am 1. August 2001

1. Berichterstatter Prof. Dr. Thomas M. Klapötke
2. Berichterstatter Priv.-Doz. Dr. Konstantin Karaghiosoff

Mündliche Prüfung am 15. Oktober 2001

Acknowledgements

My main thanks and gratitude belong to my supervisor and Doktorvater

Professor Dr. Thomas M. Klapötke

for giving me the opportunity to work and study in Munich. I would also like to thank him for his interest, enthusiasm and support of my work. I thank him for the many interesting and informative discussions we have had about this project. Also I would like to thank him for performing many quantum-chemical calculations and for teaching me how to perform these calculations for myself.

I would like to thank **Priv.-Doz. Dr. Konstantin Karaghiosoff** for acting as the second examiner, for assessing this work and for his willingness to undertake this task in English.

I am also grateful to my other assessors **Prof. Dr. Wolfgang Beck, Prof. Dr. Ingo-Peter Lorenz, Dr. David D. MacNicol** and **Prof. Dr. Matthias Westerhausen** for being willing to undertake this assessment of my thesis in English.

Thanks also to **Dr. Margaret-Jane Crawford** for her support, encouragement help and advice during my project and for being a good lab colleague to work with. I would also like to thank her for proof reading this thesis.

My thanks to **Frau Irene Scheckenbach** for all her help in assisting me to fill in the official forms when I first arrived in Munich and for her help over the past four years.

I would like to thank the following members of AK Klapötke for all their help during my project:- **Priv.-Doz. Dr. Konstantin Karaghiosoff** and **Dr. Burkhard Krumm** (NMR), **Frau Carmen Nowak** (diagrams), **Dr. Anton Hammerl** (computing problems), **Dr. Claudia Rienäcker** (drop hammer testing), **Herrn Gunnar Spieß** (Raman) and **Frau Anette Burdzy**

(solvents and reprints). Thanks also to all other members of AK Klapötke for a friendly and good working environment and making my stay in Munich a happy one.

I would like to thank my F-Pratikum student **Herrn Martin Freytag** for his help with part of my project.

Thanks also to **Prof. Dr. Heinrich Nöth, Dr. Holger Schwenk-Kircher, Prof. Dr. Peter Klüfers** and **Dr. Peter Mayer** for X-ray structure determinations. I also like to thank **Dr. Paul Mallinson and Dr. Louis Farrigia** (University of Glasgow) for assisting me with X-ray structure determinations and with charge density calculations during my stay in Glasgow. Also thanks to **Dr. David D. MacNicol** (University of Glasgow) for his kind donation of a starting material.

Finally and most importantly I would like to thank my family for all their help, support and encouragement during all of my further education. Sadly my father who died earlier this year will not be here to see the end of my work but I know he would be proud of me therefore I would like to dedicate this thesis to him and my mother.

Many thanks Mum and Dad

Abstract

The main aims of this project was to prepare derivatives of halogen and nitro substituted phenyl azides and characterise them using the following analytical methods :-

1. Infrared spectroscopy
2. Raman spectroscopy
3. Elemental analysis
4. Multinuclear NMR. spectroscopy (^1H ^{13}C ^{14}N ^{15}N ^{19}F)
5. X-ray structural analysis

The structures of all prepared halogen and nitro substituted phenyl azides were computed using the Gaussian98 programme and were fully optimised and the vibrational frequencies and zero point energies computed using a semiempirical calculation carried out at the semiempirical PM3 level of theory using a VSTO-3G basis set and ab initio at the self consistent HF level of theory using a 6-31G(d) basis set. The structures, vibrational frequencies and zero point energies for the molecules that contained either bromine or iodine were also calculated ab initio at Hartree-Fock (HF) using a quasirelativistic Stuttgart/Dresden (SDD) pseudopotential for the core electrons was applied with a Dunning/Huzinaga D95-type valence basis for the bromine or iodine atoms.

The thermal decomposition of the prepared compounds was studied experimentally using gas-phase IR spectroscopy and mass spectrometry. The explosive nature of all the prepared compounds was tested, and those that exhibited an explosive nature had the temperature of explosion measured and were also used for drophammer experiments.

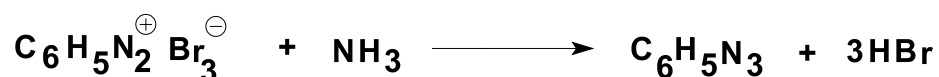
The detonation velocities of the prepared nitrophenyl azides were calculated using the Rothstein equation. This equation was also used to predict the detonation velocities of some as yet unprepared nitrophenyl azides

Another aim of this work was to prepare pentazole derivatives using a series of halogen substituted anilines and nitro substituted anilines as starting materials. It was hoped to be able to crystallise the pentazole derivatives prepared. The low temperature Raman spectra and ^{14}N NMR spectra of these derivatives were also measured.

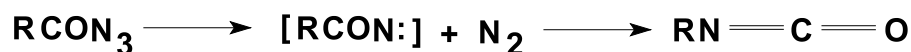
1 Introduction

1.1 Azides –Introduction

The first organic azide, phenyl azide, was synthesised by Peter Griess [1] from benzenediazonium perbromide and ammonia.



The discovery by Curtius in 1890 of the rearrangement of acyl azides to isocyanates [2] stimulated interest in organic azides and as a consequence most of the general synthetic methods were soon elucidated.



Since Curtius obtained benzyl azide from benzyl iodide and silver azide [2] not only halo but also sulfate, nitro, hydroxyl, nitrate, iodoxy and alkoxy groups have been found to enter into displacement reactions with metallic or hydrogen azides.

Other methods of preparing organic azides related to later work in this thesis

1. Nucleophilic substitution.

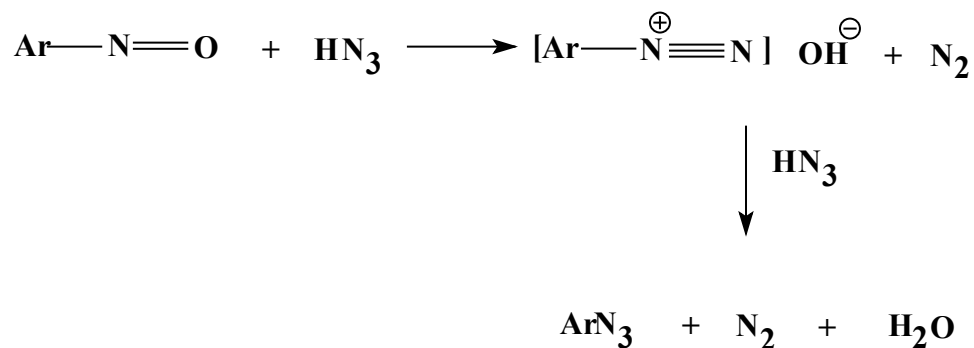
Aryl substrates containing suitable leaving or activating groups react readily with moderately strong nucleophiles such as the azide ion and a number of aromatic azides have been prepared in this manner. $\text{S}_{\text{N}}\text{Ar}$ reactions of the azide ion proceed more readily in dipolar aprotic solvents, the use of which is thus preferred with substrates of low reactivity.

2. Reaction of diazonium compounds with nucleophiles.

Aromatic azides can be synthesised from diazonium compounds using hydrazoic acid or the azide ion as the nucleophile. This reaction may be used in all cases in which a primary amine undergoes diazotization. This procedure is widely used in the synthesis of aromatic and heteroaromatic azides and the yields are usually high and often quantitative. Different procedures have been developed for this reaction, and the method used is determined by the basicity of the amine involved or the solubility of its salts.

3. Reaction of hydrazoic acid with nitroso compounds.

The synthesis aryl azides in high yields and under mild conditions by the reaction of aromatic nitroso compounds with hydrazoic acid was first reported by Maffei *et al* [3]. If the quantity of hydrazoic acid used is less than that represented in the equation below, the yield of azide decreases accordingly and the unreacted nitroso compound is present with the product.



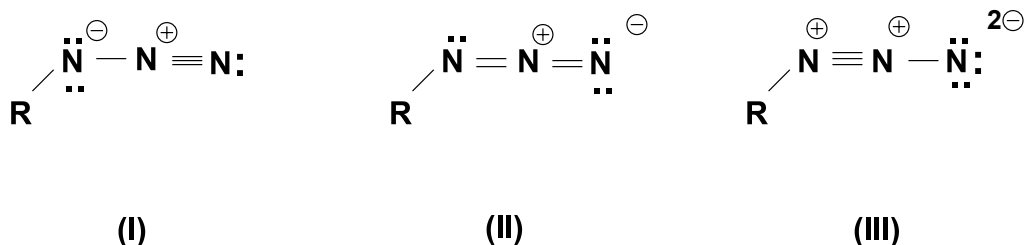
It appears that the intermediate formed from the reaction of the nitroso compound with the first molecular equivalent of hydrazoic acid interacts more rapidly with hydrazoic acid than does the nitroso compound.

Interest in the azido group has continued until the present day with the increasing awareness of the scope of reactions involving azide intermediates. For example azides react with

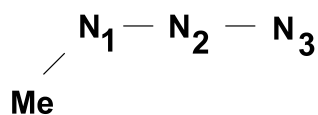
electrophiles and nucleophiles and undergo 1,3 dipolar addition reactions with olefins [4]. Furthermore, the controlled thermal or photoytic decomposition of azides yields nitrene via the elimination of nitrogen [5]. Azides have found increasing application in bio-organic chemistry, particularly in the introduction of protecting groups during peptide synthesis, the formation of the peptide link without racemisation and stereospecific syntheses of amino derivatives of steroids.

Azides – Structure

In picturing covalent azides as resonance hybrids between structures (I),(II) and (III), Pauling [6] discards structure (III) as not being a major contributor based on a consideration of the adjacent charge rule



The resulting hybrid predicts a bond order of 2.5 for N₂-N₃ and a bond order of 1.5 for N₁-N₂ (see fig IV).



(IV)

This prediction is in excellent agreement with the structure of methyl azide (IV) which was determined by Livingston and Rao using electron diffraction techniques[7]. The structural parameters for methyl azide are:-

$$\begin{aligned}
 \text{N}_2 - \text{N}_3 &= 1.12 \pm 0.01 \text{ \AA} \\
 \text{N}_1 - \text{N}_2 &= 1.24 \pm 0.01 \text{ \AA} \\
 \text{C} - \text{N}_1 &= 1.47 \pm 0.02 \text{ \AA} \\
 \angle (\text{CN}_1\text{N}_2) &= 120 \pm 2^\circ
 \end{aligned}$$

The angle $\angle(\text{CN}_1\text{N}_2)$ agrees well with the resonance hybrids (I \leftrightarrow II), since the non-bonded electron pair on N_1 should force the system into near trigonal (sp^2) hybridisation about N_1 . The linear configuration of the azido group agrees with the (sp^3) hybridisation indicated by the lack of non-bonded electron pairs on N_2 .

Considerable data on the dipole moments of organic azides are available (see table 1:1) and the data clearly support the linear structure of azido group. The dipole moment of phenyl azide is found to be 1.44 D (this is about the value of the C-N dipole contribution) and this low value is consistent with the opposing dipoles of the contributing structures (I) and (II), and suggests that the contributions of the two limiting structures are nearly equivalent. The negative end of the dipole is directed away from the benzene ring.

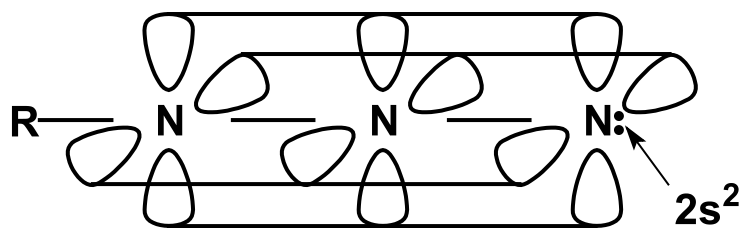
Table 1:1

Dipole moments of organic azides [8]

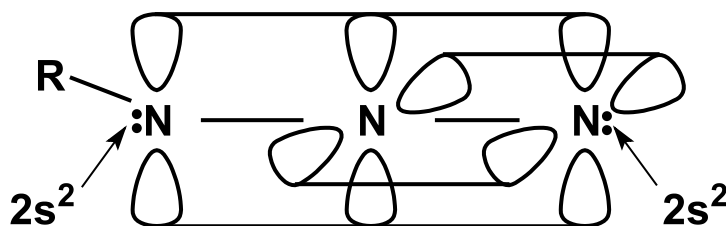
Azides	μ Debye
$C_6H_5N_3$	1.44
<i>p</i> - $CH_3C_6H_4N_3$	1.90
<i>m</i> - $CH_3C_6H_4N_3$	1.75
<i>o</i> - $CH_3C_6H_4N_3$	1.39
<i>p</i> - $ClC_6H_4N_3$	0.01
<i>m</i> - $ClC_6H_4N_3$	1.45
<i>o</i> - $ClC_6H_4N_3$	2.37
<i>p</i> - $NO_2C_6H_4N_3$	2.90
<i>m</i> - $NO_2C_6H_4N_3$	3.56
<i>o</i> - $NO_2C_6H_4N_3$	4.46

Sidgwick has used empirical bond energy values for nitrogen–nitrogen multiple bonds, (corrected for deviation due to non-bonded electron pairs) to estimate the heats of formation of the hypothetical limiting forms (I) and (II) (with $R = H$) [9]. His estimates yield values of $277 \text{ kcal mol}^{-1}$ and $288 \text{ kcal mol}^{-1}$ for structures (I) and (II) respectively. These estimates are sufficiently close to confirm the similarity in energies of the contributing structures, both of which lie below the measured value of $318.6 \text{ kcal mol}^{-1}$ for the heat of formation of hydrazoic acid. This confirms the validity of the estimate, since the heat of formation of the (more stable) hybrid ($\mathbf{I} \leftrightarrow \mathbf{II}$) should exceed the hypothetical heat of formation of either contributing structure.

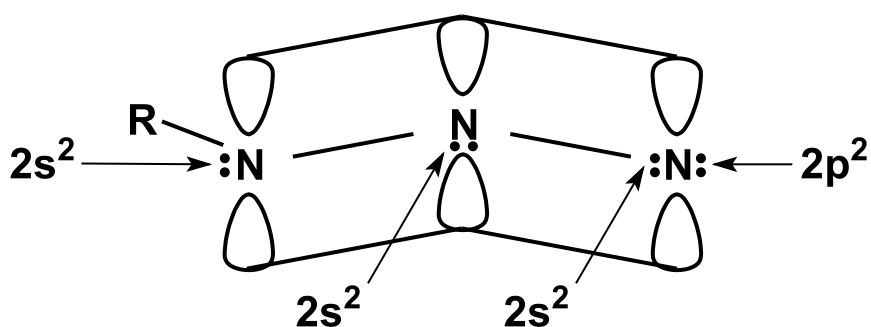
Molecular orbital calculations have been of immense value in the study of organic structural problems and Roberts [10] has studied the structure of organic azides by this approach. Organic azides could have configurations (V), (VI) and (VII) (fig below). Of these, structure (VI) represents the best picture of an organic azide and satisfies the experimental observations. .



(V)



(VI)



(VII)

The π -bond delocalisation energies of the forms (V), (VI) and (VII) have been calculated by Roberts, who used this data with the known greater stability of (VI) to estimate limits on the energy associated with the conversion of an electron pair associated with a π -bond to a lone pair of electrons. The calculated energies of the three forms are $8\alpha + 5.66\beta$, $6\alpha + 4.83\beta$ and $4\alpha + 2.83\beta$ respectively. In these forms each differ from its neighbour by one Q unit. Form (VII) differs from (VI) by only one Q unit because of the $2p^2$ unshared pair on N_3 associated with energy 2α . Thus, while going from (VI) to (VII), N_3 does not undergo any change in hybridisation. Since organic azides have the configuration (VI) one could squeeze Q between $2\alpha + 0.83\beta$ and $2\alpha + 2\beta$. Q has been taken as $2\alpha + (1.4 \pm 0.4)\beta$ assuming that organic azide

do not go over to configurations (V) and (VII), the β value for N-N bonds lying anywhere between 10 and 30 kcal mol⁻¹. The important inference from these studies is that the bending of the nitrogen chain of an organic azide does not require much energy.

Azides – electrical properties

The azide group exerts an inductive electron withdrawing effect as shown by the acid strengths of azido aliphatic acids and azido-substituted aromatic carboxylic acids. The inductive effect of the azide group has been estimated to be between that of the bromo and iodo groups from the measurement of the dissociation of substituted aromatic acids and anilinium ions [11]. Smith *et al* have determined the Hammett substituent (σ) constants for the *meta*- and *para*- azido groups to be about 0.35 and 0.10 respectively: These sigma values for the azido group are comparable to those of the fluoro group.

In the case of electrophilic substitution reactions of aromatic rings, the azido group acts as an electron donor *e.g.* the nitration of phenyl azide takes place in the *ortho* and *para* positions. Three nitro groups can be introduced to the benzene ring by nitration. The nitration of α and β naphthyl azides takes place on the ring bearing the azido group.

Azides- Characterisation

Infrared spectra of organic azides

The azido group is characterised by the asymmetric stretching frequency in the region 2160-2090 cm⁻¹, the symmetric stretching frequency in the region 1340-1180cm⁻¹ and the bending frequency around 680 cm⁻¹. The azide asymmetric and symmetric stretching bands of certain azides often appear as doublets or triplets. This has been explained on the basis of Fermi resonance interaction of the fundamentals with the overtones or combination tones of certain low lying frequencies [12]. Conjugation appears to be generally present in all azides showing azide band splittings, and the C-N stretching vibration seems to be involved in the Fermi interaction. Many organic azides show weak bands in the region of 2400 cm⁻¹, due to overtones or combination bands of the symmetric stretching vibration.

Table 1:2 Infrared Frequencies for Organic Azides [13]

RN ₃ , R =	N ₃ Asymmetric (cm ⁻¹)	N ₃ Symmetric (cm ⁻¹)
<i>n</i> -butyl	2083	1256
<i>n</i> -decyl	2092	1256
benzyl	2088	1256
cyclopentyl	2083	1256
phenyl	2114	1287
<i>p</i> -tolyl	2092	1261
<i>p</i> -bromophenyl	2110	1287
<i>p</i> -nitrophenyl	2114	1285
<i>m</i> -chlorophenyl	2096	1288
<i>p</i> -chlorophenyl	2088	1297

Ultraviolet spectroscopy

Organic azides have been studied by ultraviolet absorption techniques since the early 1930`s [14]. Alkyl azides are characterised by two relatively low intensity transactions [15]. These solvent insensitive bands centred at 287 nm and 216 nm have been described as $\pi_y \rightarrow \pi_x^*$ and $s-p_x \rightarrow \pi_y^*$, respectively. Closson and Gray also mention that the substitution of electronegative groups in the alkyl portion would lower the energy of the electrons via induction on the nitrogen atom bonded to the carbon [15]. This would increase the energy (shift to shorter wavelength) of transactions. As one would expect, the ultraviolet spectra of aromatic azides is decidedly more varied. Generally it can be said, that the intensity of the long wavelength band (*ca* 285 nm) is substantially increased.

^{14}N NMR Spectroscopy

^{14}N NMR spectroscopy is one of the most suitable methods for the characterisation of organic azides in solution. Organic azides show three nitrogen resonance signals corresponding to the three non-equivalent nitrogen atoms.



Assignment of the shifts may be made from a comparison with the shifts observed for the azide ion and the changes in the position of the highest-field (lowest frequency) resonance upon changing the R group. In no case has ^{14}N - ^{14}N spin-spin coupling been observed presumably owing to the large quadrupole moment of the nitrogen, although it has been estimated that the coupling for azide to be less than 30 Hz. The ^{14}N chemical shift for some aromatic azides are given in the table 1.3

Table 1.3 ^{14}N NMR Chemical shift for selected Organic Azides (ref. to MeNO_2).

Azide	Solvent	$\delta(\text{N}_a)$	$\delta(\text{N}_b)$	$\delta(\text{N}_c)$
PhNNN	Benzene	-286	-135	-194
PhCONNN	Benzene	-322	-140	-237
p-MeC ₆ H ₄ SO ₂ NNN	Neat	-304	-152	-209
p-NO ₂ C ₆ H ₄ NNN	Benzene	-310	-139	-211

Explosive properties of azides

In the view of the explosive and toxic nature of hydrazoic acid and its derivatives; it is pertinent to discuss the hazards of handling azides. Heat, mechanical shock or exposure to certain chemical reagents will decompose organic azides. Molecular dinitrogen is formed and the process is accompanied by the release of large amounts of energy. During controlled decomposition in solution this energy is absorbed by the solvent. In the absence of a solvent, an explosion may occur unless this energy is dissipated over the organic fragment. The larger this fragment the more effective this energy transfer becomes, hence the generally higher thermal stability of aryl azides compared with alkyl or acyl azides. In this context it has been suggested by P.A.S. Smith [4] that a threshold value is given by the ratio of $(C + O) / N$ and that a violent decomposition may occur when this ratio is lower than 3:1. Consequently organic azides have been extensively investigated as both composite explosives and initiators. Reports of the explosive character of azides have been numerous and it is therefore necessary to adopt suitable safety measures whenever handling azido compounds. Indeed some compounds, especially low molecular weight azides are so treacherous that explosions may occur for unknown reasons during procedures which have previously proved uneventful.

1.2 Aromatic nitro compounds – Introduction

The preparation of aromatic nitro compounds is most often achieved with reagents capable of forming the nitronium ion, NO_2^+ . The reagents capable of producing this ion are numerous, and the conditions employed are as varied as the aromatics being nitrated. Besides the common sulphuric acid nitric acid combination for the production of NO_2^+ , nitronium fluoroborate and other nitronium salts as well as nitrate ester, N_2O_4 , N_2O_5 and metal nitrates plus sulphuric or Lewis acids, are reagents which are believed to involve the nitronium ion as the nitrating species. Typical procedures for the introduction of a nitro group into aromatic systems consist of oxidation of nitroso and amino compounds, replacement of a diazonium ion, rearrangement of nitramines, nucleophilic displacement by aryl anions on nitrate esters and other suitable reagents such as N_2O_4 and tetranitromethane, and free-radical processes involving $\cdot\text{NO}_2$. These procedures are employed most often to overcome problems of orientation, but the sensitivity of some aromatic systems to oxidation by the usual nitrating media necessitate other method of preparing the nitroarene.

Preparative electrophilic nitration can be done in a variety of media, but the most often employed are mixed acid (nitric + sulphuric), aqueous nitric acid and nitric acid in acetic

acid. Nitronium fluoroborate (and the corresponding P, As and Sb salts) and dinitrogen pentoxide are excellent nitrating agents whose preparative value would be greater if they were more readily available and easier to prepare.

Nitrations which are predominately nucleophilic in nature are possible with suitably electron-rich aromatics *i.e.* phenoxides can be nitrated with tetranitromethane. Diazotisation of aromatic amines followed by treatment with sodium nitrite, in the presence of a copper sulphite catalyst, is a similar method to peroxide oxidation for the conversion of an amino group to a nitro group. The replacement of the diazonium group by nitrite ion can only be effected in neutral or basic conditions.

The oxides, N_2O_3 , NO_2 , N_2O_4 and N_2O_5 , when dissolved in sulphuric acid or combined with certain Lewis acids, give rise to the nitronium ion which obviously will nitrate aromatic compounds. In non-ionising solvents or in the gas phase, the use of the oxides of nitrogen in the higher oxidation states may offer some advantage over the normal methods of nitration.

Isomer distribution in the products is often quite different depending on the nitrating media. Aside from the problem of orientation in nitration, experimental conditions such as time, temperature, solvent, concentration and reagents must be selected for the proper degree of nitration of a particular aromatic compound.

It should be noted, that explosions may occur in many of the procedures in the preparation of aromatic nitro compounds, and it is therefore necessary to adopt suitable safety precautions whenever preparing these compounds.

Nitro-compounds Characterisation

Infrared spectroscopy

The nitro group has two identical NO bonds which vibrate asymmetrically, causing a strong absorption at $1556-1645\text{ cm}^{-1}$ in aliphatic nitro compounds, and symmetrically causing somewhat weaker absorption at $1390-1355\text{ cm}^{-1}$. Electronegative substituents such as halogens on the α -carbon cause the nitro stretching frequencies to diverge. Aromatic nitro groups absorb strongly in the $1530-1500\text{ cm}^{-1}$ region and somewhat weaker in the $1370-1330\text{ cm}^{-1}$ region. In addition, aromatic nitro compounds usually have strong aromatic ring absorptions between $760-705\text{ cm}^{-1}$. The usual *o-m-p* bands in the $900-700\text{ cm}^{-1}$ region are upset in the nitro aromatics and not very reliable, probably due to interaction with the out-of-plane NO_2 bending frequency. Steric effects which destroy the nitro-ring coplanarity and thus reduce conjugation make aromatic nitro groups resemble aliphatic nitro groups. The

frequency of the asymmetric NO_2 stretch in *p*-substituted nitrobenzenes has been correlated with the electron donating or withdrawing characteristics of the substituent. In nitroanilines, for example, the electron withdrawing properties of the nitro group and the electron donating properties of the amino group cause a large amount of resonance to occur in the *ortho* and *para* isomers which weaken the N-O bonds relative to the *meta* isomers, where this mesomeric effect does not occur. The strongest band in the IR spectra of nitroanilines probably involves the NO_2 symmetric stretch since it shifts as expected from mesomeric effects and the C-N(H_2) band which in an alternative assignment would be expected to shift the other way. It occurs in the pure materials at 1350 cm^{-1} in *meta*, 1305 cm^{-1} in *para* and 1245 cm^{-1} in *ortho* isomers. The usual strong nitro aromatic band near 740 cm^{-1} is also different in the *ortho* and *para* isomers. In aromatic nitro compounds some nitro group bending bands can be confused with the aromatic bands. In aromatic nitro compounds bands are usually between $890\text{-}835\text{ cm}^{-1}$ (NO_2 scissors deformation), $785\text{-}300\text{ cm}^{-1}$ (NO_2 out-of-plane wag) and $580\text{-}520\text{ cm}^{-1}$ (NO_2 in-plane rock).

Organic nitrates R-O-NO_2 are characterised by strong bands in the $1660\text{-}1625\text{ cm}^{-1}$ (NO_2 asymmetric stretch), $1285\text{-}1270\text{ cm}^{-1}$ (NO_2 symmetric stretch), $870\text{-}840\text{ cm}^{-1}$ (N-O stretch) and $710\text{-}690\text{ cm}^{-1}$ (NO_2 deformation) regions.

^{14}N NMR Spectroscopy

The ^{14}N chemical shifts of the nitro group in aromatic nitrogen compounds fall within the narrow range of -6 to -40 ppm. The ^{14}N chemical shifts of selected aromatic nitro compounds are given in the table 1.4. The nitrogen nuclei in the NO_2 group attached to an unsaturated system of carbon atoms or to an aromatic ring are more shielded than in nitroalkanes except those containing a strongly electron-attracting substituent and the nitro group on the same carbon atom. There is also evident a high field (low frequency) shift for the aromatic NO_2 group if the benzene ring is substituted with electron-attracting groups, like additional NO_2 groups, CHO or COR. However, there is no significant dependence on the position of the substituents. It seems that inductive rather than conjugative effects play the most important role in the determination of the magnetic screening of the NO_2 group nitrogen nuclei in aromatic systems. Attention is drawn to the fact that the shifts of *ortho* substituted nitrobenzenes where the nitro group may be forced out of the plane of the benzene ring, do not differ experimentally from the shifts of the corresponding *meta* and *para* substituted

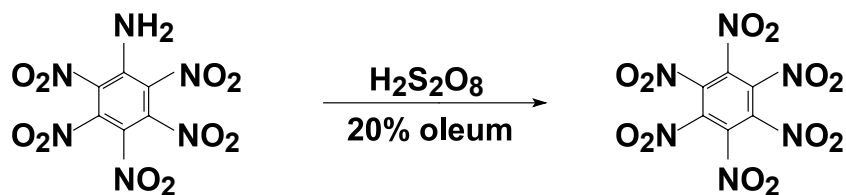
isomers. Thus from the point of view of the ^{14}N chemical shifts of the NO_2 group, aromatic rings behave as electron-attracting groups with no apparent conjugative effects. The ^{14}N resonance signals of the NO_2 group attached to a nitrogen or oxygen atom as in nitramines R_2NNO_2 and nitrate R-ONO_2 occur at higher magnetic fields (lower frequencies) when compared with C-nitro compounds. This is in accord with the general trend in ^{14}N chemical shifts for the NO_2 group.

Table 1.4 ^{14}N NMR Chemical shifts for Nitroaromatic compounds (ref to MeNO_2) [16]

Compound	Solvent	chemical shift (ppm)
Nitrobenzene	acetone	-9.3
1,2 dinitrobenzene	acetone	-13.7
1,3 dinitrobenzene	acetone	-14.7
1,4 dinitrobenzene	acetone	-13.7
1,3,5 trinitrobenzene	acetone	-18.5
2,4,6 trinitrotoluene	acetone	-14.0
hexanitrobenzene	dichloromethane	-38.5

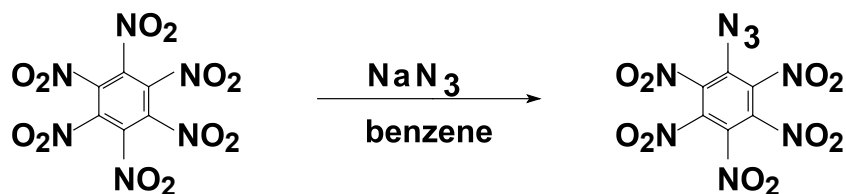
1.3 Nitrocarbons- Introduction

Nitrocarbons represent a small group of polynitro compounds composed only of nitro groups attached to carbon at the nitrogen atom. Until recently only five nitrocarbons were known:- tetranitromethane, hexanitroethane, tetranitroethylene, hexanitrobenzene and decanitrobiphenyl. Hexanitrobenzene was the first aromatic nitrocarbon to be prepared. This high-melting, somewhat stable but reactive compound, is one of the most energetic explosives known. The preparation of hexanitrobenzene was first described by Nielsen and co-workers in 1979 [17], and is readily obtained by the oxidation of pentanitroaniline in 20% oleum with peroxydisulphuric acid.



The structure of hexanitrobenzene was determined by x-ray diffraction techniques by Akopyan *et al* in 1966 [18], as noted earlier, this publication preceded any published report on the method of synthesis. The crystals are monoclinic belonging to the $I2/c$ space group. Bond lengths observed are C-C = 1.39 Å, C-N = 1.45 Å and N-O = 1.23 Å. The benzene ring is planar with co-planar C-N bonds. However each of the nitro groups is twisted out of the plane by 53°. The infrared spectrum (KBr) reveals asymmetric and symmetric NO₂ stretching frequencies at 1560 and 1320 cm⁻¹ respectively. A strong molecular ion peak is observed at 348 *m/e* in the mass spectrum (chemical ionisation (CH₄)) with very little fragmentation. The ¹³C NMR spectrum in CD₂Cl₂ shows a signal at 138.7 δ (ref. to TMS) and the ¹⁴N NMR spectrum in CD₂Cl₂ reveals a signal at -36.1 ppm (ref. to nitromethane). The density of hexanitrobenzene (2.01 g/cm³ at 25°C) is the highest reported for any explosive, and contributes to its high energetic properties [19].

The azide ion reacts efficiently with hexanitrobenzene. A solution of hexanitrobenzene in benzene reacts with aqueous sodium azide at 25°C to form pentanitrophenyl azide. Unlike the reactions of halide ions, no acid catalyst is required for this synthesis. Two crystalline forms of this powerful, very brisant explosive were isolated by crystallisation from carbon tetrachloride.



Nitrocarbons represent a very small group of compounds, only 4 new members of this class of compounds have been synthesised since tetranitromethane was first reported in 1861 [20]. They are of special interest as high energy explosives and propellant ingredients. Except for

tetranitromethane they are rather difficult to synthesise and (except tetranitromethane) they are somewhat thermally liable, slowly evolving NO_2 at ambient temperatures. The correlation of energetic properties of known nitrocarbons and their polynitro precursors with the structure is of great value in selecting new target nitrocarbons and other explosives. Theoretical calculations are important in predicting many properties of unknown nitrocarbons, including energy, density, structure, thermodynamic and kinetic stability and reactivity.

1.4 Explosives -Introduction

The use of energetic additives, mainly binders and plasticisers, is considered to be one of the practical ways to improve the energy level and other technical performances of solid propellant and gun propellants. In this aspect organic azides are attracting researchers attention more and more. Since 1970 organic azides as energetic binders or plasticisers for advanced solid propellants have been studied extensively in many countries. Organic azides possess a number of advantages, replacement of binders and/or plasticizers presently in use with energetic azides, including those containing other energetic groups, cannot only make a significant energy contributions to propellants but can also reduce or minimise the amount of flame and smoke in the exhaust gases generated during propulsion phase of solid propellants. Therefore, azides are suitable ingredients for minimum-signature propellants. During the past two decades a large number of organic azides that can or may find applications in propellants or plastic bonded explosives have been synthesised and examined. They included azidopolyethers, azidonitramines, azidonitro compounds, azidoalkanes and azidoesters. As stated above, energetic ingredients (including binders and plasticizers) used in formulating solid propellants, gun propellants or explosives, increase energy levels and appear to be the emerging tendency for the next generation of high energy dense materials (HEDM).

Since highly toxic lead azide is still widely used as an initiator in ammunition, there is a great demand to find suitable non-toxic, heavy metal free substitutes which can be used as detonators. Equally important, most solid-rocket fuels are still based on mixtures of ammonium perchlorate, aluminum and epoxy resins, which consequently generate exhaust plumes which contain large amounts of HCl and aluminum oxides. The presence of these compounds is both environmentally not desirable and, the trace of such rockets can easily be detected by radar [21].

A large number of explosives have been reported in the recent past. The selection of an explosive is made in the light of stability, reliability, safety, application and mission

requirements. At the time of development of a new explosive it is essential to keep in mind such factors, as indigenous availability of starting materials, ease of method of preparation, purity of explosive and its cost-effectiveness, in addition to its impact on the environment.

Calculating detonation velocity from molecular formula and structure.

The detonation velocity determines the characteristics and utility value of explosives and propellants. Methods of calculating the detonation velocities of a variety of explosives on the basis of their molecular formulae have been evolved by Rothstein. [22] The calculation involved making use of a factor F which can be correlated readily with the detonation velocities. Rothstein calculated the F factor values for a series of explosives *i.e.* nitroaromatics, nitrate esters, azides, etc and correlated with the detonation velocity D at TMD (theoretical maximum density) as in equation below.

$$D = \frac{F - 0.26}{0.55}$$

where F is given by

$$F = [100 \times \frac{n[\text{O}] + n[\text{N}] - (\frac{n[\text{H}]}{2n[\text{O}]}) + \frac{A}{3} - \frac{n[\text{B}]}{1.75} - \frac{n[\text{C}]}{2.5} - \frac{n[\text{D}]}{4} - \frac{n[\text{E}]}{5}}{\text{MW}}] - G$$

where

G = 0.4 for liquid explosives , G = 0 for solid explosives

A = 1 if the compound is aromatic , A = 0 otherwise

n[O] = number of oxygen atoms

n[N] = number of nitrogen atoms

n[H] = number of hydrogen atoms

n[B] = number of oxygen atoms in excess of those already available to form CO₂ and H₂O

n[C] = number of oxygen atoms doubly bonded directly to carbon as in carbonyl

n[D] = number of oxygen atoms singly-bonded directly to carbon

n[E] = number of nitrate groups existing either in a nitrate ester configuration or as a nitric acid salt such as hydrazine mononitrate

In this equation, F values are derived only from molecular formulae and structures. The detonation velocities predicted for various explosives based on this equation were found to be in good agreement with those observed [22]. Since the F factor depends solely on the molecular formula and structure and since it has a direct relationship with D, it would be possible to optimise D by selecting the required number of substituents that may be attached to a potential skeleton. In this way, efficient high energetic materials with optimum detonation velocities can be predicted, and these compounds will be very good synthetic targets. The method is, of course a qualitative technique without differentiating isomeric compounds which would introduce differing strain energies due to conformational repulsions and attractions.

1.5 Introduction to theoretical calculations

Programs

All semiempirical (PM3), ab initio (HF) and hybrid-DFT (B3LYP) calculations were carried out using the program package Gaussian 98 [23] with the input files (z matrices) being generated using the program package HyperChem [24]. All structures were fully optimised without symmetry constraints and the vibrational frequencies computed using the optimised structures. The molecular structure diagrams were generated from the Gaussian output files for the fully optimised structures using the Resview program [25].

Semiempirical PM3 Computations

Semiempirical calculations are characterised by their use of parameters derived from experimental data in order to simplify the approximation of the Schrödinger equation [26]. As such, they are relatively inexpensive (cpu time) and can be applied to large molecules.

Semiempirical methods may only be used for systems where parameters have been developed for all of the component atoms. This, fortunately, is the case for the organic type C, H, N, O, X compounds (X = halogen) studied in this thesis.

All calculations in this thesis were carried out with the program package Gaussian 98W [23] at the semiempirical PM3 level of theory using a VSTO-3G basis set [27-32]. For the semiempirical calculations the PM3 method was chosen (which differs from AM1 only in the values of the parameters) since the parameters for PM3 were derived by comparing a much larger number and wider variety of experimental versus computed molecular properties. The PM3 is a reparametrization of AM1, which is based on the neglect of diatomic differential overlap (NDDO) approximation. NDDO retains all one-center differential overlap terms when Coulomb and exchange integrals are computed.

Ab initio Computations

Since the quality of a semiempirical calculation also strongly depends on the nature of the compounds which have been used to fit the computed (versus the experimental) parameters, semiempirical calculations are often limited with respect to the prediction of molecular properties of new classes of compounds [26,33]. Therefore, it was decided also to calculate the structures and energies also ab initio at Hartree-Fock (HF) level of theory using a standard split-valence double-zeta 6-31G Pople basis set. In calculations for molecules containing iodine and bromine a quasirelativistic Stuttgart/Dresden (SDD) pseudopotential for the core electrons was applied for these elements (Br, I) with a Dunning/Huzinaga D95-type valence basis set [34-36]. The energy-consistent pseudopotentials are semi-local pseudopotentials adjusted to reproduce atomic valence-energy spectra. The adjustment of the pseudopotential parameters has been done in fully numerical calculations, valence basis sets have been generated a-posteriori via energy optimisation. The complete set of potentials includes one-component (non-relativistic and scalar-relativistic) effective-core potentials (ECP) [34].

HF calculations are very useful as a predictive tool for many systems and to compute the structures and vibrational frequencies of stable closed-shell molecules. However, the neglect of electron correlation makes the HF method unsuitable for accurate modelling of the energetics of reactions and bond dissociation. To overcome this problem, it was decided to compute the total energies for those molecules for which reaction energies were to be predicted at hybrid-DFT level of theory (see below).

Hybrid-DFT Calculations

The density functional theory (DFT) methods achieve significantly greater accuracy than HF methods (see above) at only a moderate increase in cost (cpu time). This is achieved by including some of the effects of electron correlation much less expensively than traditional correlated methods (*e.g.* MP2). In DFT, the exact exchange (HF) for a single determinant is replaced by a more general expression, the exchange-correlation functional, which can include terms accounting for both the exchange energy and the electron correlation, which is omitted from HF theory. (*N.B.* A functional is defined in mathematics as a function of a function. In DFT, functionals are functions of the electron density which itself is a function of co-ordinates in space) [27]. In other words, DFT methods compute electron correlation via general functionals of the electron density. DFT functionals partition the electronic energy into several components which are computed separately:

- (i) the kinetic energy
- (ii) the electron-nuclear interaction,
- (iii) the Coulomb repulsion
- (iv) the exchange-correlation term for the remainder of the electron-electron interaction which is usually itself divided into separate exchange and correlation components.

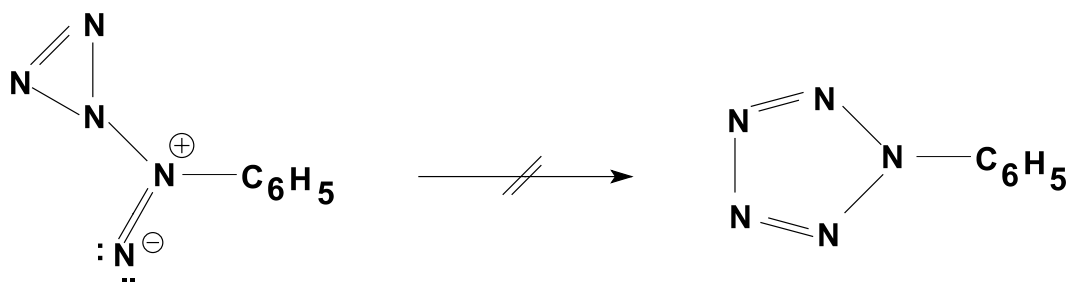
In this work, the so-called hybrid DFT method was applied in which a hybrid functional, which defines the exchange functional as a linear combination of HF, local, and gradient-corrected exchange terms is used. This exchange functional is then combined with a local and gradient corrected correlation functional. In this study Becke's three-parameter functional (B3LYP) was applied where the non-local correlation is provided by the LYP correlation functional (LYP = Lee, Yang, Parr) [37-40].

For reaction energy calculations, all structures were fully optimised at PM3/VSTO-3G level of theory with the energies computed at B3LYP/6-31G(d) level (single point calculations), notation: B3LYP/6-31G(d)//PM3/VSTO-3G.

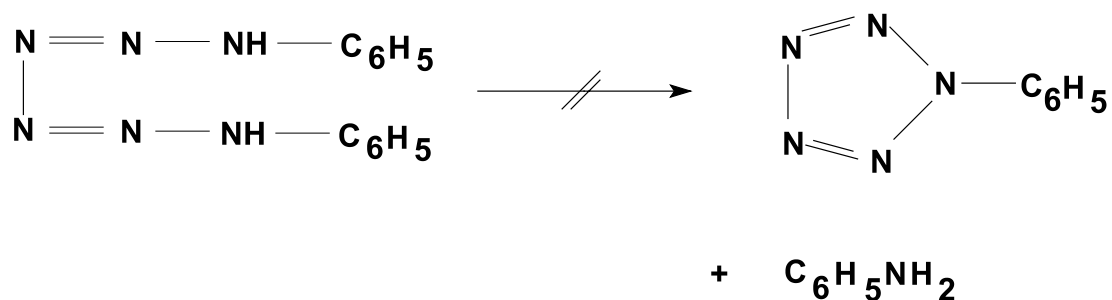
For a simple definition of the terms ab initio, basis sets, Hartree-Fock and DFT, including the Gaussian (Pople) notation of basis sets see ref. [41].

1.6 Pentazoles

The history of pentazoles began in 1903 when Hantzsch [42] tried to form phenylpentazole by the rearrangement of benzenediazonium azide. (Note that formerly the azide structure was assumed to be a three membered ring. This is documented on the Curtius monument in Heidelberg, Germany.)



Dimroth and de Montmollin [43] also had no luck when they planned to prepare phenylpentazole from a chain of six nitrogen atoms.



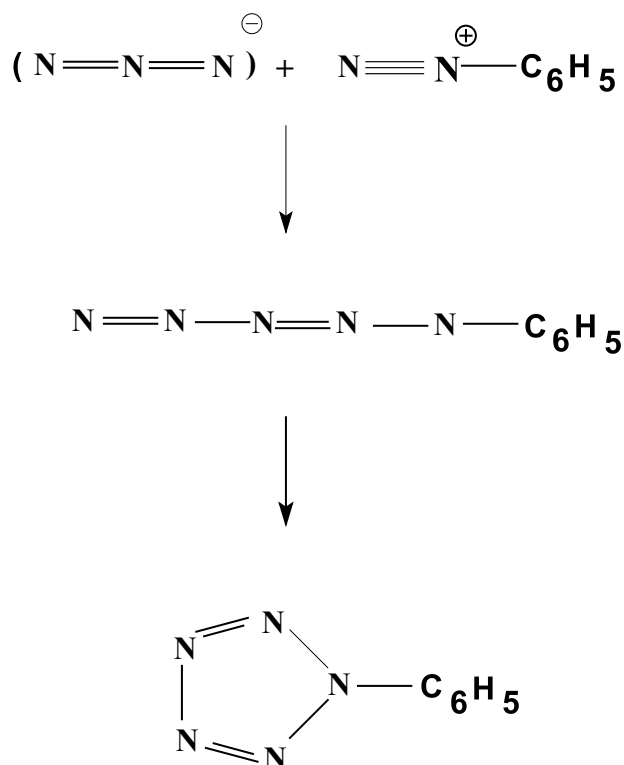
Then in 1915, Lifschitz [44] believed he had synthesised pentazole acetic acid amidrazone from tetrazolecarbonitrile. But in the same year came the rebuttal from Curtius *et al* [45] with the title ***Die sogenannten Pentazol-Verbindungen von Lifschitz***

(The so-called pentazole compounds of Lifschitz). They did not mince their words :-

Ein derartiger Reaktionsverlauf wäre im höchsten Grade überraschend ... Lifschitz glaubt die Richtigkeit seiner Auffassung mit vollkommener Sicherheit folgern zu müssen ohne weitere Prüfung in das Reich des Unmöglichen zu verweisen ... daß alle seine Beobachtungen und Folgerungen auf Irrtum beruhen von Pentazole keine Rede sein kann.

(Such a course for the reaction would be extremely surprising ... Lifschitz believes he must conclude that his interpretation is correct in perfect confidence without further proof it must be relegated to the realm of the impossible ... all his observations and conclusions are based on error.... there can be no question of pentazoles in this case.)

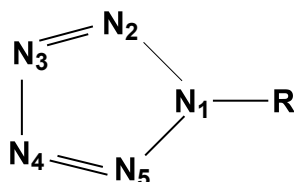
Curtius verdict hit hard and it was almost half a century before anyone again ventured to search for pentazole. Huisgen and Ugi [46,47] thus solved a classic problem in 1956 when they proved that they could link the benzenediazonium ion with the azide ion to form benzenediazoazide, which on ring-closure yielded phenylpentazole.



The X-ray structure of 4-dimethylaminophenylpentazole was determined by X-ray diffraction techniques in 1983 by Dunitz and Wallis [48] and to date this is the only known X-ray structure of a pentazole compound. The N-N bond distances in the structure lie in the range 1.30 -1.35 Å, intermediate between single bonds (1.449 Å) and double bonds (1.252 Å) thus the pentazole ring with 6π electrons can be regarded as aromatic.

^{14}N NMR evidence for the pentazole ring structure.

In 1975 Witanowski *et al* [49] predicted the ^{14}N NMR chemical shifts for the pentazole compound to be



N(1) $+75 \pm 9$ ppm (upfield from CH_3NO_2 as internal standard)

N(2), N(5) -7 ± 15 ppm

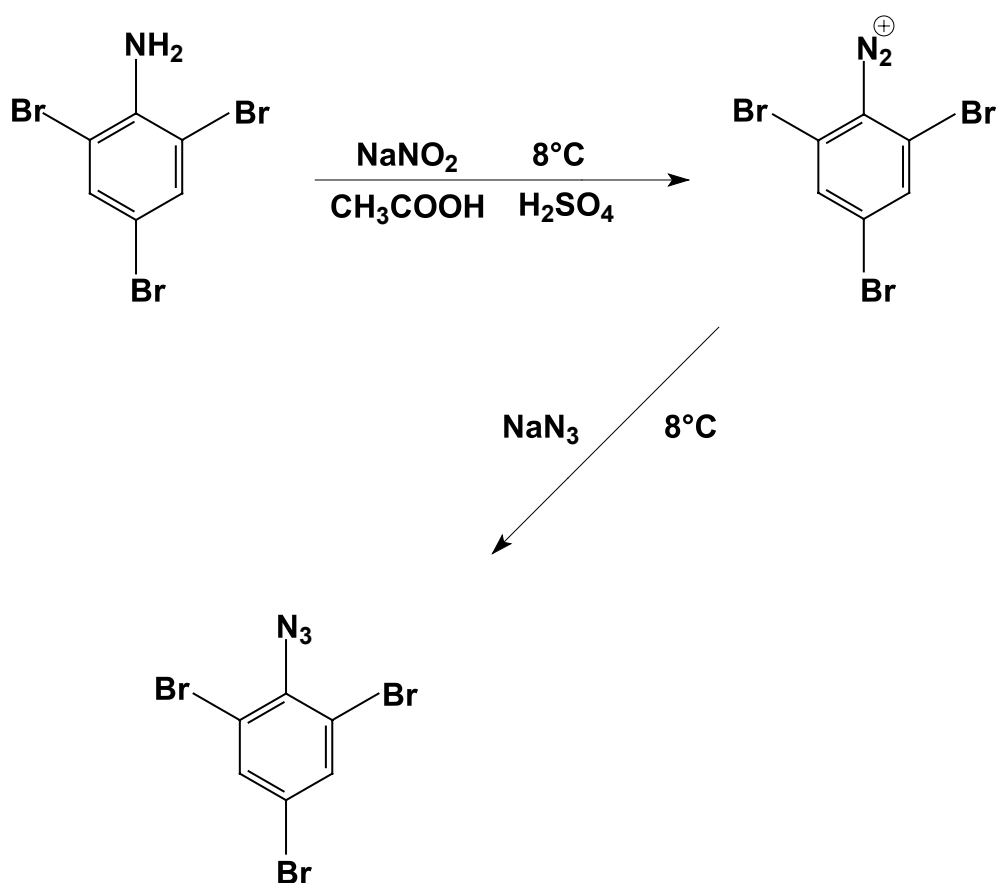
N(3), N(4) $+13 \pm 14$ ppm

They then attempted to record the ^{14}N NMR spectra of 4-dimethylaminophenylpentazole, but once the compound was dissolved in solution it immediately began to evolve gaseous dinitrogen which posed a problem in recording the spectrum. Several solvents were tried, but in all cases the only ^{14}N spectrum they obtained was that of 4-dimethylaminophenyl azide. It was eventually found that the evolution of nitrogen gas was relatively slow in a 1:1 mixture of methanol and dichloromethane. The ^{14}N NMR spectrum of this solution measured within a few hours shows a sharp signal at +70 ppm which gradually diminishes with time. This is as expected for the pyrrole type nitrogen N(1) in a decomposing pentazole. The rest of the spectrum was too weak for the broader signals to be observed.

2 Halogen substituted phenyl azides

2.1 2,4,6- tribromophenyl azide

The first halogen substituted phenyl azide to be prepared in this work was 2,4,6-tribromophenyl azide which was prepared by the reaction of 2,4,6-tribromoaniline with sodium nitrite in a mixture of glacial acetic acid and sulphuric acid at 8 °C to yield the diazonium salt. The diazonium salt was then reacted with sodium azide at 8 °C to yield 2,4,6-tribromophenyl azide as shown in the scheme below.



2,4,6-tribromophenyl azide was isolated as a pink solid and was then recrystallised from ethanol to give pink needles with a melting point of 70 - 71 °C. The elemental analysis for the 2,4,6-tribromophenyl azide was in agreement with the theoretical values, (found C, 20.0 ; H, 0.7; N, 11.8 %. calculated C, 20.2 ; H, 0.6 ; N, 11.8 %). The IR spectrum showed a strong absorption at 2109 cm⁻¹ for the asymmetric stretching vibration of the azide group and a strong absorption at 1303 cm⁻¹ for the symmetric stretching vibration of the azide group. The IR spectrum also showed a weak absorption at 3055 cm⁻¹ which is characteristic for C-H

vibrations in an aromatic ring, a strong absorption at 1534 cm^{-1} for the asymmetric stretching vibration of the C-C bond in the aromatic ring, a peak at 1370 cm^{-1} for the symmetric stretching vibration of the C-C bond and a weak absorption at 573 cm^{-1} for the deformation of the carbon bromine bond. The Raman spectrum showed two peaks at 2143 and 2100 cm^{-1} for the asymmetric stretching vibration of the azide group, a strong peak at 1301 cm^{-1} for the symmetric stretching vibration of the azide. The Raman spectrum also showed a peak at 3058 cm^{-1} which is characteristic for C-H vibrations in an aromatic ring, a peak at 1554 cm^{-1} for the asymmetric stretching vibration of the C-C bond in the aromatic ring, a peak at 1370 cm^{-1} for the symmetric stretching vibration of the C-C bond and a medium peak at 573 cm^{-1} for the deformation of the carbon bromine bond. The ab initio calculation of the vibrational frequencies for 2,4,6-tribromophenyl azide was carried out at the self consistent HF level of theory using a 6-31G(d) basis set. There is a very good agreement between the calculated frequencies and the observed IR and Raman frequencies. The calculated and observed IR and Raman frequencies are shown in Table 2:1.

Table 2:1 Comparison between the calculated and the experimental observed vibrational frequencies for 2,4,6-tribromophenyl azide

Assignment	Calculated Frequencies HF/6-31G(d) (cm^{-1})	Observed Raman Frequencies (cm^{-1})	Observed I.R. Frequencies (cm^{-1})
ν (CH)	3068	3058	3055
ν_{as} (NNN)	2397*	2143	2143
ν (CC)	1545	1554	1534
ν (CC) + ν (CN)	1447	1435	1430
ν (CC)	1360	n.o.	1370
ν_{sym} (NNN)	1307	1301	1303
δ (CC)	1168	1148	1146
δ (CC)	807	827	828
γ (CC)	729	730	729

* see footnote at the end of this chapter

The structure of 2,4,6-tribromophenyl azide was fully optimised and the vibrational frequencies and zero point energy computed using a semiempirical calculation carried out at the semiempirical PM3 level of theory using a VSTO-3G basis set and ab initio at the self consistent HF level of theory using a 6-31G(d) basis set for hydrogen and carbon and a quasirelativistic Stuttgart/Dresden (SDD) pseudopotential for the core electrons of bromine with a Dunning/Huzinaga D95-type valence basis set [34]. The fully optimised structure of 2,4,6-tribromophenyl azide is shown in the figure 2.1 below.

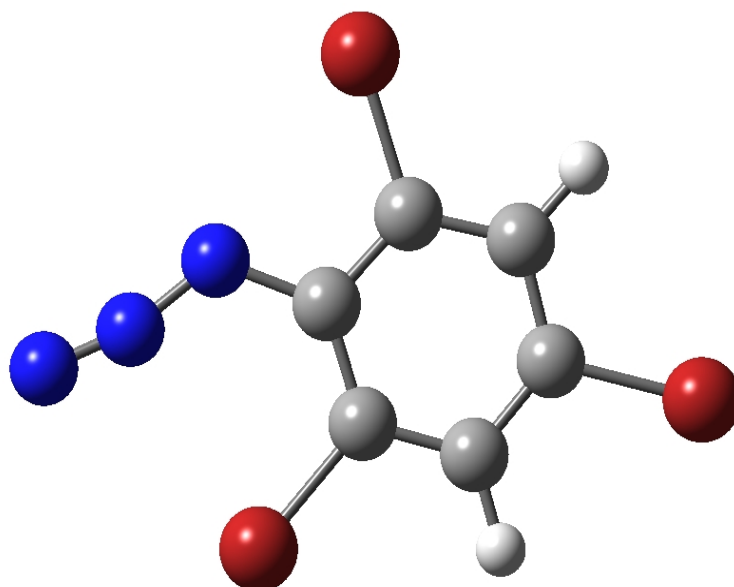


Figure 2.1 Molecular structure of 2,4,6-tribromophenyl azide fully optimised at HF/6-31G(d) level of theory

The 2,4,6-tribromophenyl azide was isolated as a pink solid which was then recrystallised from ethanol to give pink needles which were used for the x-ray structure determination. A crystal (0.08 x 0.04 x 0.03 mm) of 2,4,6-tribromophenyl azide was mounted on Siemens SMART Area-detector with Mo-K α radiation at 213 K for the crystal structure analysis. The cell dimensions were derived from the least-squares analysis of 25 independent reflections.

Intensities of 4990 reflections were surveyed in the range θ 3.80-58.10 and 1509 independent reflections satisfied the criterion $F > 4 \sigma(F)$. The crystal structure was solved by direct phasing using SHELXS [50]. H atoms were located in difference fourier synthesis. Full-matrix least squares calculations were performed on F with anisotropic thermal parameters for C, N, and Br atoms and isotropic for H atoms using SHELXL [51]. Least-squares convergence at $R = 0.0284$, $R_w = 0.0582$. The crystals are monoclinic, with space group P21/n and cell dimensions $a = 3.918(1)$, $b = 14.6728(4)$, $c = 15.6992(5)$, $\beta = 95.898(4)$.

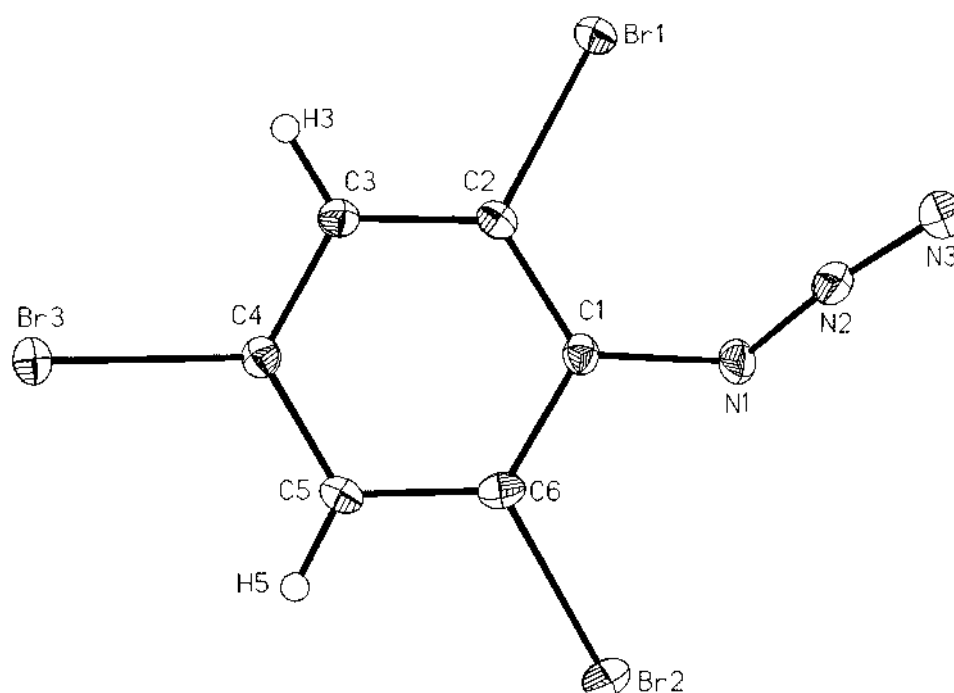


Figure 2.2 - ORTEP drawing of 2,4,6-tribromophenyl azide with the thermal ellipsoids of the C, N and Br atoms drawn at 25% probability level, H atoms are represented by spheres of radius 0.1Å.

In 2,4,6 tribromophenyl azide the bond length between the terminal nitrogen and the central nitrogen is 1.133 Å and the bond length between the central nitrogen and the nitrogen attached directly to the ring is 1.242 Å. The azide group is not linear. The angle at the central nitrogen atom is 171.3°. The angle at the nitrogen of the azide that is attached directly to the ring is 116.2° which is slightly less than the expected value of 120°.

The molecular geometries of 2,4,6-tribromophenyl azide are comparable with the structures of other 2,4,6-tribromophenyl compounds, *i.e.* 2,4,6-tribromoaniline, 2,4,6-tribromobenzene and 2,4,6-tribromocyanobenzene [52-54]. The ring carbon – carbon bond lengths are 1.377 – 1.390 Å in 2,4,6-tribromophenyl azide, 1.360 – 1.385 Å in 2,4,6-tribromoaniline, 1.392 – 1.402 Å in 2,4,6-tribromobenzene and 1.414 – 1.474 Å in 2,4,6-tribromocyanobenzene. The carbon – bromine bond lengths are 1.889 – 1.894 Å in 2,4,6 tribromophenyl azide, 1.867 – 1.895 Å in 2,4,6-tribromoaniline, 1.855 – 1.861 Å in 2,4,6-tribromobenzene and 1.838 – 1.895 Å in 2,4,6-tribromocyanobenzene. The $\angle(\text{C} - \text{C} - \text{C} (\text{ring}))$ angles are 118.1 – 122.1° in 2,4,6-tribromophenyl azide, 118.5 – 121.7° in 2,4,6-tribromoaniline and 115.7 – 123.0° in 2,4,6-tribromocyanobenzene.

The crystal packing diagram of 2,4,6 tribromophenyl azide shows that terminal N(3) atom of the azide group has two intermolecular contacts with two bromine atoms of symmetrically related molecules within the unit cell. The intermolecular distances are N(3) to Br(2)* ($x - 0.5, -y - 0.5, z - 0.5$) 3.605 Å and N(3) to Br(1)* ($x + 1, y, z$) 3.881 Å. These distances are both below the sum of the van der Waals radii of both atoms.. The crystal packing diagram of 2,4,6-tribromophenyl azide is shown in the figure 2.3

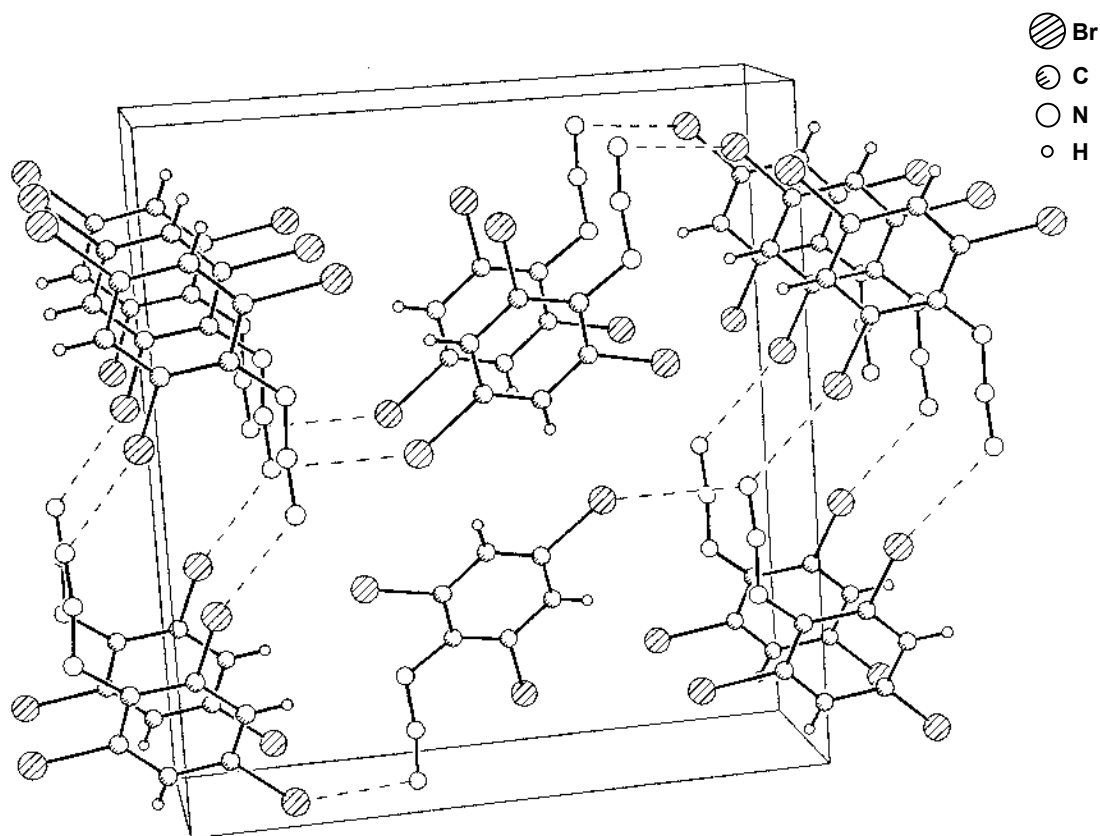


Figure 2:3 - The crystal packing diagram of 2,4,6-tribromophenyl azide showing the two intermolecular contacts between N(3) symmetrically related bromine atoms.

There is a very good agreement between the calculated bond lengths and angles and the bond length and angles in the structure determined at 213 K. The comparison of bond lengths and angles between the calculated HF/6-31G(d) structure and the X-ray structure determined at 213K of 2,4,6-tribromophenyl azide are shown in tables 2.2 and 2.3.

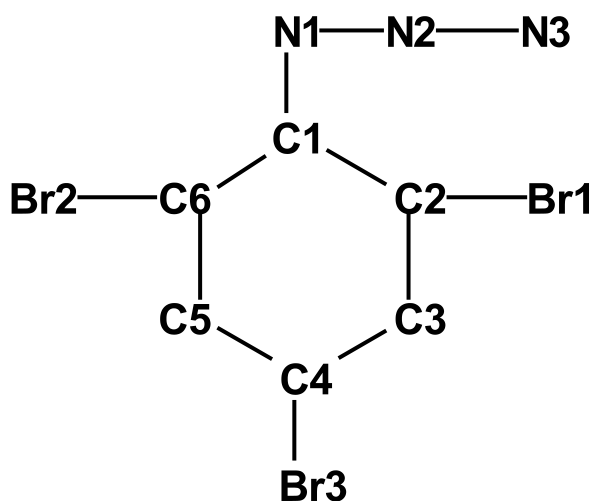


Table 2.2 Comparison of bond lengths (values given in Å) between the calculated PM3/VSTO-3G structure, HF/6-31G(d) structure, HF/SDD structure and the X-ray structure determined at 213K of 2,4,6 tribromophenyl azide.

Bond	X-ray	PM3	HF/ 6-31G(d)	HF/ SDD
Br (1) – C (2)	1.889 (4)	1.864	1.926	1.939
Br (2) – C (6)	1.889 (4)	1.858	1.916	1.930
Br (3) – C (4)	1.894 (4)	1.854	1.920	1.934
N (1) – N (2)	1.242 (5)	1.275	1.256	1.272
N (1) – C (1)	1.430 (5)	1.418	1.409	1.427
N (2) – N (3)	1.133 (5)	1.125	1.109	1.118
C (1) – C (6)	1.390 (5)	1.397	1.394	1.402
C(1) – C (2)	1.399 (6)	1.392	1.390	1.400
C (2) – C (3)	1.379 (6)	1.385	1.382	1.391
C (3) – C (4)	1.385 (5)	1.383	1.375	1.386
C (4) – C (5)	1.377 (6)	1.387	1.379	1.388
C (5) – C (6)	1.386 (6)	1.380	1.377	1.388

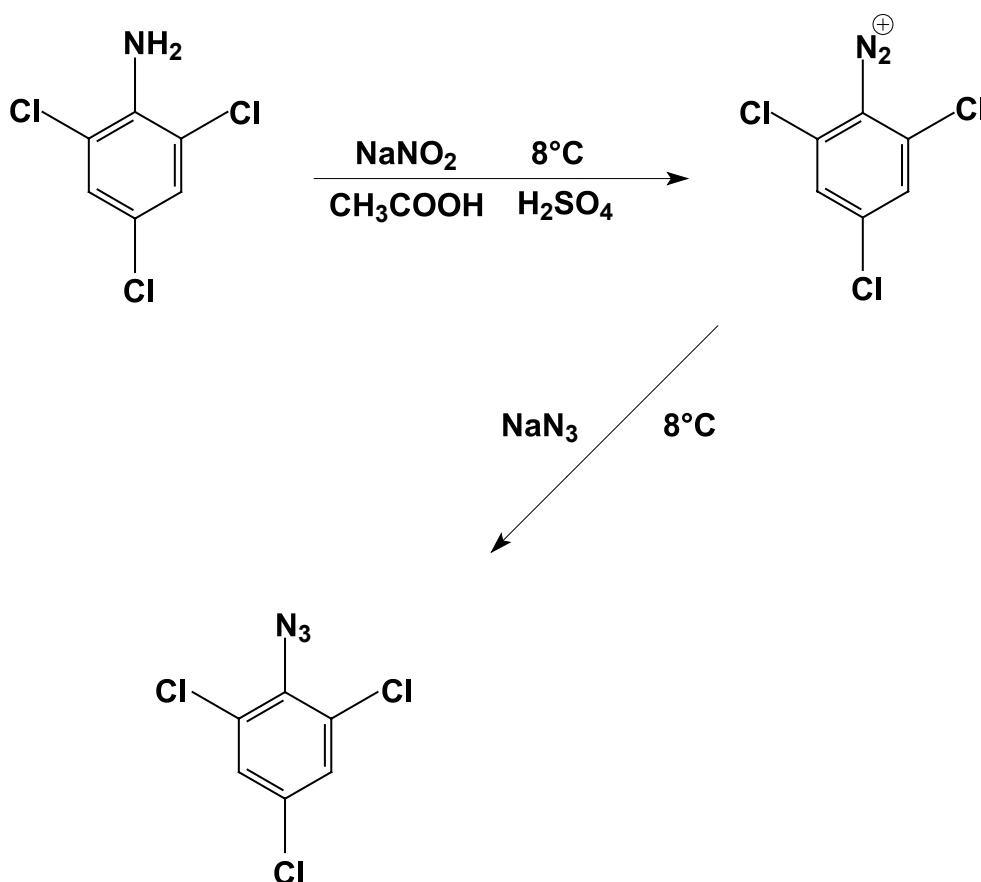
Table 2:3 Comparison of angles ($^{\circ}$) between the calculated PM3/VSTO-3G structure, HF/6-31G(d) structure, HF/SDD structure and the X-ray structure determined at 213K of 2,4,6 tribromophenyl azide.

Angle	X-ray	PM3	HF/6-31G(d)	HF/ SDD
N (2) – N (1) – C (1)	116.2 (3)	123.49	121.20	118.27
N (1) – N (2) – N (3)	171.3 (4)	165.86	167.25	169.39
C (6) – C (1) – C (2)	117.4 (4)	117.23	116.93	117.30
C (6) – C (1) – N (1)	118.1 (4)	114.90	115.92	117.21
C (2) – C (1) – N (1)	124.3 (3)	127.87	127.09	125.26
C (3) – C (2) – C (1)	122.1 (3)	122.43	121.90	121.83
C (3) – C (2) – Br (1)	118.0 (3)	117.72	116.44	116.92
C (1) – C (2) – Br (1)	119.8 (3)	119.85	121.63	121.21
C (2) – C (3) – C (4)	118.1 (4)	117.27	119.30	119.02
C (5) – C (4) – C (3)	122.0 (4)	123.38	120.64	120.95
C (5) – C (4) – Br (3)	118.6 (3)	118.29	119.68	119.50
C (3) – C (4) – Br (3)	119.3 (3)	118.33	119.67	119.55
C (4) – C (5) – C (6)	118.5 (4)	116.99	119.25	119.17
C (5) – C (6) – C (1)	121.8 (4)	122.71	121.97	121.71
C (5) – C (6) – Br (2)	118.2 (3)	117.19	117.78	117.80
C (1) – C (6) – Br (2)	120.0 (3)	120.09	120.25	120.49

The ^1H NMR spectrum shows one resonance at 7.66 ppm for the two ring hydrogens. The ^{13}C NMR spectrum shows four resonances at 136.0, 135.2, 119.2, and 119.1 ppm. for the aromatic carbons. The ^{14}N NMR spectrum shows three resonances for the azide N_{α} ($\delta = -280$ ppm), N_{β} ($\delta = -145.2$ ppm) and N_{γ} ($\delta = -155.0$ ppm).

2.2 2,4,6-trichlorophenyl azide

The next halogen substituted phenyl azide to be prepared was 2,4,6-trichlorophenyl azide which was prepared by the reaction of 2,4,6-trichloroaniline with sodium nitrite in a mixture of glacial acetic acid and sulphuric acid at 8°C to yield the diazonium salt. The diazonium salt was then reacted with sodium azide at 8°C to yield 2,4,6-trichlorophenyl azide as shown in the scheme below.



The 2,4,6-trichlorophenyl azide was isolated as a brown solid and was then recrystallised from ethanol to give brown needles that darken if exposed to continuous sunlight. The elemental analysis for the 2,4,6-trichlorophenyl azide was in agreement with the theoretical values, (found C, 32.3 ; H, 0.9 ; N, 19.0. % $\text{C}_6\text{H}_2\text{Cl}_3\text{N}_3$ calculated C, 32.4 ; H, 0.9 ; N, 18.9 %). The IR spectrum showed a strong absorption at 2130 cm^{-1} for the asymmetric stretching vibration of the azide group and a strong absorption at 1316 cm^{-1} for the symmetric stretching vibration of the azide group. The IR spectrum also showed a weak absorption at 3065 cm^{-1}

which is characteristic for C-H vibrations in an aromatic ring, a strong absorption at 1568 cm^{-1} for the asymmetric stretching vibration of the C-C bond in the aromatic ring, a peak at 1373 cm^{-1} for the symmetric stretching vibration of the C-C bond and a weak absorption at 598 cm^{-1} for the deformation of the carbon chlorine bond. The Raman spectra showed a peak at 2127 cm^{-1} for the asymmetric stretching vibration of the azide group, a strong peak at 1317 cm^{-1} for the symmetric stretching vibration of the azide. The Raman spectrum also showed a peak at 3068 cm^{-1} which is characteristic for C-H vibrations in an aromatic ring, a peak at 1570 cm^{-1} for the asymmetric stretching vibration of the C-C bond in the aromatic ring and a peak of medium intensity at 599 cm^{-1} for the deformation of the carbon chlorine bond. The ab initio calculation of the vibrational frequencies for 2,4,6-trichlorophenyl azide was carried out at the self consistent HF level of theory using a 6-31G(d) basis set. There is a very good agreement between the calculated frequencies and the observed IR and Raman frequencies. The calculated and observed IR and Raman frequencies are shown in Table 2.4.

Table 2.4 Comparison between the calculated and the experimental vibrational frequencies for 2,4,6-trichlorophenyl azide

Assignment	Calculated Frequencies HF/6-31G(d) (cm^{-1})	Observed Raman Frequencies (cm^{-1})	Observed I.R. Frequencies (cm^{-1})
ν (CH)	3055	3068	3065
ν_{as} (NNN)	2396*	2127	2130
ν (CC)	1573	1570	1568
ν (CC) + ν (CN)	1433	1449	1441
ν_{sym} (NNN)	1299	1317	1316
γ (CC)	794	n.o.	807

* see footnote at the end of this chapter

The structure of 2,4,6-trichlorophenyl azide was fully optimised and the vibrational frequencies and zero point energy computed using a semiempirical calculation carried out at the semiempirical PM3 level of theory using a VSTO-3G basis set and ab initio at the self consistent HF level of theory using a 6-31G(d) basis set. The fully optimised structure of 2,4,6- trichlorophenyl azide is shown in figure 2:4 below.

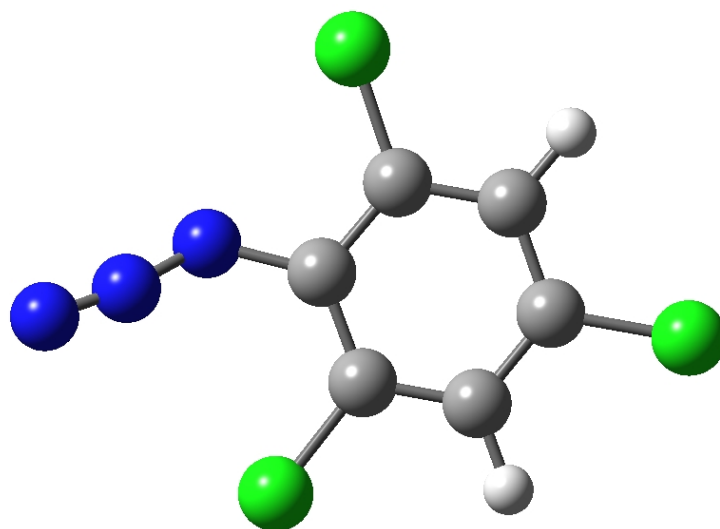


Figure 2.4 Molecular structure of 2,4,6-trichlorophenyl azide fully optimised at HF/6-31G(d) level of theory

2,4,6- trichlorophenyl azide was isolated as a brown solid and was then recrystallised from ethanol to give brown needles. A crystal (0.30 x 0.16 x 0.08 mm) of 2,4,6,trichlorophenyl azide was mounted on Siemens SMART Area-detector with Mo-K α radiation at room temperature (293 K) for structure determination. The cell dimensions were derived from the least-squares analysis of 25 independent reflections. Intensities of 862 reflections were surveyed in the range θ 5.00-49.90 and 628 independent reflections satisfied the criterion $F > 4 \sigma (F)$. The crystal structure was elucidated by direct phasing using SHELXS [50]. H atoms located in difference fourier synthesis. Full-matrix least squares calculations were performed on F with anisotropic thermal parameters for C, N, and Cl atoms and with isotropic

for H atoms using SHELXL [51]. Least-squares convergence at $R = 0.0382$, $R_w = 0.0875$. The crystals are monoclinic, with space group P21 and cell dimensions, $a = 3.835(5)$, $b = 13.29(1)$, $c = 8.349(7)\text{\AA}$, $\beta = 103.06(2)^\circ$.

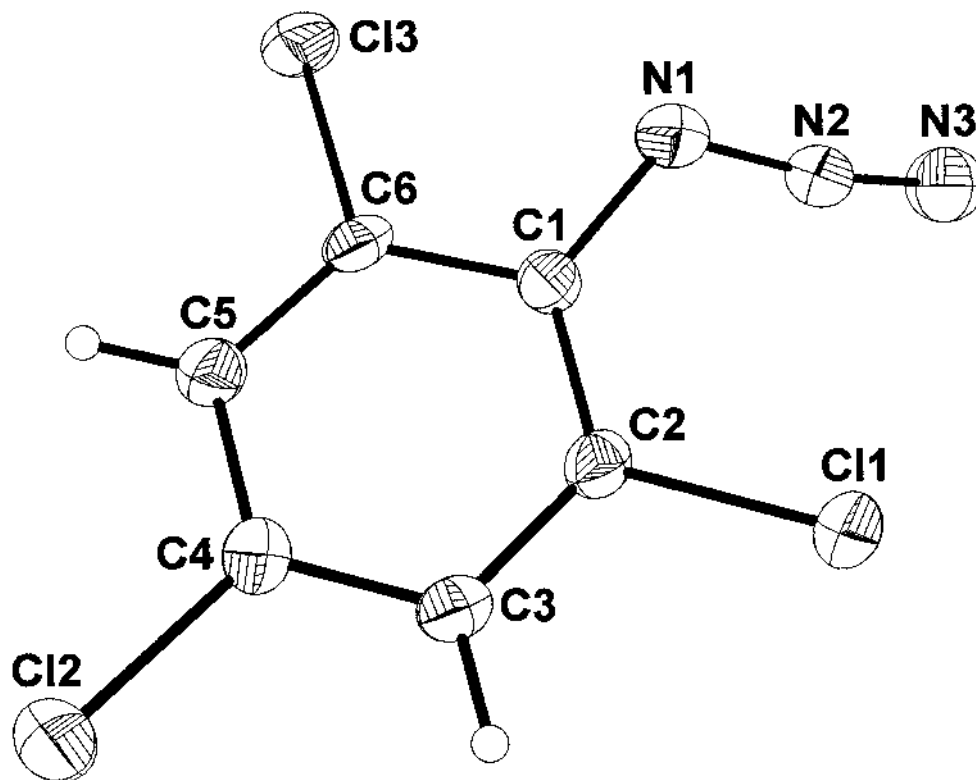


Figure 2.5 ORTEP drawing of 2,4,6-trichlorophenyl azide with the thermal ellipsoids of the C, N and Cl atoms drawn at 50 % probability level and H atoms are represented by spheres of radius 0.1Å.

In 2,4,6-trichlorophenyl azide, the bond length between the terminal nitrogen and the central nitrogen is 1.107 Å and the bond length between the central nitrogen and the nitrogen attached directly to the ring is 1.242 Å. The azide group is not linear, the (NNN) angle at the central nitrogen atom is 169.7°, whereas the angle at the nitrogen of the azide that is attached directly to the ring is 119.6° which is close to the expected value of 120°.

The molecular geometries of 2,4,6-trichlorophenyl azide is comparable with the structures of other 2,4,6-trichlorophenyl compounds, *i.e.* 2,4,6-trichloroacetanilide, 2,4,6-trichlorobenzene and 2,4,6-trichlorocyanobenzene [55-57]. The ring carbon – carbon bond lengths are 1.374 – 1.398 Å in 2,4,6-trichlorophenyl azide, 1.375 – 1.403 Å in 2,4,6-trichloroacetanilide, 1.373 – 1.413 Å in 2,4,6-trichlorobenzene and 1.381 – 1.413 Å in 2,4,6-trichlorocyanobenzene. The carbon – chlorine bond lengths are 1.721 – 1.740 Å in 2,4,6-trichlorophenyl azide, 1.721 – 1.736 Å in 2,4,6-trichloroacetanilide, 1.708 – 1.714 Å in 2,4,6-trichlorobenzene and 1.711 – 1.747 Å in 2,4,6-trichlorocyanobenzene. The $\angle(\text{C} - \text{C} - \text{C} \text{ (ring)})$ angles are 117.0 – 122.1° in 2,4,6-trichlorophenyl azide, 116.8 – 123.0° in 2,4,6-trichloroacetanilide and 117.5 – 124.6° in 2,4,6-trichlorocyanobenzene.

There is a very good agreement between the calculated bond lengths and angles in the structure determined at room temperature. A comparison of bond lengths and angles between the calculated HF/6-31G(d) structure and the structure determined using x-ray diffraction techniques at room temperature of 2,4,6 trichlorophenyl azide are shown in tables 2.5 and 2.6

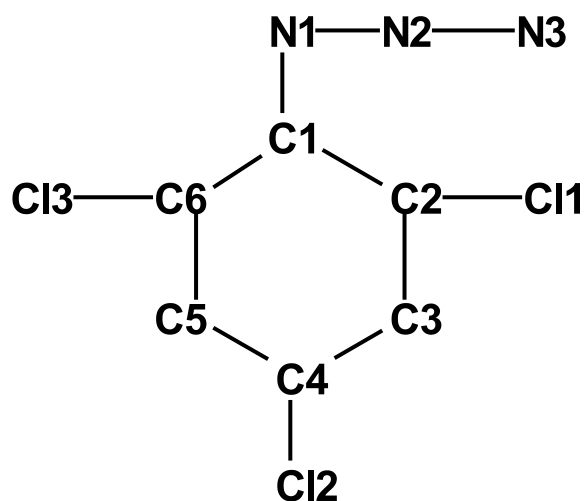


Table 2:5 Comparison of bond lengths (values given in Å) between the calculated PM3/VSTO-3G structure, HF/631G(d)structure, and the structure determined using x-ray diffraction techniques at room temperature of 2,4,6-trichlorophenyl azide

Bond	X-ray	PM3	HF/ 6-31G(d)
Cl (1) – C (2)	1.721 (6)	1.683	1.802
Cl (2) – C (4)	1.740 (7)	1.682	1.798
Cl (3) – C (6)	1.723 (7)	1.679	1.792
N (1) – N (2)	1.242 (8)	1.268	1.259
N (1) – C (1)	1.410 (9)	1.433	1.412
N (2) – N (3)	1.107 (8)	1.126	1.109
C (1) – C (6)	1.396 (9)	1.404	1.393
C(1) – C (2)	1.398 (10)	1.402	1.390
C (2) – C (3)	1.379 (9)	1.392	1.380
C (3) – C (4)	1.374 (9)	1.392	1.376
C (4) – C (5)	1.377 (10)	1.392	1.379
C (5) – C (6)	1.379 (9)	1.393	1.378

Table 2:6 Comparison of bond angles (°) between the calculated PM3/VSTO-3G structure, HF/6-31G(d) structure, and the X-ray structure determined at room temperature of 2,4,6-trichlorophenyl azide

Angle	X-ray	PM3	HF/ 6-31G(d)
N (2) – N (1) – C (1)	119.6 (6)	122.41	119.76
N (1) – N (2) – N (3)	169.7 (8)	168.87	168.20
C (6) – C (1) – C (2)	117.0 (6)	119.24	116.72
C (6) – C (1) – N (1)	116.0 (7)	116.43	117.10
C (2) – C (1) – N (1)	126.9 (6)	124.08	126.05
C (3) – C (2) – C (1)	122.1 (6)	120.53	122.36
C (3) – C (2) – Cl (1)	117.5 (5)	118.20	117.13
C (1) – C (2) – Cl (1)	120.4 (5)	121.27	120.48
C (2) – C (3) – C (4)	118.6 (6)	119.38	118.71
C (5) – C (4) – C (3)	121.6 (6)	121.02	121.15
C (5) – C (4) – Cl (2)	119.5 (5)	119.51	119.42
C (3) – C (4) – Cl (2)	118.8 (6)	119.47	119.43
C (4) – C (5) – C (6)	118.9 (6)	119.49	118.90
C (5) – C (6) – C (1)	121.7 (6)	120.33	122.14
C (5) – C (6) – Cl (3)	118.5 (5)	118.77	117.85
C (1) – C (6) – Cl (3)	119.7 (5)	120.90	120.00

The ^1H NMR spectrum shows one resonance at 7.30 ppm for the two ring hydrogens. The ^{13}C NMR spectrum shows four resonances at 133.0, 131.2, 129.9, and 128.9 ppm for the aromatic carbons. The ^{14}N NMR spectrum shows three resonances for the azide N_α ($\delta = -287$ ppm), N_β ($\delta = -144.7$ ppm) and N_γ ($\delta = -154.0$ ppm).

2.3 2,5,6-trichlorophenyl azide

The two halogen substituted phenyl azides previously described consisted of the halogen atoms in symmetrical positions *i.e.* 2,4,6 trisubstituted. Therefore the next halogen substituted phenyl azide to be prepared was 2,5,6-trichlorophenyl azide, in which the halogen atoms are in the non-symmetrical positions. 2,5,6-trichlorophenyl azide was prepared by the reaction of 2,5,6-trichloroaniline with sodium nitrite in a mixture of glacial acetic acid and sulphuric acid at 8°C to yield the diazonium salt. The diazonium salt was then reacted with sodium azide at 8°C to yield 2,5,6-trichlorophenyl azide.

The 2,5,6-trichlorophenyl azide was isolated as a brown solid and was then recrystallised from ethanol to give tan-coloured needles. The elemental analysis for the 2,5,6-trichlorophenyl azide was in agreement with the theoretical values, (found C, 32.3 ; H, 1.1 ; N, 18.5 % calculated C, 32.4 ; H, 0.9 ; N, 18.9 %). The IR spectrum showed a strong absorption at 2129 cm^{-1} for the asymmetric stretching vibration of the azide group and a strong absorption at 1293 cm^{-1} for the symmetric stretching vibration of the azide group. The I.R. spectrum also showed a weak absorption at 3077 cm^{-1} which is characteristic for C-H vibrations in an aromatic ring, a strong absorption at 1555 cm^{-1} for the asymmetric stretching vibration of the C-C bond in the aromatic ring, a peak at 1353 cm^{-1} for the symmetric stretching vibration of the C-C bond and a weak absorption at 622 cm^{-1} for the deformation of the carbon chlorine bond. The Raman spectrum of the tan coloured needles of 2,5,6-trichlorophenyl azide was not obtained as the compound fluoresced. The Raman spectrum of a saturated solution of 2,5,6-trichlorophenyl azide in acetone was obtained, however. the only peaks other than solvent peaks that were observed after 2000 scans were at 1304 cm^{-1} for the symmetric stretching vibration of the azide and 1581 cm^{-1} for the asymmetric stretching vibration of the C-C bond in the aromatic ring.

The ^1H NMR spectrum shows two resonances at 7.27 and 7.24 ppm for the two ring hydrogens. The ^{13}C NMR spectrum shows six resonances at 120.9 , 124.0 , 128.9, 131.6, 131.9 and 137.0 ppm for the aromatic carbons. The ^{14}N NMR spectrum shows three resonances for the azide N_α ($\delta = -286$ ppm), N_β ($\delta = -141.9$ ppm) and N_γ ($\delta = -153.0$ ppm).

2.4 2,4-dibromophenyl azide

2,4-dibromophenyl azide was prepared by the reaction of 2,4-dibromoaniline with sodium nitrite in a mixture of glacial acetic acid and sulphuric acid at 8°C to yield the diazonium salt. The diazonium salt was then reacted with sodium azide at 8°C to yield 2,4 - dibromophenyl azide.

2,4-dibromophenyl azide was isolated as a brown solid and was recrystallised from ethanol to give brown needlelike crystals. The elemental analysis for the 2,4-dibromophenyl azide was in agreement with the theoretical values, (found C, 25.8 ; H, 1.1 ; N, 15.1.% calculated C, 26.2 ; H, 1.1 ; N, 15.2 %). The IR spectrum showed two strong absorption at 2135 and 2103 cm^{-1} for the asymmetric stretching vibration of the azide group and a strong absorption at 1302 cm^{-1} for the symmetric stretching vibration of the azide group. The I.R. spectrum also showed a weak absorption at 3077 cm^{-1} which is characteristic for C-H vibrations in an aromatic ring, a strong absorption at 1573 cm^{-1} for the asymmetric stretching vibration of the C-C bond in the aromatic ring, a peak at 1380 cm^{-1} for the symmetric stretching vibration of the C-C bond and a weak absorption at 527 cm^{-1} for the deformation of the carbon bromine bond. The Raman spectra showed a peak at 2107 cm^{-1} for the asymmetric stretching vibration of the azide group, a strong peak at 1310 cm^{-1} for the symmetric stretching vibration of the azide. The Raman spectrum also showed a peak at 3054 cm^{-1} which is characteristic for C-H vibrations in an aromatic ring, a peak at 1572 cm^{-1} for the asymmetric stretching vibration of the C-C bond in the aromatic ring, a peak at 1382 cm^{-1} for the symmetric stretching vibration of the C-C bond.

The ^1H NMR spectrum shows three resonances at 7.60, 7.46 and 7.25 ppm for the three ring hydrogens. The ^{13}C NMR spectrum shows six resonances at 114.6 , 117.8 , 120.5, 131.6, 136.2 and 138.1 ppm for the aromatic carbons. The ^{14}N NMR spectrum shows three resonances for the azide N_α ($\delta = -280$ ppm), N_β ($\delta = -139.5$ ppm) and N_γ ($\delta = -143.8$ ppm).

2.5 2,4-dichlorophenyl azide

2,4-dichlorophenyl azide was prepared by the reaction of 2,4-dichloroaniline with sodium nitrite in a mixture of glacial acetic acid and sulphuric acid at 8°C to yield the diazonium salt. The diazonium salt was then reacted with sodium azide at 8°C to yield 2,4-dichlorophenyl azide

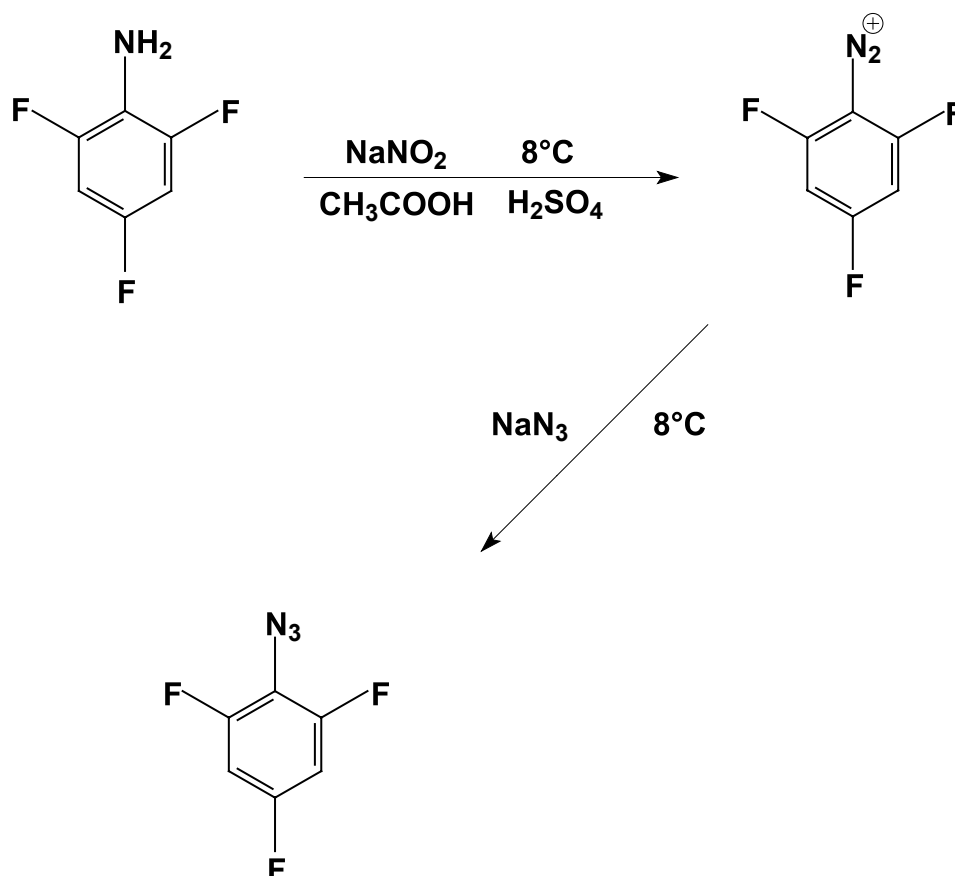
The 2,4-dichlorophenyl azide was isolated as a brown solid and recrystallised from ethanol to give very thin brown needles. The elemental analysis for the 2,4-dichlorophenyl azide was in agreement with the theoretical values, (found C, 38.1 ; H, 1.6 ; N, 22.4 %. calculated C, 38.3 ; H, 1.6 ; N, 22.4 %). The IR spectrum showed a strong absorption at 2119 cm⁻¹ for the asymmetric stretching vibration of the azide group and a strong absorption at 1306 cm⁻¹ for the symmetric stretching vibration of the azide group. The I.R. spectrum also showed a weak absorption at 3084 cm⁻¹ which is characteristic for C-H vibrations in an aromatic ring, a strong absorption at 1568 cm⁻¹ for the asymmetric stretching vibration of the C-C bond in the aromatic ring, a peak at 1388 cm⁻¹ for the symmetric stretching vibration of the C-C bond and a weak absorption at 596 for the deformation of the carbon chlorine bond. The Raman spectra showed a peak at 2121 cm⁻¹ for the asymmetric stretching vibration of the azide group, a strong peak at 1306 cm⁻¹ for the symmetric stretching vibration of the azide. The Raman spectrum also showed a peak at 3059 cm⁻¹ which is characteristic for C-H vibrations in an aromatic ring, a peak at 1581 cm⁻¹ for the asymmetric stretching vibration of the C-C bond in the aromatic ring and a peak at 1389 cm⁻¹ for the symmetric stretching vibration of the C-C bond.

The ¹H NMR spectrum shows three resonances at 7.59, 7.44 and 7.26 ppm for the three ring hydrogens. The ¹³C NMR spectrum shows six resonances at 120.4, 125.8, 128.1, 130.5, 130.6 and 136.1 ppm for the aromatic carbons. The ¹⁴N NMR spectrum shows three resonances for the azide N_α (δ = -278 ppm), N_β (δ = -139.5 ppm) and N_γ (δ = -144.9 ppm).

2.6 2,4,6-trifluorophenyl azide

The next 2,4,6 trisubstituted phenyl azide to be prepared was 2,4,6-trifluorophenyl azide which was prepared by the reaction of 2,4,6-trifluoroaniline with sodium nitrite in a mixture of glacial acetic acid and sulphuric acid at 8°C to yield the diazonium salt. The diazonium salt was then reacted with sodium azide, the solution was stirred at 8°C for one hour then poured on ice cold water. This solution was then extracted three times with chloroform. The organic

layer was then washed twice with water and 2M sodium carbonate, then dried over magnesium sulphate. The chloroform was slowly and carefully removed by distillation to yield 2,4,6-trifluorophenyl azide as red oil. Further purification of this red oil by fractional distillation was attempted but the compound decomposed on heating.



The IR spectrum showed a strong absorption at 2135 cm^{-1} for the asymmetric stretching vibration of the azide group and a strong absorption at 1309 cm^{-1} for the symmetric stretching vibration of the azide group. The IR spectrum also showed a weak absorption at 3086 cm^{-1} which is characteristic for C-H vibrations in an aromatic ring, a strong absorption at 1630 cm^{-1} for the asymmetric stretching vibration of the C-C bond in the aromatic ring, a peak at 1376 cm^{-1} for the symmetric stretching vibration of the C-C bond and a weak absorption at 576 cm^{-1} for the deformation of the carbon fluorine bond.

The Raman spectra showed a peak at 2136 cm^{-1} for the asymmetric stretching vibration of the azide group, a strong peak at 1310 cm^{-1} for the symmetric stretching vibration of the azide. The Raman spectrum also showed a peak at 3088 cm^{-1} which is characteristic for C-H

vibrations in an aromatic ring, a peak at 1636 cm^{-1} for the asymmetric stretching vibration of the C-C bond in the aromatic ring, a peak at 1374 cm^{-1} for the symmetric stretching vibration of the C-C bond and a medium peak at 576 cm^{-1} for the deformation of the carbon fluorine bond.

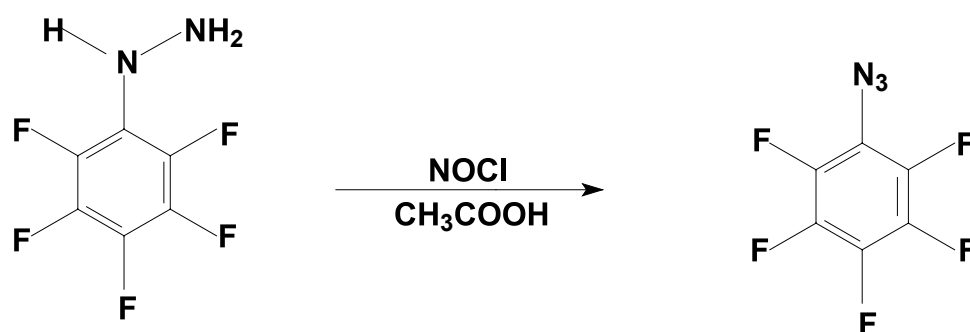
The ^1H NMR spectrum shows a resonance at 6.70 ppm for the two ring hydrogens. The ^{13}C NMR spectrum shows four resonances at 101.0 , 114.1 , 154.4 and 157.4 ppm for the aromatic carbons. The ^{14}N NMR spectrum shows three resonances for the azide N_α ($\delta = -268\text{ ppm}$), N_β ($\delta = -143.1\text{ ppm}$) and N_γ ($\delta = -153.3\text{ ppm}$). The ^{19}F -NMR shows a triplet at -112.6 ppm for the para fluorine and a multiplet at -120.3 ppm for the two ortho fluorines.

The structure of 2,4,6-trifluorophenyl azide was fully optimised and the vibrational frequencies and zero point energy computed using a semiempirical calculation carried out at the semiempirical PM3 level of theory using a VSTO-3G basis set and ab initio at the self consistent HF level of theory using a 6-31G(d) basis set. The fully optimised structure of 2,4,6-trifluorophenyl azide is shown in figure 2.6 below.

Figure 2.6 Molecular structure of 2,4,6-trifluorophenyl azide fully optimised at HF/6-31G(d) level of theory

2.7 2,3,4,5,6 pentafluorophenyl azide

2,3,4,5,6-pentafluorophenyl azide was prepared by passing a slow stream of nitrosyl chloride into a stirred solution of glacial acetic acid containing pentafluorophenyldiazine. The reaction began immediately and continued for about two hours, the solution gradually becoming deep red. The solution was left open to the atmosphere overnight and then heavily diluted with water. This solution was then extracted three times with dichloromethane. The organic layer was then washed twice with water and 2M sodium carbonate, then dried over magnesium sulphate. The dichloromethane was slowly and carefully removed by distillation to yield 2,3,4,5,6-pentafluorophenyl azide as red liquid as shown in the scheme below. Further purification by fractional distillation was attempted on this red liquid but the compound decomposed on heating.



The IR spectrum showed a strong absorption at 2130 cm^{-1} for the asymmetric stretching vibration of the azide group and a strong absorption at 1324 cm^{-1} for the symmetric stretching vibration of the azide group. The IR spectrum also showed a medium absorption at 1650 cm^{-1} for the asymmetric stretching vibration of the C-C bond in the aromatic ring.

The Raman spectra showed a peak at 2127 cm^{-1} for the asymmetric stretching vibration of the azide group, a strong peak at 1328 cm^{-1} for the symmetric stretching vibration of the azide. The Raman spectrum also showed a peak at 1655 cm^{-1} for the asymmetric stretching vibration of the C-C bond in the aromatic ring, a peak at 1468 cm^{-1} for the symmetric stretching vibration of the C-C bond and a medium peak at 586 cm^{-1} for the deformation of the carbon fluorine bond.

The ^{14}N NMR spectrum shows three resonances for the azide N_α ($\delta = -295\text{ ppm}$), N_β ($\delta = -145.0\text{ ppm}$) and N_γ ($\delta = -149.5\text{ ppm}$). The ^{19}F NMR shows a triplet at -160.4 ppm for the

para fluorine, a multiplet at -152.1 ppm for the two ortho fluorines, and a multiplet at -162.6 ppm for the two para fluorines.

The structure of 2,3,4,5,6-pentafluorophenyl azide was fully optimised and the vibrational frequencies and zero point energy computed using a semiempirical calculation carried out at the semiempirical PM3 level of theory using a VSTO-3G basis set and ab initio at the self consistent HF level of theory using a 6-31G(d) basis set. The fully optimised structure of 2,3,4,5,6-pentafluorophenyl azide is shown in figure 2.7 below.

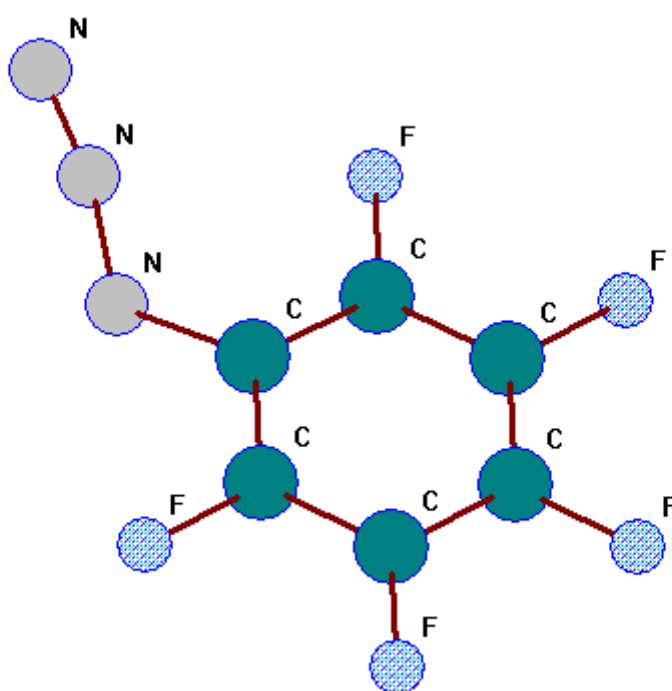


Figure 2.7 Molecular structure of 2,3,4,5,6-pentafluorophenyl azide fully optimised at HF/6-31G(d) level of theory

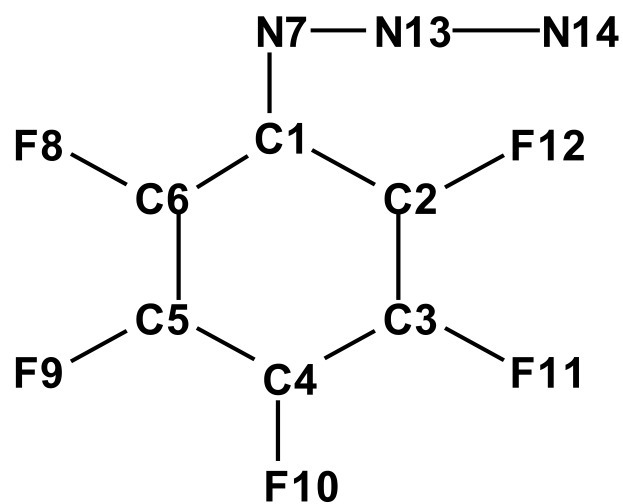


Table 2.7 Calculated HF/6-31G(d) Bond Lengths (Å) for
2,3,4,5,6-pentafluorophenyl azide

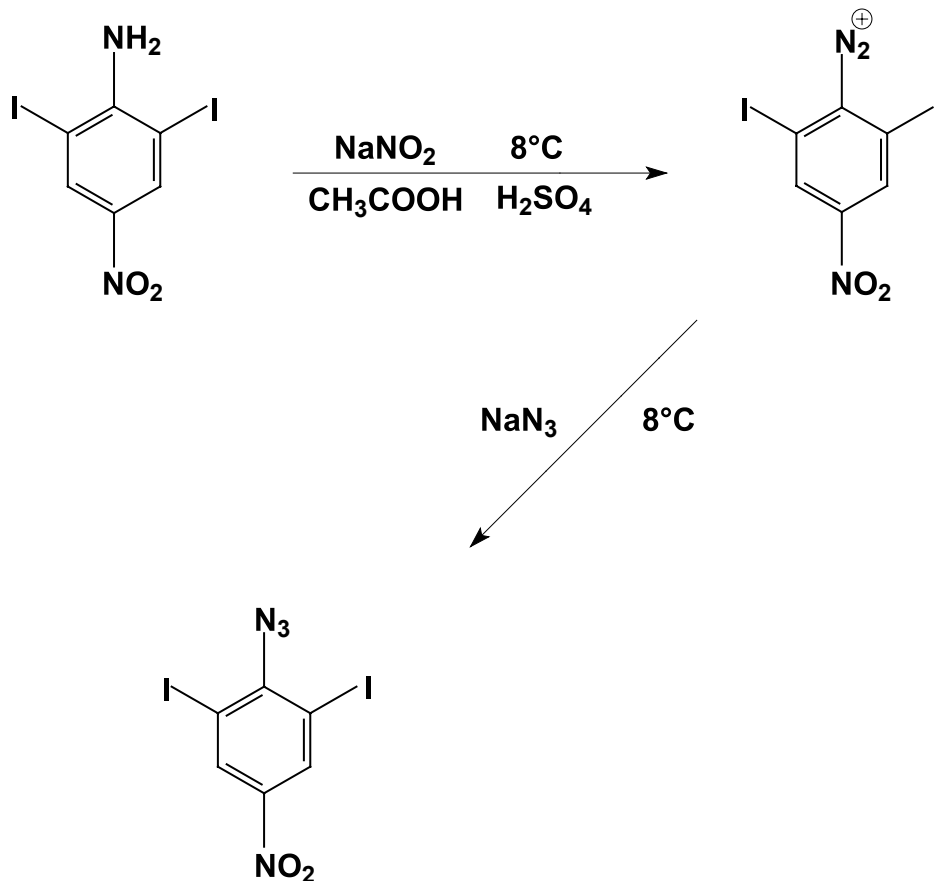
C (1) – C (6)	1.415	C (1) – C (2)	1.409
C (2) – C (3)	1.409	C (3) – C (4)	1.405
C (4) – C (5)	1.409	C (5) – C (6)	1.408
C (6) – F (8)	1.336	C (2) – F (12)	1.341
C (3) – F (11)	1.335	C (4) – F (10)	1.335
C (5) – F (9)	1.335	C (1) – N (7)	1.420
N (7) – N (13)	1.275	N (13) – N (14)	1.123

Table 2:8 Calculated HF/6-31G(d) Bond Angles (°) for
2,3,4,5,6-pentafluorophenyl azide

N (7) – N (13) – N (14)	168.0	N (13) – N (7) – C (1)	124.4
N (7) – C (1) – C (2)	126.0	C (1) – C (2) – F (12)	120.5
C (1) – C (2) – C (3)	120.9	C (2) – C (3) – F (11)	119.8
F (11) – C (3) – C (4)	120.0	C (3) – C (4) – F (10)	120.2
F (10) – C (4) – C (5)	120.2	C (4) – C (5) – F (9)	119.6
F (9) – C (5) – C (6)	120.0	C (5) – C (6) – F (8)	118.3
F (8) – C (6) – C (1)	121.2	C (6) – C (1) – N (7)	115.3

2.8 2,6-diiodo-4-nitrophenyl azide

In order to complete the series tri-halogen substituted phenyl azides several attempts were made to prepare tri-iodophenyl azide but these were not successful so in order to have a iodo substitute phenyl azide 2,6-diiodo-4-nitrophenyl azide was prepared. 2,6-diiodo-4-nitrophenyl azide was prepared by the reaction 2,6-diiodo-4 nitroaniline with sodium nitrite in a mixture of glacial acetic acid and sulphuric acid at 8°C to yield the diazonium salt. The diazonium salt was then reacted with sodium azide at 8°C to yield 2,6-diiodo-4-nitrophenyl azide



The 2,6,-diiodo-4-nitrophenyl azide was isolated as a brown solid and was then recrystallised from ethanol to give green needles. The elemental analysis for the 2,6-diiodo-4-nitrophenyl azide was in agreement with the theoretical values, (found C, 17.2 ; H, 0.5 ; N, 13.2.% calculated C, 17.3 ; H, 0.5 ; N, 13.5 %.) The IR spectrum showed a strong absorption at 2134 cm^{-1} for the asymmetric stretching vibration of the azide group, a strong absorption at 1310 cm^{-1} for the symmetric stretching vibration of the azide and an absorption at 703 cm^{-1} for the deformation of the azide group. The I.R. spectrum also showed two weak absorptions at 3084 and 3062 cm^{-1} which are characteristic for C-H vibrations in an aromatic ring, a strong absorption at 1572 cm^{-1} for the asymmetric stretching vibration of the C-C bond in the aromatic ring, a strong absorption at 1512 cm^{-1} for the asymmetric stretching vibration of the NO_2 group and a strong absorption at 1339 cm^{-1} for the symmetric stretching vibration of the NO_2 group. The Raman spectra showed a peak at 2117 cm^{-1} for the asymmetric stretching vibration of the azide group, a strong peak at 1318 cm^{-1} for the symmetric stretching vibration of the azide. The Raman spectrum also showed a peak at 3064 cm^{-1} which is characteristic for C-H vibrations in an aromatic ring, a peak at 1558 cm^{-1} for the asymmetric stretching vibration of the C-C bond in the aromatic ring, a peak at 1514 cm^{-1} for the

asymmetric stretching vibration of the NO₂ group and a strong peak at 1335 cm⁻¹ for the symmetric stretching vibration of the NO₂ group. The ab initio calculation of the vibrational frequencies for 2,6-diiodo-4-nitrophenyl azide was carried out at the self consistent HF level of theory using a 6-31G(d) basis set. There is a very good agreement between the calculated frequencies and the observed IR and Raman frequencies. The calculated and observed IR and Raman frequencies are shown in Table 2.9 .

Table 2.9 Comparisons between the calculated HF/6-31G(d) and the experimental vibrational frequencies for 2,6-diiodo-4-nitrophenyl azide

Assignment	Calculated Frequencies HF/6-31G(d) (cm ⁻¹)	Observed IR Frequencies (cm ⁻¹)	Observed Raman Frequencies (cm ⁻¹)
v (CH)	3055	3062	3064
v _{as} (NNN)	2397*	2134	2117
v (CC)	1568	1572	1558
v _{as} (NO ₂)	1513	1514	1512
v _{sym} (NO ₂)	1346	1339	1343
v _{sym} (NNN)	1323	1310	1318

* see footnote at the end of this chapter

The structure of 2,6-diiodo-4-nitrophenyl azide was fully optimised and the vibrational frequencies and zero point energy computed using a semiempirical calculation carried out at the semiempirical PM3 level of theory using a VSTO-3G basis set and ab initio at the self consistent HF level of theory using a 6-31G(d) basis set for hydrogen, carbon, nitrogen and oxygen and a quasirelativistic Stuttgart/Dresden (SDD) pseudopotential for the core electrons of iodine with a Dunning/Huzinaga D95-type valence basis set [34]. The fully optimised structure of 2,6-diiodo-4-nitrophenyl azide is shown in figure 2.8 below.

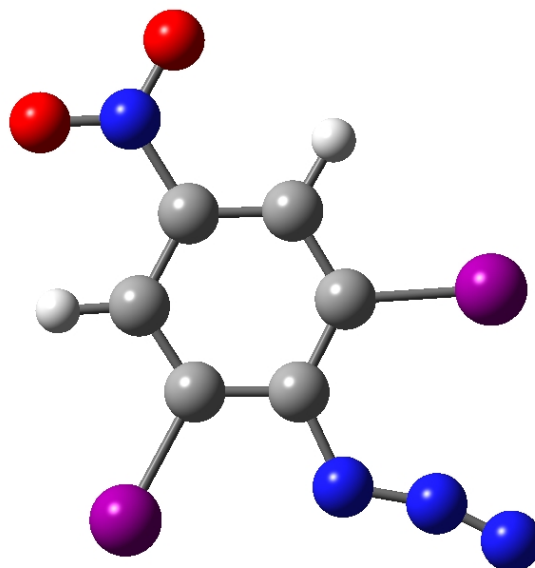


Figure 2.8 Molecular structure of 2,6-diiodo-4-nitrophenyl azide fully optimised at HF/6-31G(d) level of theory

The ^1H NMR spectrum shows one resonance at 8.64 ppm for the two ring hydrogens. The ^{13}C NMR spectrum shows four resonances at 89.9, 135.1, 145.1 and 147.5 ppm for the aromatic carbons. The ^{14}N NMR spectrum shows four resonances, one for the nitro group ($\delta = -18.7$ ppm) and three resonances for the azide N_α ($\delta = -272$ ppm), N_β ($\delta = -148.2$ ppm) and N_γ ($\delta = -151.2$ ppm).

The 2,6-diiodo-4-nitrophenyl azide was isolated as a brown solid and was then recrystallised from ethanol to give green needles which were used for x-ray structure determination.

A crystal (0.40 x 0.30 x 0.20 mm) of 2,6-diiodo-4-nitrophenyl azide was mounted on the Enraf-Nonius CAD4 diffractometer with Mo-K α radiation and cooled to 100°K using an Oxford Cryosystems cooling unit. The cell dimensions were derived from the least-squares analysis of the 25 independent reflections. Intensities of 5472 reflections were surveyed in

the range θ 2.43-26.28 and 3957 independent reflections satisfied the criterion $I \geq 2 \sigma(I)$. Three reference reflections monitored periodically showed a decline of 7 % over the period of collection.

The crystal structure was elucidated by the direct phasing program XCAD4 [58]. After preliminary least-squares adjustments of the co-ordinates and anisotropic thermal parameters of the C, N, O and I atoms, the H atoms were located in difference Fourier synthesis and subsequently included in the least-squares calculations with isotropic thermal parameters using SHELX [59]. The refinement converged at $R = 0.0337$, $R_w = 0.0726$. The crystals are monoclinic, with space group P21/c and cell dimensions $a = 8.4469(14)$, $b = 16.318(2)$, $c = 14.359(2)$, $\beta = 97.315(4)$.

There are two independent molecules in the asymmetric unit, one molecule has an ordered azide group and the other molecule has a disordered azide group. These two independent molecules are shown in the following three figures 2.9, 2.10 and 2.11

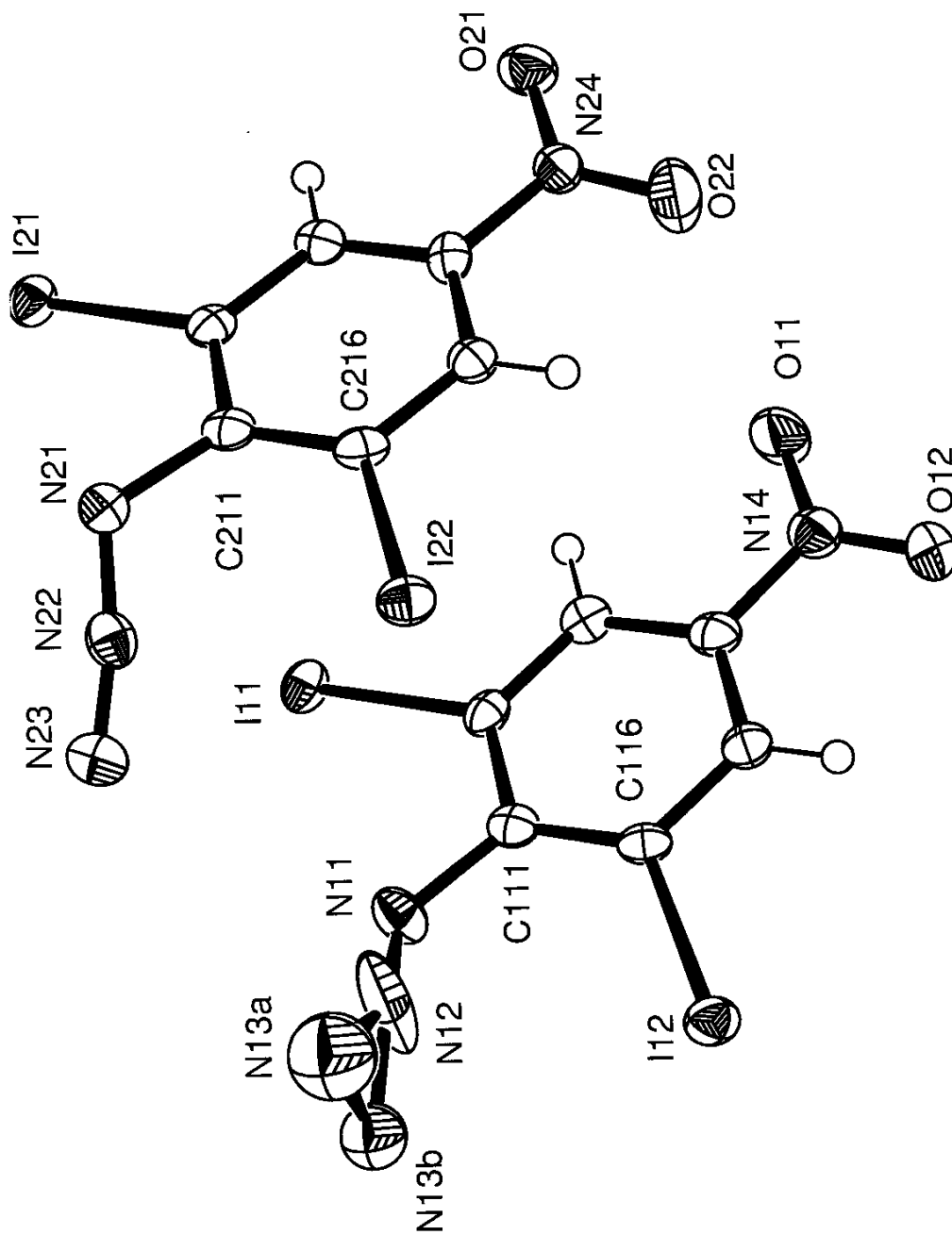


Figure 2.9

ORTEP drawing of the two independent molecules of 2,6-diiodo-4-nitrophenyl azide with the thermal ellipsoids of the C, N, O and I atoms drawn at 50 % probability level and H atoms are represented by spheres of radius 0.1 Å.

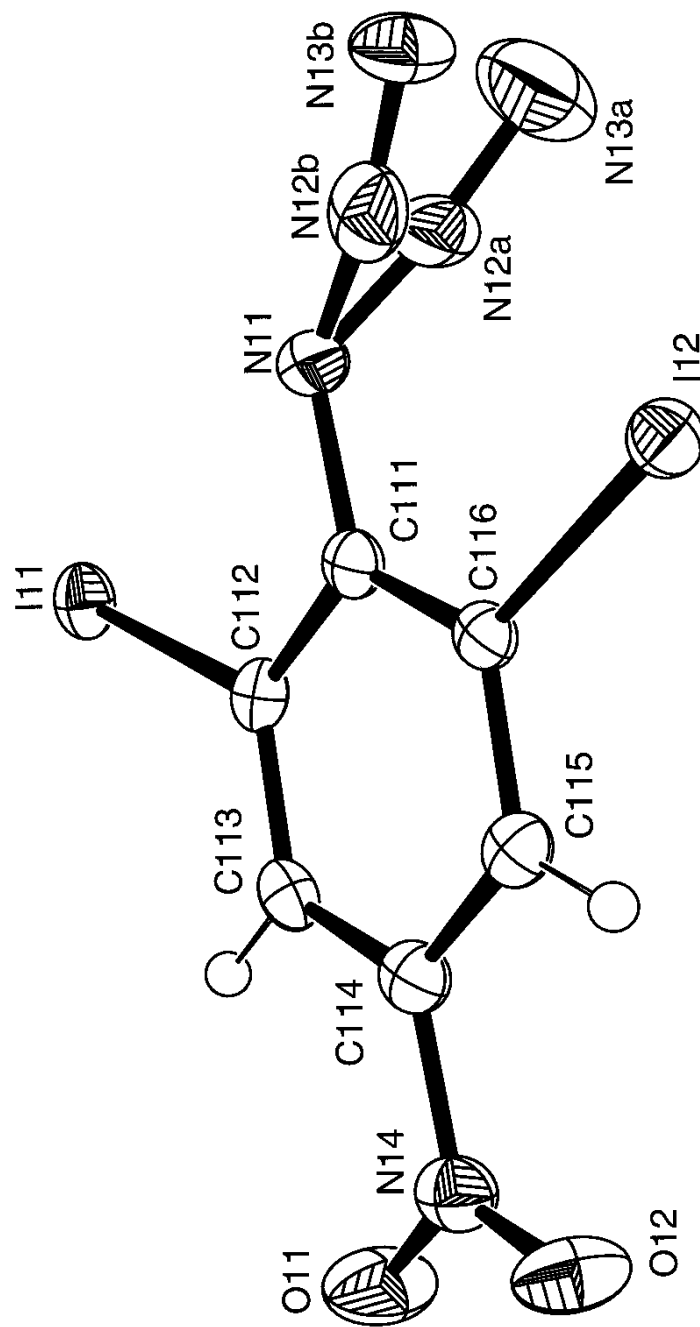


Figure 2.10 ORTEP drawing of the molecule of 2,6-diiodo-4-nitrophenyl azide with the disordered azide group with the thermal ellipsoids of the C, N, O and I atoms drawn at 50 % probability level and the H atoms are represented by spheres of radius 0.1 Å.

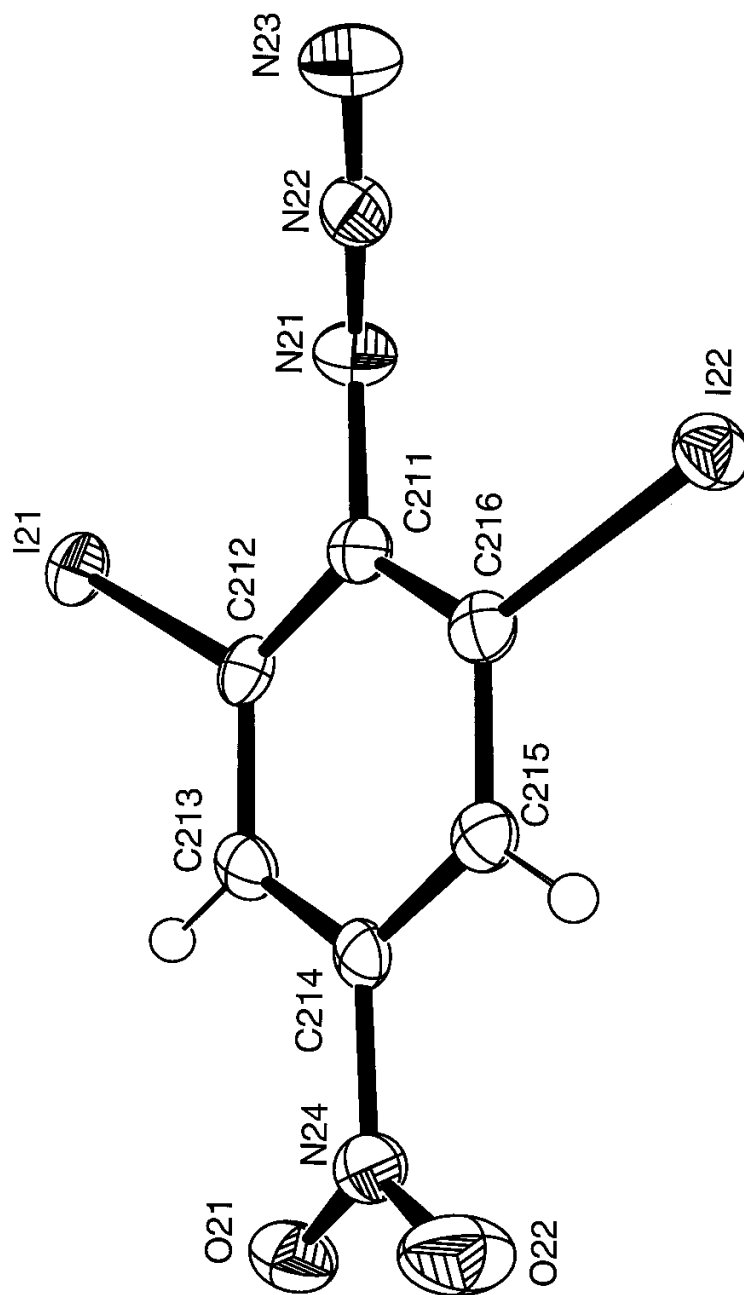


Figure 2.11

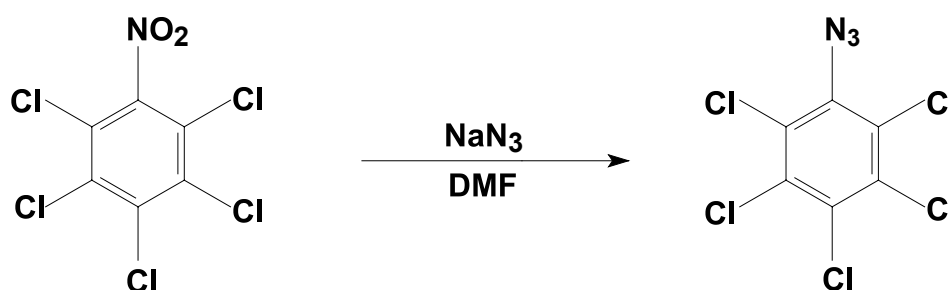
ORTEP drawing of the molecule of 2,6-diiodo-4-nitrophenyl azide with the ordered azide group with the thermal ellipsoids of the C, N, O and I atoms drawn at 50 % probability level and the H atoms are represented by spheres of radius 0.1 Å.

In the molecule with the ordered azide group the bond length between the terminal nitrogen and the central nitrogen is 1.126 Å and the bond length between the central nitrogen and the nitrogen attached directly to the ring is 1.249 Å. The azide group is not linear, with the angle at the central nitrogen atom being 170.0°. The ring carbon – carbon bond lengths are 1.369 Å. The nitrogen – oxygen bond lengths the nitro group are 1.211 – 1.233 Å The carbon – iodine bonds are 2.080 and 2.096 Å. The angle at the nitrogen of the azide that is attached directly to the ring is 119.8° which is close to the expected value of 120°. In the molecule with the disordered azide group the bond lengths between the terminal nitrogens and the central nitrogen is 1.255 and 1.287 Å and the bond length between the central nitrogen and the nitrogen attached directly to the ring is 1.149 Å. The ring carbon – carbon bond lengths are 1.369 Å. The nitrogen – oxygen bond lengths the nitro group are 1.217 – 1.227 Å The carbon – iodine bonds are 2.081 and 2.096 Å. The angle at at the nitrogen of the azide that is attached directly to the ring is 125.4 ° which is greater than the expected value of 120°. There is a most unusual intermolecular contact of 3.041 Å between O(11) and I(22) and between O(21) and I(12). This distance is well below the sum of the van der Waals radii of both atoms. This interaction is shown in figure 2.12

Figure 2.12 ORTEP drawing of 2,6-diiodo-4-nitrophenyl azide with the thermal ellipsoids of the C, N and O atoms drawn at 25 % probability showing the intermolecular contact of 3.041 Å between O(11) and I(22) and between O(21) and I(12).

2.9 2,3,4,5,6-pentachlorophenyl azide

In an attempt to replace the chlorine atoms in pentachloronitrobenzene with azide groups, pentachloronitrobenzene was reacted with sodium azide in dimethylformamide for 4 hours. After slowly evaporation of the solvent, small colourless crystals remained in the reaction vessel. The x-ray structural analysis of these crystals showed that the crystals were 2,3,4,5,6-pentachlorophenyl azide and not any of the desired azidonitrobenzene products. The reaction of sodium azide and pentachloronitrobenzene in dimethylformamide is shown in the scheme below.



The structure of 2,3,4,5,6-pentachlorophenyl azide was fully optimised and the vibrational frequencies and zero point energy computed using a semiempirical calculation carried out at the semiempirical PM3 level of theory using a VSTO-3G basis set and ab initio at the self consistent HF level of theory using a 6-31G(d) basis set. The fully optimised structure of 2,3,4,5,6-pentachlorophenyl azide is shown in the figure 2:13

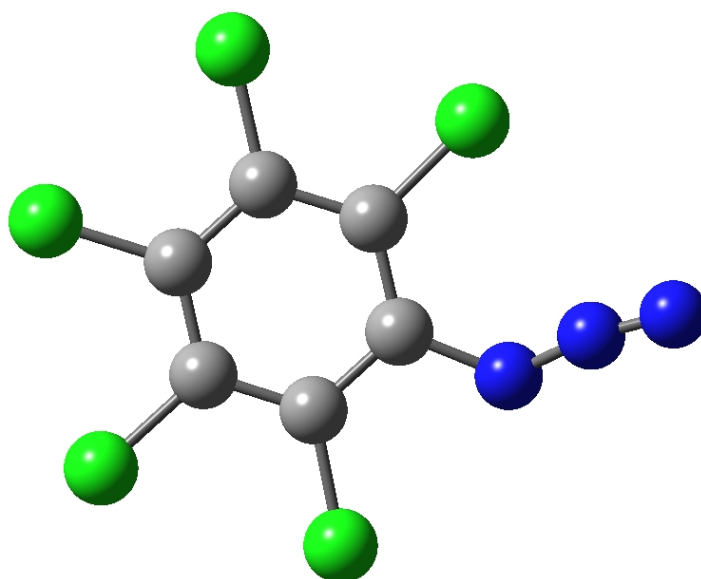


Figure 2:13 Molecular structure of 2,3,4,5,6-pentachlorophenyl azide fully optimised at HF/6-31G(d) level of theory

A crystal (0.37 x 0.07 x 0.05 mm) of 2,3,4,5,6-pentachlorophenyl azide was mounted on STOE image-plate area-detector with Mo-K α radiation at 200 K for crystal structure analysis. The cell dimensions were derived from the least-squares analysis of the 25 independent reflections. Intensities of 1200 reflections were surveyed in the range θ 2.51- 22.30 and 1029 independent reflections satisfied the criterion $I \geq 2$ sigma (I). The crystal structure was elucidated by direct phasing using SIR97 [60]. Full matrix least-squares calculations on F with anisotropic thermal parameters for C, N, and Cl atoms using SHELXL [51]. Least-squares convergence at $R = 0.0859$, $R_w = 0.2057$. The crystals are monoclinic, with space group C2/c and cell dimensions, $a = 34.293(3)$, $b = 3.7641(2)$, $c = 16.27(1)$, $\beta = 113.078(9)$.

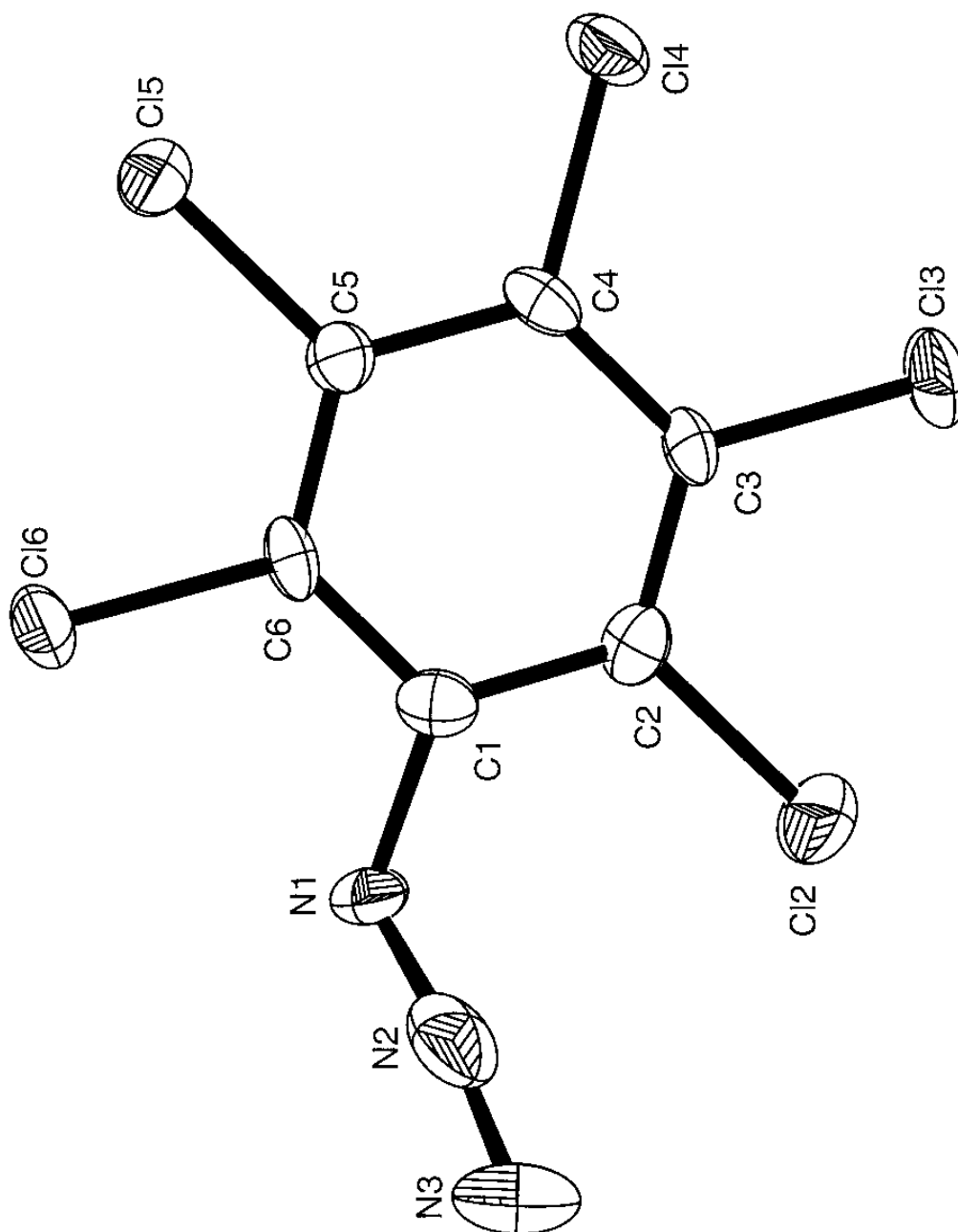


Figure 2:14 ORTEP drawing of 2,3,4,5,6-pentachlorophenyl azide with the thermal ellipsoids of the C, N and Cl atoms drawn at 50 % probability level

In 2,3,4,5,6-pentachlorophenyl azide the bond length between the terminal nitrogen and the central nitrogen is 1.172 Å and the bond length between the central nitrogen and the nitrogen attached directly to the ring is 1.233 Å. The azide group is not linear, as the angle at the central

nitrogen atom is 171.4°. The angle at the nitrogen of the azide that is attached directly to the ring is 117.4° which is slightly less than the expected value of 120°.

There is a very good agreement between the calculated bond lengths and angles and the bond length angles in the structure determined at room temperature. The comparison of bond lengths and angles between the calculated HF/6-31G(d) structure and the X-ray structure determined at room temperature of 2,3,4,5,6-pentachlorophenyl azide are shown in tables 2.10 and 2.11

Table 2.10 Comparison of bond lengths (Å) between the calculated PM3/VSTO-3G structure, HF/6-31G(d) structure, and the X-ray structure determined at 200 K of 2,3,4,5,6-pentachlorophenyl azide

Bond	X-ray	PM3	HF/631G(d)
C (1) – C (6)	1.382 (8)	1.406	1.392
C (1) – C (2)	1.397 (8)	1.402	1.389
C (1) – N (1)	1.421 (8)	1.429	1.412
C (2) – C (3)	1.384 (8)	1.397	1.383
C (2) – Cl (2)	1.729 (6)	1.682	1.790
C (3) – C (4)	1.385 (8)	1.394	1.382
C (3) – Cl (3)	1.713 (5)	1.674	1.783
C (4) – C (5)	1.401 (8)	1.396	1.386
C (4) – Cl (4)	1.721 (6)	1.673	1.783
C (5) – C (6)	1.387 (8)	1.396	1.380
C (5) – Cl (5)	1.714 (5)	1.673	1.782
C (6) – Cl (6)	1.718 (5)	1.673	1.782
N (1) – N (2)	1.233 (9)	1.270	1.261
N (2) – N (3)	1.172 (9)	1.126	1.108

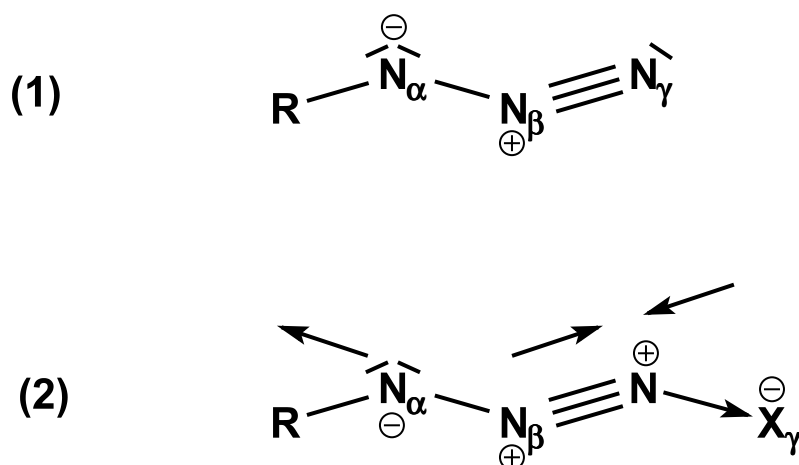
Table 2:11 Comparison of angles ($^{\circ}$) between the calculated PM3/VSTO-3G structure, HF/6-31G(d) structure, and the X-ray structure determined at 200 K of 2,3,4,5,6-pentachlorophenyl azide

Angle ($^{\circ}$)	X-ray	PM3	HF/6-31G(d)
C (6) – C (1) – C (2)	118.2 (5)	119.63	118.26
C (6) – C (1) – N (1)	116.0 (5)	115.31	116.65
C (2) – C (1) – N (1)	125.5 (5)	124.90	124.93
C (3) – C (2) – C (1)	121.5 (5)	120.01	121.13
C (3) – C (2) – Cl (2)	119.2 (4)	118.16	119.95
C (1) – C (2) – Cl (2)	119.3 (4)	121.82	118.90
C (4) – C (3) – C (2)	119.5 (5)	120.30	119.89
C (4) – C (3) – Cl (3)	120.2 (4)	119.82	120.10
C (2) – C (3) – Cl (3)	120.3 (4)	119.88	120.00
C (3) – C (4) – C (5)	119.9 (5)	119.82	119.74
C (3) – C (4) – Cl (4)	119.9 (4)	120.09	120.12
C (5) – C (4) – Cl (4)	120.1 (4)	120.08	120.14
C (6) – C (5) – C (4)	119.4 (5)	120.36	120.10
C (6) – C (5) – Cl (5)	120.8 (4)	119.90	119.90
C (4) – C (5) – Cl (5)	119.8 (4)	119.73	119.91
C (1) – C (6) – C (5)	121.4 (5)	119.86	120.87
C (1) – C (6) – Cl (6)	119.2 (4)	121.16	118.57
C (5) – C (6) – Cl (6)	119.4 (4)	118.99	120.56
N (2) – N (1) – C (1)	117.4 (5)	123.35	119.46
N (3) – N (2) – N (1)	171.4 (7)	168.47	168.13

Footnote

Generally the agreement between calculated and experimentally observed (IR, Raman) frequencies is very good at HF/6-31G(d) level of theory so that no scaling of the computed frequencies was necessary. The fact that the asymmetric azide vibration is calculated too high for 2,4,6-tribromophenyl azide, 2,4,6-trichlorophenyl azide and 2,6-diiodo-4-nitrophenyl azide may or may not be explained by strong intermolecular interactions via the N_3 group in these compounds as revealed by X-ray diffraction (see figures 2:3 and 2:12) which due to the increased (formal) charges on N_β and N_γ weaken the terminal nitrogen-nitrogen triple bond.

- (1) no intermolecular interaction
- (2) with intermolecular interaction



(the arrows indicate the asymmetric N_3 azide stretch)

3 Nitro compounds

During the last 10 years, significant advances have been made in the area of covalently bound azides, as indicated by the number of recent reviews covering various aspects of the subject [61, 62]. Recently, the convenient preparation of N_2O_5 and other nitrating agents was reported as well as the nitration of covalent non-metal compounds [63-66].

Since toxic lead azide is still widely used as the initiator in ammunition, [67] there is a great demand to find suitable non-toxic, heavy metal free substitutes which can be used as primary detonators [21]. Equally important, most solid-rocket fuels are still based on mixtures of ammonium perchlorate, aluminum and epoxy resins. Which therefore generate exhaust plumes which contain large amounts of HCl and aluminium oxides [67]. The presence of these compounds is both environmentally not desirable and the trace of such rockets can easily be detected by radar [21].

The goal of our work is to find new, metal and halogen free high energy density materials which can be used either as initiators or solid rocket propellants. In the search for such new compounds we started to combine azide and nitro groups in covalent molecules in order to provide both a fuel and oxidiser in one compound. These compounds are metal free and combust ideally to give only gaseous products (*e.g.* CO_2 and N_2).

The first compound prepared was *o*-nitrophenyl azide which was prepared by the reaction of *o*-nitroaniline with sodium nitrite at $0^\circ C$ to yield the diazonium salt which was then reacted with sodium azide at $0^\circ C$ to yield *o*-nitrophenyl azide as shown in scheme below .

The *o*-nitrophenyl azide was isolated as a light cream solid and was then recrystallised from aqueous ethanol (20% water, 80% ethanol) to yield cream coloured needles, with a melting point of 129-130°C. The elemental analysis for the *o*-nitrophenyl azide was in agreement with the theoretical values, (found C, 43.1; H, 2.5; N, 33.6 % calculated C, 43.9; H, 2.5; N, 34.1 %). The IR spectrum showed a strong absorption at 2124 cm⁻¹ for the asymmetric stretching vibration of the azide group, a strong absorption at 1295 cm⁻¹ for the symmetric stretching vibration of the azide and an absorption at 704 cm⁻¹ for the deformation of the azide group. The I.R. spectrum also showed two weak absorptions at 3106 and 3037 cm⁻¹ which are characteristic for C-H vibrations in an aromatic ring, a strong absorption at 1605 cm⁻¹ for the asymmetric stretching vibration of the C-C bond in the aromatic ring, a strong absorption at 1525 cm⁻¹ for the asymmetric stretching vibration of the NO₂ group and a strong absorption at 1354 cm⁻¹ for the symmetric stretching vibration of the NO₂ group. The Raman spectra showed a peak at 2119 cm⁻¹ for the asymmetric stretching vibration of the azide group, a strong peak at 1292 cm⁻¹ for the symmetric stretching vibration of the azide. The Raman spectrum also showed a peak at 3088 cm⁻¹ which is characteristic for C-H vibrations in an aromatic ring, a peak at 1582 cm⁻¹ for the asymmetric stretching vibration of the C-C bond in the aromatic ring, a peak at 1517 cm⁻¹ for the asymmetric stretching vibration of the NO₂ group and a strong peak at 1353 cm⁻¹ for the symmetric stretching vibration of the NO₂ group.

The ¹H NMR spectrum shows four resonances at 7.93, 7.61, 7.33 and 7.33 ppm. The ¹³C NMR spectrum shows six resonances at 140.89, 134.78, 133.95, 126.07, 124.88, and 120.68 ppm for the six aromatic carbons. The ¹⁴N NMR spectrum shows four resonances, one for the NO₂ group (δ = -12.0 ppm) and three for the azide N_α (δ = -285 ppm), N_β (δ = -140 ppm) and N_γ (δ = -146.0 ppm). The ¹⁴N NMR spectrum of *o*-nitrophenyl azide is shown in figure 3.1.

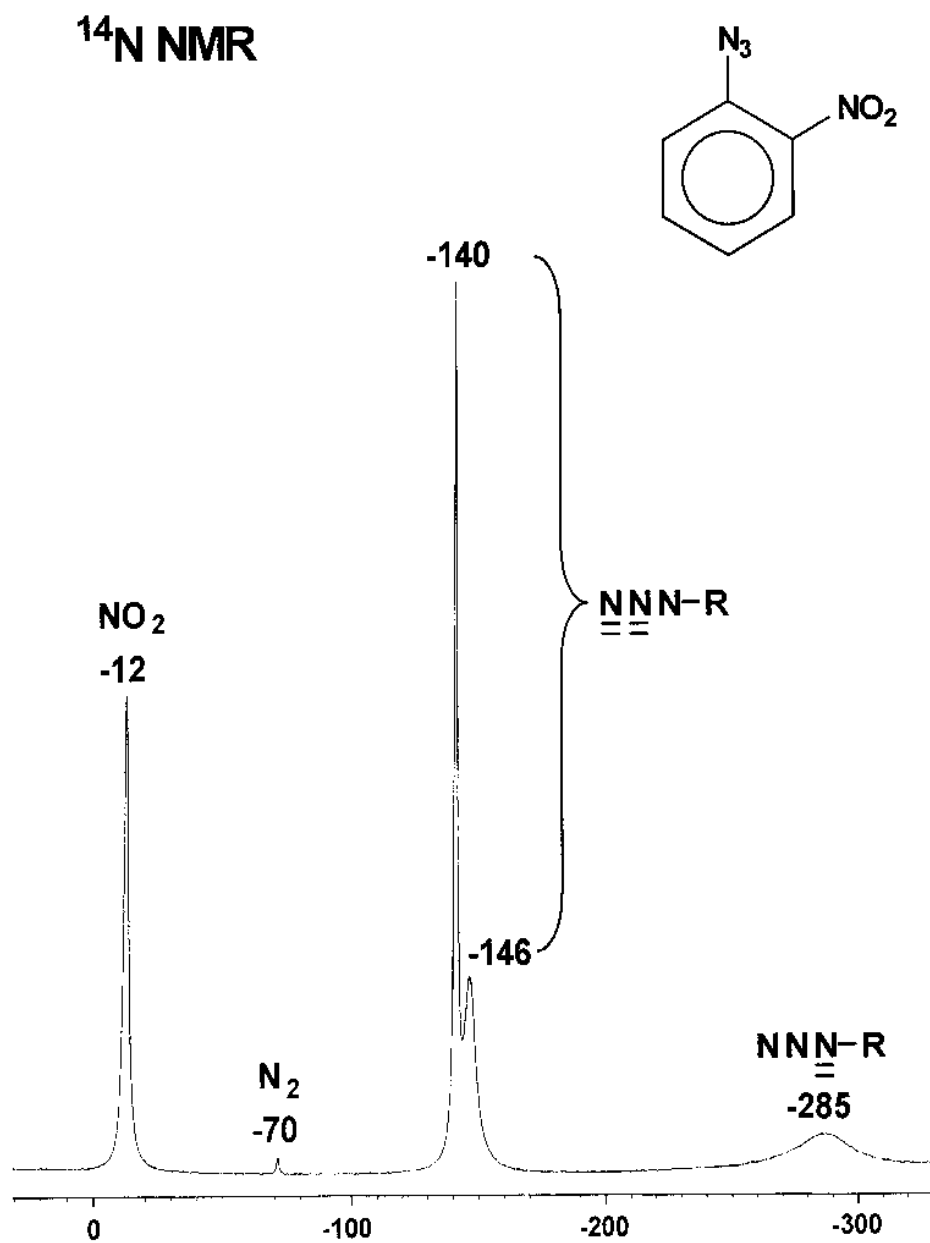
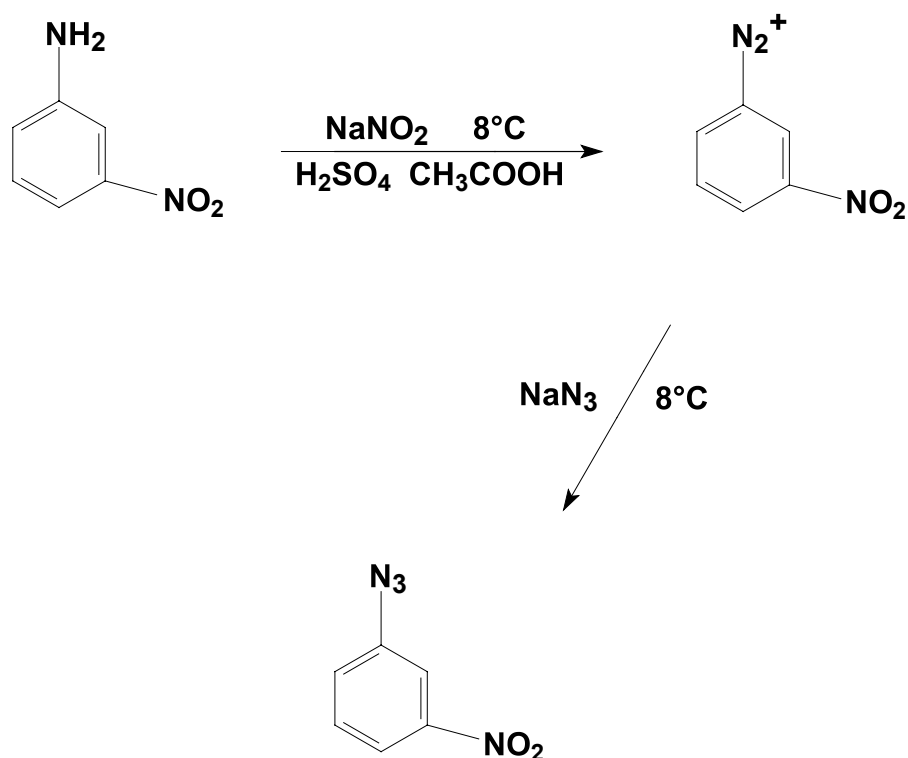


Figure 3.1 ^{14}N NMR (CDCl_3) spectrum of *o*-nitrophenyl azide

The next compound to be prepared was *m*-nitrophenyl azide which was prepared by the reaction of *m*-nitroaniline with sodium nitrite in a mixture of glacial acetic acid and sulphuric acid at 8°C to yield the diazonium salt. The diazonium salt was then reacted with sodium azide at 8°C to yield *m*-nitrophenyl azide as shown in the scheme below.



The *m*-nitrophenyl azide was isolated as a yellow solid and was then recrystallised from methanol to give thin yellow needles. The elemental analysis for the *m*-nitrophenyl azide was in agreement with the theoretical values, (found C, 43.8 ; H, 2.4 ; N, 34.1 % calculated C, 43.9 ; H, 2.5 ; N, 34.1 %). The IR spectrum showed a strong absorption at 2128 cm⁻¹ for the asymmetric stretching vibration of the azide group, a strong absorption at 1302cm⁻¹ for the symmetric stretching vibration of the azide and an absorption at 712 cm⁻¹ for the deformation of the azide group. The IR spectrum also showed two weak absorptions at 3106 and 3077 cm⁻¹ which are characteristic for C-H vibrations in an aromatic ring, a strong absorption at 1586 cm⁻¹ for the asymmetric stretching vibration of the C-C bond in the aromatic ring, a strong absorption at 1531 cm⁻¹ for the asymmetric stretching vibration of the NO₂ group and a strong absorption at 1353 cm⁻¹ for the symmetric stretching vibration of the NO₂ group. The Raman spectra showed a peak at 2131 cm⁻¹ for the asymmetric stretching vibration of the azide group, a strong peak at 1303 cm⁻¹ for the symmetric stretching vibration of the azide. The

Raman spectrum also showed a peak at 3084 cm^{-1} which is characteristic for C-H vibrations in an aromatic ring, a peak at 1582 cm^{-1} for the asymmetric stretching vibration of the C-C bond in the aromatic ring, a peak at 1530 cm^{-1} for the asymmetric stretching vibration of the NO_2 group and a strong peak at 1351 cm^{-1} for the symmetric stretching vibration of the NO_2 group. The ab initio calculation of the vibrational frequencies for *m*-nitrophenyl azide was carried out at the self consistent HF level of theory using a 6-31G(d) basis set. There is a very good agreement between the calculated frequencies and the observed IR and Raman frequencies. The calculated and observed IR and Raman frequencies are shown in Table 3.1.

Table 3.1 Comparison between the calculated and the experimental observed vibrational frequencies for *m*-nitrophenyl azide

Assignment	Calculated Frequencies HF/6-31G(d) (cm^{-1})	Observed Infra-Red Frequencies (cm^{-1})	Observed Raman Frequencies (cm^{-1})
ν_{CH} (Ar)	3066	3077	3081
$\nu_{\text{as}}\text{N}_3$	2135	2128	2137
ν_{as} CC(Ar)	1584	1586	1582
ν_{as} NO_2	1535	1531	1530
$\nu_{\text{s}}\text{N}_3$	1307	1302	1304

The ^1H NMR spectrum shows four resonances at 7.91, 7.60, 7.34 and 7.23 ppm. The ^{13}C NMR spectrum shows six resonances at 120.8, 124.0, 128.9, 131.6, 131.9, and 136.9 ppm. for the six aromatic carbons. The ^{14}N NMR spectrum shows four resonances, one for the NO_2 group ($\delta = -12.3$ ppm) and three for the azide N_α ($\delta = -287$ ppm), N_β ($\delta = -140.5$ ppm) and N_γ ($\delta = -146.0$ ppm). The ^{14}N NMR spectrum of *m*-nitrophenyl azide is shown in figure 3.2.

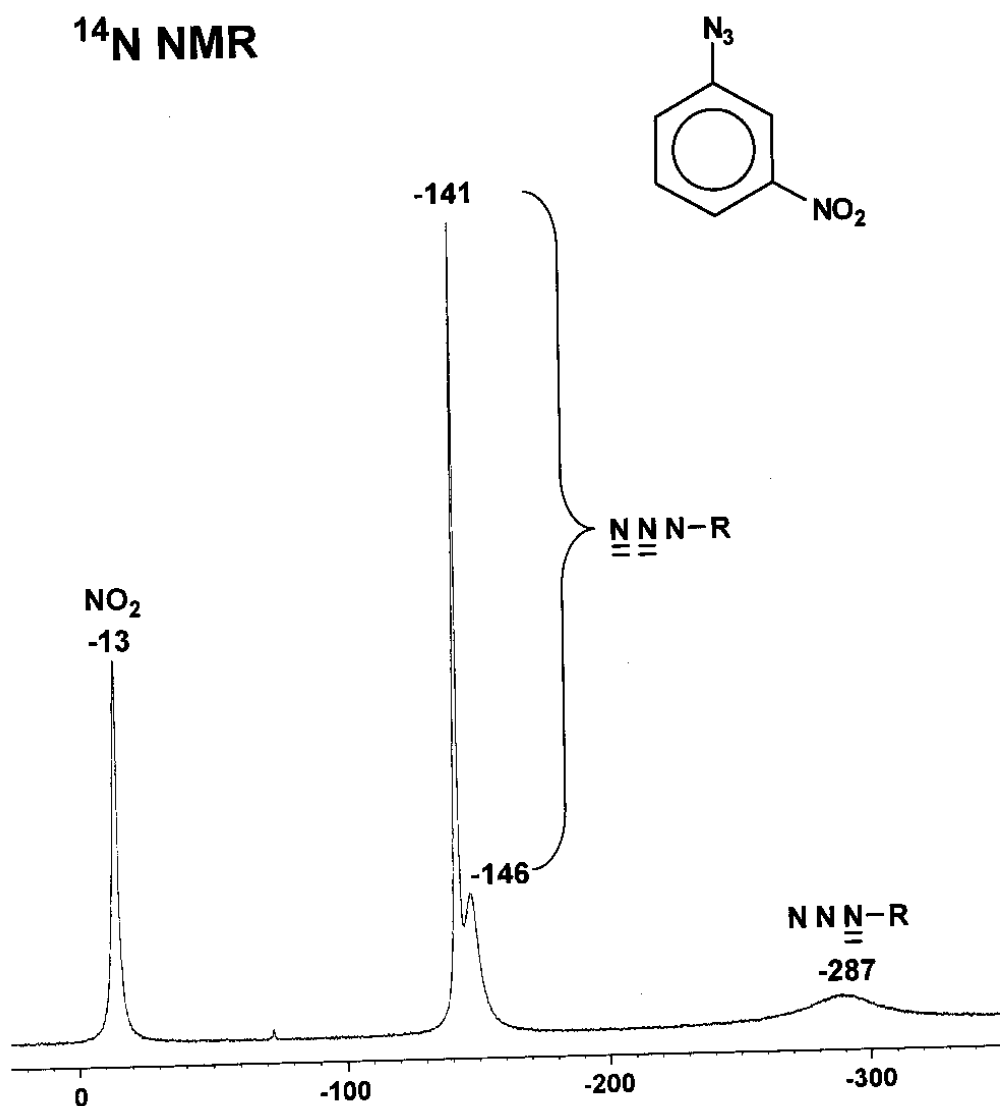


Figure 3.2 ^{14}N NMR (CDCl_3) spectrum of *m*-nitrophenyl azide

In this project we also wanted to prepare compounds which had more than one nitro group or more than one azide group on the benzene ring or a combination of both. 2,4-dinitrophenyl azide was prepared by the reaction of 2,4-dinitroaniline with sodium nitrite in a mixture of glacial acetic acid and sulphuric acid at 8 °C to yield the diazonium salt. The diazonium salt was then reacted with sodium azide at 8 °C to yield 2,4-dinitrophenyl azide

The 2,4-dinitrophenyl azide was isolated as a yellow solid and was then recrystallised from ethanol to give yellow needlelike crystals. The elemental analysis for the 2,4-dinitrophenyl

azide was in agreement with the theoretical values, (found C, 34.6 ; H, 1.4;N, 33.4 % calculated C, 34.5 ; H, 1.4 ; N, 34.0 %).The IR spectrum showed a strong absorption at 2135 cm^{-1} for the asymmetric stretching vibration of the azide group, a strong absorption at 1301 cm^{-1} for the symmetric stretching vibration of the azide and an absorption at 722 cm^{-1} for the deformation of the azide group. The I.R. spectrum also showed 2 weak absorptions at 3114 and 3077 cm^{-1} which are characteristic for C-H vibrations in an aromatic ring, a strong absorption at 1611 cm^{-1} for the asymmetric stretching vibration of the C-C bond in the aromatic ring, a strong absorption at 1558 cm^{-1} for the asymmetric stretching vibration of the NO_2 group and a strong absorption at 1345 cm^{-1} for the symmetric stretching vibration of the NO_2 group. The Raman spectra showed a peak at 2124 cm^{-1} for the asymmetric stretching vibration of the azide group, a strong peak at 1333 cm^{-1} for the symmetric stretching vibration of the azide. The Raman spectrum also showed a peak at 3097 cm^{-1} which is characteristic for C-H vibrations in an aromatic ring, a peak at 1621 cm^{-1} for the asymmetric stretching vibration of the C-C bond in the aromatic ring, a peak at 1521 cm^{-1} for the asymmetric stretching vibration of the NO_2 group and a strong peak at 1359 cm^{-1} for the symmetric stretching vibration of the NO_2 group.

The ^1H NMR spectrum shows three resonances at 7.90, 7.62 and 7.34 ppm. The ^{13}C NMR spectrum shows six resonances at 120.6, 124.7, 128.5, 130.6, 131.3, and 135.9 ppm for the six aromatic carbons. The ^{14}N NMR spectrum shows three resonances, one for the NO_2 group ($\delta = -16.1$ ppm) and two for the azide N_α ($\delta = -290$ ppm), $\text{N}_\beta, \text{N}_\gamma$ ($\delta = -144.5$ ppm) The ^{14}N NMR spectrum of 2,4-dinitrophenyl azide is shown in figure 3.3.

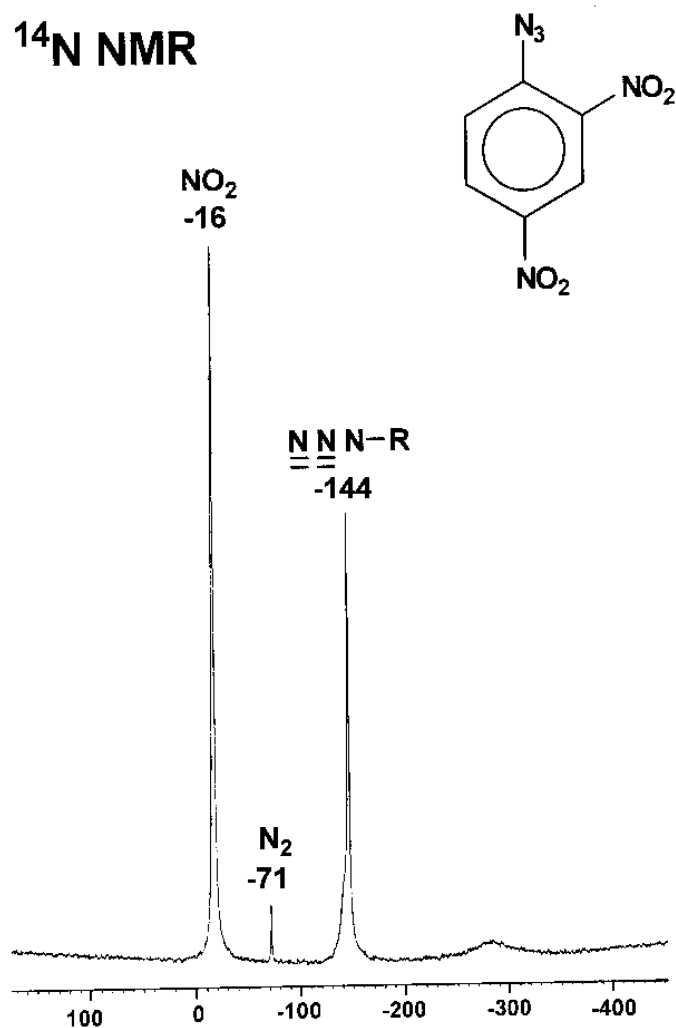
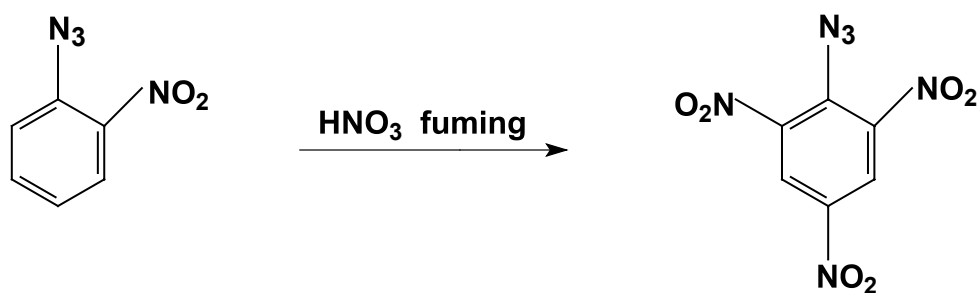


Figure 3.3 ^{14}N NMR (CDCl_3) spectrum of 2,4-dinitrophenyl azide

The next compound targeted was 2,4,6-trinitrophenyl azide which is an analogue of TNT (trinitrotoluene) a commercial explosive thus making the target compound a possible HEDM. 2,4,6-trinitrophenyl azide (picryl azide) was prepared by nitration of the previously prepared *o*-nitrophenyl azide with fuming nitric acid as shown in the scheme below



The 2,4,6-trinitrophenyl azide was isolated as a yellow powder and was recrystallised from methanol to yield yellow needles with a melting point of 89-90°C, dec. The elemental analysis for 2,4,6-trinitrophenyl azide was in agreement with the theoretical values, (found C, 27.8 ; H, 0.8 ; N, 32.6 % calculated C, 28.4 ; H, 0.8 ; N, 33.1 %). The IR spectrum showed a strong absorption at 2137 cm^{-1} for the asymmetric stretching vibration of the azide group, a strong absorption at 1288 cm^{-1} for the symmetric stretching vibration of the azide and an absorption at 623 cm^{-1} for the deformation of the azide group. The IR spectrum also showed two weak absorptions at 3108 and 3096 cm^{-1} which are characteristic for C-H vibrations in an aromatic ring, a strong absorption at 1603 cm^{-1} for the asymmetric stretching vibration of the C-C bond in the aromatic ring, a strong absorption at 1536 cm^{-1} for the asymmetric stretching vibration of the NO_2 group and a strong absorption at 1351 cm^{-1} for the symmetric stretching vibration of the NO_2 group. The Raman spectra showed a peak at 2127 cm^{-1} for the asymmetric stretching vibration of the azide group, a strong peak at 1287 cm^{-1} for the symmetric stretching vibration of the azide. The Raman spectrum also showed a peak at 1556 cm^{-1} for the asymmetric stretching vibration of the C-C bond in the aromatic ring, a peak at 1537 cm^{-1} for the asymmetric stretching vibration of the NO_2 group and a strong peak at 1350 cm^{-1} for the symmetric stretching vibration of the NO_2 group. The ab initio calculation of the vibrational frequencies for 2,4,6-trinitrophenyl azide was carried out at the self consistent HF level of theory using a 6-31G(d) basis set with a scaling factor of 0.89 [26].

There is a very good agreement between the scaled calculated frequencies and the observed IR and Raman frequencies. The calculated scaled and observed IR and Raman frequencies are shown in Table 3.2.

Table 3:2 The calculated HF/6-31G(d) , scaled and observed I.R. and Raman frequencies (cm^{-1}) for 2,4,6-trinitrophenyl azide

Assignment	Calculated Frequencies (unscaled) HF/6-31G(d)	Calculated Frequencies (scaled) F = 0.89	Observed Infra-Red Frequencies	Observed Raman Frequencies
ν_{CH} (Ar)	3487	3103	3108	3107
ν_{CH} (Ar)	3485	3101	3096
$\nu_{\text{as}}\text{N}_3$	2396	2133	2137	2127
$\nu_{\text{as}}\text{CC}$ (Ar)	1817	1617	1603	1612
$\nu_{\text{as}}\text{NO}_2$	1498	1333	1351	1350
$\nu_{\text{s}}\text{N}_3$	1418	1262	1288	1287
δCH	1330	1184	1181	1182
γCH	865	770	773

The ^1H NMR spectrum shows one resonance at 8.93 ppm for the two ring hydrogens. The ^{13}C NMR spectrum shows four resonances at 144.21, 142.54, 133.94 and 123.88 ppm. The ^{14}N NMR spectrum shows four resonances, one for the NO_2 groups ($\delta = -22.7$ ppm) and three for the azide N_α ($\delta = -290$ ppm), N_β ($\delta = -143.1$ ppm) and N_γ ($\delta = -153.2$ ppm).

2,4,6-trinitrophenyl azide (picryl azide) was recrystallised from methanol to yield yellow needle like crystals but in every batch of crystals grown there were a few regular hexagonal crystals which were the crystals used for x-ray structural determination. A crystal (0.40 x 0.20 x 0.16 mm) of 2,4,6-trinitrophenyl azide (picryl azide) was mounted on the Enraf-Nonius CAD4 diffractometer with Mo-K α radiation at room temperature for crystal structure analysis. The cell dimensions were derived from the least-squares analysis of the 25 independent reflections. Intensities of 2320 reflections were surveyed in the range θ 4.01-26.3 and 1670 independent reflections satisfied the criterion $I \geq 2\sigma(I)$. Three reference reflections monitored periodically showed a decline of 3% over the period of collection.

The crystal structure was elucidated by the direct phasing program XCAD4 [58]. After preliminary least-squares adjustments of the co-ordinates and anisotropic thermal parameters

of the C, N and O atoms, the H atoms were located in difference Fourier synthesis and subsequently included in the least-squares calculations with isotropic thermal parameters using SHELX [59]. The refinement converged at $R = 0.0429$, $R_w = 0.1286$. The crystals are orthorhombic with space group *Pbca* and cell dimensions $a = 10.16(1)$, $b = 12.60(1)$, $c = 14.32(1)$.

The crystal structure was also determined at 120 K. A crystal (0.40 x 0.20 x 0.16 mm) of 2,4,6-trinitrophenyl azide (picryl azide) was mounted on the Enraf-Nonius CAD4 diffractometer with Mo-K α radiation and cooled to 120 K using an Oxford Cryosystems cooling unit. The cell dimensions were derived from the least-squares analysis of the 25 independent reflections. Intensities of 2490 reflections were surveyed in the range θ 4.01-26.3 and 1252 independent reflections satisfied the criterion $I \geq 3\sigma(I)$. Three reference reflections monitored periodically showed a decline of 2% over the period of collection.

The crystal structure was elucidated by the direct phasing program XCAD4 [58]. After preliminary least-squares adjustments of the co-ordinates and anisotropic thermal parameters of the C, N and O atoms, the H atoms were located in difference Fourier synthesis and subsequently included in the least-squares calculations with isotropic thermal parameters using SHELX [59]. The refinement converged at $R = 0.045$, $R_w = 0.053$. The crystals are orthorhombic with space group *Pbca* and cell dimensions $a = 10.16(5)$, $b = 12.60(5)$, $c = 14.32$.

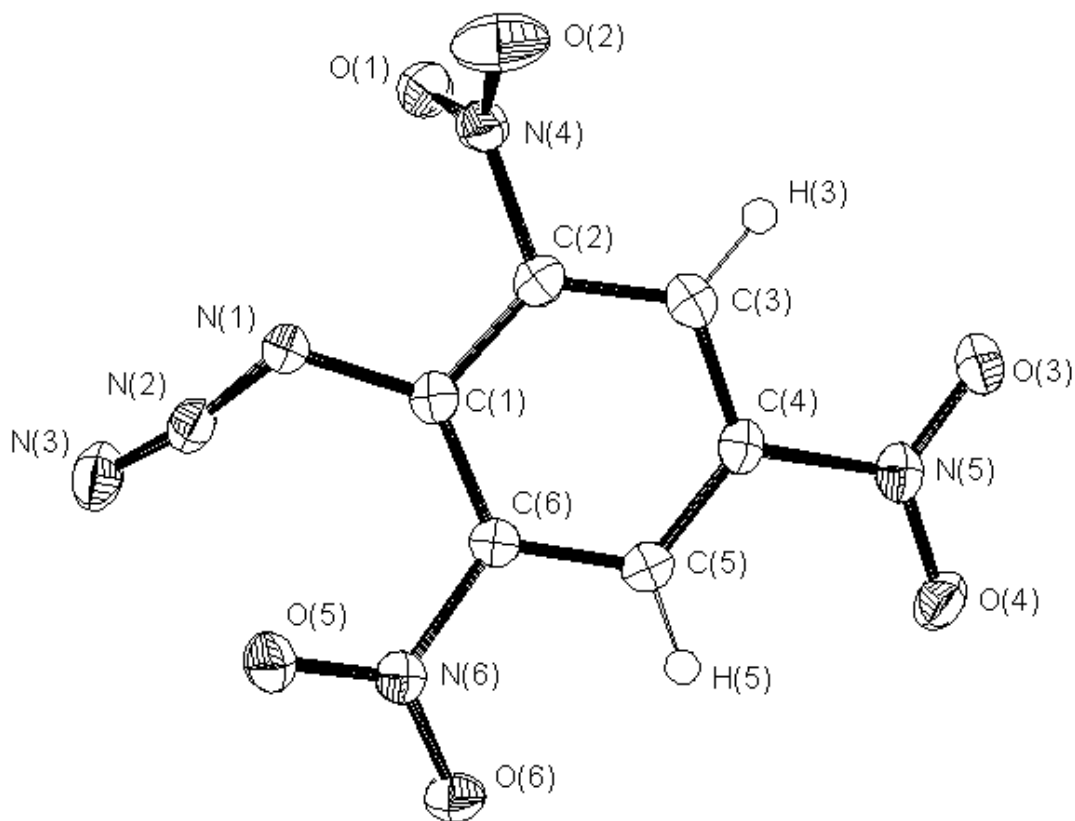


Figure 3.4 ORTEP drawing of 2,4,6-trinitrophenyl azide (picryl azide) with the thermal ellipsoids of the C, N and O atoms drawn at 50 % probability level and H atoms are represented by spheres of radius 0.1 Å.

The bond length between the terminal nitrogen and the central nitrogen is 1.114 Å and the bond length between the central nitrogen and the nitrogen attached directly to the ring is 1.250 Å. The ring carbon – carbon bond lengths are 1.369 – 1.401 Å. The nitrogen – oxygen bond lengths the nitro groups are 1.202 – 1.224 Å. The azide group is not linear and the angle at the central nitrogen atom (N2) is 169.9° whereas the angle at N1 is 119.4° which is close to the expected value of 120°. The benzene nucleus has internal angles greater than 120° at the carbon atoms attached to the nitro groups.

There is a most unusual intermolecular contact of 2.761(4) Å between O(1) and N(5) (at 0.5+x, 0.5-y, 1-z). This distance is well below the sum of the van der Waals radii of both atoms. This interaction maybe caused by electrostatic interactions or by crystal packing forces. This interaction is shown in the figure 3.5 below.

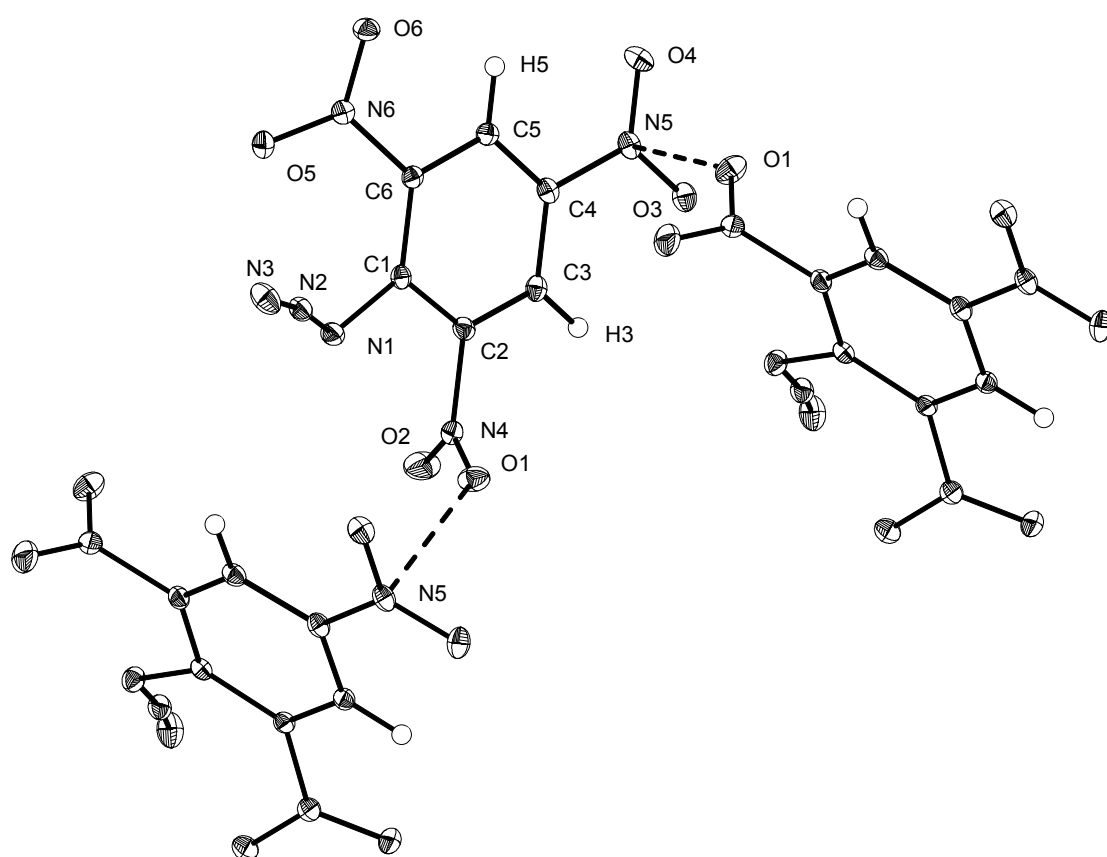


Figure 3.5 ORTEP drawing of 2,4,6-trinitrophenyl azide (picryl azide) with the thermal ellipsoids of the C, N and O atoms drawn at 25 % probability showing the intermolecular contact of 2.761(4) Å between O(1) and N(5)

The structure of 2,4,6-trinitrophenyl azide was fully optimised and the vibrational frequencies and zero point energy computed using a semiempirical calculation carried out at the semiempirical PM3 level of theory using a VSTO-3G basis set and ab initio at the self consistent HF level of theory using a 6-31G(d) basis set. The fully optimised structure of 2,4,6-trinitrophenyl azide is shown in figure 3.6

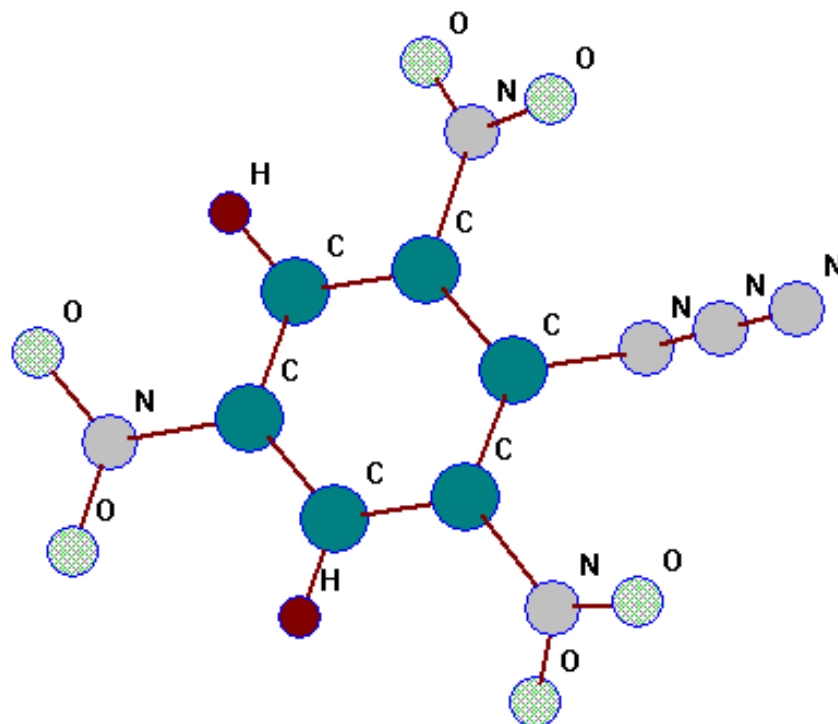


Figure 3.6 Molecular structure of 2,4,6-trinitrophenyl azide fully optimised at HF/6-31G(d) level of theory

There is very good agreement between the calculated bond lengths and angles and the bond length angles in the room temperature structure and the 120 K structure. The comparison of bond lengths and angles between the calculated HF/6-31G(d) structure and the X-ray structures determined at room temperature and 120 K of 2,4,6-trinitrophenyl azide are shown in tables 3.3 and 3.4.

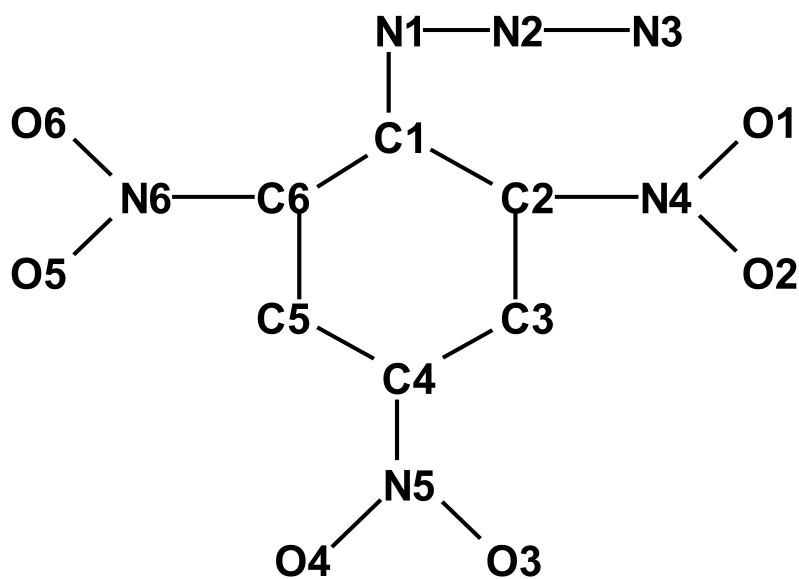


Table 3:3 Comparison of bond lengths (Å) between the calculated HF/6-31G(d) structure and the X-ray structures determined at room temperature and 120 K of 2,4,6-trinitrophenyl azide

Bonds	Room Temperature Structure	120 K Structure	Calculated Structure HF/6-31G(d)
C (1) – N (1)	1.395 (2)	1.402 (3)	1.415
C (1) – C (2)	1.394 (3)	1.396 (3)	1.394
C (1) – C (6)	1.401 (3)	1.400 (3)	1.394
C (2) – N (4)	1.473 (3)	1.471 (3)	1.447
C (2) – C (3)	1.369 (3)	1.375 (3)	1.379
C (3) – C (4)	1.377 (3)	1.382 (3)	1.380
C (4) – C (5)	1.357 (3)	1.366 (3)	1.380
C (4) – N (5)	1.475 (2)	1.469 (3)	1.446

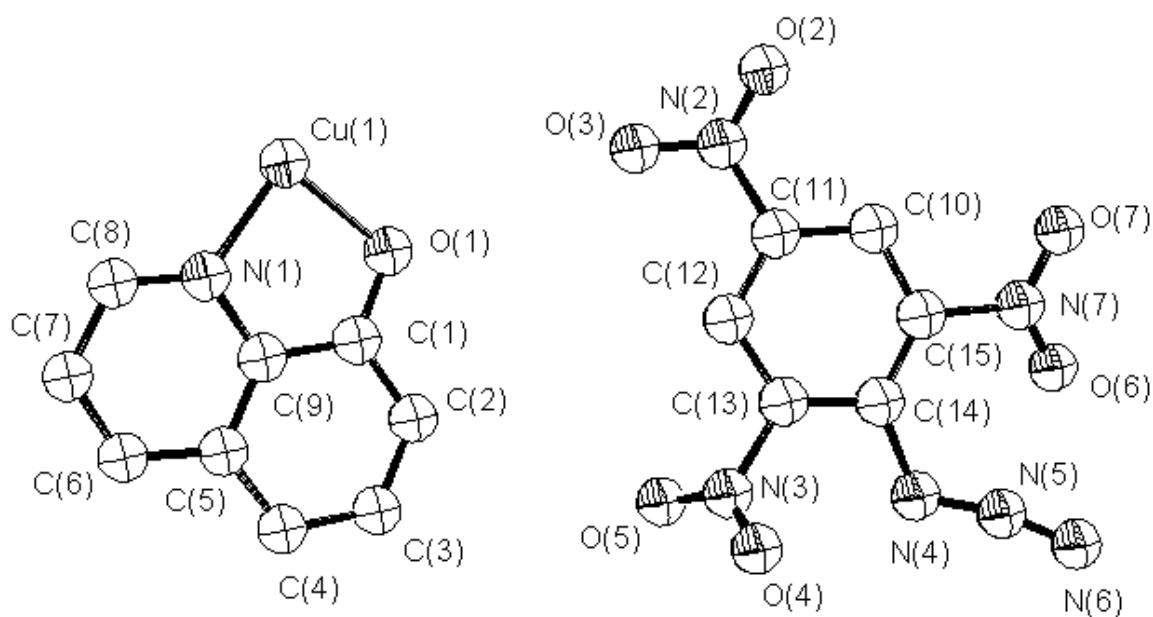
C (5) – C (6)	1.386 (3)	1.389 (3)	1.379
C (6) – N (6)	1.459 (3)	1.466 (3)	1.447
N (4) – O (1)	1.202 (2)	1.216 (3)	1.223
N (4) – O (2)	1.210 (3)	1.224 (3)	1.223
N (5) – O (3)	1.220 (2)	1.230 (3)	1.223
N (5) – O (4)	1.218 (2)	1.218 (3)	1.223
N (6) – O (5)	1.214 (2)	1.216 (3)	1.223
N (6) – O (6)	1.224 (2)	1.230 (3)	1.223
N (1) – N (2)	1.250 (3)	1.253 (3)	1.266
N (2) – N (3)	1.114 (2)	1.115 (3)	1.102

Table 3:4 Comparison of angles (°) between the calculated HF/6-31G(d) structure and the X-ray structures determined at room temperature and 120 K of 2,4,6-trinitrophenyl azide

Angles	Room Temperature Structure	120 K Structure	Calculated Structure HF/6-31G(d)
C (6) – C (1) – N (1)	129.9 (2)	130.3 (2)	120.90
C (6) – C (1) – C (2)	115.7 (2)	115.8 (2)	116.30
N (1) – C (1) – C (2)	114.3 (2)	113.7 (2)	121.52
N (4) – C (2) – C (1)	117.6 (2)	117.9 (2)	120.28
C (3) – C (2) – C (1)	124.6 (2)	124.6 (2)	122.64
N (4) – C (2) – C (3)	117.8 (2)	117.5 (2)	117.07
C (4) – C (3) – C(2)	116.3 (2)	116.0 (2)	118.31

C (5) – C (4) – C (3)	122.9 (2)	123.2 (2)	121.07
C (5) – C (4) – N (5)	118.9 (2)	118.4 (2)	119.40
N (5) – C (4) – C (3)	118.2 (2)	118.4 (2)	119.40
C (6) – C (5) – C (4)	119.2 (2)	118.7 (2)	118.27
C (5) – C (6) – C (1)	121.1 (2)	121.4 (2)	122.70
N (6) – C (6) – C (5)	116.2 (2)	115.8 (2)	117.08
N (6) – C (6) – C (1)	122.5 (2)	122.6 (2)	120.20
N (2) – N (1) – C (1)	119.4 (2)	119.5 (2)	118.73
N (3) – N (2) – N (1)	169.9 (2)	170.5 (2)	169.77
C (2) – N (4) – O (1)	118.2 (2)	117.7 (2)	117.86
C (2) – N (4) – O (2)	116.9 (2)	116.9 (2)	117.52
O (1) – N (4) – O (2)	124.8 (2)	125.5 (2)	124.56
C (4) – N (5) – O (3)	117.9 (2)	117.6 (2)	117.71
C (4) – N (5) – O (4)	117.3 (2)	117.9 (2)	117.70
O (4) – N (5) – O (3)	124.8 (2)	124.4 (2)	124.57
O (6) – N (6) – C (6)	118.6 (2)	118.4 (2)	117.86
O (5) – N (6) – C (6)	117.8 (2)	117.4 (2)	117.46
O (5) – N (6) – O (5)	123.6 (2)	124.1 (2)	124.61

The crystal structure of the molecular complex of bis-8-hydroxy-quinolinatocopper (II) and picryl azide was determined by x-ray diffraction methods by Bailey and Prout in 1965 [68]. The crystals contain isolated bis-8-hydroxy-quinolinatocopper (II) molecules and isolated picryl azide molecules in the ratio of 1:2. The resulting arrangement is such that metal complexes alternate with pairs of picryl azide molecules in stacks perpendicular to the *ab* plane. An ORTEP drawing of the molecular complex of bis-8-hydroxy-quinolinatocopper (II) and picryl azide with the thermal ellipsoids of the Cu, C, O and N atoms drawn at 50 % probability level is shown below in figure 3:7, the H atoms have been removed for clarity.



The geometries of the molecular complex of bis-8-hydroxy-quinolinatocopper (II) and picryl azide and the picryl azide structure described previously in this chapter can be compared. The geometries of azide group are very similar the bond length between the terminal nitrogen and the central nitrogen is 1.114 Å in picryl azide structure and 1.119 Å in the complex, furthermore the bond length between the central nitrogen and the nitrogen attached directly to the ring is 1.250 Å in picryl azide and 1.243 Å in the complex. The azide group in both cases is not linear with an angle of 169.9° in picryl azide and 168.4° in the complex. The ring

carbon – carbon bond lengths in picryl azide are 1.369 – 1.401 Å and 1.373 – 1.410 Å in complex. The nitrogen – oxygen bond lengths in the nitro groups are also very similar 1.202 – 1.224Å in both the picryl azide and 1.160 – 1.216Å in the complex. A selection of bond lengths and angles in both the picryl azide and the related complex are summarised in the tables below 3.5 and 3.6

Table 3.5 A comparison of bond lengths (Å) in picryl azide and complex of bis-8-hydroxy-quinolinatocopper (II) and picryl azide

Copper complex	Bond	Picryl azide
1.119	N(3) – N(2)	1.114
1.243	N(2) – N(1)	1.250
1.445	N(1) – C(1)	1.395
1.465, 1.507, 1.519	C – N (NO ₂)	1.459, 1.473, 1.475
1.373 – 1.410	C – C (ring)	1.369 – 1.401
1.160 – 1.216	N – O	1.202 – 1.224

Table 3:6 A comparison of angles (°) in picryl azide and complex of bis-8-hydroxy-quinolinatocopper (II) and picryl azide

Copper complex	Angle	Picryl azide
168.3	N(3) – N(2) – N(1)	169.9
112.0	N(1)- C(1) – C(2)	114.3
131.9	N(1) –C(1) – C(6)	129.9
115.9 – 124.2	C – C – C (ring)	115.7 - 124.6
122.1, 122.5, 128.4	O – N – O (NO ₂)	123.6, 124.8, 124.8

After a successful low temperature crystal structure determination of picryl azide it was thought that this compound maybe a good molecule for an experimental charge density study as it fitted the criteria for such a study :-

- (1) **high resolution** - better than 0.5 Å
- (2) **low temperature** – to reduce thermal vibrations of the atoms
- (3) **very accurate intensity measurements** – errors must be smaller than bond electron effects
- (4) **chemical suitability** – sufficiently small molecules, composed of atoms $Z < 35$, with minimal hydrogen content.
- (5) **crystal suitability** – ordered structure, appropriate size, well-characterised morphology, preferably centrosymmetric and with high symmetry so as to reduce the size of the asymmetric unit and the number of parameters require to fit the charge density study.
- (6) **corrections** - for absorption, extinction, background and thermal diffuse scattering (TDS). In fact it is best to avoid crystals showing sizeable extinction and/or TDS effects.

The same hexagonal crystal as used in the structural determination was then used to begin a larger data collection for a charge density study at 120 K. After about two days, it was noticed that there was a large error in the intensities of the standard intensity reflections set at the start of the collection, thus indicating a problem with the crystal.. The data collection was stopped at this point and the crystal examined under a microscope and it was observed that the crystal had cracked. This experiment was repeated several times with a new crystal each time but the crystals always cracked after being cooled to 120 K for 2-3 days. As this is not long enough to collect enough data for a experimental charge density study, it was decided to attempt to get crystals of better quality. As it was not possible to carry out an experimental charge density study of these crystal, a theoretical charge density study was then calculated using the same data set as was used for determining the structure at 120K.

The ab initio wavefunction was calculated for the crystalline molecular geometry as determined in the 120 K experiment for picryl azide using GAMESS [69]. A 6-31G(d) basis set was used, at the Hartree-Fock level. The AIMPAC SADDLE program locates (3,-1) (bond) critical points in all bonds, and a (3+1) (ring) critical point at the centre of the ring [70]. Using the GRID program the Laplacian maps in the plane of the ring, the plane of N3 N2 N1, and the plane of N2 N1 C1 were also computed. The N-N triple bond is quite markedly "thicker" than the N2 - N1 bond, and lone pairs on N3 and N1 are visible. The Laplacian maps are shown in figures 3:8, 3:9 and 3:10.

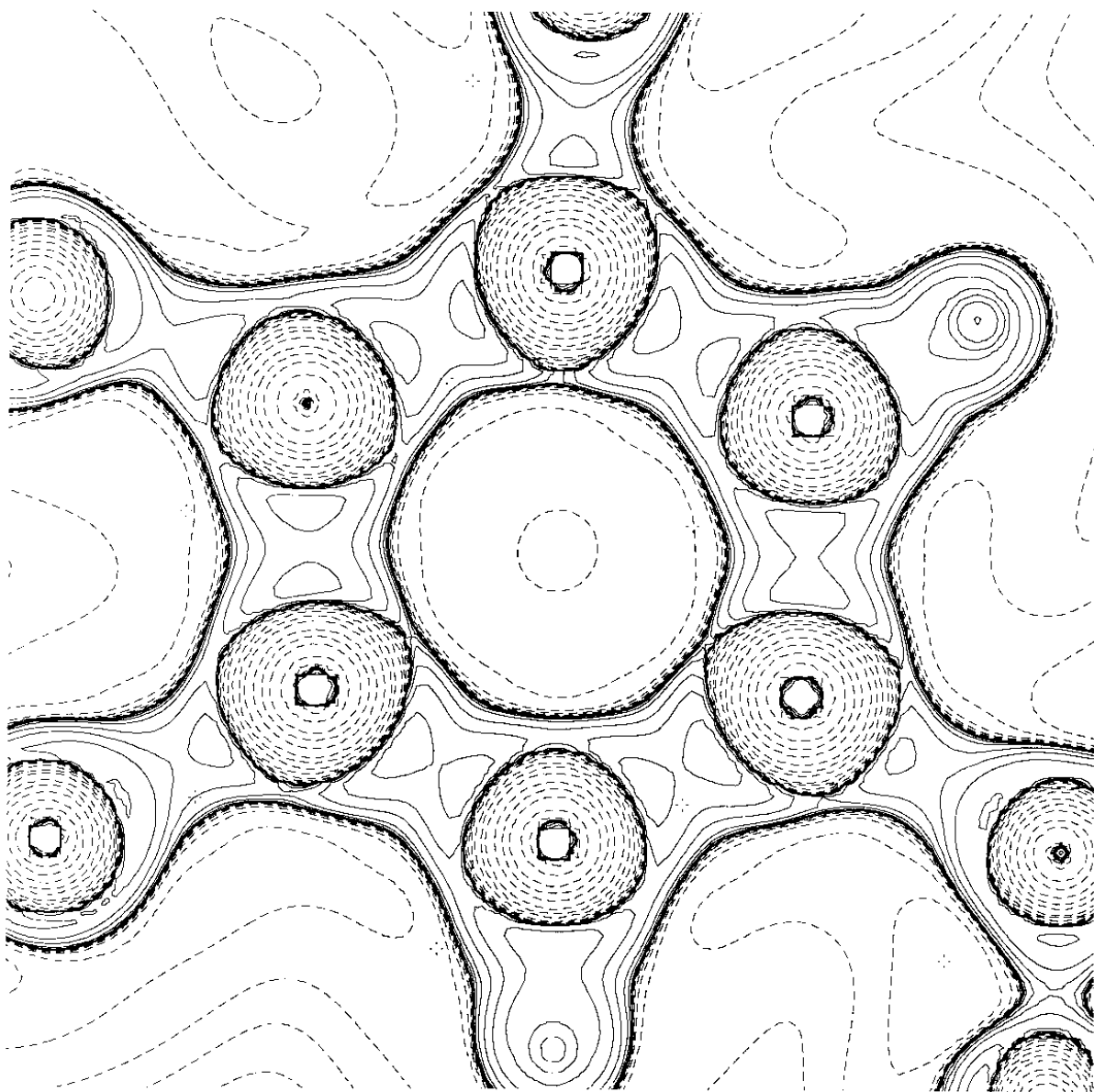


Figure 3.8 Laplacian map in the plane of the ring of picryl azide

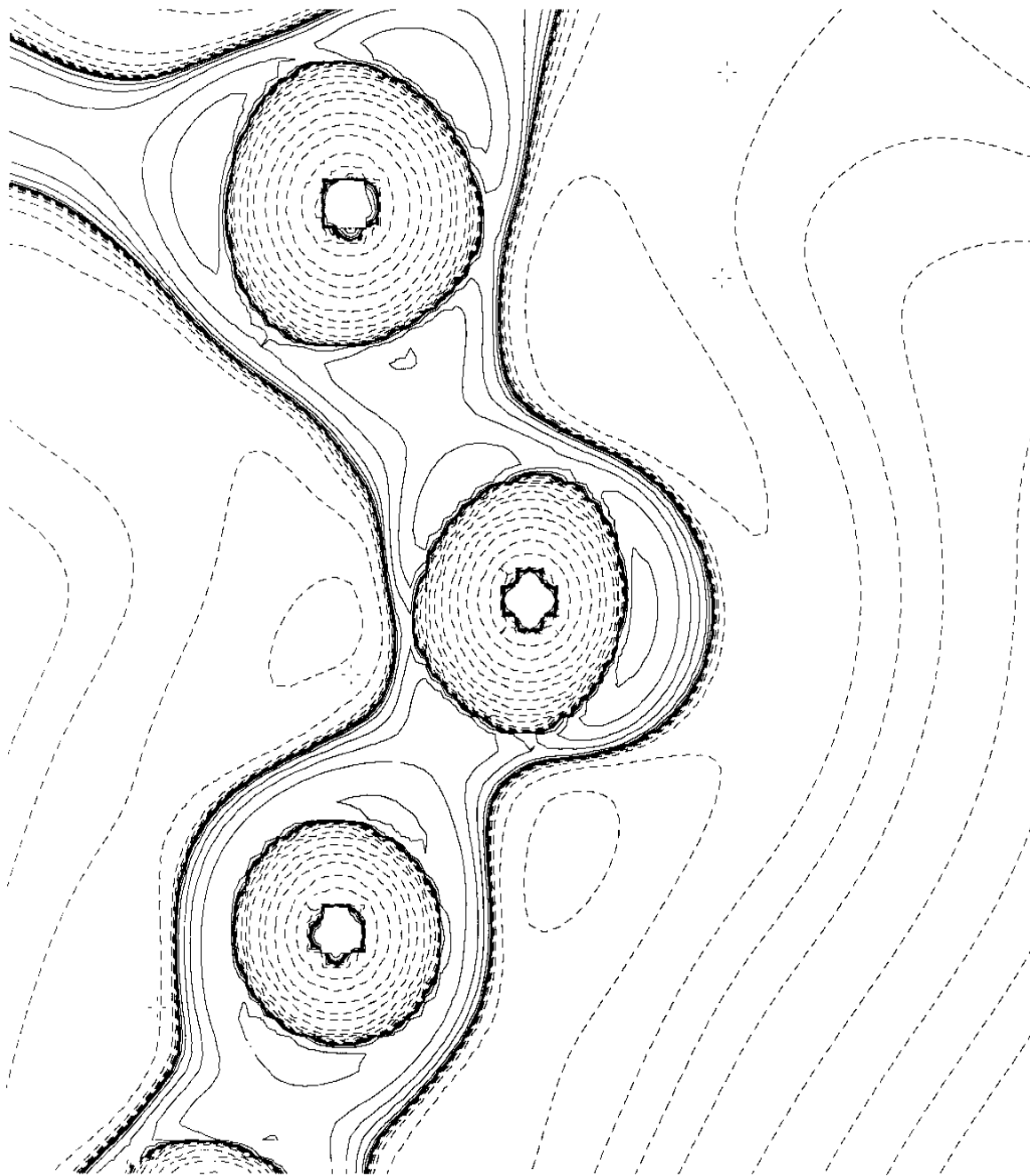


Figure 3.9 Laplacian map in the plane of N2 N1 C1 of picryl azide

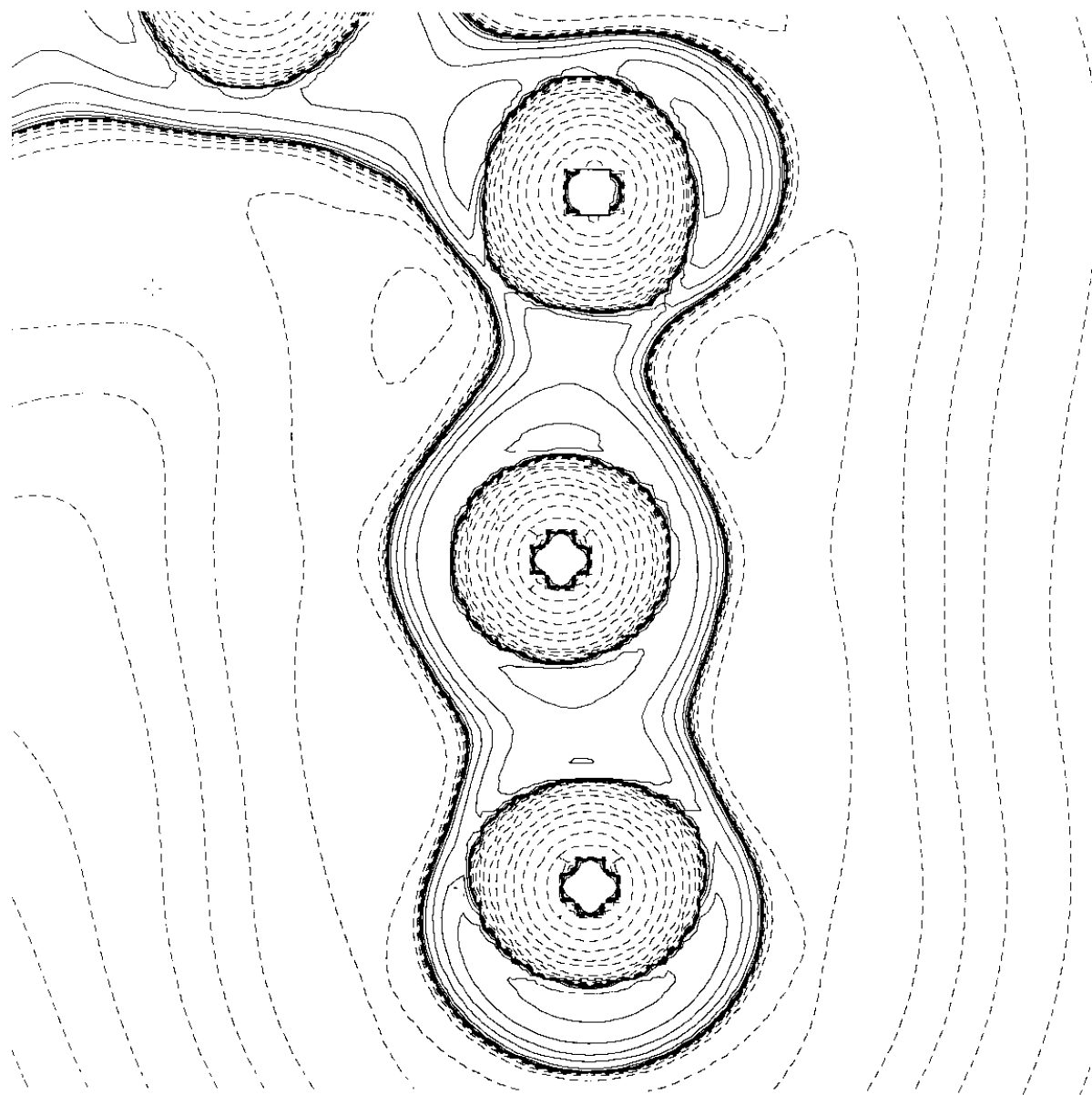


Figure 3.10 Laplacian map in the plane of N1 N2 N3 of picryl azide

2,4,6-trinitrophenyl azide only showed very moderate impact sensitivity (drop hammer testing) and often deflagrates upon ignition but explosions were also observed to have occurred. Therefore it was not possible to determine the accurate temperature of explosion of 2,4,6-trinitrophenyl azide using the sand bath technique as with the other compounds discussed later. It was observed that if a sample was placed in the sand bath at room temperature and the bath was gradually warmed up to 250°C no explosion occurred. The compound was observed to decompose as it was slowly warmed up in the sand bath, this decomposition was monitored using variable temperature Raman spectroscopy. It can be seen from the spectra in figure 3.11 that the compound decomposes around its melting point and no spectra could be obtained of the brown tar-like material left in the sample vial at temperatures above the melting point. The explosive properties of this compound are discussed in more detail in later chapters of this thesis.

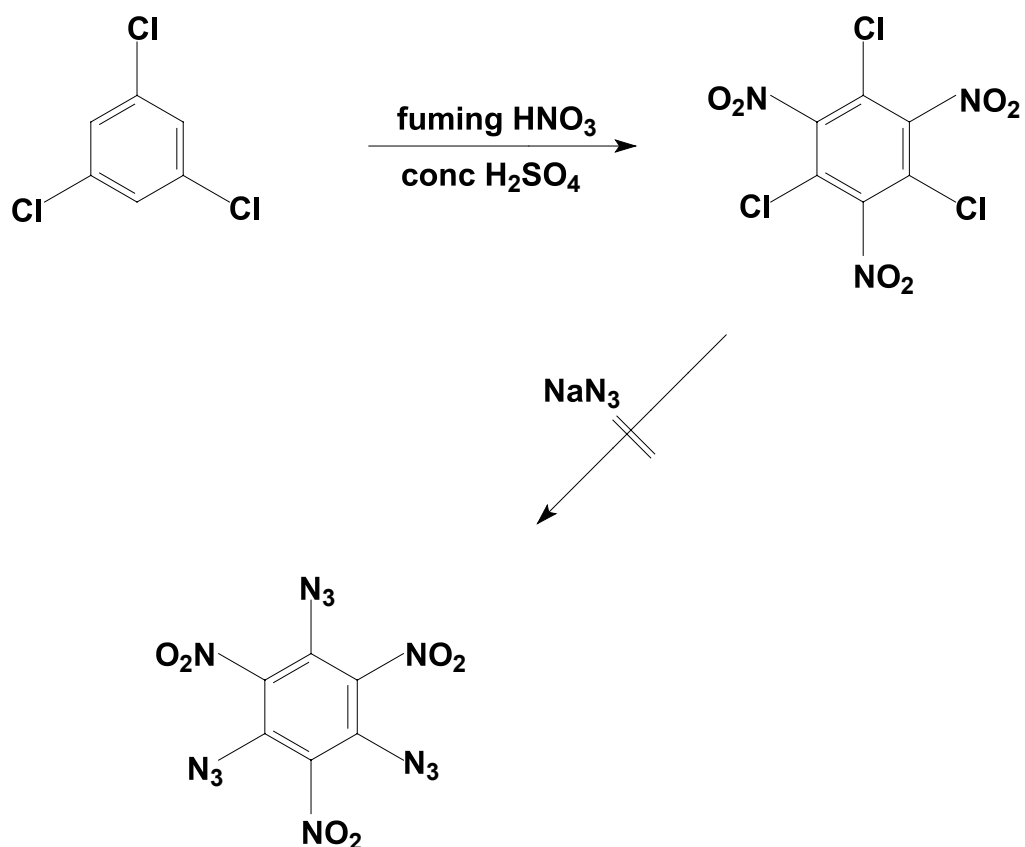
Figure 3.11 Raman spectra of 2,4,6-trinitrophenyl azide at 25°C , 50°C, 75°C and 100°C

After the preparation of picryl azide, nitration of the last two positions on the benzene ring to yield pentanitrophenyl azide was attempted. The preparation of pentanitrophenyl azide was attempted in 4 different ways:

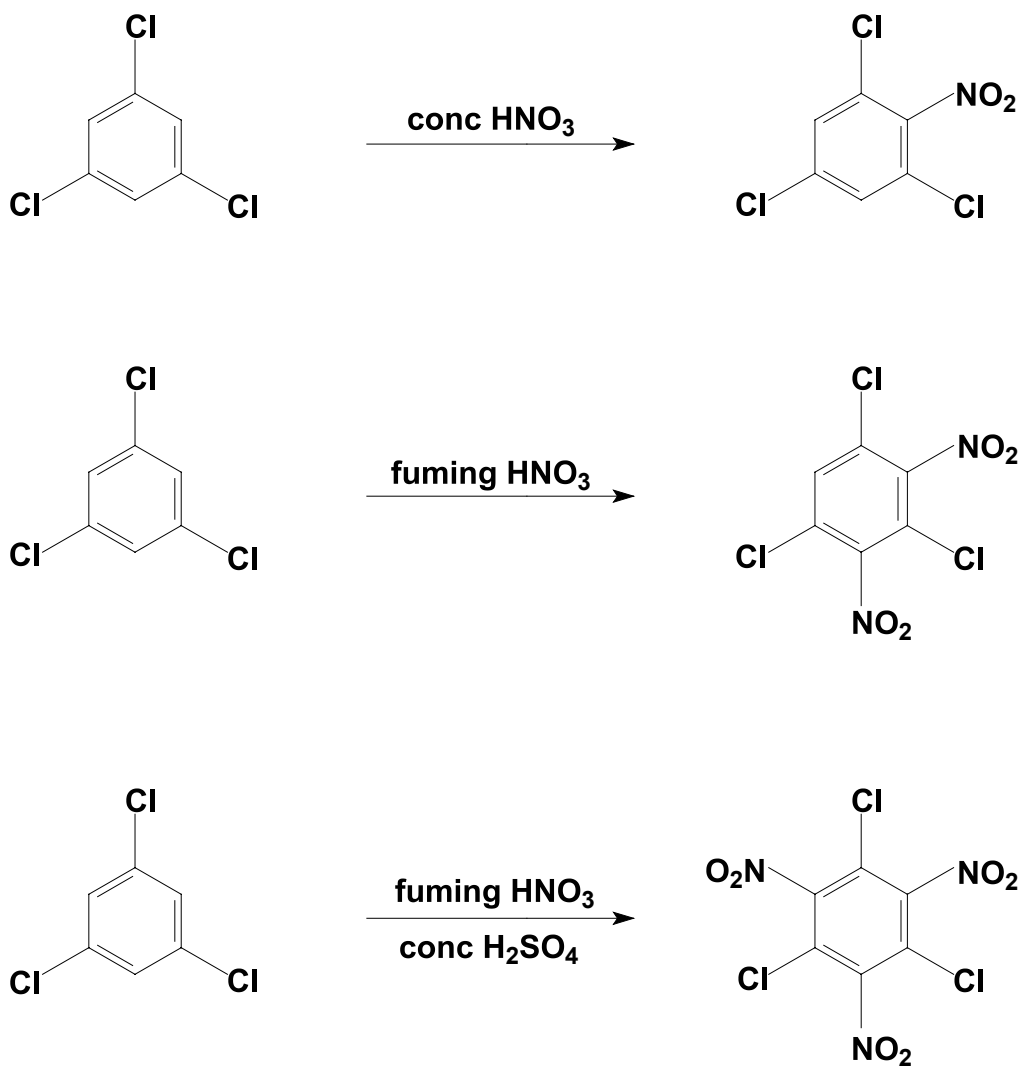
- (1) **nitration of *o*-nitrophenyl azide with $\text{HNO}_3 / \text{H}_2\text{SO}_4$** :- as previously described in this chapter, the nitration of *o*-nitrophenyl azide with a mixture of fuming nitric acid and concentrated sulphuric acid yielded 2,4,6-trinitrophenyl azide (picryl azide). In this experiment a large excess of the nitrating mixture was used in an attempt to prepare pentanitrophenyl azide, but unfortunately this again only yielded 2,4,6-trinitrophenyl azide.
- (2) **nitration of *o*-nitrophenyl azide with N_2O_5** :- *o*-nitrophenyl azide was dissolved in dichloromethane in a 100 mL round bottom flask. This solution was then cooled to -50°C with stirring. Dinitrogen pentoxide was dissolved in dichloromethane at -50°C and added to a special dropping funnel which was surrounded by a dichloromethane-dry ice bath. The dinitrogen pentoxide solution was slowly and carefully added dropwise to the azide solution over the period of 45 minutes making sure the temperature remained at -50°C . When addition was complete, the solution was stirred at -50°C for a further 60 minutes then allowed to warm up to room temperature. The solvent was then carefully removed to yield a yellow powder which on analysis was 2,4,6-trinitrophenyl azide (picryl azide) and not the desired product pentanitrophenyl azide.
- (3) **nitration of picryl azide with N_2O_5** :- picryl azide was dissolved in dichloromethane in a 100 mL round bottom flask. The solution was then cooled to -50°C whilst stirring. Dinitrogen pentoxide was dissolved in dichloromethane at -50°C and added to a special dropping funnel which was surrounded by a dichloromethane-dry ice bath. The dinitrogen pentoxide solution was slowly and carefully added dropwise to the azide solution over the period of 45 minutes making sure the temperature remained at -50°C . After addition, it was observed that no reaction had occurred and only the starting material was recovered when the solvent was evaporated.
- (4) **reaction of pentanitroaniline with sodium azide via a diazonium salt** :- pentanitroaniline was prepared by nitration of 3,5-dinitroaniline by using a modification of the method of Flürscheim [71]. 3,5-dinitroaniline was dissolved in 100% sulphuric acid

and cooled to 5°C. 100% nitric acid was added dropwise over 10 minutes, during which time the temperature was maintained below 8°C. The reaction mixture was then heated for 1 hour at 70-75 °C and finally cooled in an ice bath. The yellow solid was filtered, air dried at the pump for 10 minutes and then dissolved in dichloroethane to yield pentanitroaniline as clear yellow plates with a melting point of 192-200°C dec. (lit 193-202 °C) [71]. The pentanitroaniline was then reacted with sodium nitrite at 0°C to yield the diazonium salt which was then reacted with sodium azide at 0°C to yield pentanitronitrophenyl azide as a yellow solid. However this solid was not stable at room temperature and rapidly decomposed given off nitrogen gas. The Raman spectrum was recorded at 0° C and indicate the presence of an organic azide, but as yet this product has not been isolated at room temperature.

In an attempt to prepare trinitrotriazidobenzene ($C_6N_{12}O_6$), trichlorobenzene ($C_6H_3Cl_3$) was reacted with a mixture of fuming nitric acid and concentrated sulphuric acid to yield trichlorotrinitrobenzene ($C_6N_3O_6Cl_3$). The trichlorotrinitrobenzene was then reacted with an excess of sodium azide in dichloromethane, but this reaction mixture was explosive and each time the reaction was attempted a small explosion occurred. The reaction was then attempted at low temperatures but at these temperatures there was no reaction. Thus it was not possible to prepare trinitrotriazidobenzene by this method (as shown in the scheme below). So another method for the preparation of trinitrotriazidobenzene had to be found.



Jackson and Wing reported that the extent of nitration of trichlorobenzene was dependent on the nitration agent used [72]. The reaction of trichlorobenzene with concentrated nitric acid gave the mono nitration, the reaction with fuming nitric acid gave di-nitration and the reaction with a mixture of fuming nitric acid and concentrated sulphuric acid resulted in tri-nitration. These three reactions are shown in the scheme below.



In a new attempt to prepare trinitrotriazidobenzene ($\text{C}_6\text{N}_{12}\text{O}_6$), trichlorobenzene was reacted with fuming nitric acid to yield trichlorodinitrobenzene. The trichlorodinitrobenzene was dissolved in a boiling mixture of acetone and methanol. A hot solution of sodium azide in water and methanol was then added. This mixture was then boiled under reflux for 90 minutes, and then filtered and the residual sodium chloride was washed three times with hot ethanol. The filtrate and washings were cooled in a fridge at 0°C overnight to yield triazidodinitrobenzene (DNNTA). The triazidodinitrobenzene was then nitrated with fuming nitric acid to give trinitrotriazidobenzene (TNNTA). This was not only a successful route to prepare trinitrotriazidobenzene but also yielded another compound triazidodinitrobenzene which could also be a target a HEDM. The scheme for this preparation is shown below

The 1,3,5-triazido-2,4-dinitrobenzene was isolated by cooling in the fridge overnight as a brown solid and recrystallised from ethanol to yield yellow needles with a melting point of

107-108°C. The elemental analysis for carbon and nitrogen in 1,3,5-triazido-2,4-dinitrobenzene was in agreement with the theoretical values, (found C, 24.5 ; N, 52.6 % calculated C, 24.7 ; N, 52.9%). The micro-analyst was unable to determine an accurate value for hydrogen due to its low percentage in the molecule. The IR spectrum showed a strong absorption at 2137 cm^{-1} for the asymmetric stretching vibration of the azide group, a strong absorption at 1269 cm^{-1} for the symmetric stretching vibration of the azide and an absorption at 682 cm^{-1} for the deformation of the azide group. The IR spectrum also showed a weak absorption at 3077 cm^{-1} which is characteristic for C-H vibrations in an aromatic ring, a strong absorption at 1605 cm^{-1} for the asymmetric stretching vibration of the C-C bond in the aromatic ring, a strong absorption at 1535 cm^{-1} for the asymmetric stretching vibration of the NO_2 group and a strong absorption at 1364 cm^{-1} for the symmetric stretching vibration of the NO_2 group. The Raman spectrum showed a peak at 2135 cm^{-1} for the asymmetric stretching vibration of the azide group, a strong peak at 1284 cm^{-1} for the symmetric stretching vibration of the azide. The Raman spectrum also a peak at 1579 cm^{-1} for the asymmetric stretching vibration of the C-C bond in the aromatic ring, a peak at 1529 cm^{-1} for the asymmetric stretching vibration of the NO_2 group and a strong peak at 1340 cm^{-1} for the symmetric stretching vibration of the NO_2 group.

The ^1H NMR spectrum shows one resonance at 6.83 ppm for the one ring hydrogen. The ^{13}C NMR spectrum shows four resonances at 137.50, 127.63, 108.57 and 103.51 ppm. The ^{14}N NMR spectrum shows four resonances, one for the NO_2 group ($\delta = -22.4$ ppm) and three for the azide N_α ($\delta = -290$ ppm), N_β ($\delta = -146.8$ ppm) and N_γ ($\delta = -150.9$ ppm). The ^{14}N NMR spectrum of 1,3,5-triazido-2,4-dinitrobenzene is shown in figure 3.12 .

¹⁴N NMR

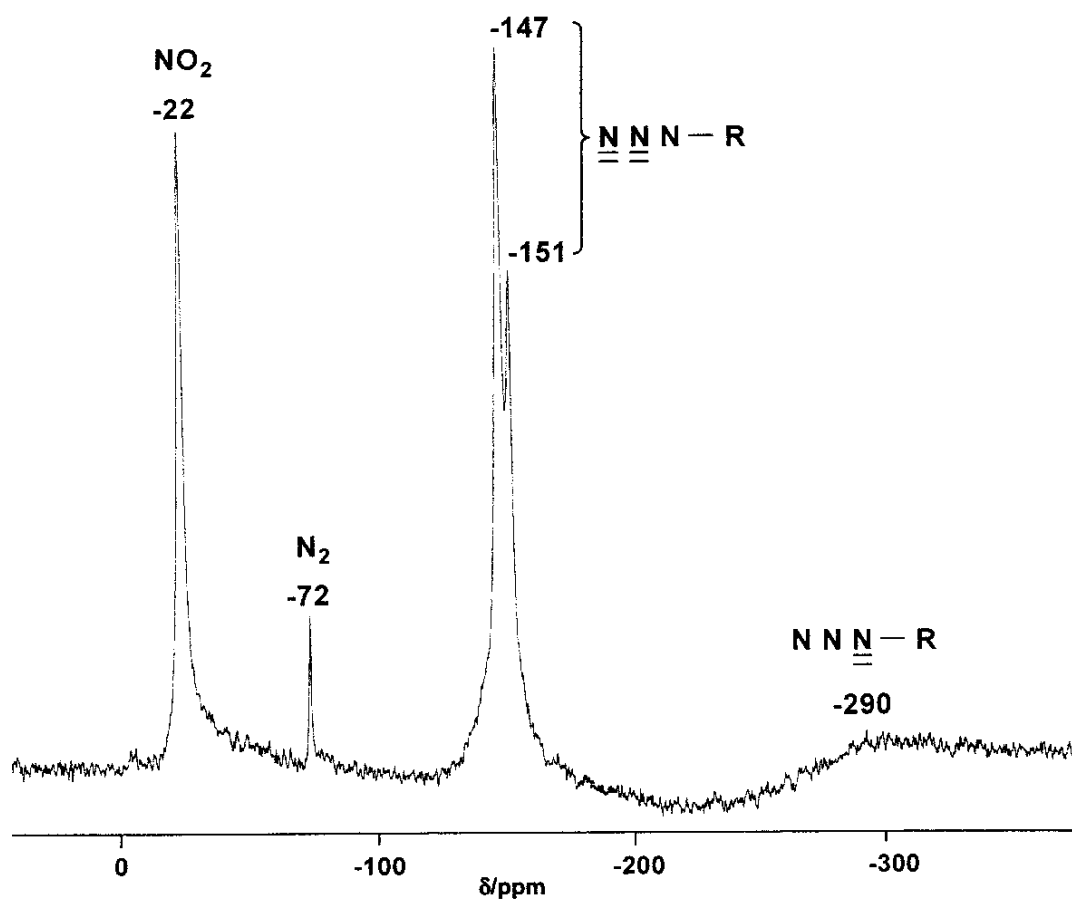
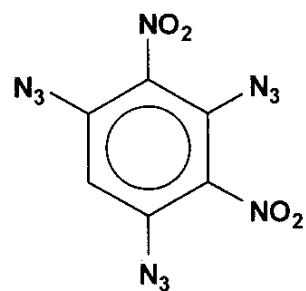


Figure 3.12 ¹⁴N NMR (CDCl₃) spectrum of 1,3,5-triazido-2,4-dinitrobenzene

The structure of 1,3,5-triazido-2,4-dinitrobenzene was fully optimised and the vibrational frequencies and zero point energy computed using a semiempirical calculation carried out at the semiempirical PM3 level of theory using a VSTO-3G basis set and ab initio at the self consistent HF level of theory using a 6-31G(d) basis set. The fully optimised structure of 1,3,5-triazido-2,4-dinitrobenzene is shown in the figure 3:13

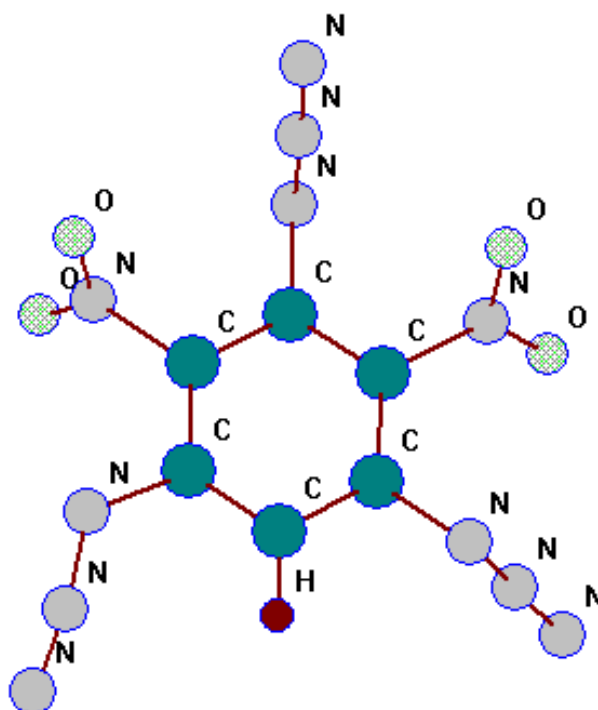


Figure 3:13 Molecular structure of 1,3,5-triazido-2,4-dinitrobenzene fully optimised at HF/6-31G(d) level of theory.

1,3,5-triazido 2,4, dinitrobenzene was found to be impact-sensitive (drop hammer testing) and detonate violently upon ignition. The temperature at which 1,3,5-triazido 2,4-dinitrobenzene exploded was determined by putting 10 mg of the compound in a small glass sample vial and placing this vial into a sand bath at a pre-determined temperature and monitoring if an explosion occurred. 1,3,5-triazido 2,4-dinitrobenzene exploded immediately at all temperatures above 156°C, so the explosion temperature for 1,3,5-triazido 2,4-dinitrobenzene is 156°C. However if a sample was placed in the sand bath at room temperature and the bath

was gradually warmed up to 250°C no explosion was observed to occur. The compound was observed to decompose as it was slowly warmed up in the sand bath, this decomposition was monitored using variable temperature Raman spectroscopy. It can be seen from the spectrum in figure 3.14 that the compound decomposes around its melting point and no spectrum could be obtained of the brown tar-like material left in the sample vial at temperatures above the melting point. The explosive properties of this compound are discussed in more detail in later chapters of this thesis.

Figure 3.14 Raman spectra of 1,3,5-triazido-2,4-dinitrobenzene at 25°C , 60°C, 90°C and 120°C

1,3,5-triazido-2,4,6-trinitrobenzene was precipitated as yellow plates from the reaction mixture and the addition of water to the reaction mixture yielded some more yellow solid. The combined solids were further recrystallised from acetic acid to yield bright yellow plates with a melting point of 128-130°C. The elemental analysis for 1,3,5-triazido 2,4,6 trinitrobenzene was in agreement with the theoretical values, (found C, 21.3 ;N, 49.3 % calculated C, 21.4 ; N, 50.0%). The IR spectrum showed a strong absorption at 2121 cm^{-1} for the asymmetric stretching vibration of the azide group, a strong absorption at 1343 cm^{-1} for the symmetric stretching vibration of the azide and an absorption at 603 cm^{-1} for the deformation of the azide group. The IR spectrum also showed a strong absorption at 1599 cm^{-1} for the asymmetric stretching vibration of the C-C bond in the aromatic ring, a strong absorption at 1542 cm^{-1} for the asymmetric stretching vibration of the NO_2 group and a strong absorption at 1370 cm^{-1} for the symmetric stretching vibration of the NO_2 group. The Raman spectra showed a peak at 2141 cm^{-1} for the asymmetric stretching vibration of the azide group, a strong peak at 1340 cm^{-1} for the symmetric stretching vibration of the azide. The Raman spectrum also showed a peak at 1568 cm^{-1} for the asymmetric stretching vibration of the C-C bond in the aromatic ring and a peak at 1541 cm^{-1} for the asymmetric stretching vibration of the NO_2 group. The ^{13}C NMR spectrum shows two resonances at 140.9 and 102.0 ppm The ^{14}N NMR spectrum shows four resonances, one for the NO_2 group ($\delta = -27.6$ ppm) and three for the azide N_α ($\delta = -290$ ppm), N_β ($\delta = -144.4$ ppm) and N_γ ($\delta = -153.0$ ppm). The ^{14}N NMR spectrum of 1,3,5-triazido 2,4,6 trinitrobenzene is shown in figure 3.15.

^{14}N NMR

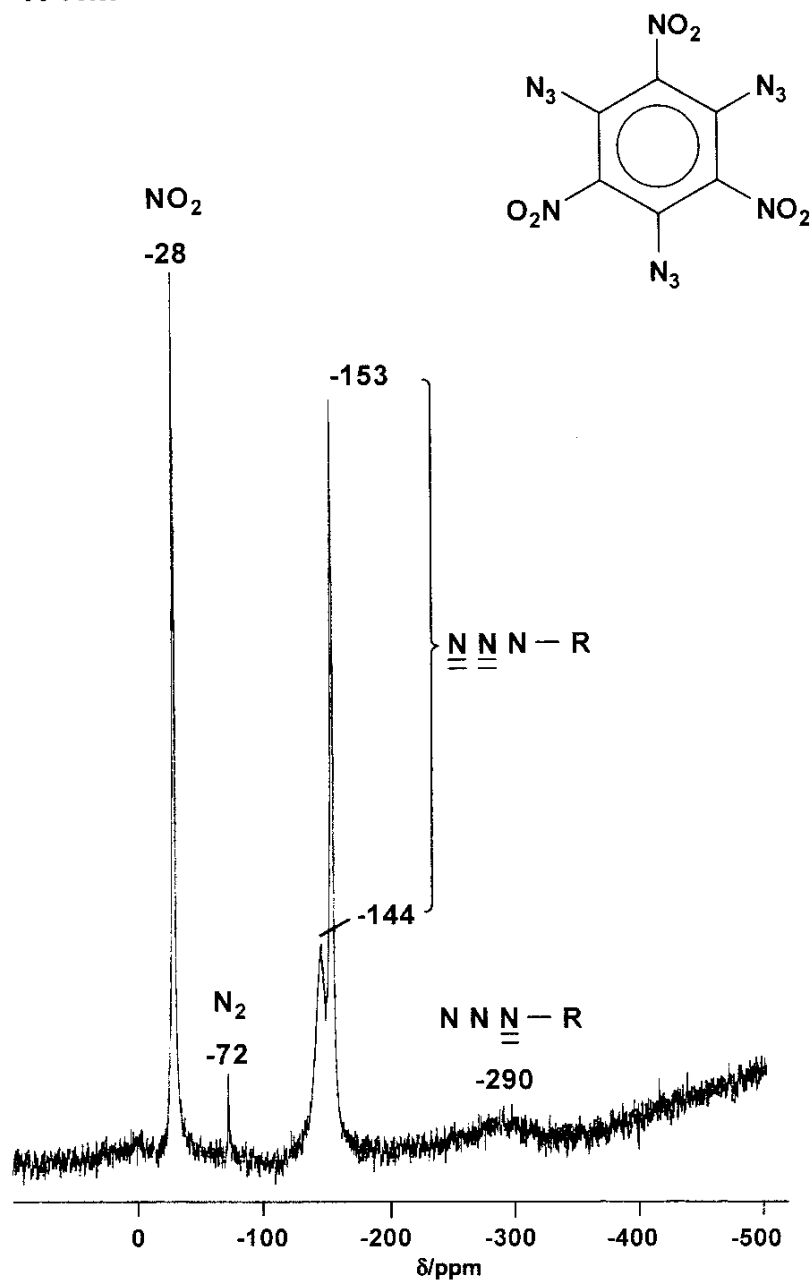


Figure 3.15 ^{14}N NMR (CDCl_3) spectrum of 1,3,5-triazido 2,4,6-trinitrobenzene

The structure of 1,3,5-triazido 2,4,6-trinitrobenzene was fully optimised and the vibrational frequencies and zero point energy computed using a semiempirical calculation carried out at the semiempirical PM3 level of theory using a VSTO-3G basis set and ab initio at the self

consistent HF level of theory using a 6-31G(d) basis set. The fully optimised structure of 1,3,5-triazido 2,4,6-trinitrobenzene is shown in figure 3.16

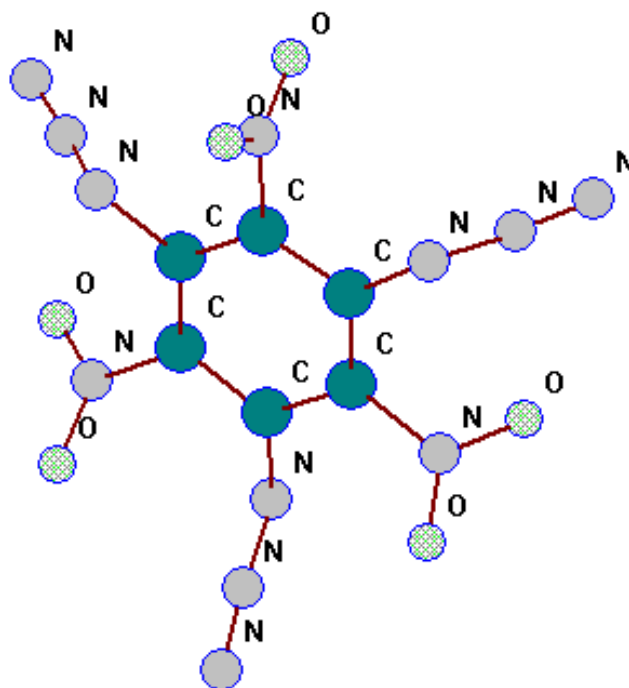


Figure 3.16 Molecular structure of 1,3,5-triazido 2,4,6-trinitrobenzene fully optimised at HF/6-31G(d) level of theory.

Table 3.7 Calculated HF/6-31G(d) and observed I.R. and Raman frequencies for 1,3,5-triazido 2,4,6-trinitrobenzene (cm^{-1})

Assignment	Calculated Frequencies HF/6-31G(d)	Observed Infra-Red Frequencies	Observed Raman Frequencies
$\nu_{\text{as}} \text{N}_3$	2132	2121	2141
$\nu_{\text{as}} \text{CC}(\text{Ar})$	1569	1599	1568
$\nu_{\text{as}} \text{NO}_2$	1544	1542	
$\nu_{\text{s}} \text{N}_3$	1335	1343	1340

1,3,5-triazido 2,4,6-trinitrobenzene was found to be impact-sensitive (drop hammer testing) and detonate violently upon ignition. The temperature at which 1,3,5-triazido 2,4,6-trinitrobenzene exploded was determined by putting 10 mg of the compound in a small glass sample vial and placing this vial into a sand bath at a pre-determined temperature and monitoring if an explosion occurred. 1,3,5-triazido 2,4,6-trinitrobenzene exploded immediately at all temperatures above 168°C , so the explosion temperature for 1,3,5-triazido 2,4,6-trinitrobenzene is 168°C . However if a sample was placed in the sand bath at room temperature and the bath was gradually warmed up to 250°C no explosion was observed. The compound was observed to decompose as it was slowly warmed up in the sand bath, this decomposition was monitored using variable temperature Raman spectroscopy. It can be seen from the spectrum in figure 3.17 that the compound decomposes around its melting point and the spectrum obtained at temperatures above the melting point is that of a brown oil remaining in the sample vial. The explosive properties of this compound are discussed in more detail in later chapters of this thesis.

Figure 3.17 Raman spectra of 1,3,5-triazido 2,4,6-trinitrobenzene at 30°C , 60°C, 100°C and 150°C.

In the next section it was decided to prepare compounds that contained either multiple azide or nitro groups which were not directly bonded to the central benzene ring. These compounds would also be tested as potential HEDM. The first compound prepared was hexakis (azidomethyl) benzene. Hexakis (bromomethyl) benzene was prepared by the literature method of Backer, by the reaction hexamethylbenzene and bromine in ethylene bromide [73]. Hexakis (bromomethyl) benzene was then reacted with a slight excess of sodium azide in dimethyl formamide at room temperature for 2 hours. The reaction mixture was then poured onto water and the hexakis (azidomethyl) benzene was collected by suction filtration and washed twice with water and then twice with methanol . The full preparation is shown in the scheme below.

Hexakis (bromomethyl) benzene was isolated as a white solid. The elemental analysis for the hexakis (bromomethyl) benzene was in agreement with the theoretical values, (found C, 22.5 ; H, 1.8 % calculated C, 22.5 ; H, 1.9 %). The IR spectrum also showed 2 absorptions at 3030 and 2997 cm^{-1} which are characteristic for C-H vibrations in an aromatic ring, a strong absorption at 1576 cm^{-1} for the asymmetric stretching vibration of the C-C bond in the aromatic ring and a strong absorption at 1312 cm^{-1} for the symmetric stretching vibration of the C-C bond in the aromatic ring. The Raman spectrum showed two peaks at 3035 cm^{-1} and 2996 cm^{-1} which are characteristic for C-H vibrations in an aromatic ring, a peak at 1573 cm^{-1} for the asymmetric stretching vibration of the C-C bond in the aromatic ring, and a peak at 1309 cm^{-1} for the symmetric stretching vibration of the C-C bond in the aromatic ring. The ^1H NMR spectrum shows one resonance at $\delta = 3.34$ ppm for the methyl hydrogens.

The hexakis (azidomethyl) benzene was isolated as a white solid with a melting point of 163.5°C. The elemental analysis for the hexakis (azidomethyl) benzene was in agreement with the theoretical values, (found C, 35.5 ; H, 2.9 ; N, 62.4 % calculated C, 35.3 ; H, 2.9 ; N, 61.8%). The IR spectrum showed a strong absorption at 2117 cm^{-1} for the asymmetric stretching vibration of the azide group, a strong absorption at 1272 cm^{-1} for the symmetric stretching vibration of the azide group. The IR spectrum also showed 2 absorptions at 3011 and 2963 cm^{-1} which are characteristic for C-H vibrations in an aromatic ring, a strong absorption at 1570 cm^{-1} for the asymmetric stretching vibration of the C-C bond in the aromatic ring and a strong absorption at 1358 cm^{-1} for the symmetric stretching vibration of the C-C bond in the aromatic ring. The Raman spectrum showed a peak at 2117 cm^{-1} for the asymmetric stretching vibration of the azide group, a strong peak at 1270 cm^{-1} for the symmetric stretching vibration of the azide. The Raman spectrum also showed two peaks at 3010 cm^{-1} and 2961 cm^{-1} which are characteristic for C-H vibrations in an aromatic ring, a peak at 1568 cm^{-1} for the asymmetric stretching vibration of the C-C bond in the aromatic ring and a peak at 1357 cm^{-1} for the symmetric stretching vibration of the C-C bond in the aromatic ring. The ^1H NMR spectrum shows one resonance at 3.31 ppm for the CH_2 hydrogens. The ^{13}C NMR spectrum shows two resonances at 47.1 ppm for the CH_2 carbons and 136.4 ppm for the ring aromatic carbons. The ^{14}N NMR spectrum shows two resonances, N_β ($\delta = -134.1$ ppm) and N_γ ($\delta = -170.1$ ppm). The ^{15}N NMR spectrum shows three resonances three for the azide N_α ($\delta = -306.2$ ppm), N_β ($\delta = -134.4$ ppm) and N_γ ($\delta = -168.9$ ppm).

The structure of hexakis (azidomethyl) benzene was fully optimised and the vibrational frequencies and zero point energy computed using a semiempirical calculation carried out at the semiempirical PM3 level of theory using a VSTO-3G basis set and ab initio at the self consistent HF level of theory using a 6-31G(d) basis set. The fully optimised structure of hexakis (azidomethyl) benzene is shown in figure 3.18

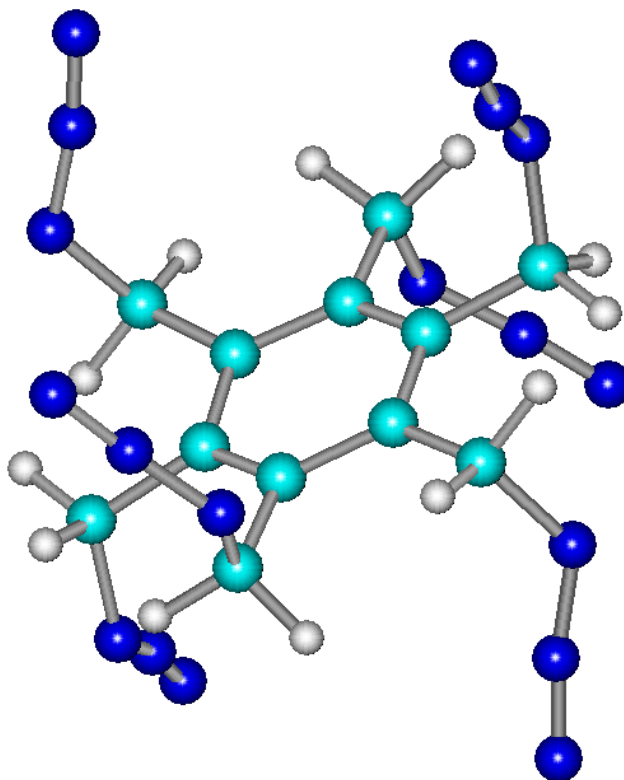
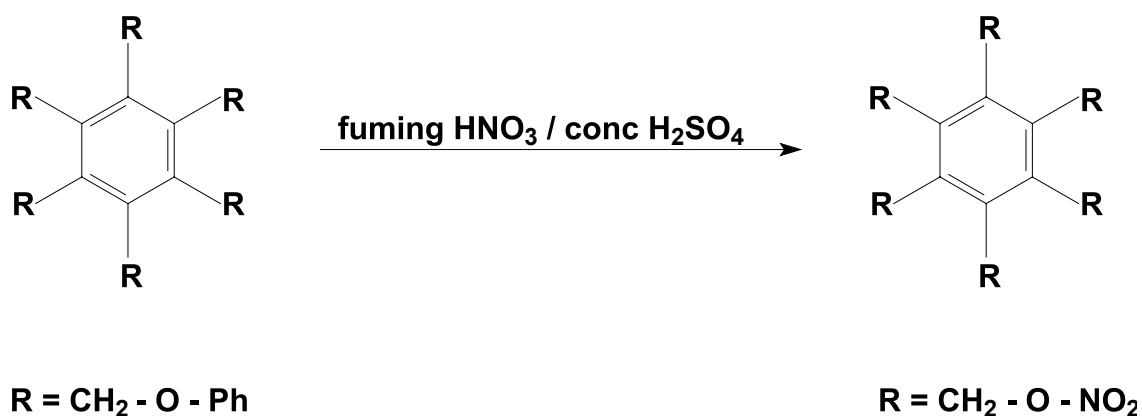


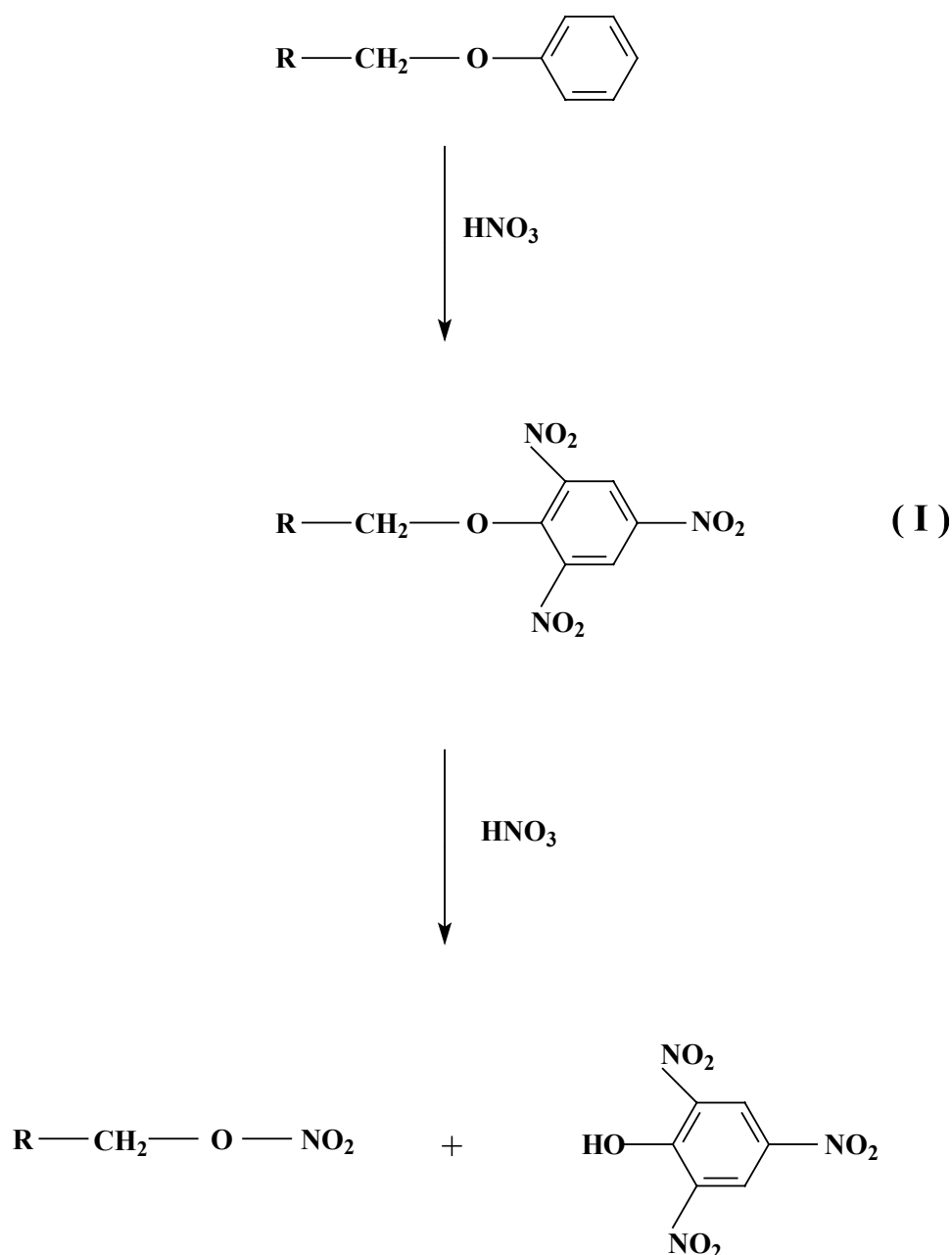
Figure 3.18 Molecular structure of hexakis (azidomethyl) benzene fully optimised at HF/6-31G(d) level of theory.

Hexakis (phenoxy)methyl benzene was chosen as a starting material with the idea of attempting to nitrate several positions on the six external benzene rings. Hexakis (phenoxy)methyl benzene was slowly added to fuming nitric acid over a period of 60 minutes. This solution was stirred for 10 minutes before concentrated sulphuric acid was added dropwise, after this addition was complete the solution was then stirred at room

temperature for 7 days. The acid was then poured onto a ice cooled water and a white solid was precipitated. The precipitate was collected by suction filtration and washed twice with ice cold water. The solid was then dried in a dessicator over phosphorus pentoxide overnight. When the solid was analysed it was found that the product was hexakis (methylnitrate) benzene ($C_6-(-CH_2- O- NO_2)_6$) and not one of the desired products. This reaction was carried out several times changing the reaction conditions *i.e.* reaction time and temperature but the final product was always the same. If the strength of the nitrating agent was reduce *i.e.* using more dilute nitric acid no reaction was observed to occur and the starting material was recovered from the reaction mixture. The scheme for the reaction is shown below.



A proposed mechanism for the reaction of hexakis (phenoxymethyl) benzene with fuming nitric acid to yield hexakis (methylnitrate) benzene is shown in the scheme below. It is proposed that tri-nitration of six external benzene rings initially takes place to yield (I) as an intermediate, but as the picrate group is a strong leaving group, it reacts with acidic proton to form picric acid and the nitrate ion bonds to the CH_2 group to form hexakis (methylnitrate) benzene. It would be useful if the intermediate (I) could be isolated as this was the original target molecule.



Hexakis (methylnitrate) benzene ($\text{C}_6 - (-\text{CH}_2-\text{O}-\text{NO}_2)_6$) was isolated as a white solid with a melting point of 176-177°C. The elemental analysis for the hexakis (methylnitrate) benzene was in agreement with the theoretical values, (found C, 28.90; H, 2.19; N, 15.64 % calculated C, 27.28 ; H, 2.28 ; N, 15.91 %). The IR spectrum showed 2 weak absorptions at 3025 and 2960 cm^{-1} which are characteristic for C-H vibrations in an aromatic ring, a strong absorption at 1644 cm^{-1} for the asymmetric stretching vibration of the C-C bond in the aromatic ring, a strong absorption at 1524 cm^{-1} for the asymmetric stretching vibration of the NO_2 group, a strong absorption at 1348 cm^{-1} for the symmetric stretching vibration of the NO_2 group and a strong absorption at 1280 cm^{-1} for symmetric stretching vibration of the $-\text{O}-\text{NO}_2$ group. The

Raman spectrum also showed two peaks at 3024 and 2960 cm^{-1} which are characteristic for C-H vibrations in an aromatic ring, a peak at 1596 cm^{-1} for the asymmetric stretching vibration of the C-C bond in the aromatic ring, a peak at 1524 cm^{-1} for the asymmetric stretching vibration of the NO_2 group, a strong peak at 1350 cm^{-1} for the symmetric stretching vibration of the NO_2 group and a strong absorption at 1281 cm^{-1} for symmetric stretching vibration of the $-\text{O}-\text{NO}_2$ group.

The ^1H NMR spectrum shows one resonance at 3.08 ppm for the CH_2 hydrogens. The ^{13}C NMR spectrum shows two resonances at 68.4 ppm for the CH_2 carbons and at 136.7 ppm for the ring carbons. The ^{14}N NMR spectrum shows one resonance at -44.3 ppm for the NO_2 group.

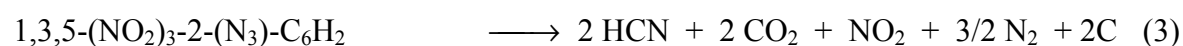
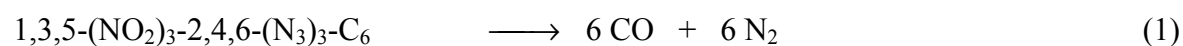
The structure of hexakis (methylnitrate) benzene was fully optimised and the vibrational frequencies and zero point energy computed using a semiempirical calculation carried out at the semiempirical PM3 level of theory using a VSTO-3G basis set and ab initio at the self consistent HF level of theory using a 6-31G(d) basis set. The fully optimised structure of hexakis (methylnitrate) benzene is shown in figure 3.19

Figure. 3.19 Molecular structure of hexakis (methylnitrate) benzene fully optimised at HF/6-31G(d) level of theory.

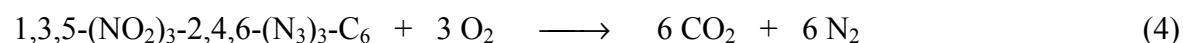
4 Decomposition and Explosion experiments

4.1 Thermal decomposition of TNMA , DNTA and TNTA

The thermal decomposition of three nitrophenyl azides, 1,3,5-(NO₂)₃-2,4,6-(N₃)₃-C₆ (TNTA), 1,3-(NO₂)₂-2,4,6-(N₃)₃-C₆H (DNTA) and 1,3,5-(NO₂)₃-2-(N₃)-C₆H₂ (TNMA) was studied experimentally using gas-phase IR spectroscopy. For the experiments a dry 120 mL stainless steel (T 316 SS) bomb was loaded with 100 mg either of the compounds TNTA, DNTA or TNMA and evacuated. The steel bomb was then heated for 20 mins to 300°C and the reaction products were detected by gas-phase IR spectroscopy. Dinitrogen, N₂, was detected by its characteristic purple gas-phase discharge colour using a high-frequency brush electrode (Tesla coil). The thermal decomposition products shown in eqs. (1) - (3) were all undoubtedly identified by gas-phase IR spectroscopy and gas discharge (N₂). Whereas reaction (1) only yielded CO and N₂, reaction (2) produced in addition to CO and N₂, HCN and traces carbon soot. In reaction (3) HCN, CO₂, NO₂, N₂ and carbon soot were found.



The combustion of 1,3,5-(NO₂)₃-2,4,6-(N₃)₃-C₆ (TNTA) in an O₂ atmosphere (two fold excess) yielded CO₂, N₂, very small amounts of NO₂ and traces of N₂O (eq. 4).



In a further experiment exploring the potential of TNTA as a solid fuel was mixed the material with the stoichiometric amount (*cf.* eq. (5)) of NH₄NO₃ and heated the mixture under vacuum for 20 mins. to 300°C. The reaction products identified by gas phase IR spectroscopy and gas discharge were CO₂, N₂, H₂O and small amounts of N₂O and NO₂ (eq. 5).

No carbon soot was found to be left after the reaction in the steel bomb was complete. The formation of some NO₂ and N₂O in the reaction of TNTA with NH₄NO₃ indicates a relatively

high combustion temperature otherwise the formation of endothermic nitrogen oxides would not be expected, especially since neither NO₂ nor N₂O was detected in reaction (1) (see above).



Thermally all three compounds are stable up to temperatures over 100°C and show only very moderate to low hygroscopy.

In addition to the combustion experiments of TNTA with NH₄NO₃ in a steel bomb under vacuum 1:6 molar ratio mixtures of these two components were ignited under atmospheric conditions and ambient pressure with a magnesium igniter, the mixture detonated violently.

The IR spectra for the decompositions (1-3 , 6, 7 and 8) and combustion experiments (4 and 5) were recorded using a Perkin Elmer 983 high-resolution spectrophotometer and a 10 cm gas cell (p = 2 torr) fitted with KBr plates. The Infra Red spectra for the decompositions (1-3) and combustion experiments (4 and 5) are shown in figures (4.1- 4.5)

Figure 4.1 IR of the gaseous product CO of the thermal decomposition of 1,3,5-(NO₂)₃-2,4,6-(N₃)₃-C₆ (TNTA).

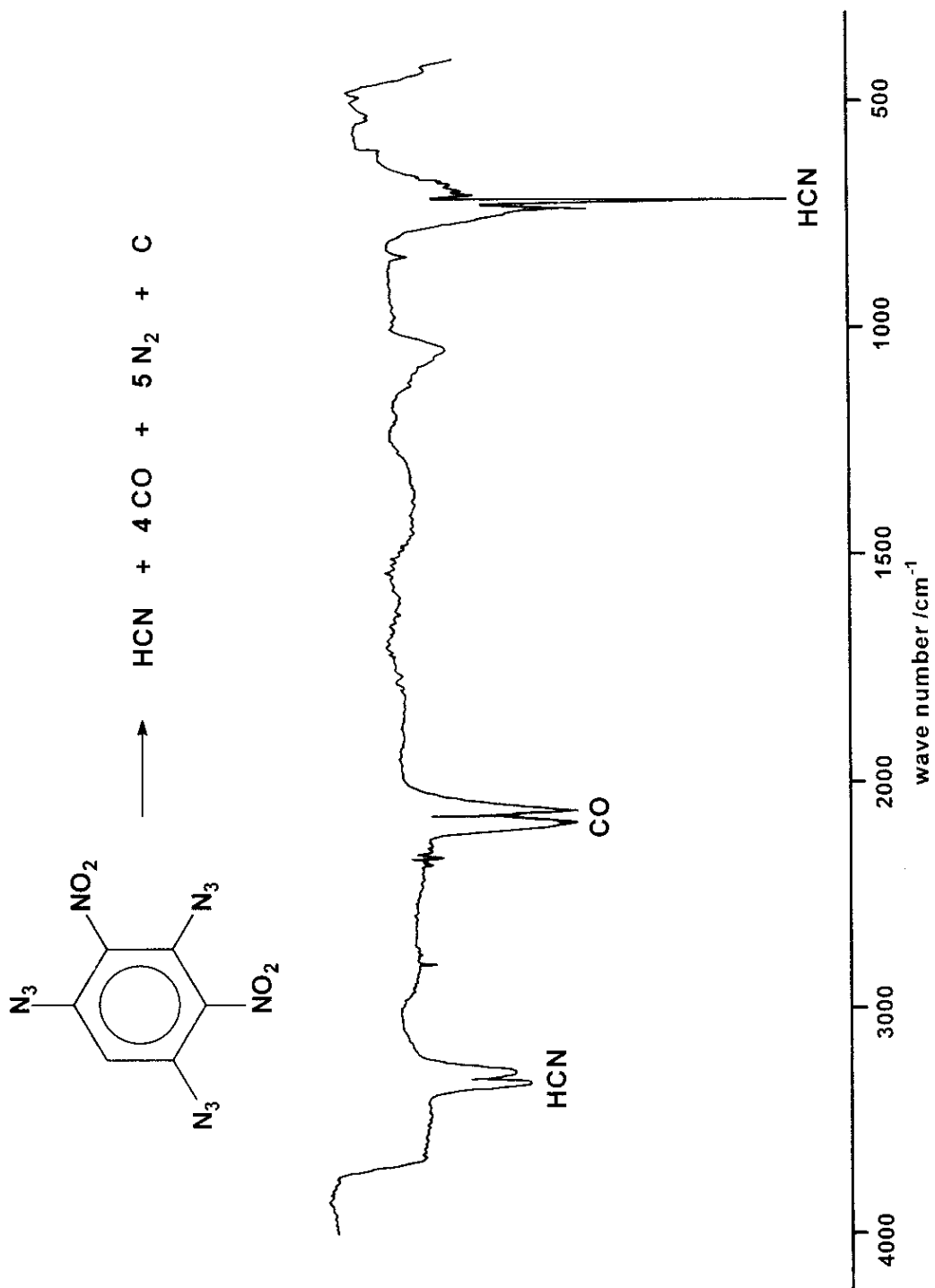


Figure 4.2 IR of the gaseous products of the thermal decomposition of 1,3-(NO₂)₂-2,4,6-(N₃)₃-C₆H (DNTA).

Figure 4.3 IR spectrum of the gaseous products of the thermal decomposition of 1,3,5-(NO₂)₃-2-(N₃)-C₆H₂ (TNMA).

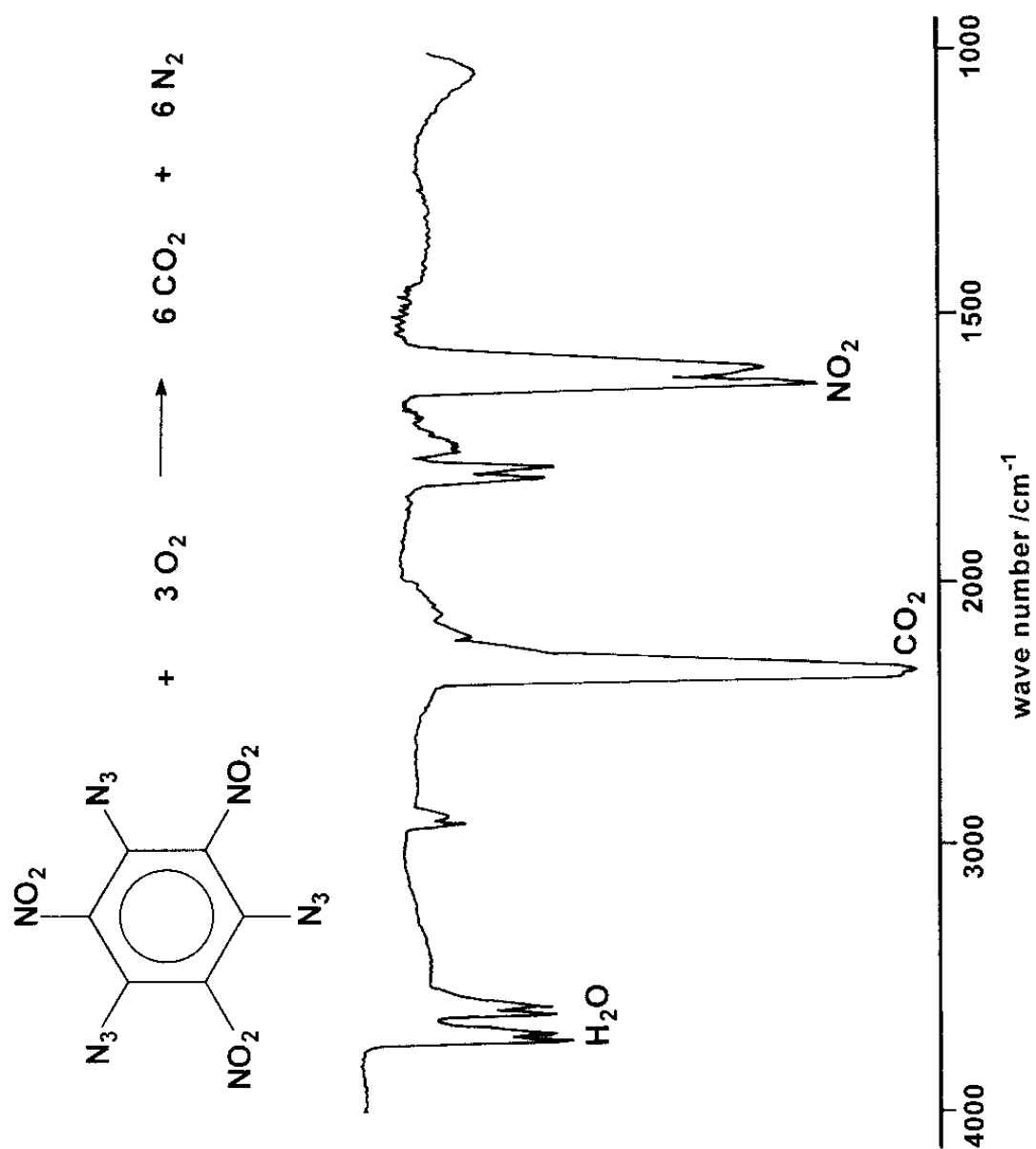


Figure 4.4 IR spectrum for the gaseous products of the combustion of 1,3,5-(NO₂)₃-2,4,6-(N₃)₃-C₆ (TNTA) in an O₂ atmosphere (two fold excess).

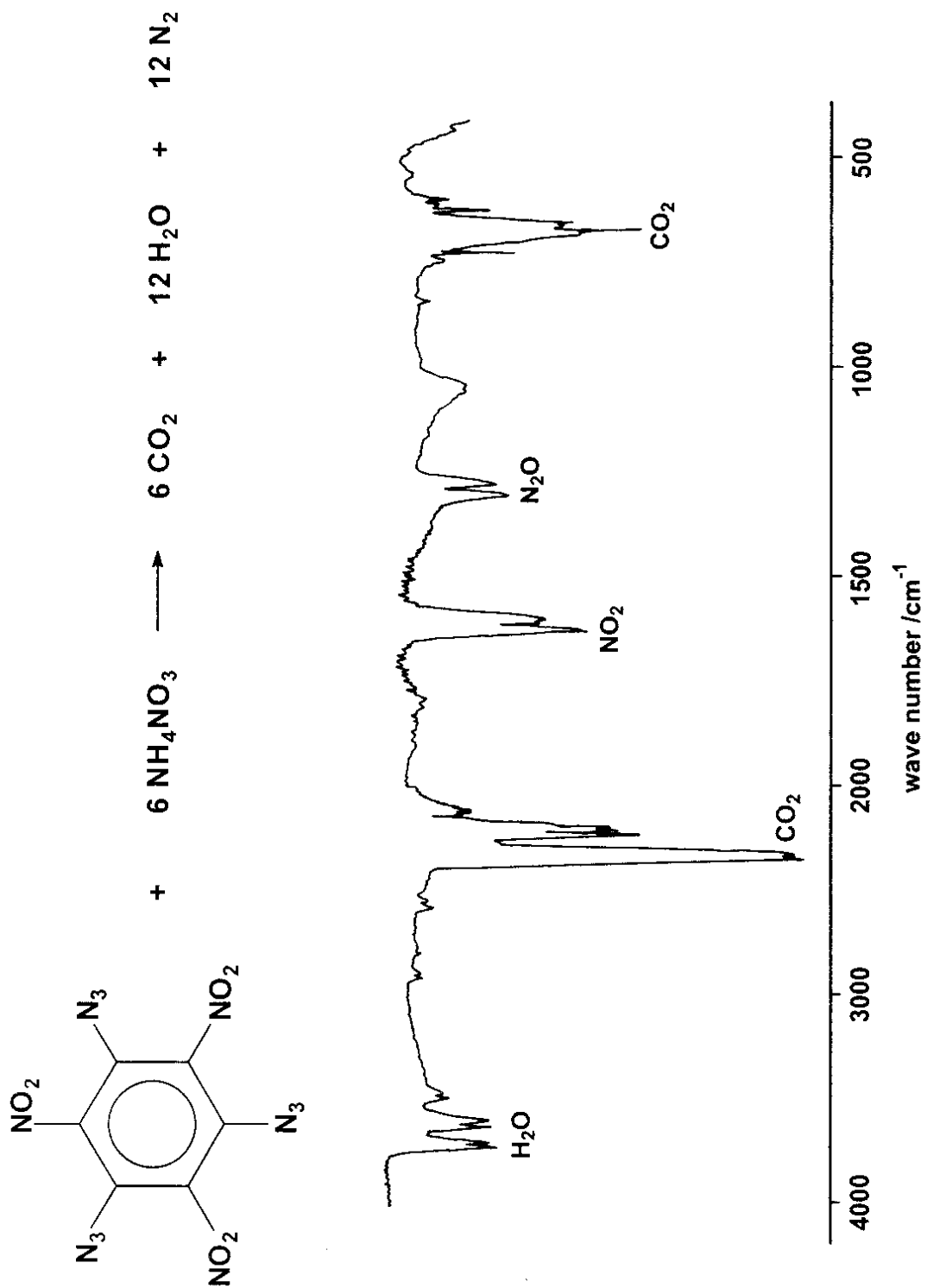


Figure 4.5 IR spectrum of the gaseous products for the combustion of TNTA with NH_4NO_3 at 300°C .

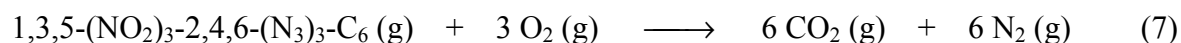
4.2 Computational Aspects

The structures of all compounds considered were fully optimised and the vibrational frequencies and zero point energies computed using semiempirical calculations at the PM3 level of theory (Table 4.1). Finally, more accurate total energies were computed at the fully optimised PM3 structures using the hybrid method at the B3LYP level of theory (Table 4.1).

The calculated total energies (Table 4.1) can be used to predict theoretically the heat of the decomposition reaction of 1,3-5-(NO₂)₃-2,4,6-(N₃)₃-C₆. The heat of reaction (6) was calculated ($\Delta U^{\text{el}} = -368.6 \text{ kcal mol}^{-1}$), which, after correction for zero-point energies (*zpe*, (Table 4.1); $\Delta U^{\text{vib}} = -33.1 \text{ kcal mol}^{-1}$), differences in rotational ($\Delta U^{\text{rot}} = 21/2 \text{ RT}$) and translational ($\Delta U^{\text{tr}} = 33/2 \text{ RT}$) degrees of freedom, and the work term ($p\Delta V = 11 \text{ RT}$), was converted into the ΔH° value at room temperature (enthalpy value): $\Delta H^\circ (6) = -379.2 \text{ kcal mol}^{-1}$.



Since reaction (6) represents the decomposition (and not combustion) of 1,3-5-(NO₂)₃-2,4,6-(N₃)₃-C₆ we also decided to look at the combustion of 1,3-5-(NO₂)₃-2,4,6-(N₃)₃-C₆ in oxygen according to eq. (7).



The calculated total energies (Table 4.1) can be used to predict theoretically the heat of the combustion reaction of 1,3-5-(NO₂)₃-2,4,6-(N₃)₃-C₆ in an oxygen atmosphere. The heat of reaction (7) was calculated ($\Delta U^{\text{el}} = -792.7 \text{ kcal mol}^{-1}$), which, after correction for zero-point energies (*zpe*, Table 4.1; $\Delta U^{\text{vib}} = -20.5 \text{ kcal mol}^{-1}$), differences in rotational ($\Delta U^{\text{rot}} = 15/2 \text{ RT}$) and translational ($\Delta U^{\text{tr}} = 12 \text{ RT}$) degrees of freedom, and the work term ($p\Delta V = 8 \text{ RT}$), was converted into the ΔH° value at room temperature (enthalpy value):

$$\Delta H^\circ (7) = -796.9 \text{ kcal mol}^{-1}.$$

In order to estimate more reliably the energy release with a practically usable oxidiser, we decided to calculate the energy of reaction (8) introducing ammonium nitrate, NH₄NO₃, and using an energy cycle as shown in scheme 1 : $\Delta E^\circ (8) = -883.6 \text{ kcal mol}^{-1}$.

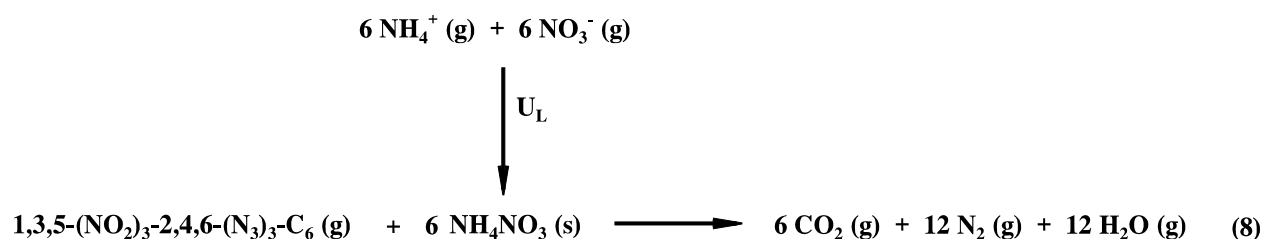
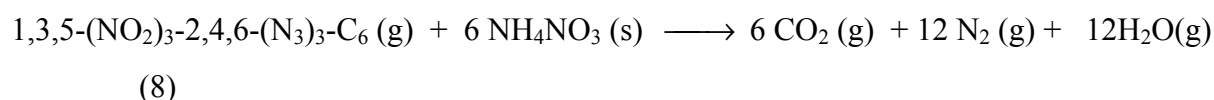
The lattice energy of NH_4NO_3 of $U_L = 157.1 \text{ kcal mol}^{-1}$ (see scheme 4.1) was converted into the lattice enthalpy ΔH_L according to eq. (9) [74]

$$\text{Eq.(9)} \quad U_L(\text{NH}_4\text{NO}_3) = \Delta H_L - [(3/2 - 2) (3/2 - 2)] RT$$

$$\therefore \Delta H(\text{NH}_4\text{NO}_3) = 158.3 \text{ kcal mol}^{-1}$$

with this value ΔE° (8) could be converted into ΔH° (8) = -908.9 kcal mol⁻¹.

The calculated enthalpy value of -908.9 kcal mol⁻¹ makes the 1:6 molar mixture of 1,3,5-(NO₂)₃-2,4,6-(N₃)₃-C₆ and NH_4NO_3 a very promising high energy density material (*HEDM*) the potential of which we are going to explore in more detail in future studies [75].



Scheme 4.1 Energy cycle to estimate the heat of reaction (8).

The total electronic energies for 1,3,5-(NO₂)₃-2,4,6-(N₃)₃-C₆, NH_4^+ , NO_3^- , CO_2 , N_2 and H_2O were taken from the B3LYP/6-31G(d)//PM3/VSTO-3G(d) Computational results (Tab. 4:1).

The lattice energy of NH_4NO_3 was calculated using the linear relationship $U_L = 556.3 V_M^{-0.33} (\text{\AA}) + 26.3$; ¹³ $V_M(\text{NH}_4\text{NO}_3)$ was taken to be equal to 77 \AA^3 , which was estimated from the density in the solid state ($d(\text{NH}_4\text{NO}_3) = 1.720 \text{ g cm}^{-3}$) [76].

Table 4:1 Computed total energies and zero point energies

	$E^{\text{PM3 a}} /$ a.u.	$zpe^{\text{PM3 a}} /$ kcal mol ⁻¹	$-E^{\text{B3LYP b}} /$ a.u.	Symmetry	<i>NIMAG</i> ^c
1,3,5-(NO ₂) ₃ -2,4,6-(N ₃) ₃ -C ₆	0.393316	75.7	1336.412619	C ₁	0
1,3-(NO ₂) ₂ -2,4,6-(N ₃) ₃ -C ₆ H	0.392401	73.5	1131.945568	C ₁	0
1,3,5-(NO ₂) ₃ -2-(N ₃)-C ₆ H ₂	0.137496	71.3	1009.285757	C ₁	0
CO	-0.031502	3.3	113.309436	C _{∞v}	0
N ₂	0.027952	3.8	109.523966	D _{∞h}	0
CO ₂	-0.135584	6.9	188.580425	D _{∞h}	0
NO ₂	-0.003034	6.2	205.069992	C _{2v}	0
HCN	0.052476	10.3	93.422622	C _{∞v}	0
NH ₄ ⁺	0.244454	32.6	56.890763	T _d	0
NO ₃ ⁻	-0.148786	9.7	280.333232	D _{3h}	0
O ₂	-0.006703	3.0	150.316546	D _{∞h}	0
H ₂ O	-0.085159	14.5	76.408066	C _{2v}	0

a fully optimised at the PM3 level of theory using a VSTO-3G(d) basis set,
PM3/VSTO-3G(d)

b B3LYP single point calculation at the fully optimised PM3 structure using a 6-31G(d)
basis set, B3LYP/6-31G(d)//PM3/VSTO-3G(d)

c *NIMAG* = number of imaginary frequencies

4.3 Thermal decomposition of halogen substituted phenyl azides

The thermal decomposition of halogen substituted phenyl azides was studied experimentally using gas-phase IR spectroscopy. For the experiments a dry 120 mL stainless steel (T 316 SS) bomb was loaded with 100 mg of the compound and evacuated. Then the steel bomb was heated for 20 mins to 300°C and the reaction products were detected by gas-phase IR spectroscopy as previously described in this chapter.

The thermal decomposition of 2,4,6-tribromophenyl azide yielded only N₂ and a brown oil remained in the bomb. This experiment was repeated twice more each time increasing the time of heating to 40 and 60 minutes respectively, again both experiments only yielded N₂ and a brown oil remained in the bomb. It was not possible to identify this brown oil either by IR or Raman spectroscopy and attempts to purify it by distillation resulted in a brown tar. The thermal decompositions of 2,4,6-trichlorophenyl azide and 2,4,5-trichlorophenyl azide both yielded HCl, N₂, Cl₂ and carbon soot. The thermal decomposition products shown in eqs. (9) and (10) were all undoubtedly identified by gas-phase IR spectroscopy, gas discharge (N₂) and mass spectrometry. It was also possible to detect the presence of chlorine gas by smell when the bomb was opened.



The thermal decompositions of both 2,4,6-trifluorophenyl azide and 2,3,4,5,6-pentafluorophenyl azide were not carried out as it was noted during their preparation that both compounds decomposed during attempts to purify them by fractional distillation.

4.4 Thermal decomposition of hexakis (azidomethyl) benzene

The thermal decomposition of hexakis (azidomethyl) benzene was studied experimentally using gas-phase IR spectroscopy. For this experiment a dry 120 mL stainless steel (T 316 SS) bomb was loaded with 100 mg of hexakis (azidomethyl) benzene and evacuated. Then the steel bomb was heated for 40 mins to 500°C and the reaction products were detected by gas-phase IR spectroscopy as previously described in this chapter.

The thermal decomposition of hexakis (azidomethyl) benzene yielded HCN, N₂, H₂ and carbon soot. The thermal decomposition products shown in eq. (11) were all undoubtedly identified by gas-phase IR spectroscopy, gas discharge (N₂) and mass spectrometry. The Infra Red spectrum and the mass spectrum of the gaseous products of the thermal decomposition of hexakis (azidomethyl) benzene are shown in figs. (4:6) and (4:7)

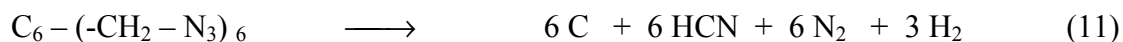


Figure 4.6 Mass spectrum of the gaseous products of the thermal decomposition of hexakis (azidomethyl) benzene.

Figure 4.7 IR spectrum of the gaseous products of the thermal decomposition of hexakis (azidomethyl) benzene.

A possible valence bond (VB) mechanism for the thermal decomposition of hexakis (azidomethyl) benzene $C_6(CH_2-N_3)_6$ is presented in figure 4:8 in which (for clarity) only the decomposition of two of the six $-CH_2 - N_3$ substituents is explicitly shown.

The final decomposition products of this VB mechanism are nicely in accord with the experimentally observed species HCN, N_2 , H_2 and carbon (*cf.* eq 11).

The VB formulations shown in Figure 4:8 exploit the singlet diradical character which is present in 1,3-dipolar molecules , such as the azide substituents in $C_6(CH_2-N_3)_6$ [77].

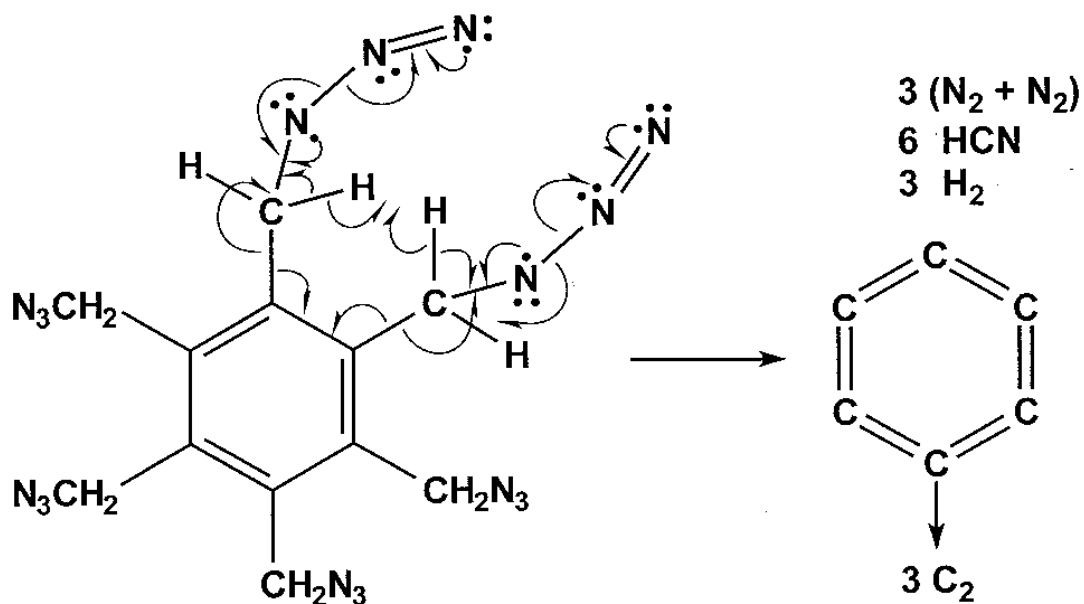
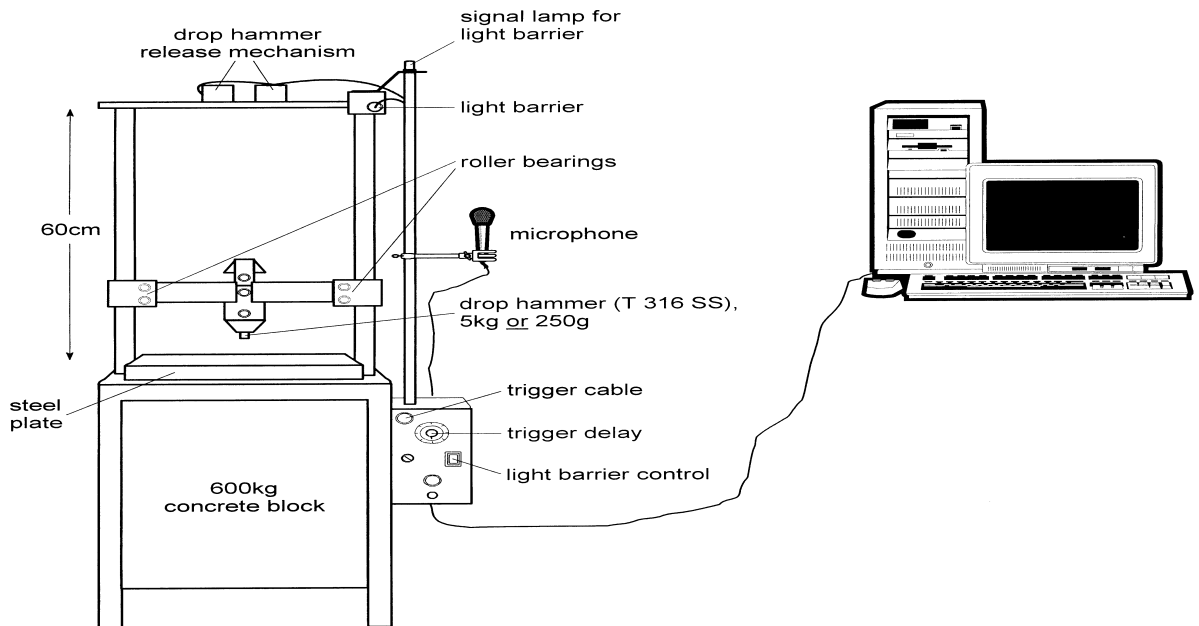


Figure 4.8 Valence bond (VB) mechanism for the thermal decomposition of hexakis (azidomethyl) benzene $C_6(CH_2-N_3)_6$.

4.5 Drophammer Testing of TNMA, DNTA and TNTA

Apparatus

A schematic diagram of the drophammer is shown in figure 4:9. The apparatus is based on a 600 kg concrete block, on top of which a replaceable steel plate for the samples was fixed. A 60 cm height metal frame contains the drophammer release mechanism, the light barrier and a sledge with roller bearings for the drophammer. A small box beside the block contains the electronic devices like the light barrier control and trigger delay. The distance between the microphone (from beyerdynamic, model M101 N(C)) and the impact area was fixed to 140 cm and the distance between the drophammer bottom and the impact area was 52 cm. For all experiments, the Hewlett-Packard HP VEE software, version 4.01 (1997) was used. Two programs have been developed based on this program, one for recording the measurements and the other for the interpretation of the data.



Experimental

The samples for the impact test were dried at 50°C in an oven over night and placed between two sheets of sandpaper (180 grit). The samples were placed directly onto the steel plate in the impact area. For data collection the following parameters were used (for software see above), scan rate: 200 000 , no. of scans 65536, range of voltage ± 1.25 V. The drophammer was finally released from a safe place outside the room with a remote control.

Results

Physical Background

To interpret the measured data it was necessary to adjust the specific data of the microphone used by applying the following physical equations [78].

acoustic intensity: I : acoustic energy, which hits one square metre per second;
unit [W/m^2].

$$\text{acoustic level: } L = 10 \cdot \lg \left(\frac{I}{I_0} \right), \quad \text{unit [dB]} \quad (1)$$
$$I_0 = 10^{-12} \text{ W}/\text{m}^2$$

acoustic pressure

$$\text{level (absolute): } L = 20 \cdot \lg \left(\frac{p}{p_0} \right), \quad p_0 = 2 \cdot 10^{-5} \text{ Pa} \quad (2)$$

specific data of the

$$\text{used microphone: } 1.0 \text{ mV} \quad 0.769 \text{ Pa} \quad (3)$$

These equations (1)-(3) have been integrated into the interpretation program to get the maximum values of voltage, pressure level and absolute acoustic level for each measured explosion.

The order of the acoustic level is $TNMA < DNTA < TNTA$, but the values for DNTA and TNTA are very similar. Even the weakest of the investigated organic explosives (TNMA) is more powerful than AgN_3 or $Pb(N_3)_2$, if the acoustic level is interpreted as somewhat proportional to the detonation power.

The average values of max. abs. acoustic level in [dB] for TNMA, DNTA and TNTA for all weights measured are given in Table 4.2.

The drophammer experiments for 30 mg DNTA and for 20 mg/30 mg TNTA gave a output greater than the detectable range. The results for all other experiments are given in Tables 4.3-4.8.

Table 4.2. Average values of max. abs. acoustic level in [dB] for TNMA, DNTA and TNTA for various weights.

Substance	Amount [mg]	Average value of max. abs. acoustic level [dB]
1,3,5-trinitro-2-monoazidobenzene (TNMA)	10	141.06
	20	149.58
	30	151.96
1,3-dinitro-2,4,6-triazidobenzene (DNTA)	10	147.61
	20	151.24
1,3,5-trinitro-2,4,6-triazidobenzene (TNTA)	10	146.28

Table 4.3 Drophammer tests for 10 mg samples of TNMA

Drophammer 5 kg, 2*Sandpaper 180, TNMA 10 mg
 Scan rate: 200 000
 No. of Scans: 65536
 Voltage Range ± 1.25 V
 2 of 10 samples failed

Sample No.	max. voltage [V]	Max.acoustic pressure [Pa]	max. abs. acoustic level [dB]
1	0.4631	356.2	145
2	0.1566	120.5	135.6
3	0.3642	280.1	142.9
4			
5	0.2897	222.8	140.9
6	0.2683	206.4	140.3
7	0.145	111.5	134.9
8	0.3733	287.2	143.1
9	0.5076	390.5	145.8
10			

Table 4.4 Drophammer tests for 20 mg samples of TNMA

Drophammer 5 kg, 2*Sandpaper 180, TNMA 20 mg
Scan rate: 200 000
No. of Scans: 65536
Voltage Range ± 1.25 V
3 of 25 samples failed.

Sample No.	max. voltage [V]	Max. acoustic pressure [Pa]	max. abs. acoustic level [dB]
1	0.7042	541.7	148.7
2	0.4869	374.5	145.4
3	1.054	810.8	152.2
4	0.9612	739.4	151.4
5	0.703	540.8	148.6
6	0.659	507	148.1
7	0.554	504.1	148
8	0.5528	425.2	146.6
9	0.5076	390.5	145.8
10	0.841	646.9	150.2
11	1.25		
12	1.072	824.9	152.3
13	1.074	825.8	152.3
14	1.136	873.7	152.8
15	0.9612	739.4	151.4
16	1.146	881.2	152.9
17	0.9154	704.2	150.9
18	0.5687	437.4	146.8
19	0.6267	482.1	147.6
20	0.6151	473.1	147.5
21	0.7372	567.1	149.1
22	1.105	850.2	152.6

Table 4.5 Drophammer tests for 30 mg samples of TNMA

Drophammer 5 kg, 2*Sandpaper 180, TNMA 30 mg
Scan rate: 200 000
No. of Scans: 65536
Voltage Range ± 1.25 V
1 of 10 samples failed

Sample No.	max. voltage [V]	Max. acoustic pressure [Pa]	max. abs. acoustic level [dB]
1	0.9185	706.5	151
2	1.25		
3	1.25		
4	1.25		
5	1.25		
6	1.232	947.4	153.5
7	1.204	926.3	153.3
8	0.8684	668	150.5
9	0.9747	749.7	151.5

Table 4.6 Drophammer tests for 20 mg samples of DNTA

Drophammer 5 kg, 2*Sandpaper 180, DNTA 20 mg
Scan rate: 200 000
No. of Scans: 65536
Voltage Range ± 1.25 V
0 of 10 sample failed

Sample No.	max. voltage [V]	Max. acoustic pressure [Pa]	max. abs. acoustic level [dB]
1	0.573	440.7	146.9
2	0.9069	697.6	150.9
3	0.7897	607.4	149.6
4	1.091	839.4	152.5
5	1.25	961.5	153.6
6	0.9942	764.8	151.7
7	0.9307	751.9	151.1
8	1.034	795.8	152
9	0.9509	731.4	151.3
10	0.7738	595.2	149.5

Table 4.7 Drophammer tests for 10 mg samples of DNTA

Drophammer 5 kg, 2*Sandpaper 180, DNTA 10 mg
Scan rate: 200 000
No. of Scans: 65536
Voltage Range ± 1.25 V
1 of 25 samples failed

Sample No.	max. voltage [V]	Max. acoustic pressure [Pa]	max.abs. acoustic level [dB]
1	0.8935	687.3	150.7
2	0.5784	445	146.9
3	0.676	520.6	148.3
4	0.7421	570.8	149.1
5	0.4502	346.3	144.8
6	0.4264	328	144.3
7	0.7897	607.4	149.6
8	0.5437	418.2	146.4
9	0.764	587.7	149.4
10	0.7695	592	149.4
11	0.8684	668	150.5
12	0.8104	623.4	149.9
13	0.6291	483.9	147.7
14	0.7121	547.8	148.8
15	0.5162	397.1	146
16	0.504	387.7	145.7
17	0.7067	543.6	148.7
18	0.7689	591.5	149.4
19	0.6047	465.2	147.3
20	0.5339	410.7	146.2
21	0.5797	445.9	147
22	0.5064	389.5	145.8
23	0.4307	331.3	144.4
24	0.5443	418.7	146.4

Table 4.8 Drophammer tests for 10 mg samples of TNTA

Drophammer 5 kg, 2*Sandpaper 180, TNTA 10 mg
Scan rate: 200 000
No. of Scans: 65536
Voltage Range ± 1.25 V
4 of 25 samples failed

Sample No.	max. voltage [V]	Max. acoustic pressure [Pa]	max. abs. acoustic level [dB]
1	0.3715	285.8	143.1
2	0.6432	494.7	147.9
3	0.5919	455.3	147.1
4	0.5931	456.2	147.2
5	1.026	789.2	151.9
6	0.4887	375.9	145.5
7	0.3678	282.9	143
8	0.3874	298	143.5
9	0.4161	320	144.1
10	0.6841	526.2	148.4
11	0.6126	471.3	147.4
12	0.2183	167.9	138.5
13	0.761	585.4	149.3
14	0.6145	472.7	147.5
15	0.4087	314.4	143.9
16	0.7665	589.6	149.4
17	0.5229	402.2	146.1
18	0.8764	674.1	150.6
19	0.4447	342.1	144.7
20	0.4118	316.8	144
21	0.7079	544.5	148.7

4.6 Calculating the detonation velocity from molecular formula and structure for TNMA , DNTA and TNTA.

The detonation velocities of TNMA, DNTA and TNTA were calculated on the basis of their molecular formulae and structure using the formula evolved by Rothstein [22]. The calculation involved making use of a factor F which can be correlated readily with the detonation velocities D (ms⁻¹).

$$D = \frac{F - 0.26}{0.55}$$

where F is given by

$$F = [100 \times \frac{n[\text{O}] + n[\text{N}] - (\frac{n[\text{H}]}{2n[\text{O}]}) + \frac{A}{3} - \frac{n[\text{B}]}{1.75} - \frac{n[\text{C}]}{2.5} - \frac{n[\text{D}]}{4} - \frac{n[\text{E}]}{5}}{\text{MW}}] - G$$

where

G = 0.4 for liquid explosives , G = 0 for solid explosives

A = 1 if the compound is aromatic , A = 0 otherwise

n[O] = number of oxygen atoms

n[N] = number of nitrogen atoms

n[H] = number of hydrogen atoms

n[B] = number of oxygen atoms in excess of those already available to form CO₂ and H₂O

n[C] = number of oxygen atoms doubly bonded directly to carbon as in carbonyl

n[D] = number of oxygen atoms singly-bonded directly to carbon

n[E] = number of nitrate groups existing either in a nitrate ester configuration or as a nitric acid salt such as hydrazine monnitrate

The calculated factor (F) and detonation velocities (D) for TNMA, DNTA and TNTA are shown in Table 4.9. The calculated detonation velocities (D) are in agreement with the drophammer tests for these compounds *i.e* the values for detonation velocities (D) show $TNMA < DNTA < TNTA$, but the values for DNTA ($9.185 \text{ mm } \mu\text{s}^{-1}$) and TNTA ($9.441 \text{ mm } \mu\text{s}^{-1}$) are very similar.

Table 4.9 Calculated factor (F) and detonation velocities (D) for TNMA, DNTA and TNTA.

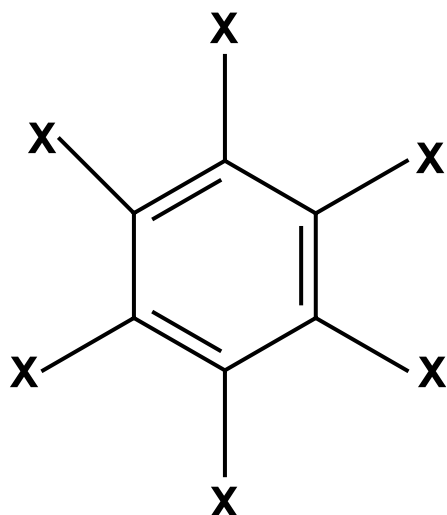
Compound	Formula	Molecular Weight (gmol^{-1})	Factor F	Detonation Velocity ($\text{mm } \mu\text{s}^{-1}$)
TNMA	$\text{C}_6\text{H}_2\text{N}_6\text{O}_6$	254.12	4.786	8.229
DNTA	$\text{C}_6\text{H}_1\text{N}_{11}\text{O}_6$	323.14	5.312	9.185
TNTA	$\text{C}_6\text{N}_{12}\text{O}_6$	336.14	5.453	9.441

4.7 Calculating the detonation velocity from molecular formula and structure for a series of azido and nitro substituted benzenes.

The detonation velocities were calculated using the Rothstein equation (as above) for all possible compounds where a benzene ring is only substituted by either azido or nitro groups. The results of these calculations are shown in table 4.10. It can be concluded from these results that as the number of azido groups on the benzene ring increases the F factor and detonation velocity also increase.

Hexanitrobenzene was the first prepared by Nielsen and co-workers in 1979 [20]. This high-melting, somewhat stable but reactive compound is one of the most energetic explosives known. The density of hexanitrobenzene (2.01 g/cm^3 at 25°C) is the highest reported for any explosive and contributes to its high energetic properties. As hexanitrobenzene is one of the most energetic explosives known today we can predict from these calculations that the other compounds would make good targets as possible explosives if they could be synthesised. The 1,3,5-(NO₂)₃-2,4,6-(N₃)₃-C₆ (TNTA) has been synthesised during this project and the explosive properties of this compound are discussed elsewhere in this thesis.

The calculated F factors and detonation velocities of several commercial explosives are given in table 4.11 for comparison.



where **X = either N₃ or NO₂**

Table 4.10 Calculated detonation velocities from molecular formula and structure for a series of azido and nitro substituted benzenes*

No. of nitro groups	No. of azide Groups	Formula	Molecular Weight (gmol ⁻¹)	Factor F	Detonation Velocity (mm μs ⁻¹)
0	6	C ₆ N ₁₈	324.18	5.654	9.807
1	5	C ₆ N ₁₆ O ₂	328.17	5.585	9.682
2	4	C ₆ N ₁₄ O ₄	332.15	5.518	9.560
3	3	C ₆ N ₁₂ O ₆	336.14	5.453	9.441
4	2	C ₆ N ₁₀ O ₈	340.12	5.389	9.325
5	1	C ₆ N ₈ O ₁₀	344.11	5.326	9.210
6	0	C ₆ N ₆ O ₁₂	348.09	5.267	9.103

* all compounds are assumed to be solids

Table 4.11 Calculated F factors and detonation velocities of several commercial explosives

Abb.	Name	Density (g/cm ³)	Molecular Weight (g mol ⁻¹)	Factor F	Detonation Velocity (mm μs ⁻¹)
HMX	Cyclotetramethylene Tetranitramine	1.90	296	5.24	9.05
RDX	Cyclotrimethylene Trinitramine	1.83	222	5.18	8.95
PETN	Pentaerythritol Tetranitrate	1.77	316	4.71	8.09
TNT	Trinitrotoluene	1.65	227	3.93	6.67
OCTOL	HMX-TNT	1.83	278	4.88	8.40
COMP B-3	RDX-TNT	1.74	221	4.71	8.09

5 Calculations of compounds of the type $C_6(NO_2)_{6-n}(N_3)_n$

In chapters (2 and 3) the experimental (X-ray) and computed structures of the following compounds 2,4,6,tribromophenyl azide, 2,4,6,trichlorophenyl azide, 2,6,di-iodo-4-nitrophenyl azide, 2,4,6-trinitrophenyl azide, and 2,3,4,5,6-pentachlorophenyl azide were compared. The computations were done at the semiempirical PM3 level of theory using a VSTO-3G* basis set and ab initio at the self consistent HF level of theory using a 6-31G(d) basis set. Whereas generally both levels seem to give reasonably good to good agreement with the experimental data especially for the nitro (-NO₂) compounds the HF computed structures and frequencies were found to be better at HF/6-31G(d) level. This gives credence to those predicted structures for compounds where the X-ray data are not yet available due to either poor crystal quality or due to the fact they have not yet been synthesised.

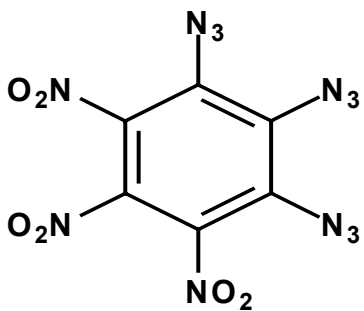
In this chapter we describe the semiempirical PM3 and the ab initio (at the self consistent HF level of theory using a 6-31G(d) basis set) calculations carried out on series of compounds of the type $C_6(NO_2)_{6-n}(N_3)_n$ (with $n = 0, 1 \dots 6$) which have the potential to be use as explosives. We will discuss the total energies (E), the zero point energies (zpe) and optimised structures of all thirteen isomers of compounds of the type $C_6(NO_2)_{6-n}(N_3)_n$. Of the compounds in this series the preparation of hexanitrobenzene was first described by Nielsen and co-workers in 1979 [20]. This high-melting, somewhat stable but reactive compound is one of the most energetic explosives known. The X-ray structure of hexanitrobenzene was reported by Akopyan *et al* in 1966 [18] as noted earlier, this publication preceded any published report bond lengths observed are C-C = 1.39 Å, C-N = 1.45 Å and N-O = 1.23 Å. the benzene ring is planar with coplanar C-N bonds. However each of the nitro groups is twisted out of the plane by 53°. This known X-ray structure will allow us to make a comparison between that structure and the optimised calculated structure for that compound. The chemistry of 1,3,5-triazido 2,4,6 trinitrobenzene is discussed in a previous chapter of this thesis.

The molecular structures of all thirteen isomers of compounds of the type $C_6(NO_2)_{6-n}(N_3)_n$ are displayed in figure 5.1 with the abbreviated and rational names given in table. 5.1.

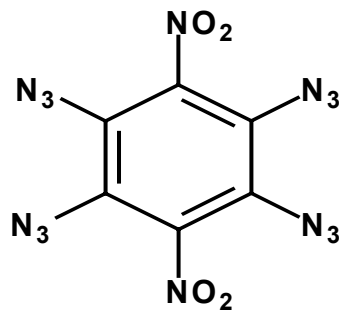
Table 5.1 Abbreviations used in this chapter for all possible isomers of compounds of the type $C_6(NO_2)_{6-n}(N_3)_n$ (with $n = 0,1 \dots 6$).

Abbreviation	Compound Name
HNB	hexanitrobenzene
PNP	pentanitrophenyl azide
DATN1	1,2-diazido 3,4,5,6-tetranitrobenzene
DATN2	1,3-diazido 2,4,5,6-tetranitrobenzene
DATN3	1,4-diazido 2,3,5,6-tetranitrobenzene
TATN	1,3,5-triazido 2,4,6-trinitrobenzene
TATN2	1,2,3-triazido 4,5,6-trinitrobenzene
TATN3	1,2,4-triazido 3,5,6-trinitrobenzene
TADN	2,3,5,6-tetraazido 1,4-dinitrobenzene
TADN2	1,2,3,4-tetraazido 5,6-dinitrobenzene
TADN3	1,3,5,6-tetraazido 2,4-dinitrobenzene
PANB	penta-azidonitrobenzene
HAB	hexa-azidobenzene

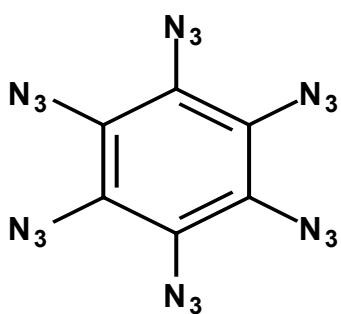
Figure 5.1 Abbreviations and structures of all possible isomers of compounds of the type $C_6(NO_2)_{6-n}(N_3)_n$ (with $n = 0, 1 \dots 6$).



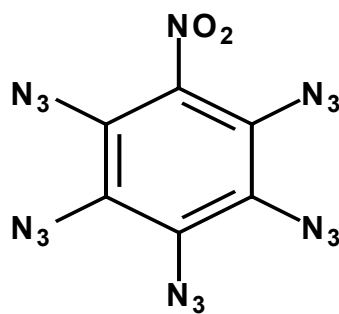
TATN2



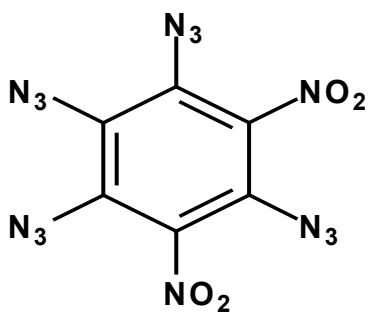
TADN



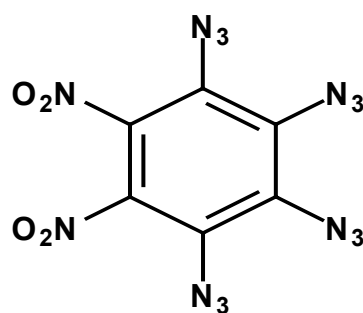
HAB



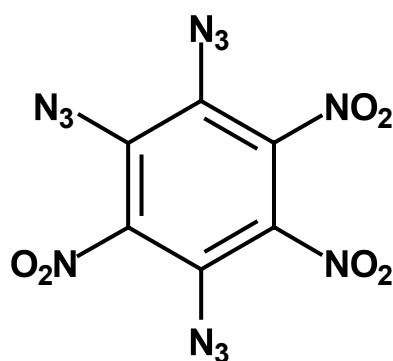
PANB



TADN3



TADN2



TATN3

Table 5.2 shows the PM3 and HF predicted structures, total energies (E) and the zero point energies (zpe) of all possible isomers of compounds of the type $C_6(NO_2)_{6-n}(N_3)_n$ (with $n = 0, 1 \dots 6$). All computed isomers represent true minima (TM, NIMAG = 0) on their potential energy surface.

As can be seen from table 5.2 changing from hexanitrobenzene (HNB) to hexaazidobenzene (HAB) the total energies increase (PM3 : more positive, HF : less negative). As expected between different structural isomers the energies are very similar. For the diazido-tetranitro (DATN) series at HF level the 1,3-diazido isomer is virtually energetically identical to the 1,4 diazido isomer ($\Delta E = 0.05 \text{ kcal mol}^{-1}$) with the 1,2 azido isomer as expected being less stable by $2.1 \text{ kcal mol}^{-1}$. Again as expected for the triazido-trinitro (TATN) series the symmetrically substituted 1,3,5- triazido isomer (TATN) is favoured at HF level by $3.5 \text{ kcal mol}^{-1}$ over the 1,2,3 triazido isomer (TATN2) and by $4.1 \text{ kcal mol}^{-1}$ over the 1,2,4 triazido isomer (TATN3). For the tetra-azido-dinitro (TADN) series the 1,3,5,6 tetra-azido isomer (TADN3) is favoured at HF level by 1 kcal mol^{-1} over the 1,2,3,4 tetra-azido isomer (TADN2) and by $4.3 \text{ kcal mol}^{-1}$ over the 2,3,5,6 tetra-azido isomer (DATN). All molecules predicted in table 5.2 possess true minima on their potential energy surfaces (NIMAG = 0). While all zero-point energy (zpe) values are as expected very similar, for a certain molecule the HF value always lies approximately $1\text{-}2 \text{ kcal mol}^{-1}$ above the PM3 level. This may be attributed to the fact that electron correlation is totally ignored at HF level whereas the PM3 method empirically accounts for some but not all correlation causing lower frequencies and therefore also lower zero-point energy values.

Table 5.2 PM3 and HF predicted structures, total energies (E) and the zero point energies (zpe) of all possible isomers of compounds of the type $C_6(NO_2)_{6-n}(N_3)_n$ (with $n = 0, 1 \dots 6$).

Compound	E^{PM3}	zpe^{PM3}	$E^{HF/6-31G}$	$zpe^{HF/6-31G}$
	a.u.	kcal mol ⁻¹	a.u.	kcal mol ⁻¹
HNB	0.072332	74.7	-1450.518290	75.7
PNP	0.179942	75.0	-1409.785176	76.3
DATN1	0.288921	75.3	-1369.044531	76.4
DATN2	0.290307	75.3	-1369.047888	76.8
DATN3	0.283368	75.4	-1369.047809	76.1
TATN	0.393316	75.7	-1328.307383	76.9
TATN2	0.401888	75.6	-1328.301800	77.0
TATN3	0.404912	75.5	-1328.300768	76.8
TADN	0.517315	75.6	-1287.547243	76.5
TADN2	0.518275	75.7	-1287.552448	77.2
TADN3	0.512806	75.8	-1287.554049	76.9
PANB	0.637025	75.8	-1246.798394	77.3
HAB	0.760377	75.8	-1206.044096	78.0

5.1 Structural Discussion

The structures and energies (see table 5.2) of all thirteen isomers of compounds of the type $C_6(NO_2)_{6-n}(N_3)_n$ have been calculated at semiempirical PM3 and ab initio at HF level of theory. The molecular structures are displayed in figure 5.1 with the abbreviated and rational names given in table 5.1.

Qualitatively, the structures are very similar at PM3 and at HF level of theory. All compounds possess an essentially planar aromatic C_6 backbone which is substituted with nitro ($-NO_2$) and/or azido ($-N_3$) groups. In all compounds both the nitro and azido groups show structural parameters which are in good accord with increased valence bond (VB) considerations. For example, in the symmetrically substituted TATN isomer (HF/6-31G level) the terminal N-N bond in the azide units corresponds with 1.10 Å almost to a triple bond whereas the $N_\alpha-N_\beta$ bond corresponds with 1.27 Å to a very strong single or better a weak double bond [79]. For comparison, typical values for N-N single, double and triple bonds are as follows: 1.45 Å, 1.24 Å and 1.098 Å [80]. The N atoms of the nitro groups lie as it is the case for all NO_2 substituted isomers which are discussed in this thesis within the C_6 plane whereas the two oxygen atoms are rotated above and below the plane, respectively. The N-O bond lengths are with 1.22 – 1.23 Å relatively short and correspond nearly to N=O double bonds with typical N-O single and N=O double bond values being 1.44 Å and 1.20 Å, respectively [80]. It is noteworthy to stress that in this compound all azide groups – though significantly out of the C_6 plane – point to the same direction (*i.e.* all “up” or all “down”).

Whereas - as already stated above - usually the six carbon atoms with the six N atoms directly bound to C form a plane and the two oxygen atoms of the NO_2 groups and the central and terminal N atoms of the azide ($-N_3$) substituents are rotated below and above this plane some of the molecules under investigation show some additional remarkable structural features. The symmetrically substituted TATN has essentially C_s symmetry with the mirror plane being perpendicular to the C_6 plane. The hexaazido derivative (HAB) is nearly a planar molecule with a molecular symmetry very close to C_{6h} . This result may be surprising but both the PM3 and the HF calculation were performed in C_1 without any symmetry constraints and were started in “real” C_1 symmetry with the azide groups being alternating *up* and *down*.

It can generally be stated that the azide groups tend to move more to positions within or close to the C_6 plane whereas the nitro groups are always arranged with a torsion angle of between 45° and 90° (perpendicular) to the C_6 plane. For example, in PNP, all five NO_2 groups are rotated significantly out of the aromatic plane whereas the one N_3 group lies essentially within the C_6 plane. The same is true for DATN2 where again the O atoms of the NO_2 groups are below and above the C_6 plane whereas in this case the two azide units are almost within the C_6 plane. On the other hand, in DATN1 the four NO_2 groups are “out of plane” with one N_3 moiety pointing above and the second one (in *ortho*-position) pointing below the C_6 plane. In the tetraazido dinitro derivative (TADN2) the four azide groups are arranged in an up-down-up-down fashion. Finally, the pentaazido nitro benzene compound has the two azide groups in *ortho* position out of the C_6 plane whereas the remaining three N_3 groups lie still slightly but significantly less out of the plane with a much smaller torsion angle.

The optimised structures of all thirteen isomers of compounds of the type $C_6(NO_2)_{6-n}(N_3)_n$ are shown in figures 5.2 – 5.14.

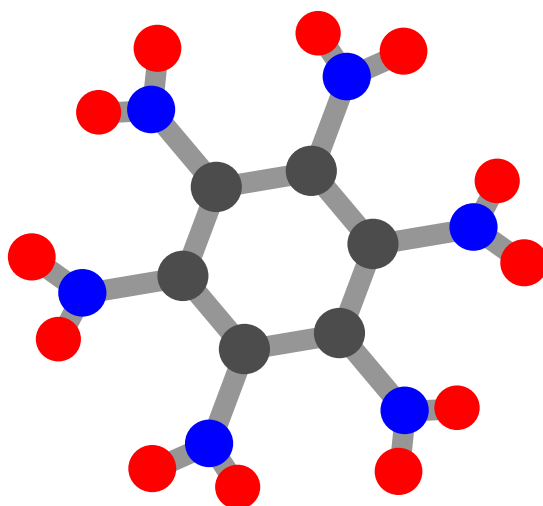


Figure 5:2 Molecular structure of hexanitrobenzene fully optimized at HF/6-31G(d) level level of theory.

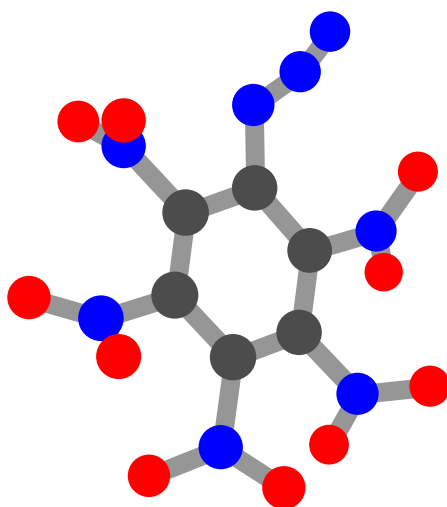


Figure 5.3 Molecular structure of pentanitrophenyl azide fully optimized at HF/6-31G(d) level level of theory.

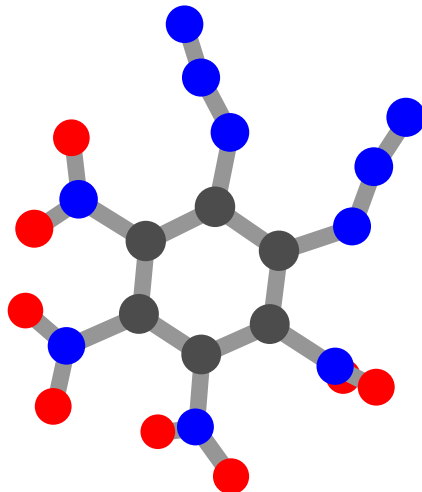


Figure 5:4 Molecular structure of 1,2-diazo 3,4,5,6-tetranitrobenzene fully optimized at HF/6-31G(d) level level of theory

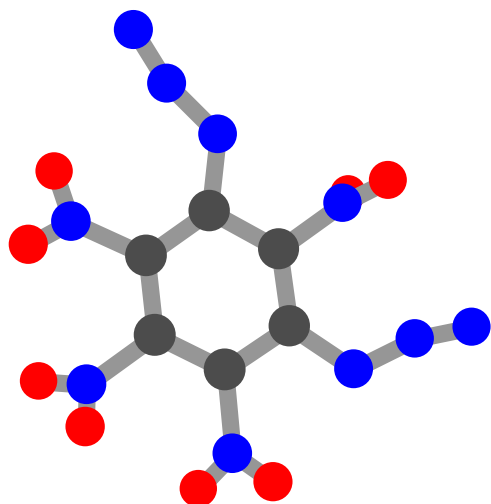


Figure 5.5 Molecular structure of 1,3-diazo 2,4,5,6-tetranitrobenzene fully optimized at HF/6-31G(d) level level of theory.

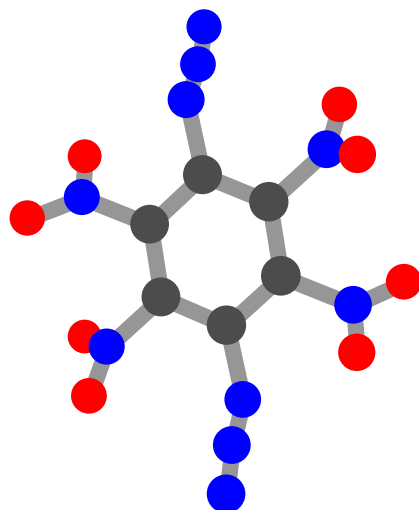


Figure 5.6 Molecular structure of 1,4-diazo 2,3,5,6-tetranitrobenzene fully optimized at HF/6-31G(d) level level of theory.

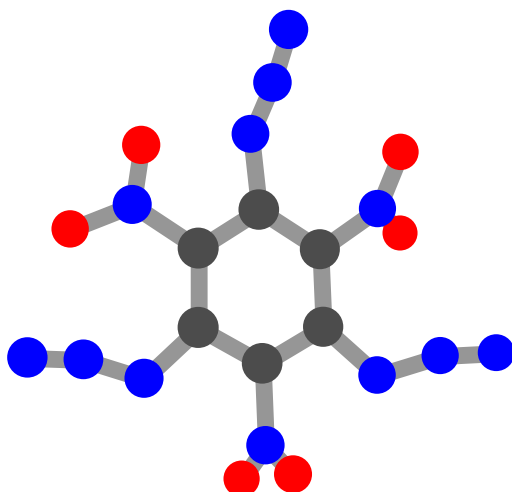


Figure 5:7 Molecular structure of 1,3,5-triazido 2,4,6-trinitrobenzene fully optimized at HF/6-31G(d) level level of theory

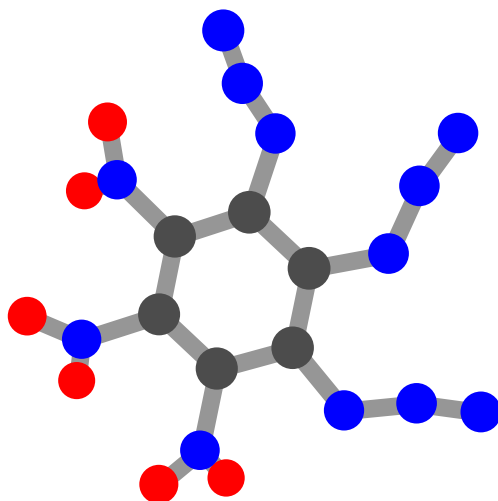


Figure 5.8 Molecular structure of 1,2,3-triazido 4,5,6-trinitrobenzene fully optimized at HF/6-31G(d) level level of theory.

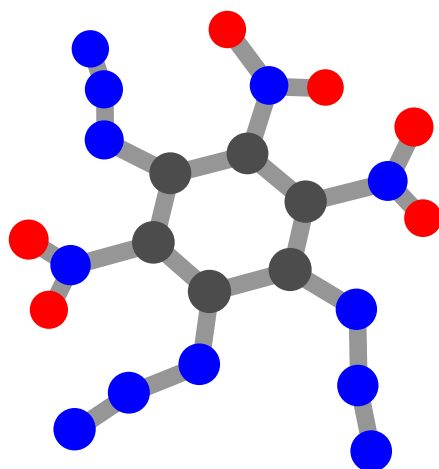


Figure 5.9 Molecular structure of 1,2,4-triazido 3,5,6-trinitrobenzene fully optimized at HF/6-31G(d) level level of theory.

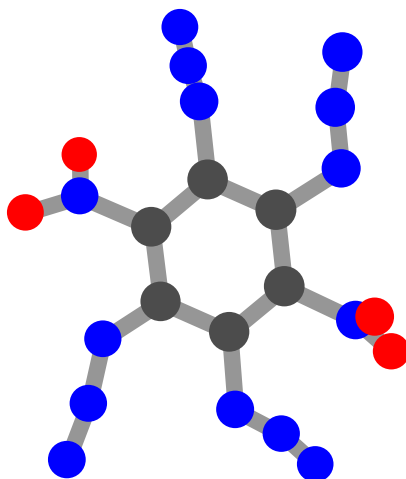


Figure 5.10 Molecular structure of 2,3,5,6-tetra-azido 1,4-dinitrobenzene fully optimized at HF/6-31G(d) level level of theory.

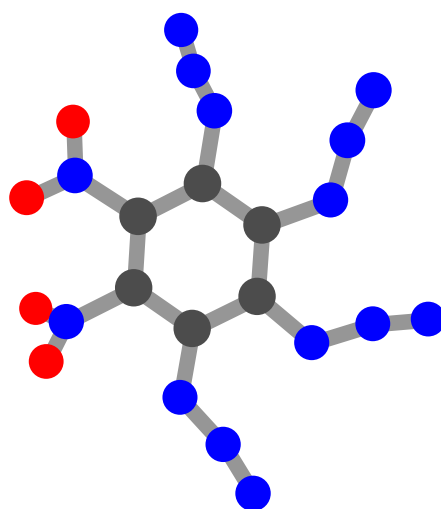


Figure 5.11 Molecular structure of 1,2,3,4-tetra-azido 5,6-dinitrobenzene fully optimized at HF/6-31G(d) level level of theory.

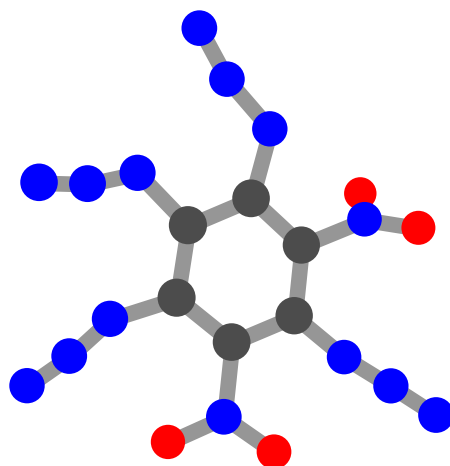


Figure 5.12 Molecular structure of 1,3,5,6-tetra-azido 2,4-dinitrobenzene fully optimized at HF/6-31G(d) level level of theory.

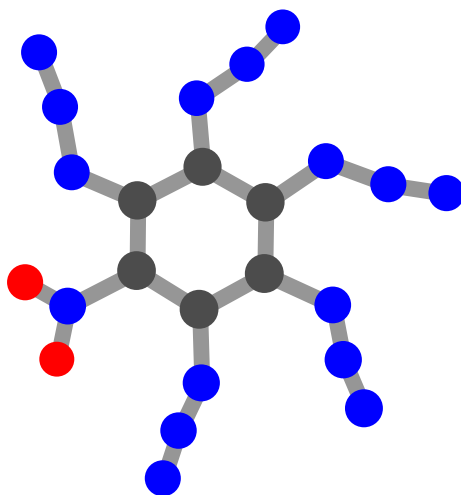


Figure 5.13 Molecular structure of penta-azido nitrobenzene fully optimized at HF/6-31G(d) level level of theory.

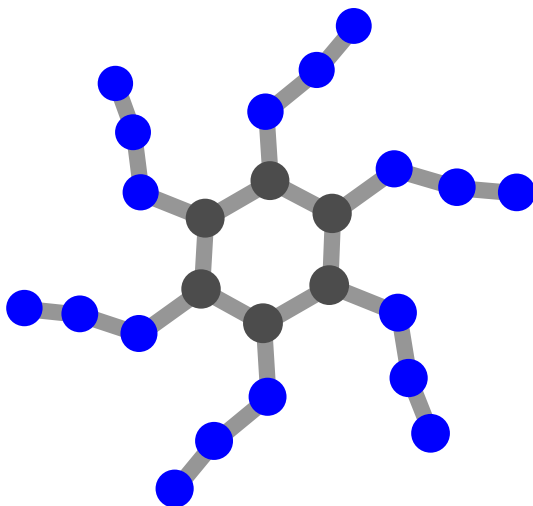


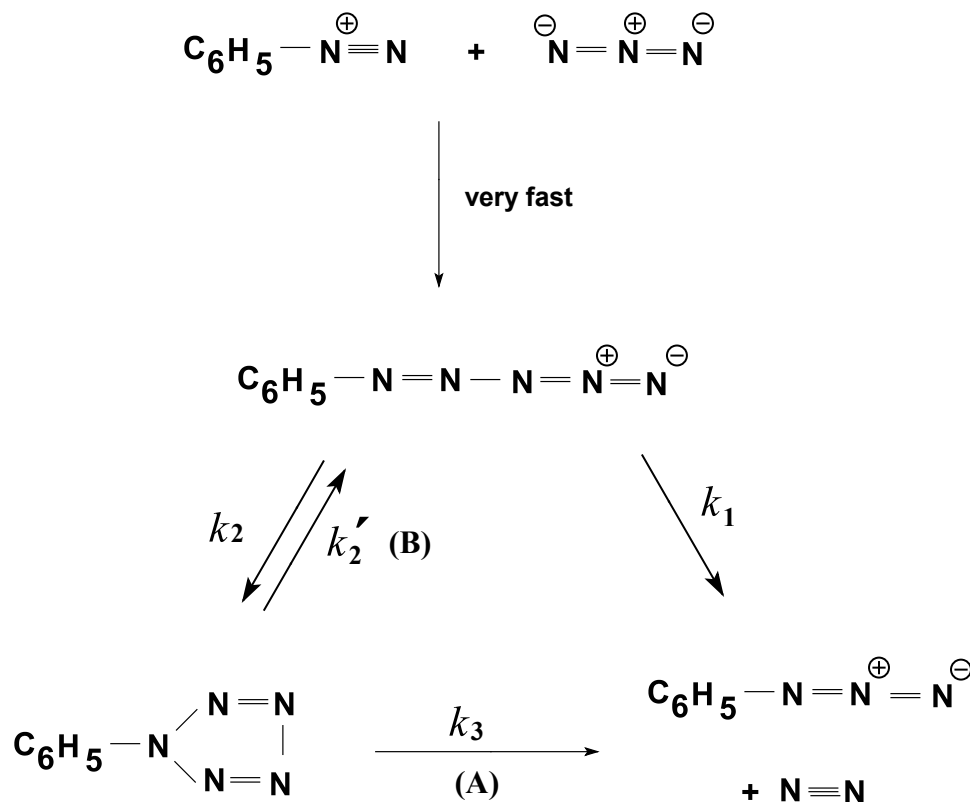
Figure 5.14 Molecular structure of hexa-azido benzene fully optimized at HF/6-31G(d) level level of theory.

6. Pentazoles

As previously described in the introduction of this thesis the thermally unstable product obtained by Huisgen and Ugi in 1957 by the reaction of benzenediazonium chloride with lithium azide in methanol at $-40\text{ }^{\circ}\text{C}$ was formulated as phenylpentazole on the basis of ^{15}N labelling studies (see reaction scheme 6.1 below) [47]. In the main reaction (65%) of the benzenediazo azide decomposes at low temperature (-50°C in methanol) to yield phenyl azide and primary nitrogen, simultaneously the remaining (35%) of benzenediazo azide undergoes ring closure to form phenylpentazole. At 0°C the phenylpentazole decomposes to yield phenyl azide and secondary nitrogen. Using ^{15}N labelled benzenediazonium chloride allowed the determination of the decomposition of phenylpentazole which yielded equal amounts of labelled and unlabelled nitrogen whereas the decomposition of benzenediazo azide only yielded unlabelled nitrogen

Scheme 6.1 Reaction scheme for the reaction of ^{15}N labelled benzenediazonium chloride with lithium azide.

In 1958, Huisgen and Ugi [81] studied the decomposition rates of series of substituted phenylpentazoles. The reaction scheme for the decomposition of the phenylpentazoles is shown below.



The rate of decomposition of the phenylpentazoles can be calculated using the following equation:-

$$k_{\text{(decomp.)}} = \frac{k_2' \times k_1}{k_1 + k_2}$$

The rates of decomposition for series of substituted phenylpentazoles are given in table 6.1 . Huisgen also noted that it had been possible to increase the half-life of phenylpentazole in methanol at 0°C from 13 minutes to nearly 2 hours. They postulated that electron-donating aryl substituents help to make the phenylpentazole more stable whereas electron-withdrawing aryl substituents increase the destabilisation of the phenylpentazole.

Table 61 Rates of decomposition of substituted phenylpentazoles ArN₅ in Methanol at 0°C

ArN ₅ (Ar =)	Rate of Decomposition k 10 ⁴ sec ⁻¹
<i>p</i> -NO ₂ -C ₆ H ₄ -	59 ± 5
<i>m</i> -NO ₂ -C ₆ H ₄ -	36 ± 4
<i>m</i> -Cl-C ₆ H ₄ -	23 ± 1.5
<i>p</i> -Cl-C ₆ H ₄ -	12.1 ± 0.7
C ₆ H ₅ -	8.41 ± 0.2
<i>m</i> -CH ₃ -C ₆ H ₄ -	7.6 ± 0.5
<i>m</i> -OH-C ₆ H ₄ -	7.1 ± 0.3
β- Naphthyl-	6.1
<i>p</i> -CH ₃ -C ₆ H ₄ -	5.6 ± 0.2
<i>p</i> -OH-C ₆ H ₄ -	3.2 ± 0.1
<i>p</i> -C ₂ H ₅ O-C ₆ H ₄ -	3.0 ± 0.2
<i>p</i> -(CH ₃) ₂ N-C ₆ H ₄ -	1.67 ± 0.1

The most stable derivative reported to decompose at 50°C is *p*-dimethylamino pentazole. The X-ray structure of 4-dimethyl-aminophenylpentazole was solved in 1983 by Dunitz and Wallis [48] and to date this is the only known X-ray structure of a pentazole compound. The N-N bond distances in the structure lie in the range 1.30-1.35 Å intermediate between single bonds (1.449 Å) and double bonds (1.252 Å) so the pentazole ring with its 6π electrons can be regarded as aromatic. The theoretical N-N distance of 1.29 Å calculated for the D_{6h} hexazine [48] fits in nicely with the average N-N distance of 1.32 Å in the pentazole. An ORTEP drawing of 4-dimethyl-aminophenylpentazole with the thermal ellipsoids of the C

and N atoms drawn at 50% probability level is shown in figure 6:1, the H atoms have been removed for clarity.

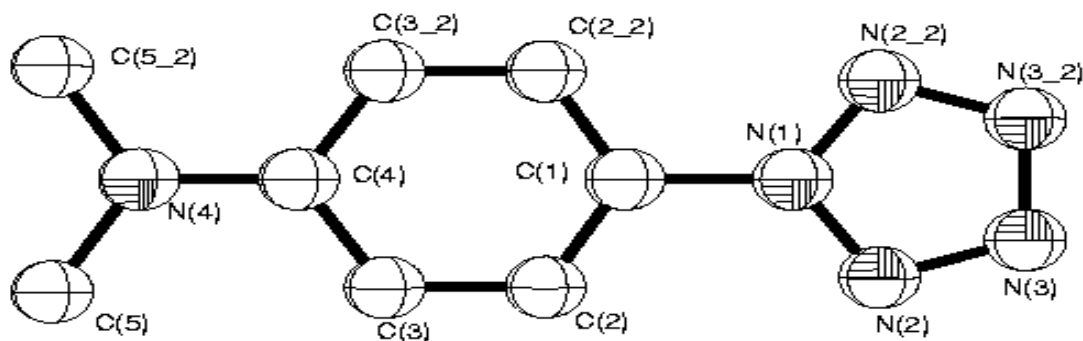


Figure 6.1 ORTEP drawing of 4-dimethyl-aminophenylpentazole with the thermal ellipsoids of the C and N atoms drawn at the 50 % probability level.

In this work, attempts were made to prepare pentazole derivatives using a series of halogen substituted anilines and nitro substituted anilines as starting materials. The anilines used were 2,4,6 tribromoaniline, 2,4,6 trichloroaniline, 2,4,5 trichloroaniline, 2,4, dibromoaniline, 2,4 dichloroaniline, 2,4,6 trifluoroaniline, *o* nitroaniline, *m* nitroaniline and 2,4, dinitroaniline. It was hoped to be able to crystallise the pentazole derivatives prepared and also record ^{14}N NMR spectra of these derivatives. The pentazoles were prepared using either of the two following standard methods:-

Method 1 :- The aniline (0.125 mmol) in water (10 mL) was treated dropwise with conc. hydrochloric acid (2.5 ml) at 0-2°C and sodium nitrite (0.96g, 0.014 mmol) in water (6 mL) was added also at 0-2°C. The solution was then cooled to -20°C and at this temperature a precooled solution of sodium azide (0.9 g, 0.014 mmol) and sodium acetate (1.7 g, 20 mmol) in water (20 mL) was added. After 30 minutes the solid pentazole was filtered off using a filter funnel that had been precooled in liquid nitrogen. The solid collected was then stored in the freezer at a temperature below -20° C.

Method 2 :- The diazonium salt was prepared as previously described and isolated at 0°C.

The diazonium salt (20 mmol) was dissolved in 50mL of water/methanol mixture (2:3), 50mL of petroleum ether (60-80 °C) were added and this solution was stirred at -35° for 20 minutes. Sodium azide (1.73 g, 27 mmol) in water (10mL) was added and the solution stirred for a further 10 minutes. The solid formed was then filtered at -35°C using a precooled filter funnel and stored in the freezer.

The problem with both of the above methods is that when the pentazole is formed, there is also some of the corresponding azide present. It is very difficult and sometimes impossible to separate both of these compounds at low temperatures. On several occasions the filtering of the solid at low temperature proved difficult and the pentazole was lost due to decomposition. For these reasons, when attempting to obtain crystals of the pentazole the solid was dissolved in the crystallising solvent without any attempt to separate the pentazole and azide. The samples were then placed in a freezer at -28°C and stored for several weeks, unfortunately the only crystals obtained were that of the corresponding azide in two of the samples. The other samples had precipitate at the bottom of the sample which on analysis was found to be the corresponding phenyl azide.

The Raman spectra of the isolated pentazoles were recorded at -50°C using a Vantacon cold cell but only very weak signals were observed during the first ten scans corresponding to the pentazole, then after first ten scans the expected peaks for the corresponding azide were observed. The decomposition of the pentazole to the corresponding azide at -50°C in the Raman tube may have been caused by the laser beam striking the sample, as the pentazoles had been stored for several days in the freezer without any decomposition. It was decided to attempt to monitor the preparation of the pentazole by Raman spectroscopy and record the spectra of the pentazole as it was produced. A 10 mm glass tube (similar to 10 mm NMR tube) was placed in the cold cell and cooled to -15°C. The diazonium salt was prepared in the 10 mm tube as previously described. The spectrum of the diazonium salt was recorded and the cell then cooled to -50°C. Whilst recording the spectra the precooled azide solution was added to the tube and five scans after the addition the spectrum of the phenyl azide was observed, the recording of the spectra was continued for a further 30 minutes at which time a spectrum of the phenyl azide similar to those described in previous chapters was observed. The experiment was repeated several times using different substituted anilines as starting materials but the observations were always the same. The Raman spectra of the diazonium salt,

diazonium salt and azide (after 5 scans) and the phenyl azide from a typical experiment are shown in figure 6.2.

Figure 6.2 Raman spectra (1064 nm, 100 mW) of diazonium salt , diazonium salt and azide (after 5 scans) and the phenyl azide.

In 1985 Philipsborn et al [82] reported the first ^{15}N NMR spectrum of a pentazole. They used the most stable pentazole known *p*-dimethylamino pentazole for this experiment. They also used ^{15}N labelled diazonium salt in the preparation where the terminal nitrogen of the diazonium salt was labelled, this yielded *p*-dimethylamino pentazole where the nitrogen in the N2 position of the pentazole ring was labelled.



The ^{15}N NMR spectrum of *p*-dimethylamino pentazole was recorded at -35°C using a solution of 80 mg in 10 mL CDCl_3 and the spectrum of the labelled pentazole was recorded at -20°C using a solution of 25mg in 10 ml CDCl_3 . The ^{15}N NMR spectrum of *p*-dimethylaminopentazole at -35°C showed four signals, one for the $\text{N}(\text{CH}_3)_2$ group ($\delta = -324.6$ ppm), and three for the five nitrogen atoms of the pentazole ring N1 ($\delta = -80.0$ ppm), N2 N5 ($\delta = -27.1$ ppm) and N3 N4 ($\delta = +4.9$ ppm). The sample of *p*-dimethylamino pentazole was warmed up to 25°C and the ^{15}N NMR spectrum recorded again, this showed four signals assigned to the decomposition product *p*-dimethylaminophenyl azide, one for the $\text{N}(\text{CH}_3)_2$ group ($\delta = -335.0$ ppm) and three for the azide N_α ($\delta = -292.7$ ppm), N_β ($\delta = -134.4$ ppm) and N_γ ($\delta = -147.0$ ppm). The ^{15}N NMR spectrum of the labelled pentazole showed the signal for the N2 atom ($\delta = -27.5$ ppm).

In 1996 Butler *et al* [83] reported the first proton and carbon-13 NMR spectra of arylpentazoles and also a proton NMR kinetic study of the influence of substituents on the degradation of pentazole rings. The pentazoles were prepared at temperatures below -10°C by coupling diazonium salts with azide ions following the previously described procedure of Huisgen and Ugi. The pentazoles were soluble in 1:1 (v/v) mixtures of methanol-dichloromethane as suggested previously by Witanowski *et al* [49] and the spectra were measured in this solvent mixture using fully deuterated solvents. Spectra were measured in temperature the range 0 - 15°C where the pentazole was observed to disappear being replaced by the corresponding azide. The chemical shifts were not influenced by temperature or the presence of the azide over the range -40 to 15°C . It proved possible to measure the rates of disappearance of the proton signals for a series of *p*-substituted 1-arylpentazoles at -5°C . These rates were measured for solutions made up at -40°C and raised to -5°C for the kinetic measurements which were reproducible to $\pm 3\%$. Varying quantities of aryl azide

were present in all cases but these did not influence the rates suggesting that the azide is produced in a slow step after the rate-determining step in the degradation of the pentazole. This was important for the rate measurements since they also could not produce solutions of pentazoles which did not contain azides. It was not possible to measure the disappearance of 1(*p*-nitrophenyl) pentazole at this temperature (-5°C) as it was too fast, nor that of 1(*p*-diaminomethyl) pentazole because it was too slow. The behaviour of these two substituted pentazoles readily showed the qualitative substituent trend; strongly electron-donating aryl substituents stabilised the system and slowed the degradation while electron-withdrawing substituents destabilised the ring and enhanced the degradation. The values of the rates of the degradation for this series of *p*-substituted 1-arylpentazoles are in agreement with the results obtained from measurements of nitrogen evolution reported by Huisgen and Ugi [81].

In 1998 Butler *et al* [84] reported further proton NMR experiments and also a further pentazole ^{15}N NMR experiment. They examined the reaction of *p*-chlorophenyldiazonium with the azide ion in the temperature range -80 to -85°C in $\text{CD}_3\text{OD}/\text{D}_2\text{O}$ (4:1 v/v) using 400MHz ^1H NMR and also ^{15}N NMR with samples prepared from ^{15}N labelled *p*-chloroaniline. They use two different techniques to prepared the NMR samples :- (1) the diazonium salt was dissolved in the $\text{CD}_3\text{OD}/\text{D}_2\text{O}$ mixture at -40°C and then cooled in the probe to -90°C , a separate solution of sodium azide in $\text{CD}_3\text{OD}-\text{D}_2\text{O}$ as cooled to -90°C and added dropwise to the NMR tube containing the diazonium solution while still within the probe. (2) this method is similar to the method used in this thesis. The diazonium solution was frozen solid in the NMR tube; the azide solution was then added and also frozen in the NMR tube to allow mixing when the temperature was raised to -85°C . In both the ^1H NMR and ^{15}N NMR it was possible to record the spectra before pentazole signals were present or when the pentazole was in the early stages of formation This was the most important experimental observation as it means pentazole is formed late in the reaction. In all cases the aryl azide was strongly present in the earliest spectra. In early spectra where the pentazole signals were first seen the ratio of pentazole to azide was 1:10 and these changed to a final consistent ratio of 1:4 with time. The results were successfully reproduced many times but in the earliest spectra the resolution was poor due to the fact that dinitrogen gas is being evolved from the solution. The results also showed that the ^{15}N atom remained bonded to aryl group throughout the reaction.

In this work attempts were made to measure the ^{14}N NMR spectra of the pentazoles prepared at -50°C . The solvent used for these measurements was a 1:1 mixture of methanol and dichloromethane as suggested by Witanowski *et al* [49]. When the pentazole was dissolved in

the solution it immediately began to evolve gaseous dinitrogen which indicated that decomposition of the pentazole had started to occur, and this caused problems in recording the spectrum. In these spectra the only peaks observed were those which could be attributed to the corresponding azide and gaseous dinitrogen. There was also a problem transferring the sample at -50°C to the precooled probe, in that the time it took for the auto-sampler to load the sample, most samples had warmed to a temperature at which the pentazole had started to decompose, and again the only peaks observed were those of the corresponding azide and gaseous nitrogen. In order to overcome this problem it was decided to prepare the pentazole in the NMR tube already in the probe. This was done by dissolving the diazonium salt in dichloromethane and placing this solution in the NMR tube and freezing it solid with liquid nitrogen and then the azide solution was added on top and also frozen solid, the NMR tube was then placed in the probe at -50°C . The two layers were allowed to mix in the NMR tube as it obtained equilibrium at -50°C . The ^{14}N NMR spectrum was recorded from the moment the tube was placed in the probe. A method similar to this was also used by Butler *et al* in 1998 [84]. In most of the spectra recorded using this method it was possible to see very small signals in the predicted region for the nitrogen atoms of the pentazole for about 30 minutes, but again the strongest signals belonged to the corresponding azide. The signals in the predicted pentazole region were not much stronger than the noise so we were not able to assign these with any confidence. However in the experiment using the above method for 2,4-dichlorophenylpentazole we were able to see clearly three distinctive signals in the expected range for the nitrogen atoms in a pentazole. This experiment was carried out several times and each time we observed the same spectra. As well as the three signals of the pentazole there are two signals of the 2,4-dichlorophenyl azide present. The spectrum of this experiment can be seen in figure 6.3. When the sample was allowed to warm up to room temperature the three signals for the pentazole disappear but the two signals for the azide remain as can be observed in figure 6.4. The signals can be tentatively assigned in the spectrum of 2,4-dichlorophenylpentazole and 2,4-dichlorophenyl azide as N1 ($\delta = -176.0$ ppm), N2 N5 ($\delta = -72.0$ ppm), N3 N4 ($\delta = -24.0$ ppm) for the pentazole and N $_{\beta}$ ($\delta = -135.0$ ppm) and N $_{\gamma}$ ($\delta = -141.0$ ppm) for the azide. Although the values we obtained for the ^{14}N spectrum of the 2,4-dichlorophenylpentazole are shifted from the values previously reported (see table 6:2) we are certain that the signals have been assigned correctly due to the fact that no other nitrogen-containing substance could be present at -50°C and that the signals disappear as the temperature is raised which is in accordance with the pentazole decomposing to the azide. This is the first reported ^{14}N NMR spectrum of a pentazole.

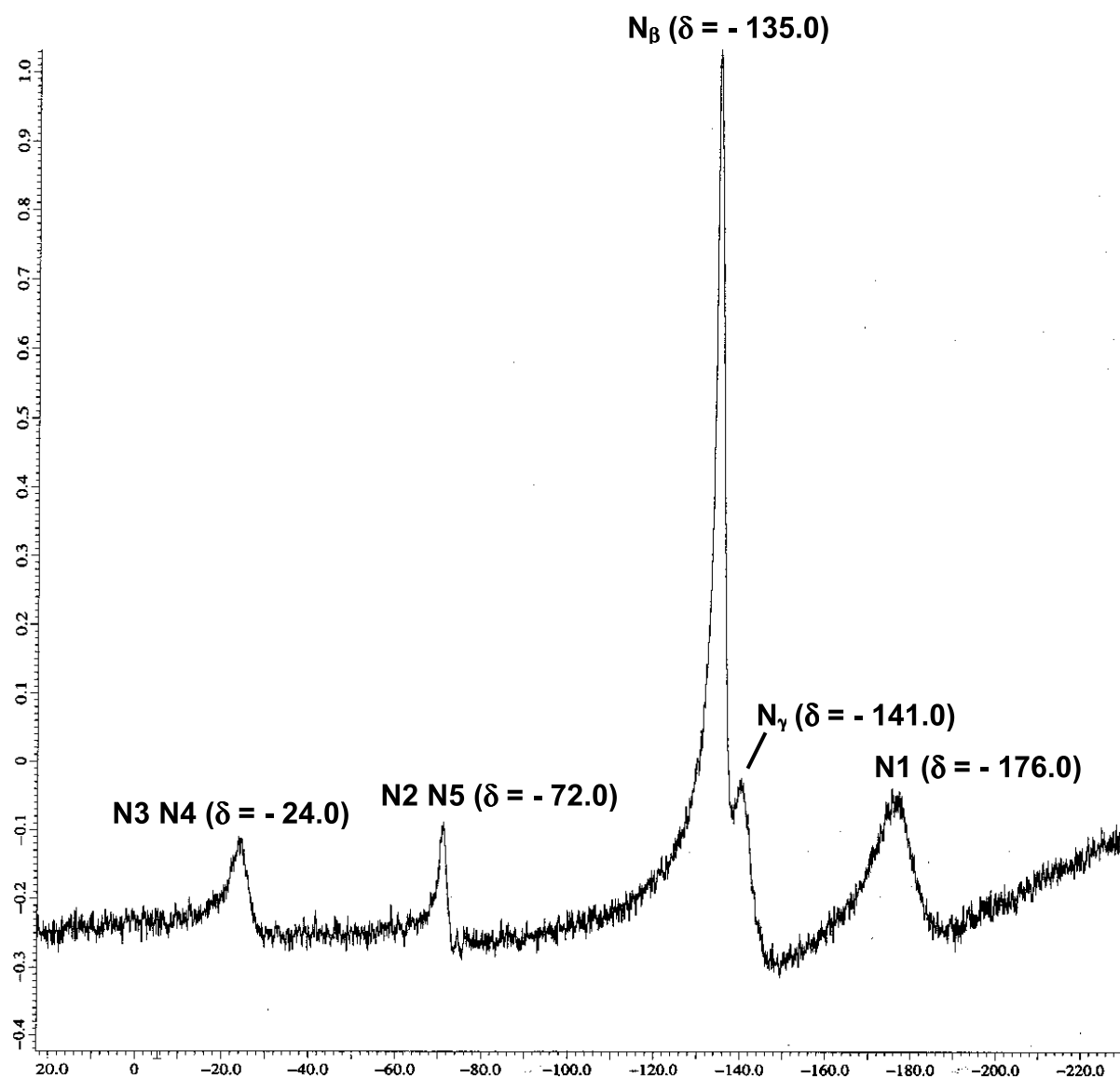


Figure 6.3 ^{14}N NMR (CH_2Cl_2) spectrum of 2,4, dichlorophenylpentazole and 2,4 dichlorophenyl azide at -50°C .

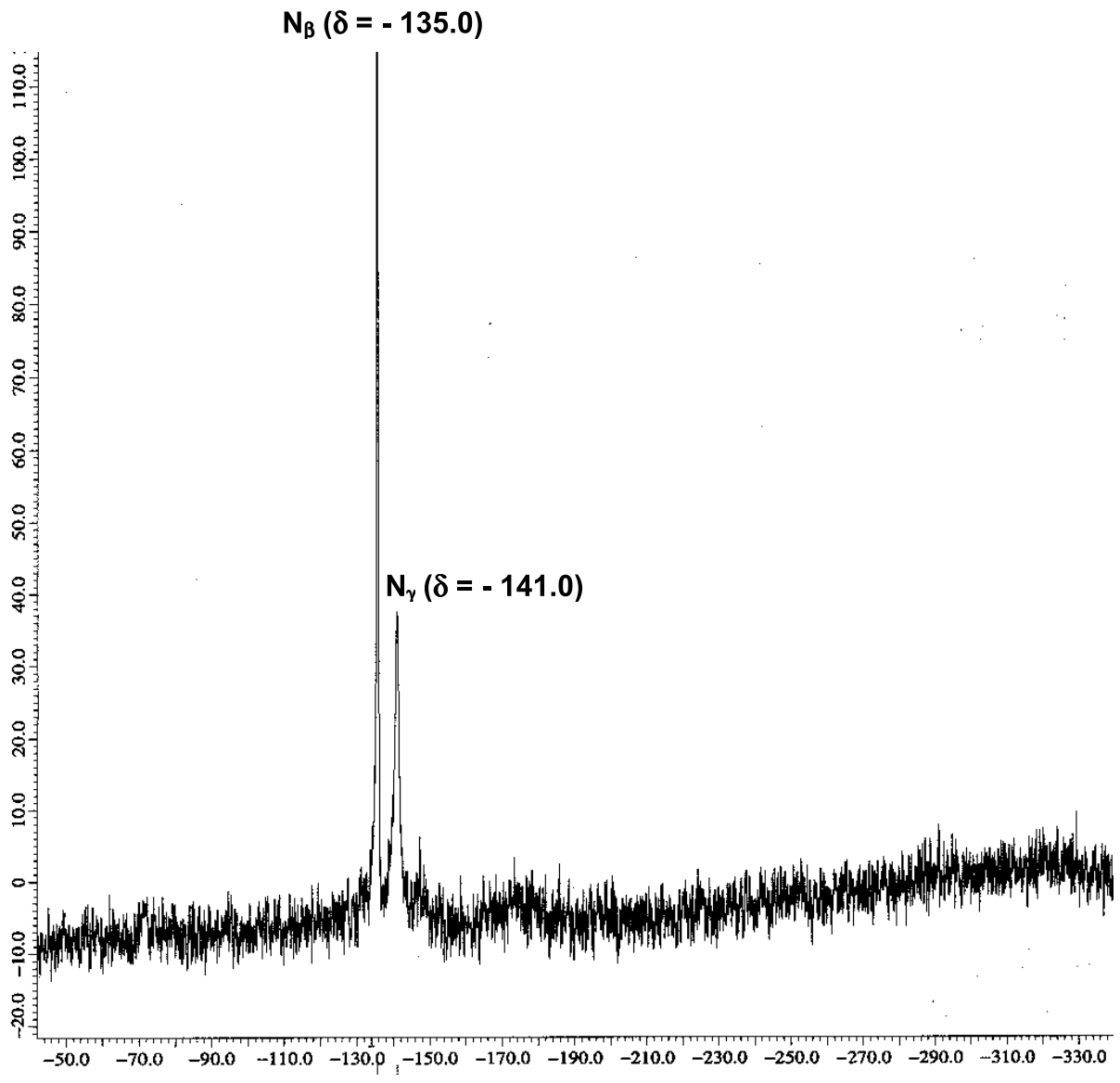


Figure 6.4 ^{14}N NMR (CH_2Cl_2) spectrum of 2,4 dichlorophenyl azide at 25° C.

Table 6.2 Comparison of the reported $^{14}\text{N}/^{15}\text{N}$ chemical shifts for pentazoles.

	N1 (δ / ppm)	N2 N5 (δ / ppm)	N3 N4 (δ / ppm)
Phenylpentazole ⁽¹⁾	-75 \pm 9	+7 \pm 15	-13 \pm 14
4-dimethylaminophenylpentazole ⁽²⁾	-80.0	-27.1	+ 4.9
4-dimethylaminophenylpentazole ⁽³⁾ (^{15}N labelled)		-27.5	
<i>p</i> -chloropentazole ⁽⁴⁾	-82.7		
2,4 dichloropentazole ⁽⁵⁾	-176.0	-72.0	-24.0

- (1) values predicted by Witanowski *et al* 1975 [49]
- (2) Philipsborn *et al* 1985 [82]
- (3) Philipsborn *et al* 1985 [82]
- (4) Butler *et al* 1998 [84]
- (5) this work

The interest of the quantum chemists in pentazoles was initiated by Ferris and Bartlett [85] when they asked the question *Hydrogen Pentazole, Does It Exist ?* They employed ab initio calculations such as *n*th order many-body perturbation theory, MBPT(*n*) whose better known variant is the *n*th order Møller-Plesset perturbation theory, MP*n*. The MBPT(*n*) procedure takes account of all terms to a predetermined final order *n* for the electron correlation. In the coupled cluster (CC) theory, on the other hand certain contributions from the MBPT formalism are summated for all order *n*. Use of the DZP basis set with these procedures yielded the anticipated structural parameters for cyclic HN₅ with C_{2v} symmetry and proof that it represents a minimum on the energy hypersurface. The energy barrier for potential decomposition into HN₃ and N₂ was given at MBPT(2) level as 19.8 kcal mol⁻¹. The question in the above reference *Does it exist* can, of course not yet be answered on these grounds alone. In 1993 Janoschek [86] calculated the kinetic stability of hydrogen pentazole using similar computational methods such as HF, MP2, MP4 and CCSD. The results of these calculations

are given in table 6.3. The height of the activation barrier would suggest that hydrogen pentazole could potentially be detected under gas-phase conditions.

Table 6:3 The activation barrier ΔE (kcal mol⁻¹) incorporating the zero-point vibrational correction for the decomposition $\text{HN}_5 \rightarrow \text{HN}_3 + \text{N}_2$ calculated with several methods.

Method	ΔE (kcal mol ⁻¹)
HF 6-31G*	36.9
MP2 6-31G*	13.7
MP4 6-31G*	18.9
MBPT(2) DZP [7]	19.8
CCSD 6-31G*	20.9

The structures of phenyl pentazole and phenyl azide were fully optimised and the vibrational frequencies and zero point energies computed using semiempirical calculations at the PM3 level of theory, more accurate total energies were computed at BLYP/6-31G(d) level of theory. The calculated total energies can be used to predict theoretically the heat of the decomposition of phenyl pentazole to phenyl azide and nitrogen (as shown in the equation below).

The heat of decomposition for the above reaction was calculated ($\Delta E^{el} = -38.6 \text{ kcal mol}^{-1}$), which, after correction for zero-point energies; differences in rotational ($\Delta U^{rot} = RT$) and translational ($\Delta U^{tr} = 3/2 RT$) degrees of freedom, and the work term ($p\Delta V = RT$), was converted into the ΔH° value at room temperature (enthalpy value): $\Delta H^\circ [\text{BLYP/6-31G(d)}] = -39.6 \text{ kcal mol}^{-1}$.

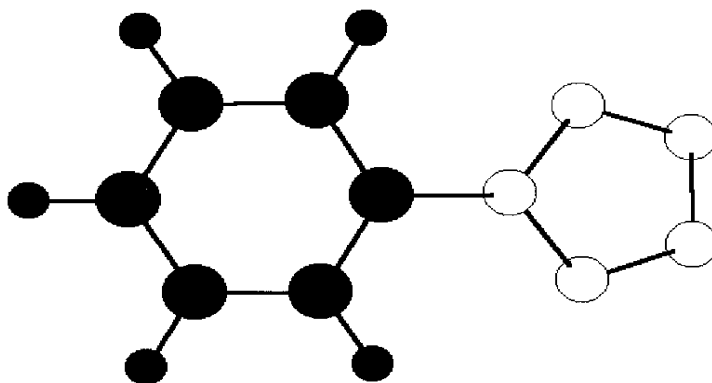


Figure 6.5 Molecular structure of phenylpentazole fully optimised at BLYP/6-31G(d) level of theory.

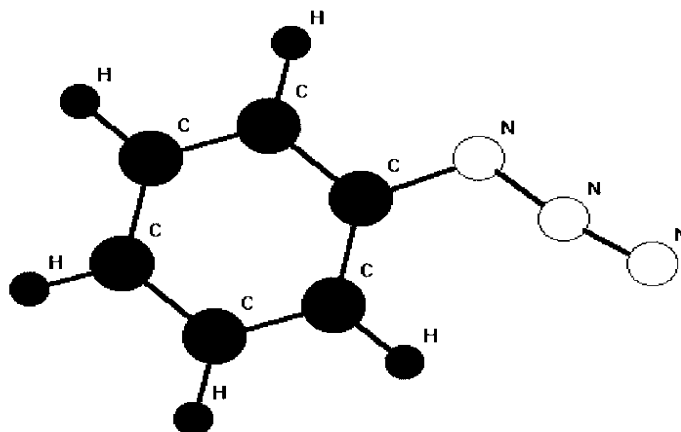


Figure 6.6 Molecular structure of phenyl azide fully optimised at BLYP/6-31G(d) level of theory.

It can be seen that the calculated bond lengths and angles for the pentazole ring in phenylpentazole at BLYP/6-31G(d) level of theory compare favourable with the x-ray structure determination of 4-dimethyl-aminophenylpentazole by Wallis and Dunitz [48] . A comparison of both compounds is shown in table 6.4.

Table 6.4 Comparison of the bond lengths (Å) and angles (°) of the x-ray structure of 4-dimethyl-aminophenylpentazole and the calculated structure of phenyl pentazole at BLYP/6-31G(d) level of theory.

	Phenyl pentazole BLYP/6-31G(d)	X-ray 4-dimethyl- aminophenylpentazole [48]
C – N1	1.436	1.438
N1-N2	1.357	1.321
N2-N3	1.314	1.309
N3-N4	1.376	1.347
N4-N5	1.314	1.309
N5 N1	1.357	1.321
N2-N1-N5	111.33	112.1
N2-N3-N4	109.20	108.8
N1-N2-N3	105.12	105.8

7 Experimental

7.1 Symbols and abbreviations

Symbol/Abbreviation	Description	Units
ν	Wavenumber	cm^{-1}
δ	Chemical shift	ppm
J	Coupling constant	Hz
m/z	Mass/charge ratio	m/e
RT	Room temperature	
xs	Excess	
s	singlet (NMR) strong (IR)	
m	multiplet (NMR) medium (IR)	
w	weak	
vw	very weak	
t	triplet	
TMS	tetramethylsilane	
Mpt	melting point	$^{\circ}\text{C}$
ν_s	symmetric vibration	
ν_{as}	asymmetric vibration	
Mo-K α	Molybdenum radiation	
M	Molar	1M = 1mol L $^{-1}$

7.2 SI and non SI units used in this thesis

Entity	Symbol	Unit	Conversion into SI units
Length	Å	Angstrom	$1 \text{ Å} = 10^{-10} \text{ m}$
Temperature	°C	° Celsius	$^{\circ}\text{C} = \text{K} - 273.1$
Pressure	bar atm	Bar Atmosphere	$1 \text{ bar} = \text{N/m}^2$ $= \text{kg/ms}^2$
Time	min h	minute hour	$1 \text{ min} = 60\text{s}$ $1 \text{ h} = 3600\text{s}$
Wavenumber	cm^{-1}	Wavenumber	
Energy	eV Cal a.u. H	Electron volt calorie atomic units Hartree	$1 \text{ eV} = 1.6022 \cdot 10^{-19} \text{ J}$ $1 \text{ H} = 27.2 \text{ eV}$ $= 627.089 \text{ kcal/mol}$ $= 2622.5 \text{ kJ/mol}$
Angle	∠	Degree	deg°

7.3 Analytical Techniques and Instruments used

Analytical Technique	Instrument
^1H NMR Spectroscopy (ref. TMS)	Jeol 270MHz/400MHz NMR Spectrometers
^{13}C NMR Spectroscopy (ref. TMS)	Jeol 270MHz/400MHz NMR Spectrometers
^{14}N NMR Spectroscopy (ref. MeNO_2)	Jeol 400MHz NMR Spectrometer
^{15}N NMR Spectroscopy (ref. MeNO_2)	Jeol 270MHz NMR Spectrometer
^{19}F NMR Spectroscopy (ref. CFCl_3)	Jeol 400MHz NMR Spectrometer
IR Spectroscopy	Perkin-Elmer 983G Spectrometer
Raman Spectroscopy	Perkin-Elmer R2000 spectrometer
C, H, N Analysis	L.M.U. analytical service
Melting Point determination	Büchi Melting Point B-540
X-ray structure determination	CAD4 Enraf-Nonius diffractomer Siemens SMART Area detector

All NMR spectra were determined in CDCl_3 at room temperature unless otherwise stated. IR spectra were determined as either KBr discs or as Nujol mulls. Not all melting points were measured due to the explosive nature of these compounds.

7.4 Chemicals used in this project.

Chemical	Source	Purification
2,4,6 – tribromoaniline	Aldrich	
glacial acetic acid	Grüssing	
sulphuric acid (conc)	Riedel de Haen	
sodium nitrite	J.T. Baker	
urea	Fluka	
sodium azide	Fluka	recryst. from methanol
2,4,6 – trichloroaniline	Aldrich	
2,4,5 – trichloroaniline	Aldrich	
2,4, dibromoaniline	Aldrich	
2,4- dichloroaniline	Aldrich	
2,4,6 – trifluoroaniline	Aldrich	
sodium carbonate	Fluka	
magnesium sulphate	Aldrich	dried 150°C
nitrosyl chloride	Prepared by Prof Klapötke	
pentafluorophenylhydrazine	Fluorochem	
p-methoxyaniline	Aldrich	
2,6 diiodo-4 nitroaniline	Aldrich	
o-nitroaniline	Aldrich	
m-nitroaniline	Synchemica	
2,4, dinitroaniline	Aldrich	recryst. from ethanol
nitric acid (fuming)	Fluka	
3,5 – dinitroaniline	Aldrich	

dinitrogen pentoxide	Prepared by Dr J.Geith
1,3,5 trichlorobenzene	Aldrich
phosphorus pentoxide	Grüssing
Hexakis (phenoxy)methyl Benzene	Donated by Dr. D. D. MacNicol (University of Glasgow)
Hexakis (bromomethyl) Benzene	Donated by Dr. D. D. MacNicol (University of Glasgow)

Solvents used in this project

Solvent	Source	Method use to dry solvent
Chloroform	Merck	Molecular sieves
Dimethyl sulphoxide	Bayer	Molecular sieves
Deuterated Chloroform	Merck	Molecular sieves
Dichloromethane	Riedel de Hæn	CaH ₂
Acetone	Merck	Molecular sieves
Deuterated Acetone	Merck	Molecular sieves
Methanol	Merck	Na
Ethanol	Merck	Na
Ether	Merck	Na
Dimethyl formamide	Bayer	CaH ₂
Dichloroethane	Riedel de Hæn	Molecular sieves
Carbon tetrachloride	Merck	P ₄ O ₁₀
Hexane	Riedel de Hæn	Na

Thermal decomposition experiments

The thermal decomposition experiments required the use of a metal vacuum line. The metal vacuum line is constructed of a metal which is unreactive, in this case a Monel line is used. The metal vacuum line has a steel pressure gauge fitted allowing us to measure the amount of gas produced during decomposition reaction. The vacuum line also has 6 mm Whitey valves to connect the reaction vessels and gas cell to the line (see figure 7:1). For the thermal decomposition experiments a dry 120 mL stainless steel (T 316 SS) bomb was loaded with 100 mg of compound. The stainless steel bomb was then connected to a metal vacuum line and evacuated. The steel bomb was then heated with a hot blast for 20 mins to 300°C and the reaction products were detected by gas-phase IR spectroscopy. The IR spectra were recorded using a Perkin Elmer 983 high-resolution spectrophotometer and a 10 cm gas cell (p = 2 torr) fitted with KBr plates. Dinitrogen, N₂, was detected by its characteristic purple gas-phase discharge colour using a high-frequency brush electrode (Tesla coil).

Figure 7:1 Metal vacuum line with bomb and IR gas cell connected.

Preparation of 2,4,6-tribromophenyl azide

To a stirred solution of 2,4,6-tribromoaniline (7.59 g, 23.0 mmol) in glacial acetic acid (150 mL) and 96% sulphuric acid (30 mL) at 8°C was added dropwise a solution of sodium nitrite (1.725 g, 25.0 mmol) in water (5 mL). After 30 minutes, solution of urea (0.20 g, 3.3 mmol) in water (0.5 mL) was added, followed 10 minutes later by a solution of sodium azide (1.725 g, 26.5 mmol) in water (5 mL). The solution was stirred at 8°C for one hour and water (200 mL) was added slowly with cooling. The precipitate was collected by suction filtration and recrystallised from ethanol to give pink needles (mpt. 70-71°C). Found C, 20.00; H, 0.69; N, 11.81. $C_6H_2Br_3N_3$ requires C, 20.25 ; H, 0.56 ; N, 11.80 %. ^{13}C NMR ($CDCl_3$) δ = 119.1 , 119.2 , 135.2, 136.0 ppm. 1H NMR ($CDCl_3$) δ = 7.66 ppm (2H). ^{14}N NMR ($CDCl_3$) δ = -145.2 (N_β), -155.0 (N_γ), -280 (br, N_α) ppm. IR (cm^{-1} , KBr , RT.) 3055 (w, ν_{CH}), 2109 (s, $\nu_{as}N_3$), 1534 (m, $\nu_{as} CC(Ar)$), 1430 (s, ν_{CC}), 1370 (m, ν_{CC}), 1303 (s, $\nu_s N_3$), 1146 (m, δ_{CC}) 850 (s, δ_{CC}); 573 (w, δCBr) 364 (w, γN_3). Raman (1064 nm, RT, 200 mW, 200 scans) 3058 (m, ν_{CH}), 2143 and 2100 (m, $\nu_{as}N_3$), 1554 (s, $\nu_{as} CC(Ar)$), 1370 (m, ν_{CC}), 1301 (s, $\nu_s N_3$), 1045 (m, δ_{CH}), 827 (m, δ_{CC}), 573 (m, δ_{CBr}), 365 (m, γN_3), 234 (s).

Preparation of 2,4,6-trichlorophenyl azide

To a stirred solution of 2,4,6-trichloroaniline (4.51 g, 23.0 mmol) in glacial acetic acid (150 mL) and 96% sulphuric acid (30 mL) at 8°C was added dropwise a solution of sodium nitrite (1.725 g, 25.0 mmol) in water (5 mL). After 30 minutes a solution of urea (0.20 g, 3.3 mmol) in water (0.5 mL) was added, followed 10 minutes later by a solution of sodium azide (1.725 g, 26.5 mmol) in water (5 mL). The solution was stirred at 8°C for one hour and water (200 mL) was added slowly with cooling. The precipitate was collected by suction filtration and recrystallised from ethanol to give brown needles Found C, 32.25; H, 0.94; N, 18.99. C₆H₂Cl₃N₃ requires C, 32.39; H, 0.90; N, 18.99%. ¹³C NMR (CDCl₃) δ = 128.9, 129.9, 131.1, 133.0 ppm. ¹H NMR (CDCl₃) δ = 7.30 ppm (2H). ¹⁴N NMR (CDCl₃) δ = -144.7 (N_γ), -154.0 (N_β), -287 (br, N_α) ppm. IR (cm⁻¹, KBr, RT.) 3065 (w, νCH), 2130 (s, ν_{as}N₃), 1568 (m, ν_{as}CC(Ar)), 1441 (s, νCC), 1373 (m, νCC), 1316 (s, ν_sN₃), 1137 (m, δCC) 807 (s, γ ring) 598 (w, δ CCl). Raman (1064 nm, RT, 200 mW, 200 scans) 3068 (m, νCH), 2127 (m, ν_{as}N₃), 1570 (s, ν_{as}CC(Ar)), 1449 (m, νCC + νCN), 1317 (s, ν_sN₃), 1067 (m, δCH), 852 (m, γ ring), 599 (m, δCCl), 380 (m, γN₃), 195 (s).

Preparation of 2,4,5-trichlorophenyl azide

To a stirred solution of 2,4,5-trichloroaniline (4.51 g, 23.0 mmol) in glacial acetic acid (150 mL) and 96% sulphuric acid (30 mL) at 8°C was added dropwise a solution of sodium nitrite (1.725 g, 25.0 mmol) in water (5 mL). After 30 minutes, a solution of urea (0.20 g, 3.3 mmol) in water (0.5 ml) was added, followed 10 minutes later by a solution of sodium azide (1.725 g, 26.5 mmol) in water (5 mL). The solution was stirred at 8°C for one hour and water (200 mL) was added slowly with cooling. The precipitate was collected by suction filtration and recrystallised from ethanol to give tan coloured needles Found C, 32.32 ; H, 1.14 ; N, 18.53. C₆H₂Cl₃N₃ requires C, 32.39 ; H, 0.90 ; N, 18.99%. ¹³C NMR (CDCl₃) δ = 120.9 , 124.0 , 128.9, 131.6, 131.9, 137.0 ppm. ¹H NMR (CDCl₃) δ = 7.27, 7.24 ppm. ¹⁴N NMR (CDCl₃) δ = -141.9 (N_γ), -153.0 (N_β), -286 (br, N_α) ppm. IR (cm⁻¹, KBr , RT.) 3077 (w, vCH), 2129 (s, v_{as}N₃), 1555 (m, v_{as} CC(Ar)), 1454 (s, vCC), 1353 (m, vCC), 1293 (s, v_s N₃), 1127 (m, δCC) 877 (s, γ ring) 622 (w, δ CCl). Raman (1064 nm, RT, 400 mW, 2000 scans, sat. solution in acetone) 1581 (m, v_{as} CC(Ar)), 1304 (m, v_s N₃),

Preparation of 2,4-dibromophenyl azide

To a stirred solution of 2,4-dibromoaniline (6.36 g, 23.0 mmol) in glacial acetic acid (150 mL) and 96 % sulphuric acid (30 mL) at 8°C was added dropwise a solution of sodium nitrite (1.725 g, 25.0 mmol) in water (5 mL). After 30 minutes, a solution of urea (0.20 g, 3.3 mmol) in water (0.5 mL) was added, followed 10 minutes later by a solution of sodium azide (1.725 g, 26.5 mmol) in water (5 mL). The solution was stirred at 8°C for one hour and water (200 mL) was added slowly with cooling. The precipitate was collected by suction filtration and recrystallised from ethanol to give brown needlelike crystals. Found C, 25.82 ; H, 1.11 ; N, 15.13. $C_6H_3Br_2N_3$ requires C, 26.02 ; H, 1.09 ; N, 15.17%. ^{13}C NMR ($CDCl_3$) δ = 114.6, 117.8, 120.5, 131.6, 136.2, 138.1 ppm. 1H NMR ($CDCl_3$) δ = 7.60 (1H), 7.46 (1H), 7.25 (1H) ppm. ^{14}N NMR ($CDCl_3$) δ = -139.5 (N_γ), -143.8 (N_β), -280 (br, N_α) ppm. IR (cm^{-1} , KBr, RT.) 3077 (w, ν_{CH}), 2135/2103 (s, $\nu_{as}N_3$), 1573 (m, $\nu_{as}CC(Ar)$), 1468 (s, ν_{CC}), 1380 (m, ν_{CC}), 1302 (s, $\nu_s N_3$), 1157 (m, δ_{CC}) 881 (s, γ ring) 527 (w, δ CBr). Raman (1064 nm, RT, 400 mW, 300 scans) 3054 (m, ν_{CH}), 2107 (w, $\nu_{as}N_3$), 1572 (m, $\nu_{as}CC(Ar)$), 1462 (w, ν_{CC}), 1382 (w, ν_{CC}), 1310 (s, $\nu_s N_3$), 1159 (w, δ_{CC}) 820 (s, γ ring), 654 (m).

Preparation of 2,4-dichlorophenyl azide

To a stirred solution of 2,4-dichloroaniline (4.32 g, 23.0 mmol) in glacial acetic acid (150 mL) and 96% sulphuric acid (30 mL) at 8°C was added dropwise a solution of sodium nitrite (1.725 g, 25.0 mmol) in water (5 mL). After 30 minutes, a solution of urea (0.20 g, 3.3 mmol) in water (0.5 mL) was added, followed 10 minutes later by a solution of sodium azide (1.725 g, 26.5 mmol) in water (5 mL). The solution was stirred at 8°C for one hour and water (200 mL) was added slowly with cooling. The precipitate was collected by suction filtration and recrystallised from ethanol to give very thin brown needles. Found C, 38.13 ; H, 1.60 ; N, 22.39. C₆H₃Cl₂N₃ requires C, 38.32 ; H, 1.60 ; N, 22.35%. ¹³C NMR (CDCl₃) δ = 120.4, 125.8, 128.1, 130.5, 130.6, 136.1 ppm. ¹H NMR (CDCl₃) δ = 7.59 (1H), 7.44 (1H), 7.26 (1H) ppm. ¹⁴N NMR (CDCl₃) δ = -139.5 (N_γ), -144.9 (N_β), -278 (br, N_α) ppm. IR (cm⁻¹, KBr, RT.) 3084 (w, νCH), 2119 (s, ν_{as}N₃), 1568 (m, ν_{as}CC(Ar)), 1477 (s, νCC), 1388 (m, νCC), 1306 (s, ν_sN₃), 1148 (m, δCC) 884 (s, γ ring), 596 (w, δ CCl). Raman (1064 nm, RT, 400 mW, 200 scans) 3059 (m, νCH), 2121 (w, ν_{as}N₃), 1581 (m, ν_{as}CC(Ar)), 1474 (w, νCC), 1389 (w, νCC), 1306 (s, ν_sN₃), 1158 (w, δCC), 840 (s, γ ring), 666 (m).

Preparation of 2,4,6-trifluorophenyl azide

To a stirred solution of 2,4,6-trifluoroaniline (3.98 g, 23.0 mmol) in glacial acetic acid (150 mL) and 96% sulphuric acid (30 mL) at 8°C was added dropwise a solution of sodium nitrite (1.725 g, 25.0 mmol) in water (5 mL). After 30 minutes, a solution of urea (0.20 g, 3.3 mmol) in water (0.5 mL) was added, followed 10 minutes later by a solution of sodium azide (1.725 g, 26.5 mmol) in water (5 mL). The solution was stirred at 8°C for one hour then poured on ice cold water (150 mL). This solution was then extracted 3 times with chloroform (25 mL). The organic layer was then washed twice with water and 2M sodium carbonate, then dried over magnesium sulphate. The chloroform was slowly and carefully removed by distillation to yield 2,4,6-trifluorophenyl azide as red oil. Further purification of this red oil by fractional distillation was attempted but the compound decomposed on heating. ^{13}C NMR (CDCl_3) $\delta = 101.0, 114.1, 154.4, 157.4$ ppm. ^1H NMR (CDCl_3) $\delta = 6.70$ (2H) ppm. ^{14}N NMR (CDCl_3) $\delta = -143.1$ (N_γ), -153.3 (N_β), -268 (br, N_α) ppm. ^{19}F -NMR (CDCl_3) $\delta = -112.6$ (t, 1F) -120.3 (m, 2F) ppm. IR (cm^{-1} , nujol, RT.) 3086 (w, ν_{CH}), 2135 (s, ν_{asN_3}), 1630 (m, $\nu_{\text{as CC(Ar)}}$), 1507 (s, ν_{CC}), 1376 (m, ν_{CC}), 1309 (s, $\nu_{\text{s N}_3}$), 1157 (m, δ_{CC}) 895 (s, γ ring) 576 (w, δ CF). Raman (1064 nm, RT, 400 mW, 500 scans) 3088 (m, ν_{CH}), 2136 (w, ν_{asN_3}), 1636 (m, $\nu_{\text{as CC(Ar)}}$), 1505 (w, ν_{CC}), 1374 (w, ν_{CC}), 1310 (s, $\nu_{\text{s N}_3}$), 1001 (m, δ_{CC}) 895 (s, γ ring), 654 (m) 576 (s, δ CF).

Preparation of 2,3,4,5,6-pentafluorophenyl azide

A slow stream of nitrosyl chloride (ca. 2.0 g, 30 mmol) was passed into a stirred solution of glacial acetic acid (20 mL) containing pentafluorophenylhydrazine (6.0 g, 30mmol). The reaction began immediately and continued for about 2 hours, the solution gradually becoming deep red. The solution was left open to the atmosphere overnight and then heavy diluted with water (100 mL). This solution was then extracted 3 times with dichloromethane (25 mL). The organic layer was then washed twice with water and 2M sodium carbonate, then dried over magnesium sulphate. The dichloromethane was slowly and carefully removed by distillation to yield 2,3,4,5,6 pentafluorophenyl azide as red liquid. Further purification by fractional distillation was attempted on this red liquid but the compound decomposed on heating. ^{14}N NMR (CDCl_3) $\delta = -145.0$ (N_γ), -149.5 (N_β), -295 (br, N_α) ppm. ^{19}F NMR (CDCl_3) $\delta = -152.1$ (m, 2F), -160.4 (t, 1F), -162.6 (m, 2F) ppm. IR (cm^{-1} , nujol, RT.) 2130 (s, $\nu_{\text{as}}\text{N}_3$), 1650 (m, $\nu_{\text{as}}\text{CC}(\text{Ar})$), 1470 (s, ν_{CC}), 1324 (s, $\nu_{\text{s}}\text{N}_3$), 1157 (m, δ_{CC}) 895 (s, γ ring). Raman (1064 nm, RT, 400 mW, 500 scans) 2127 (w, $\nu_{\text{as}}\text{N}_3$), 1655 (m, $\nu_{\text{as}}\text{CC}(\text{Ar})$), 1468 (w, ν_{CC}), 1328 (s, $\nu_{\text{s}}\text{N}_3$), 894 (s, γ ring), 586 (m) 525 (s, δ CF).

Preparation of p-methoxyphenyl azide

To a stirred solution of p-methoxyaniline (2.83 g, 23.0 mmol) in glacial acetic acid (150 mL) and 96% sulphuric acid (30 mL) at 8°C was added dropwise a solution of sodium nitrite (1.725 g, 25.0 mmol) in water (5 mL). After 30 minutes a solution of urea (0.20 g, 3.3mmol) in water (0.5mL) was added, followed 10 minutes later by a solution of sodium azide (1.725 g, 26.5mmol) in water (5 mL). The solution was stirred at 8°C for one hour and water (200 mL) was added slowly with cooling. The precipitate was collected by suction filtration and recrystallised from methanol to give light brown (tan) needles which darken on standing.

Found C, 56.22 ; H, 4.60 ; 99N, 28.16. $C_7H_7O_1N_3$ requires C, 56.36 ; H, 4.73 ; N, 28.17%. ^{13}C NMR (D6-Acetone) δ = 54.9 (CH₃), 115.2, 119.9, 131.9, 157.3 ppm. 1H NMR (D6-Acetone) δ = 4.08 (CH₃) , 7.21(2H) ppm. ^{14}N NMR (D6-Acetone) δ = -142.7 (N _{γ}), -151.6 (N _{β}), -292 (br, N _{α}) ppm. IR (cm⁻¹, KBr , RT.). 3057 (w, vCH), 2132 (s, v_{as}N₃), 1582 (m, v_{as}CC(Ar)), 1504 (s, vCC), 1455 (m, v(C-OCH₃)), 1302 (s, v_s N₃), 1246 (m, δ CC), 1172 (m), 827 (s, γ ring) 622 (m), 399 (w, γ N₃). Raman (1064 nm, RT, 200 mW, 500 scans) 3058 (m, vCH), 2103 (w, v_{as}N₃), 1606 (m, v_{as} CC(Ar)), 1502 (m, vCC), 1304 (s, v_s N₃), 1174 (m, δ CC), 828 (s, γ ring) 644 (m).

Preparation of 2,6-diiodo-4-nitrophenyl azide

To a solution of 2,6-diiodo-4 nitroaniline (8.951 g, 23 mmol) in glacial acetic acid (150 mL) and concentrated sulphuric acid (30 mL) at 8 °C was added dropwise a solution of sodium nitrite (1.725 g, 25 mmol) in water (5 mL). After 30 minutes a solution of urea (0.2 g, 3.3 mmol) in water (0.5 mL) was added, followed 10 minutes later by a solution of sodium azide (1.725 g, 26.5 mmol) in water (5 mL). The solution was stirred at 8 °C for one hour and water (200 mL) was added slowly with cooling. The precipitate was collected by suction filtration and recrystallised from ethanol to yield the title compound as green needles. Found LC, 17.25 ; H, 0.47 ; N, 13.20. C₆H₂N₄O₂I₂ requires C, 17.32 ; H, 0.48 ; N, 13.47%. ¹³C NMR (CDCl₃) δ = 89.9, 135.1, 145.1, 147.5 ppm. ¹H NMR (CDCl₃) δ = 8.64 (2H) ppm. ¹⁴N NMR (CDCl₃) δ = -18.7 (NO₂), -148.2 (N_γ), -151.2 (N_β), -272 (br, N_α) ppm. IR (cm⁻¹, KBr) 3084 (vw, νCH(Ar)), 3062 (vw, νCH(Ar)), 2134/2100 (s, br, ν_{as}N₃), 1572 (m, ν_{as}CC(Ar)), 1512 (s, br, ν_{as}NO₂), 1339 (s, br, ν_sNO₂), 1310 (m, br, ν_sN₃), 1192 (w, δCH), 1122 (m, νCN), 740 (m, γCH), 703 (m, δN₃) 517 (w, δCNN). Raman (1064nm, RT, 200mW, 500 scans) 3064 (vw, νCH(Ar)), 2117 (vw, ν_{as}N₃), 1558 (m, ν_{as}CC(Ar)), 1514 (m, ν_{as}NO₂), 1335 (s, br, ν_sNO₂), 1318 (s, ν_sN₃), 1267 (w, δCH), 1124 (w, νCN), 892 (m).

Preparation of 2-nitrophenyl azide

A mixture of *o*-nitroaniline (28 g, 0.2 mol), water (80 ml) and concentrated hydrochloric acid (45 mL, 0.54 mmol) was placed in a 500 mL flask. The flask was cooled to 0°C and then sodium nitrite (14.5 g, 0.21 mol) in water (50 mL) was added dropwise. After one hour of stirring at 0°C, the yellow solution was suction filtered from the trace of insoluble impurities and poured into a 2 litre beaker surrounded by an ice bath. With stirring sodium azide (13.0 g, 0.20 mol) in 50mL water was added. Immediately the product began to precipitate as a light cream solid. After the nitrogen evolution had ceased, the product was collected on a Buchner funnel and washed twice with ice cold water and then dried in air overnight. The crude 2-nitrophenyl azide was then recrystallised from aqueous ethanol (20 % water, 80 % ethanol) to yield cream coloured needles, (m.pt. 129-130°C). Found C, 43.08 ; H, 2.54 ; N, 33.63. C₆H₄N₄O₂ requires C, 43.91 ; H, 2.46 ; N, 34.14%. ¹H NMR (CDCl₃) δ = 7.93 (dd, J= 7.9, 1.5 Hz, 1H), 7.61 (d_{ψt}, J= 7.9, 1.4 Hz, 1H), 7.33 (dd, J= 8.4, 1.0 Hz, 1H), 7.25 (d_{ψt}, J= 7.7, 1.1 Hz, 1H)ppm. ¹³C NMR (CDCl₃) δ = 140.89, 134.78, 133.95, 126.07, 124.88, 120.68 ppm. ¹⁴N NMR (CDCl₃) δ = -12.0 (NO₂), -140.4 (N_β), 146.2 (N_γ), -285 (N_α) ppm. IR (cm⁻¹, KBr) 3106 (vw, νCH(Ar)), 3037 (vw, νCH(Ar)), 2460 (vw, νCH(Ar)), 2308 (vw), 2124 (s, br, ν_{as}N₃), 1605 (s, ν_{as} CC(Ar)), 1525 (s, br, ν_{as} NO₂), 1445.3 (vw), 1354 (s, br, ν_s NO₂), 1295 (s, br, ν_s N₃), 1168 (m, δCH), 1155 (m, νCN), 776 (m, γCH), 743 (s, γCH (1,2 disubt. Aromatic)), 704 (m, δN₃) 530 (w, δCNN). Raman (1064nm, RT, 100mW, 436 scans) 3088 (m, νCH(Ar)), 2119 (m, ν_{as}N₃), 1602 (m, ν_{as} CC(Ar)), 1582 (m, ν_{as} CC(ar)), 1517 (m, ν_{as} NO₂), 1444 (m), 1353(s, br, ν_s NO₂), 1292 (s, ν_s N₃), 1170 (m, δCH), 1140 (w, νCN), 640 (m).

Preparation of *m*-nitrophenyl azide

To a stirred solution of *m*-nitroaniline (3.17 g, 23.0 mmol) in glacial acetic acid (150 mL) and 96% sulphuric acid (30 mL) at 8°C was added dropwise a solution of sodium nitrite (1.725 g, 25.0 mmol) in water (5 mL). After 30 minutes a solution of urea (0.20 g, 3.3 mmol) in water (0.5 mL) was added, followed 10 minutes later by a solution of sodium azide (1.725 g, 26.5 mmol) in water (5 mL). The solution was stirred at 8°C for one hour and water (200 mL) was added slowly with cooling. The precipitate was collected by suction filtration and recrystallised from methanol to give yellow needles Found C, 43.78; H, 2.37 ; N, 34.15. C₆H₄N₄O₂ requires C, 43.91 ; H, 2.46 ; N, 34.14%. ¹H NMR (CDCl₃) δ = 7.91 (dd, J= 7.9, 1.5 Hz, 1H), 7.60 (dψt, J= 7.9, 1.4 Hz, 1H), 7.34 (dd, J= 8.4, 1.0 Hz, 1H), 7.23 (dψt, J= 7.7, 1.1 Hz, 1H) ppm. ¹³C NMR (CDCl₃) δ = 120.8, 124.0, 128.9, 131.6, 131.9, 136.9 ppm. ¹⁴N NMR (CDCl₃) δ = -12.3 (NO₂), -140.5 (N_β), -146.0 (N_γ), -287 (N_α) ppm. IR (cm⁻¹, KBr) 3106 (vw, νCH(Ar)), 3077 (vw, νCH(Ar)), 2415 (vw, νCH(Ar)), 2128 (s, br, ν_{as}N₃), 1613 (m, ν_{as} CC(Ar)), 1531 (s, br, ν_{as}NO₂), w), 1353 (s, br, ν_sNO₂), 1302 (m, br, ν_sN₃), 1144 (w, δCH), 1155 (m, νCN), 736 (m, γCH), 712 (m, δN₃) 534 (w, δCNN). Raman (1064 nm, RT, 100 mW, 400 scans) 3084 (m, νCH(Ar)), 2131 (m, ν_{as}N₃), 1582 (m, ν_{as} CC(Ar)), 1530 (m, ν_{as} NO₂), 1351 (s, br, ν_sNO₂), 1303 (s, ν_sN₃), 1281 (m, δCH), 654 (m).

Preparation of 2,4-dinitrophenyl azide

To a stirred solution of 2,4-dinitroaniline (4.21 g, 23.0 mmol) in glacial acetic acid (150 mL) and 96% sulphuric acid (30 mL) at 8°C was added dropwise a solution of sodium nitrite (1.725 g, 25.0 mmol) in water (5 mL). After 30 minutes a solution of urea (0.20 g, 3.3mmol) in water (0.5 mL) was added, followed 10 minutes later by a solution of sodium azide (1.725 g, 26.5 mmol) in water (5 mL). The solution was stirred at 8°C for one hour and water (200 mL) was added slowly with cooling. The precipitate was collected by suction filtration and recrystallised from ethanol to give yellow needlelike crystals. Found C, 34.65 ; H, 1.37 ; N, 32.06. C₆H₃N₅O₄ requires C, 34.46 ; H, 1.44 ; N, 33.48%. ¹H NMR (CDCl₃) δ = 7.90 (1H), 7.62 (1H), 7.34 (1H) ppm. ¹³C NMR (CDCl₃) δ = 120.6, 124.7,128.5, 130.6, 131.3, 135.9 ppm. ¹⁴N NMR (CDCl₃) δ = -16.1 (NO₂), -144.7 (N_β,N_γ), -290 (N_α)ppm. IR (cm⁻¹, KBr) 3114 (vw, νCH(Ar)), 3077 (vw, νCH(Ar)), 2135 (s, br, ν_{as}N₃) , 1611 (m, ν_{as} CC(Ar)), 1558 (s, br, ν_{as} NO₂), w), 1345 (s, br, ν_s NO₂), 1301 (m, br, ν_s N₃), 1186 (w, δCH), 1156 (m, νCN), 743 (m, γCH), 722 (m, δN₃) 533 (w, δCNN).Raman (1064 nm, RT, 100 mW, 400 scans) 3097 (vw, νCH(Ar)), 2124 (vw, ν_{as}N₃), 1621 (m, ν_{as} CC(Ar)), 1521 (m, ν_{as} NO₂), 1389 (s, br, ν_sNO₂), 1333 (s, ν_sN₃), 1163 (w, δCH), 1140 (w, νCN), 885 (m).

Preparation of 2,4,6-trinitrophenyl azide (picryl azide)

2-nitrophenyl azide was prepared as previously described. To a well-stirred mixture of nitric acid (25 mL, fuming 90 %) and sulphuric acid (25 mL, concentrated) which had been cooled to 0°C was added 2-nitrophenyl azide (5.0 g, 0.31 mmol). After being stirred at 0°C for one hour, the reaction mixture was poured onto ice and the solid collected and washed with ice cold water. 2,4,6 trinitrophenyl azide was recrystallised from methanol to yield yellow needles (m.pt. 89-90°C, dec). Found C, 27.83 ; H, 0.79 ; N, 32.61. C₆H₂N₆O₆ requires C, 28.36 ; H, 0.69 ; N, 33.07%. ¹H NMR (CDCl₃) δ = 8.93 (s, 2H) ppm. ¹³C NMR (CDCl₃) δ = 144.21, 142.54, 133.94, 123.88 ppm. ¹⁴N NMR (CDCl₃) δ = -22.7 (br, NO₂), -143.1 (N_γ), -153.2 (N_β), -290 (br, N_α) ppm. IR (cm⁻¹, KBr, RT.) 3108 (m, νCH(Ar)), 3096 (w, νCH(Ar)), 2243 (w, νCN), 2137(s, br, ν_{as}N₃), 1603 (s, ν_{as} CC(Ar)), 1536 (vs, br, ν_{as} NO₂), 1351 (s, br, ν_sNO₂), 1288 (s, br, ν_sN₃), 1181 (m, δCH), 1120 (m, νCN), 773 (vw, γCH), 623 (m, δN₃) 520 (w, δCNN). Raman (1064 nm, RT, 200 mW, 100 scans) 2127 (w, ν_{as}N₃), 1612 (m, ν_{as} CC(Ar)), 1556 (m, ν_{as} CC(ar)), 1537 (w, ν_{as} NO₂), 1350(s, br, ν_sNO₂), 1287 (m, ν_sN₃), 1182 (m, δCH), 827 (m), 522 (w).

Preparation of 1,3,5-triazido-2,4-dinitrobenzene

1,3,5-Trichloro-2,4-dinitrobenzene (10.0g) was dissolved in a boiling mixture of acetone (55 mL) and methanol (20 mL). A hot solution of sodium azide (8.2 g) in water (30 mL) and methanol (30 mL) was then added. This mixture was then boiled under reflux for 90 minutes and then filtered and the residual sodium chloride was washed three times with hot ethanol (3 x 5 mL). The filtrate and washings were cooled in a fridge at 0°C overnight. The crude triazidodinitrobenzene was collected and air-dried and then recrystallised from ethanol to yield yellow needles (m.pt. 107-108°C). Found C, 24.51 ; H, 0.00; N, 52.63. C₆H₁N₁₁O₄ requires C, 24.75 ; H, 0.35 ; N, 52.92%. ¹H NMR (CDCl₃) δ = 6.83 (s, 1H) ppm. ¹³C NMR (CDCl₃) δ = 137.50, 127.63, 108.57, 103.51 ppm. ¹⁴N NMR (CDCl₃) δ = -22.4 (br, NO₂), -146.8 (N_γ), -150.9 (N_β), -290 (br, N_α) ppm. IR (cm⁻¹, KBr, RT.) 3077 (w, νCH(Ar)), 2280 (vw, νCN), 2137 (s, br, ν_{as}N₃), 1605 (m, ν_{as} CC(Ar)), 1545 (s, ν_{as} NO₂), 1364 (s, br, ν_sNO₂), 1269 (s, ν_sN₃), 1165 (w, δCH), 818 (vw, γCH), 682 (m, δN₃) 527 (w, δCNN). Raman (1064 nm, RT, 200 mW, 1000 scans) 2135 (w, ν_{as}N₃), 1579 (m, ν_{as} CC(Ar)), 1529 (m, ν_{as} NO₂), 1340 (s, br, ν_sNO₂), 1284 (s, ν_sN₃), 1145 (m, δCH), 830 (m), 451 (w).

Preparation of 1,3,5-triazido-2,4,6-trinitrobenzene

1,3,5-Triazido-2,4-dinitrobenzene (4 g) was slowly added to fuming nitric acid (20 mL) when all the solid was in solution , concentrated sulphuric acid (4 mL) was added dropwise and the solution allowed to stand at room temperature . After about 2 hours pale yellow plates started to separate and 4 hours later the mixture was cooled to 0°C. The next day the solid was filtered and washed with water. The filtrate was diluted with an equal volume of water and the impure material that separated was crystallised from acetic acid. The combined solids were further recrystallised from acetic acid to yield bright yellow plates (m.pt. 128-130°C). Found C, 21.26 ; N, 49.34. C₆N₁₂O₆ requires C, 21.44 ; N, 50.00%. ¹³C NMR (CDCl₃) δ = 140.9 102.0 ppm. ¹⁴N NMR (CDCl₃) δ = -27.6 (NO₂), -144.4 (N_γ), -153.0 (N_β), -290 (br, N_α) ppm. IR (cm⁻¹, KBr , RT.) 2232 (vw, νCN), 2121 (s, ν_{as}N₃), 1599 (m, ν_{as} CC(Ar)), 1542 (s, ν_{as} NO₂), 1370 (m, ν_s NO₂), 1343 (s, ν_s N₃), 893 (w, νCN), 603 (m, δN₃) 579 (w, δ NO₂) 520 (w, δCNN). Raman (1064 nm, RT, 200 mW, 1111 scans) 2146 (m, ν_{as}N₃) , 1568 (s, ν_{as} CC(Ar)), 1541 (m, ν_{as} NO₂), , 1340 (s, ν_s N₃), 1144 (m, δCH), 819 (m), 499 (w).

Preparation of pentanitroaniline

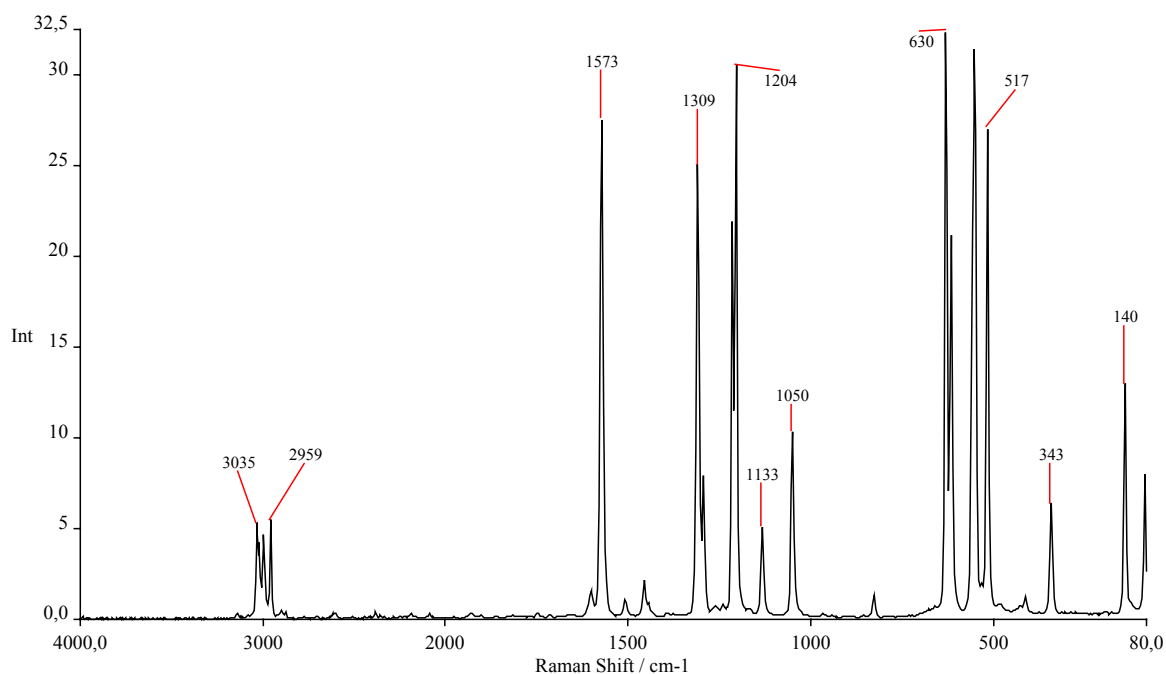
Pentanitroaniline was prepared by nitration of 3,5 - dinitroaniline by using a modification of the method of Flürscheim [71]. 3,5 – dinitroaniline (2.0 g, 11 mmol) was dissolved in 100% sulphuric acid (80 mL) and cooled to 5°C. One hundred percent nitric acid (5 mL, 7.6 g, 120 mmol) was added dropwise over 10 minutes during which time the temperature was held below 8°C. The reaction mixture was then heated for 1 hour at 70-75 °C and finally cooled in an ice bath. The yellow solid was filtered, air dried at the pump for 10 minutes and then dissolved in dichloroethane (70 ml). The organic layer was carefully decanted from the residual sulphuric acid, concentrated to 25 mL , and allowed to crystallise at –20° C overnight to yield pentanitroaniline as clear yellow plates (1.46 g, 52 %), mp 192-200°C dec (lit 193-202 °C) [71] ¹⁴N NMR (CDCl₃) δ = -26.6 (NO₂), -29.9 (NO₂), -31.0 (NO₂) ppm. IR (cm⁻¹, KBr) 1615 (m, v_{as} CC(Ar)), 1544 (s, br, v_{as} NO₂), w), 1360 (s, br, v_s NO₂), 824 (m). Raman (1064 nm, RT, 100 mW, 400 scans), 1621 (m, v_{as} CC(Ar)), 1540 (m, v_{as} NO₂), 1364 (s, br, v_s NO₂), 1171 (m), 918 (m), 826 (m).

Preparation of hexakis (methylnitrate) benzene (C₆- (-CH₂- O- NO₂)₆)

Hexakis (phenoxy)methyl benzene (2.00 g, 2.80 mmol) was slowly added to fuming nitric acid (40 mL) over a period of 60 minutes. This solution was stirred for 10 minutes before concentrated sulphuric acid (10 mL) was added dropwise, after this addition was complete the solution was then stirred at room temperature for 7 days. The acid was then poured onto a ice cooled water (200 mL) and a white solid was precipitated. The precipitate was collected by suction filtration and washed twice with ice cold water. The solid was then dried in a dessicator over phosphorus pentoxide overnight. (mpt 176-177°C). Found C, 28.90 ; H, 2.19 ; N, 15.64. C₁₂H₁₂N₆O₁₈ requires C, 27.28 ; H, 2.28 ; N, 15.91%. ¹H NMR (CDCl₃) δ = 3.08 (s, CH₂) ppm. ¹³C NMR (CDCl₃) δ = 68.4 (CH₂), 136.7 (ring C) ppm. ¹⁴N NMR (CDCl₃) δ = -44.3 (br, NO₂) ppm. IR (cm⁻¹, KBr , RT.) 3025 (m, CH), 2960 (w, CH), 1644 (m, ν_{as} CC(Ar)), 1547(m, ν_{as} CC(ar)), 1524 (w, ν_{as} NO₂), 1384 (s, ν_s NO₂), 1348(m, ν_s NO₂), 1280 (s, ν_s -O-NO₂), 1220 (w, δCH), 995 (s, CC ring), 583 (w, NO₂). Raman (1064 nm, RT, 200 mW, 200 scans) 3024 (m, CH), 2960 (s, CH), 1629 (m, ν_{as} CC(Ar)), 1596 (m, ν_{as} CC(ar)), 1524 (w, ν_{as} NO₂), 1369 (s, ν_s NO₂), 1350(s, ν_s NO₂), 1281 (s, ν_s -O-NO₂), 1221 (m, δCH), 990 (s, CC ring), 838 (m), 563 (s, NO₂).

Preparation of hexakis (bromomethyl) benzene

Hexakis (bromomethyl) benzene was prepared by the literature method of Backer by the reaction hexamethylbenzene and bromine in ethylene bromide[73]. Found C, 22.52 ; H, 1.84 . $C_{12}H_{12}Br_6$ requires C, 22.52 ; H, 1.90 %. 1H NMR (DMSO- D_6) δ = 3.34 (s, CH_2) ppm. IR (cm^{-1} , KBr , RT) 3030 (s, ν_{CH}), 2997 (m, ν_{CH}), 1576 (s, ν_{as} CC(Ar)), 1312 (s, ν_{CC}), 1048 (m, δ_{CH}), 624 (m, δ_{CBr}). Raman (1064 nm, RT, 200 mW, 200 scans) 3035 (m, ν_{CH}), 2996 (m, ν_{CH}), 2959 (m, ν_{CH}), 1573 (s, ν_{as} CC(Ar)), 1309 (s, ν_{CC}), 1050 (m, δ_{CH}), 630 and 616 (s, δ_{CBr}).



Preparation of hexakis (azidomethyl) benzene

Hexakis (bromomethyl) benzene (0.50 g, 0.78 mmol) and a slight excess of sodium azide (0.40 g, 6.15 mmol) were stirred i dimethyl formamide (25 mL) at room temperature for 2 hours. The reaction mixture was then poured into water and the solid was collected by suction filtration and washed twice with water (25 mL) and then twice with methanol (25 mL).

The yield of hexakis (azidomethyl) benzene was (0.29 g, 0.72 mmol, 92.3 %) (mpt 163.5°C). Found C, 35.48 ; H, 2.95 ; N, 62.41. C₁₂H₁₂N₁₈ requires C, 35.29 ; H, 2.96 ; N, 61.74%. ¹H NMR (DMSO-D6) δ = 3.31 (s, CH₂) ppm. ¹³C NMR (DMSO-D6) δ = 47.1 (CH₂), 136.4 (ring C) ppm. ¹⁴N NMR (DMSO-D6) δ = -134.1 (N_γ), -170.1 (N_β) ppm. ¹⁵N NMR (DMSO-D6) δ = -134.4 (N_γ), -168.9 (N_β), -306.2 (N_α) ppm. IR (cm⁻¹, KBr , RT.) 3011(m, vCH), 2963 (m, vCH), 2117 (m, v_{as}N₃), 1570 (s, v_{as} CC(Ar)), 1358 (m, vCC), 1272 (m, v_s N₃), 1212, (m, δCH), 874 (s , δCC). Raman (1064 nm, RT, 200 mW, 200 scans)). 3010(m, vCH), 2961 (m, vCH), 2117 (m, v_{as}N₃), 1568 (s, v_{as} CC(Ar)), 1357 (m, vCC), 1270 (m, v_s N₃), 1212, (m, δCH), 876 (s , δCC)

Preparation of 1,3,5 trichloro-2,4-dinitrobenzene

100 mL of fuming nitric acid was stirred in a 250 mL conical flask at room temperature. Over a period of 90 minutes 1,3,5-trichlorobenzene (20.0 g, 110.2 mmol) was slowly and carefully added to this flask (N.B. if the addition was made too quickly then NO₂ gas was evolved.).

This solution was stirred at room temperature for a further 60 minutes and then poured on to ice to precipitate a cream solid. This solid was then recrystallised to 1,3,5 trichlorobenzene-2,4 dinitro benzene (9.83 g, 36.2 mmol, 32.9%). Found C, 26.37; H, 0.00 ; N, 10.31. C₆H₁Cl₃N₂O₄ requires C, 26.55 ; H, 0.37 ; N, 10.32%. ¹³C NMR (CDCl₃) δ = 120.8, 128.7, 130.7, 147.0 ppm. ¹H NMR (CDCl₃) δ = 7.67 ppm. ¹⁴N NMR (CDCl₃) δ = -24.1 (NO₂) ppm. IR (cm⁻¹, KBr , RT.) 3084 (w, vCH), 1618 (m, v_{as} CC(Ar)), 1575 (s, vCC), 1550 (s,br, v_{as} NO₂), 1357 (s, v_sNO₂), 1176 (m, δCC), 946 (s,vCCl), 881 (s, γ ring) 598(m, δ NO₂).Raman (1064 nm, RT, 200 mW, 200 scans) 3082 (m, vCH), 1620 (m, v_{as} CC(Ar)), 1546 (s,, v_{as} NO₂), 1357 (m, v_s NO₂), 1172 (w, δCC) , 950 (s,vCCl), 595 (m, δ NO₂).

Attempt to prepare pentanitrophenyl azide by the reaction of *o*-nitrophenyl azide with N₂O₅ in dichloromethane at -50°C:

o-nitrophenyl azide (0.820 g, 5 mmol) was dissolved in 30 mL of dichloromethane in a 100 mL round bottom flask. This solution was then cooled to -50°C with stirring. Dinitrogen pentoxide (2.700 g, 25 mmol) was dissolved in 40 mL of dichloromethane at -50°C and added to a special dropping funnel which was surrounded by a dichloromethane-dry ice bath. The dinitrogen pentoxide solution is slowly and carefully added dropwise to the azide solution over the period of 45 minutes making sure the temperature remains at -50°C. When the addition was complete the solution stirred at -50°C for a further 60 minutes then allowed to warm up to room temperature. The solvent was then carefully removed to yield a yellow powder which on analysis was 1,3,5 trinitrophenyl azide (picryl azide) and not the desired product pentanitrophenyl azide. Found C, 27.94 ; H, 0.70 ; N, 32.81. C₆H₂N₆O₆ requires C, 28.36 ; H, 0.69 ; N, 33.07%. ¹H NMR (CDCl₃) δ = 8.93 (s, 2H) ppm. ¹³C NMR (CDCl₃) δ = 144.21, 142.54, 133.94, 123.88 ppm. ¹⁴N NMR (CDCl₃) δ = -22.7 (br, NO₂), -143.1 (N_γ), -153.2 (N_β), -290 (br, N_α) ppm. IR (cm⁻¹, KBr , RT.) 3108 (m, vCH(Ar)), 3096 (w, vCH(Ar)), 2243 (w, vCN), 2137(s, br, v_{as}N₃), 1603 (s, v_{as} CC(Ar)), 1536 (vs, br, v_{as} NO₂), 1351 (s, br, v_s

NO₂), 1288 (s, br, ν_s N₃), 1181 (m, δ CH), 1120 (m, ν CN), 773 (vw, γ CH), 623 (m, δ N₃) 520 (w, δ CNN). Raman (1064 nm, RT, 200 mW, 100 scans) 2127 (w, ν_{as} N₃), 1612 (m, ν_{as} CC(Ar)), 1556 (m, ν_{as} CC(ar)), 1537 (w, ν_{as} NO₂), 1350(s, br, ν_s NO₂), 1287 (m, ν_s N₃), 1182 (m, δ CH), 827 (m), 522 (w).

Crystallographic data of 2,4,6-tribromophenyl azide at 213K

C₆H₂N₃Br₃, $M_r = 355.84$, monoclinic, P21/n, $a = 3.918(1)$, $b = 14.6728(4)$,
 $c = 15.6992(5)$, $\alpha = 90.00$, $\beta = 95.898(4)$, $\gamma = 90.00^\circ$, $V = 897.81(4) \text{ \AA}^3$, $Z = 4$,
 $D_x = 2.633 \text{ g cm}^{-3}$, $\lambda (\text{Mo-K}\alpha) = 0.71069 \text{ \AA}$, $\mu = 13.423 \text{ mm}^{-1}$, $F(000) = 656$,
 $T = 213 \text{ K}$, $R = 0.0284$ and $R_w = 0.0582$ for 1509 independent reflections

Crystal dimensions 0.08 x 0.04 x 0.03 mm. Siemens SMART Area-detector, Mo K α radiation. Intensities of 4990 reflection surveyed in the range θ 3.80-58.10 ; h -5 \rightarrow 5, k -1 \rightarrow 17, l -20 \rightarrow 20 ; 1509 independent reflections with $F > 4\sigma(F)$. Structure determined by direct phasing using SHELXS. H atoms located in difference fourier synthesis. Full- matrix least squares calculations on F with anisotropic thermal parameters for C, N, and Br atoms and isotropic for H atoms using SHELXL. Least-squares convergence at $R = 0.0284$, $R_w = 0.0582$, S 1.125 for 115 parameters.

Crystallographic data of 2,4,6-trichlorophenyl azide at 293K

C₆H₂N₃Cl₃, $M_r = 222.46$, monoclinic, P21, $a = 3.835(5)$, $b = 13.29(1)$, $c = 8.349(7)$, $\alpha = 90.00$, $\beta = 103.06(2)$, $\gamma = 90.00^\circ$, $V = 414.6(7) \text{ \AA}^3$, $Z = 2$, $D_x = 1.782 \text{ g cm}^{-3}$, $\lambda (\text{Mo K}\alpha) = 0.71069 \text{ \AA}$, $\mu = 1.043 \text{ mm}^{-1}$, $F(000) = 220$, $T = 293 \text{ K}$, $R = 0.0382$ and $R_w = 0.0875$ for 628 independent reflections.

Crystal dimensions 0.30 x 0.16 x 0.08 mm. Siemens SMART Area-detector, Mo-K α radiation. Intensities of 862 reflection surveyed in the range θ 5.00-49.90 ; h 0 \rightarrow 4, k 0 \rightarrow 15, l -9 \rightarrow 9 ; 628 independent reflections with $F > 4\sigma(F)$. Structure determined by direct phasing using SHELXS. H atoms located in difference fourier synthesis. Full- matrix least squares

calculations on F with anisotropic thermal parameters for C, N, and Cl atoms and isotropic for H atoms using SHELXL. Least-squares convergence at $R = 0.0382$, $R_w = 0.0875$, $S = 1.101$ for 109 parameters.

Crystallographic data of 2,4,6-trinitrophenyl azide (picryl azide) at 298K

$C_6H_2N_6O_6$, $M_r = 254.116$, orthorhombic, Pbc a , $a = 10.16(1)$, $b = 12.60(1)$, $c = 14.32(1)$, $\alpha = 90.00$, $\beta = 90.00$, $\gamma = 90.00^\circ$, $V = 1833(13) \text{ \AA}^3$, $Z = 8$, $D_x = 1.841 \text{ g cm}^{-3}$, $\lambda (\text{Mo-K}\alpha) = 0.71069 \text{ \AA}$, $\mu = 0.167 \text{ mm}^{-1}$, $F(000) = 1024$, $T = 298 \text{ K}$, $R = 0.0429$ and $R_w = 0.1286$ for 1670 independent reflections.

Crystal dimensions 0.40 x 0.20 x 0.16 mm. Enraf-Nonius CAD4 diffractometer, Mo-K α radiation. Cell dimensions from setting angles of 25 independent reflections with θ 13.0-17.0°. Intensities of 2320 reflection surveyed in the range θ 4.01-26.3; scan time 60 secs, $h = 12 \rightarrow 1$, $k = -6 \rightarrow 15$, $l = -17 \rightarrow 3$; 1670 independent reflections with $I \geq 2\sigma(I)$. Three reference reflections monitored periodically showed a decline of 3 % over the period of collection. Structure determined by direct phasing using XCAD4. H atoms located in difference fourier synthesis. Full-matrix least squares calculations on F with anisotropic thermal parameters for C; N and O atoms and isotropic for H atoms using SHELXL. Least-squares convergence at $R = 0.0429$, $R_w = 0.1286$, $S = 1.139$ for 171 parameters.

Crystallographic data of 2,4,6-trinitrophenyl azide (picryl azide) at 120K

$C_6H_2N_6O_6$, $M_r = 254.116$, orthorhombic, Pbc a , $a = 10.16(5)$, $b = 12.60(5)$, $c = 14.32(5)$, $\alpha = 90.00$, $\beta = 90.00$, $\gamma = 90.00^\circ$, $V = 1834.07(1) \text{ \AA}^3$, $Z = 8$, $D_x = 1.841 \text{ g cm}^{-3}$, $\lambda (\text{Mo-K}\alpha) = 0.71069 \text{ \AA}$, $\mu = 0.166 \text{ mm}^{-1}$, $F(000) = 1024$, $T = 120$, $R = 0.045$ and $R_w = 0.053$ for 1252 independent reflections.

Crystal dimensions 0.40 x 0.20 x 0.16 mm. Enraf-Nonius CAD4 diffractometer, Mo-K α radiation. Cell dimensions from setting angles of 25 independent reflections with θ 13.0-17.0°. Intensities of 2490 reflection surveyed in the range θ 4.01-26.3; scan time 60 secs; $h = 12 \rightarrow 1$, $k = -2 \rightarrow 15$, $l = -17 \rightarrow 2$; 1252 independent reflections with $I \geq 3\sigma(I)$. Three reference reflections monitored periodically showed a decline of 2 % over the period of collection. Structure determined by direct phasing using XCAD4. H atoms located in

difference fourier synthesis. Full-matrix least squares calculations on F with anisotropic thermal parameters for C, N and O atoms and isotropic for H atoms using SHELXL. Least-squares convergence at $R = 0.045$, $R_w = 0.053$, $S = 1.881$ for 171 parameters.

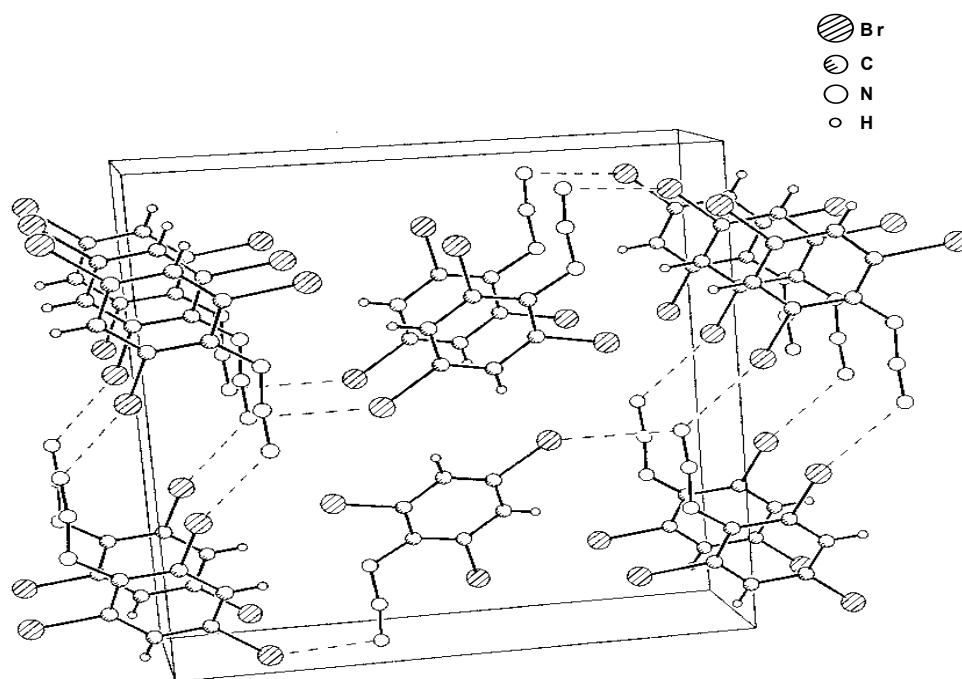
Crystallographic data of 2,6-diiodo-4-nitrophenyl azide at 100K

$C_6H_2N_4O_2I_2$, $M_r = 415.91$, monoclinic, P21/c, $a = 8.4469(14)$, $b = 16.318(2)$, $c = 14.359(2)$, $\alpha = 90.00$, $\beta = 97.315(4)$, $\gamma = 90.00^\circ$, $V = 1963.1(1) \text{ \AA}^3$, $Z = 8$, $D_x = 2.815 \text{ g cm}^{-3}$, λ (Mo- $K\alpha$) = 0.71069 \AA , $\mu = 6.38 \text{ mm}^{-1}$, $F(000) = 1504$, $T = 100 \text{ K}$, $R = 0.0337$ and $R_w = 0.0726$ for 3957 independent reflections.

Crystal dimensions $0.40 \times 0.30 \times 0.20 \text{ mm}$. Enraf- Nonius CAD4 diffractometer, Mo $K\alpha$ radiation. Cell dimensions from setting angles of 25 independent reflections with θ 9.2 - 12.5° . Intensities of 5472 reflection surveyed in the range θ 2.43 - 26.28 ; scan time 60 secs; h $-10 \rightarrow 1$, k $-20 \rightarrow 2$, l $-17 \rightarrow 17$; 3957 independent reflections with $I \geq 2\sigma(I)$. Three reference reflections monitored periodically showed a decline of 7 % over the period of collection. Structure determined by direct phasing using XCAD4. H atoms located in difference fourier synthesis. Full-matrix least squares calculations on F with anisotropic thermal parameters for C, N, O and I atoms and isotropic for H atoms using SHELXL. Least-squares convergence at $R = 0.0337$, $R_w = 0.0726$, $S = 1.20$ for 248 parameters.

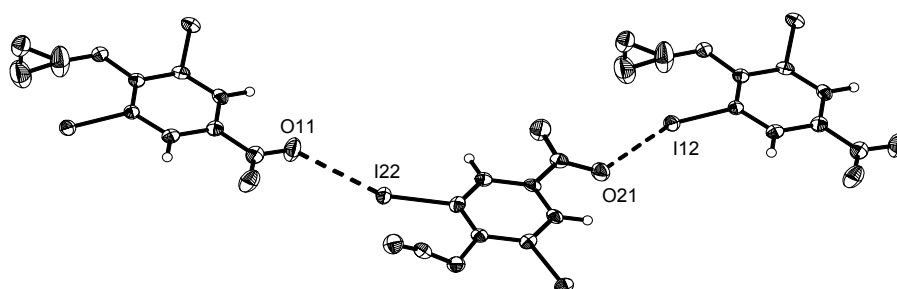
8. Summary

2,4,6-tribromophenyl azide was synthesised as previously described and fully characterised using Infrared and Raman spectroscopy, elemental analysis, NMR spectroscopy (^1H , ^{13}C , ^{14}N) and X-ray structural analysis. 2,4,6-tribromophenyl azide was recrystallised from ethanol to give pink needles which are monoclinic, with space group P21/n. The crystal packing diagram of 2,4,6-tribromophenyl azide shows that every terminal N(3) atom of the azide group has two intermolecular contacts with two bromine atoms of symmetrically related molecules within the unit cell. The intermolecular distances are N(3) to Br(2)* ($x - 0.5, -y - 0.5, z - 0.5$) 3.605 Å and N(3) to Br(1)* ($x + 1, y, z$) 3.881 Å. These distances are both below the sum of the van der Waals radii of both atoms. The crystal packing diagram of 2,4,6-tribromophenyl azide is shown in the figure below.



2,4,6-tribromophenyl azide

2,6-diiodo-4-nitrophenyl azide was synthesised as previously described and fully characterised using Infrared and Raman spectroscopy, elemental analysis, NMR. spectroscopy (^1H , ^{13}C , ^{14}N) and X-ray structural analysis. 2,6-diiodo-4-nitrophenyl azide was recrystallised from ethanol to give green needles which are monoclinic, with space group P21/c. There are two independent molecules in the asymmetric unit, one molecule has an ordered azide group and the other molecule has a disordered azide group. There is a most unusual intermolecular contact of 3.041 Å between O(11) and I(22) and between O(21) and I(12). This distance is well below the sum of the van der Waals radii of both atoms. The crystal packing is a chain with alternate ordered and disordered molecules linked by this oxygen –iodine intermolecular contact (see figure below)

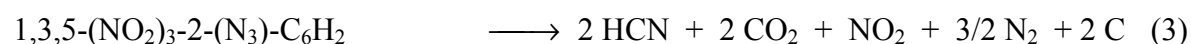


2,6-diiodo-4-nitrophenyl azide

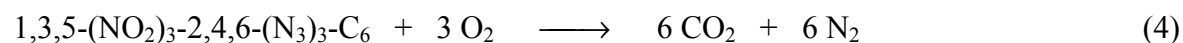
The ab initio calculations of the vibrational frequencies for all of the **halogen phenyl azides** derivatives were carried out at the self consistent HF level of theory using a 6-31G(d) basis set. Generally the agreement between calculated and experimentally observed (IR, Raman) frequencies is very good at HF/6-31G(d) level of theory for all derivatives prepared so that no scaling of the computed frequencies was necessary. The fact that the asymmetric azide vibration is calculated too high for 2,4,6-tribromophenyl azide, 2,4,6-trichlorophenyl azide

and 2,6-diiodo-4-nitrophenyl azide may or may not be explained by strong intermolecular interactions via the N₃ group in these compounds as revealed by X-ray diffraction which due to the increased formal) charges on N_β and N_γ weaken the terminal nitrogen-nitrogen triple bond.

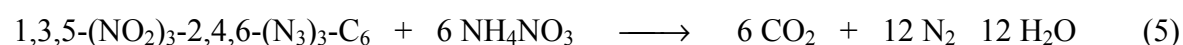
The thermal decomposition of three **nitrophenyl azides**, 1,3,5-(NO₂)₃-2,4,6-(N₃)₃-C₆ (TNTA), 1,3-(NO₂)₂-2,4,6-(N₃)₃-C₆H (DNTA) and 1,3,5-(NO₂)₃-2-(N₃)-C₆H₂ (TNMA) was studied experimentally using gas-phase IR spectroscopy



The combustion of 1,3,5-(NO₂)₃-2,4,6-(N₃)₃-C₆ (TNTA) in an O₂ atmosphere (two fold excess) yielded CO₂, N₂, very small amounts of NO₂ and traces of N₂O (eq. 4).



In a further experiment exploring the potential of TATA as a solid fuel we mixed the material with the stoichiometric amount (*cf.* eq. (5)) of NH₄NO₃



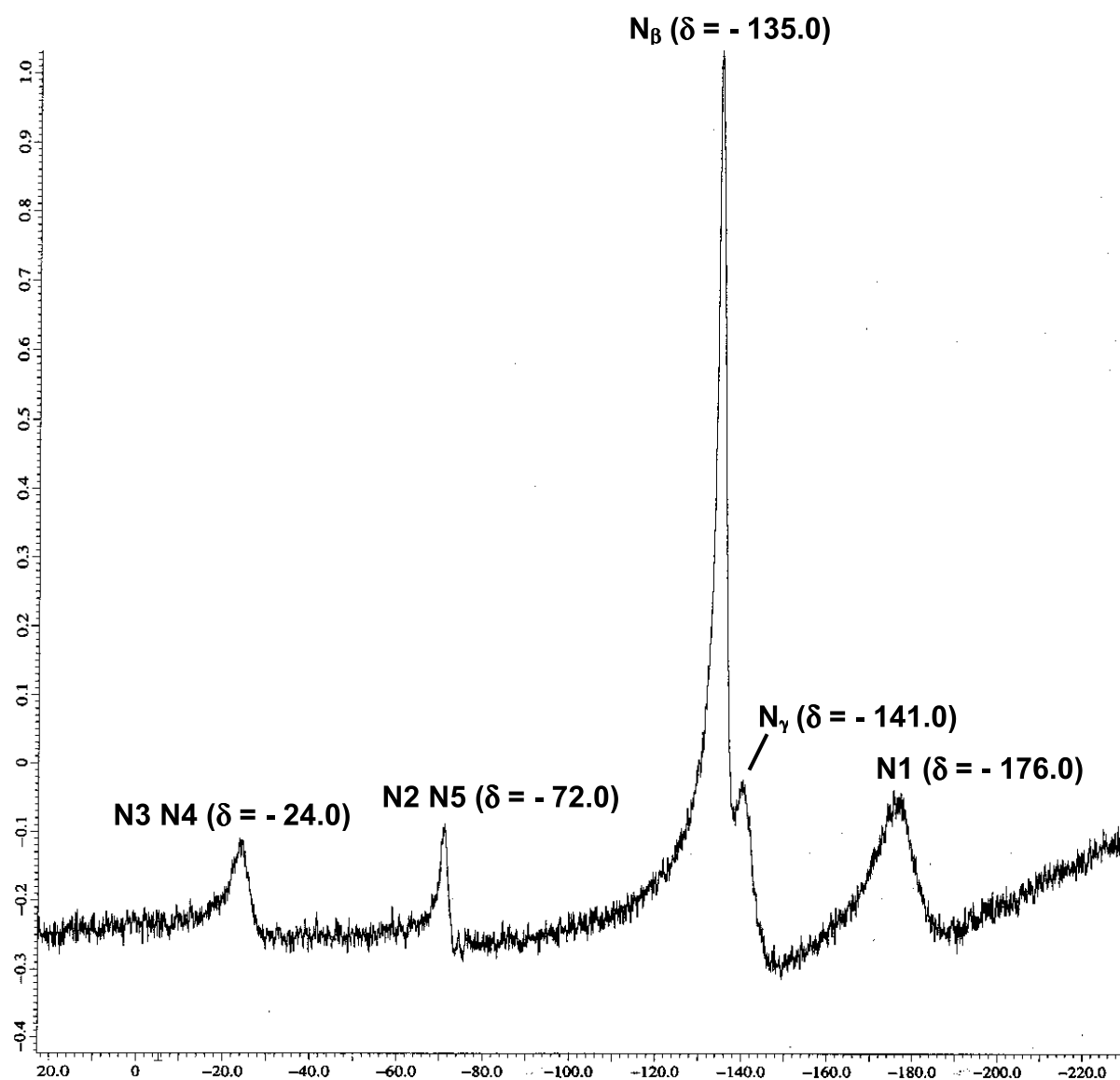
The calculated enthalpy value of -908.9 kcal mol⁻¹ makes the 1:6 molar mixture of 1,3,5-(NO₂)₃-2,4,6-(N₃)₃-C₆ and NH₄NO₃ a very promising high energy density material (*HEDM*) the potential of which we are going to explore in more detail in future studies.

In the **drophammer testing** of TNMA, DNTA and TNTA the order of the acoustic level is TNMA < DNTA < TNTA, but the values for DNTA and TNTA are very similar. Even the weakest of the investigated organic explosives (TNMA) is more powerful than AgN₃ or Pb(N₃)₂, if the acoustic level is interpreted as somewhat proportional to the detonation power.

The calculated factor (F) and detonation velocities (D) for TNMA, DNTA and TNTA were calculated using the Rothstein equation that calculates the detonation velocities of a variety of explosives on the basis of their molecular formulae. The calculated detonation velocities (D) are in agreement with the drophammer tests for these compounds *i.e* the values for detonation velocities (D) show TNMA < DNTA < TNTA, but the values for DNTA (9.185 mm μs⁻¹) and TNTA (9.441 mm μs⁻¹) are very similar. TNMA, DNTA and TNTA have higher calculated F factors and detonation velocities than several commercial explosives.

In order to measure the ¹⁴N NMR spectrum of a **pentazole**, the pentazole was prepared in the NMR tube already in the probe. This was done by dissolving the diazonium salt in dichloromethane and placing this solution in the NMR tube and freezing it solid with liquid nitrogen and then the azide solution was added on top and also frozen solid, the NMR tube was then placed in the probe at -50°C. The two layers were allowed to mix in the NMR tube as it obtained equilibrium at -50°C. The ¹⁴N NMR spectrum was recorded from the moment the tube was placed in the probe. In most of the spectra recorded using this method it was possible to see very small signals in the predicted region for the nitrogen atoms of the pentazole for about 30 minutes but again the strongest signals belong to the corresponding azide. The signals in the predicted pentazole region were not much more than the noise signal so we were not able to assign these with any confidence. However in the experiment using the above method for 2,4-dichlorophenylpentazole we were able to see three clearly distinctive signals in the expected range for the nitrogen atoms in a pentazole. This experiment was carried out several times and each time we observed the same spectra. As well as the three signals of the pentazole there are two signals of the 2,4-dichlorophenyl azide present. The spectrum of this experiment can be seen in figure below. When the sample was allowed to warm up to room temperature the three signals for the pentazole disappear but the two signals of the azide remain. We can tentatively assign the signals in the spectrum of 2,4-dichlorophenylpentazole and 2,4-dichlorophenyl azide as N₁ (δ = -176.0) ppm, N₂ N₅ (δ = -72.0) ppm, N₃ N₄ (δ = -24.0) ppm for the pentazole and N_β (δ = -135.0) ppm and N_γ (δ = -141.0) ppm for the azide. Although the values we obtained for the ¹⁴N spectrum of the 2,4-dichlorophenyl

pentazole are shifted from the values previously reported, we are certain that the signals have been assigned correctly due to the fact that no other nitrogen containing substance could be present at -50°C and that the signals disappear as the temperature is raised which is in accordance with the pentazole decomposing to the azide. This is the first reported ^{14}N NMR spectrum of a pentazole.



^{14}N NMR spectrum of 2,4-dichlorophenylpentazole and 2,4-dichlorophenyl azide at -50°C .

9. References

1. P. Griess, *Ber.*, **1869**, 2, 370.
2. T. Curtius, *Ber.*, **1890**, 23, 3023.
3. S. Maffei & A.M. Rivolta, *Gazz. Chim. Ital.*, **1954**, 84, 750
4. P.A.S. Smith, *Open-Chain Nitrogen Compounds Vol 2*, Benjamin, New York, **1966** pp211-256.
5. A.O. Beckman & R.G. Dickenson, *J. Am. Chem. Soc.*, **1928**, 50, 1870.
6. L. Pauling, *The Nature of the Chemical Bond 3rd Ed*, Cornell University Press, Ithaca, New York, **1960**.
7. R.L. Livingston & C.N.R. Rao, *J. Phys. Chem.*, **1960**, 60, 756
8. A.L. McClellan, *Tables of Experimental Dipole Moments*, Freeman & Co., San Francisco, **1963**.
9. N.V. Sidgwick, *Chemical Elements and their Compounds Vol 1*, Oxford Clarendon Press, **1950**.
10. J.D. Roberts, *Ber. Dt. Chem. Ges.*, **1961**, 94, 273.
11. P.A.S. Smith, J.H. Hall & R.O. Kann, *J. Am. Chem. Soc.*, **1962**, 84, 485
12. E. Lieber, C.N.R. Rao, A.E. Thomas, E. Oftedahl, E. Minnis & C.V.N. Numbury, *Spectrochim Acta*, **1963**, 19, 115
13. S. Patai, *The Chemistry of the Azido group*, Interscience Publishers, **1971**, p23
14. A. Hantzsch, *Ber.*, **1934**, 67B, 1674
15. W.D. Closson & H.B. Gray, *J. Am. Chem. Soc.*, **1963**, 85, 290
16. M. Witanowski & G.A. Webb, *Nitrogen NMR*, Plenum Press, London, **1973**
17. A.T. Nielsen, R.L. Atkins, & W.P. Norris, *J. Org. Chem.*, **1979**, 44, 1181
18. Z.A. Akopyan, T. Zu. Struchkov & V.G. Dashevskii, *Zh. Strukt. Khim.*, **1966**, 7, 408
19. A. T. Nielsen, *Nitrocarbons*, VCH Verlagsgesellschaft, Weinheim, **1995**.
20. L. Schischkoff, *Justus Liebigs Ann. Chem.*, **1861**, 119, 247

21. R. Farnfield, Environmental Effects of Blasting – Recent Experiences in Explosives in the Service of Man, The Royal Society of Chemistry , Brookcraft, Bath, **1997**, p153
22. L.R. Rothstein & R. Petersen, *Propellants Explos.*, **1979**, 4, 56-60
23. Gaussian 98, Revision A.3,
M. J. Frisch, G. W. Trucks, H. B. Schlegel, G. E. Scuseria, M. A. Robb, J. R. Cheeseman, V. G. Zakrzewski, J. A. Montgomery, Jr., R. E. Stratmann, J. C. Burant, S. Dapprich, J. M. Millam, A. D. Daniels, K. N. Kudin, M. C. Strain, O. Farkas, J. Tomasi, V. Barone, M. Cossi, R. Cammi, B. Mennucci, C. Pomelli, C. Adamo, S. Clifford, J. Ochterski, G. A. Petersson, P. Y. Ayala, Q. Cui, K. Morokuma, D. K. Malick, A. D. Rabuck, K. Raghavachari, J. B. Foresman, J. Cioslowski, J. V. Ortiz, B. B. Stefanov, G. Liu, A. Liashenko, P. Piskorz, I. Komaromi, R. Gomperts, R. L. Martin, D. J. Fox, T. Keith, M. A. Al-Laham, C. Y. Peng, A. Nanayakkara, C. Gonzalez, M. Challacombe, P. M. W. Gill, B. Johnson, W. Chen, M. W. Wong, J. L. Andres, C. Gonzalez, M. Head-Gordon, E. S. Replogle, and J. A. Pople, Gaussian, Inc., Pittsburgh PA, 1998.
24. HyperChem 5.0, Molecular Visualization and Simulation Program Package, Hypercube, Gainesville, FL, 1997
25. Resview, version 2.26 (04.09.1998) H. Schwenk-Kircher, 1998
26. J. B. Foresman, & A. Frisch, Exploring Chemistry with Electronic Structure Methods 2nd edn., Gaussian, Inc., Pittsburgh, PA, **1993**, chapter 6.
27. J. J. P. Stewart, *J. Comp. Chem.*, **1989**, 10, 209
28. J. J. P. Stewart, *J. Comp. Chem.*, **1989**, 10, 221.
29. M. Dewar, W. Thiel, *J. Am. Chem. Soc.*, **1977**, 99, 4499
30. M. J. S. Dewar, M. L. McKee, H. S. Rzepa, *J. Am. Chem. Soc.*, **1978**, 100, 3607
31. M. J. S. Dewar, E. G. Zoebisch, E. F. Healy, *J. Am. Chem. Soc.*, **1985**, 107, 3902
32. M. J. S. Dewar, C. H. Reynolds, *J. Comp. Chem.*, **1986**, 2, 140
33. T. M. Klapötke, A. Schulz and R. D. Harcourt, *Quantum Chemical Methods in*

Main-Group Chemistry, Wiley, Chichester, New York, **1998**, p. 89.

34. <http://www.theochem.uni-stuttgart.de>
35. G. Igel-Mann, H. Stoll, H. Preuss, *Mol. Phys.*, **1988**, 65, 1321
36. A. Bergner, M. Dolg, W. Kuechle, H. Stoll, H. Preuss, *Mol. Phys.*, **1993**, 80, 1431.
37. C. Lee, W. Yang, R. G. Parr, *Phys. Rev.*, **1988**, B 37, 785
38. A. Miehlich, A. Savin H.Stoll, & H.Preuss, *Chem. Phys. Lett.*, **1989**, 157, 200
39. A. D. Becke, *Phys. Rev.*, **1988**, A 38, 3098
40. P. M. W. Gill, in *Encyclopedia of Computational Chemistry*, P. v. R. Schleyer (ed.), Vol. 1, Wiley, Chichester, 1998, p. 678.
41. T. M. Klapötke and I. C. Tornieporth-Oetting, *Nichtmetallchemie*, VCH Verlagsgesellschaft, Weinheim 1994 p.76.
42. A. Hantzsch, *Ber. Dtsch. Chem. Ges.*, **1903**, 36, 2056
43. O. Dimroth, & de Montmollin. *Ber. Dtsch. Chem. Ges.*, **1910**, 43, 2964
44. J. Lifschitz, *Ber. Dtsch. Chem. Ges.*, **1915**, 48, 410
45. T.Curtius, , A. Darapsky, & E.Müller, *Ber. Dtsch. Chem. Ges.*, **1915**, 48
46. R. Huisgen, & I. Ugi, *Angew. Chem.*, **1956**, 68, 705
47. R. Huisgen, & I. Ugi, *Chem. Ber.*, **1957**, 90, 2914
48. J.D. Wallis, & J.D. Dunitz, *J.Chem.Soc.Chem.Commun.*, **1983**, 910

49. M. Witanowski, L. Stefaniak, H. Januszewski & K. Bahadur, *J. Cryst. Mol. Struct.*, **1975**, 5, 137
50. G.M. Sheldrick 1997. SHELXS 97 - Program for Crystal Structure Solution, University of Gottingen, Germany
51. G.M. Sheldrick 1997. SHELXL 97 - Program for the Refinement of Crystal Structures, University of Gottingen, Germany
52. A.T. Christensen & K.O. Stromme, *Acta Cryst.*, **1969**, B25, 657
53. H.J. Milledge & L.M. Pont, *Acta Cryst.*, **1960**, 13, 285
54. V.B. Carter & D. Britton, *Acta Cryst.*, **1972**, B28, 945
55. S.C. Nyburg, J.K. Fawcett & J.T. Szymanski, *Acta Cryst.*, **1987**, C43, 2452
56. A. Belaraj, Nguyen-Ba-Chanh & Y. Haget, *Zh Strukt Khim.*, **1971**, 12, 736
57. V.G. Andrianov & A.F. Korotkevich, *J. Appl. Cryst.*, **1984**, 17, 211
58. CAD4 Express Software (1994) Enraf-Nonius, Delft, The Netherlands. : K. Harms, & S. Wocadlo, (1995) XCAD-4 Program for Processing CAD-4 Diffractometer Data. University of Marburg, Germany
59. G.M. Sheldrick **1993**. SHELX 93 - Program for the Refinement of Crystal Structures, University of Gottingen, Germany
60. SIR97 Cascarano et al, *Acta Cryst A.*, **1996**, C79
61. I. C. Tornieporth-Oetting, T. M. Klapötke, *Angew. Chem.* **1995**, 107, 509; *Angew. Chem. Int. Ed. Engl.*, **1995**, 34, 511.
62. Covalent Inorganic Non-Metal Azides, I. C. Tornieporth-Oetting, T. M. Klapötke, in: Combustion Efficiency and Air Quality, I. Hargittai, T. Vidoczy (Eds.), Plenum Press, New York, **1995**, p. 51.
63. R. W. Millar, M. E. Colclough, P. Golding, P. J. Honey, N. C. Paul. A. J. Sanderson, M. J. Stewart, *Phil. Trans. R. Soc. Lond. A*, **1992**, 339, 305.
64. D. Harris, J. C. Trebellas, H. B. Jonassen, *Inorg. Synth.*, **1967**, 9, 83.
65. J. Trofimova, G. Spieß and T. M. Klapötke, *Intl. J. of Vibrational Spectroscopy*, **1998**, Vol. 2 (1), section 2c.
66. N. Paul, Modern Explosives and Nitration Techniques, in *Explosives in the Service of Man*, The Royal Society of Chemistry, Bookcraft, Bath, 1997, p. 79.

67. H. Feuer and A. T. Nielsen (eds.), *Nitro Compounds*, VCH Verlagsgesellschaft, Weinheim, 1990. J. Köhler, R. Meyer, *Explosivstoffe*, 7th edn., VCH Verlagsgesellschaft, Weinheim, 1991.
68. A.S. Bailey & C.K. Prout, *J.Chem. Soc.*, **1965**, 4867.
69. GAMESS Schmidt, M.W.; Baldrige, K.K.; Boatz, J.H.; Elbert, S.T.; Gordon, M.S.; Jensen, J.J.; Koseki, S.; Matsunaga, N.; Nguyen, K.A.; Su, S.; Windus, T.L.; Dupuis, M.; Montgomery, J.A. *J. Comp. Chem.* **1993**, 14, 1347.
70. AIMPAC Biegler-Koenig, F.W.; Bader, R.F.W.; Tang, T.H. *J. Comput. Chem.*, **1982**, 3, 317.
71. B.Flürscheim, & E.L Holmes, *J.Chem. Soc.*, **1928**, 3041
72. C.L. Jackson & J.F. Wing, *Amer.Chem.Journ.*, 9, 348
73. H.J. Backer, *Rec. Trav. Chim.*, **1935**, 54, 745
74. H.D.B. Jenkins, H.K. Roobottom, J. Passmore & L. Glasser, *Inorg Chem.*, **1999**, 38, 3609
75. T. M. Klapötke, *Chem. Ber.*, **1997**, 130, 443; and references therein.
76. Aldrich Catalogue, Sigma-Aldrich Chemie GmbH, Steinheim (1996-1997), p. 114.
77. R. D. Harcourt, F. Wang & T.M. Klapötke, *J. Mol. Model.* in press
78. <http://iva.uni-ulm.de/PHYSIK/VORLESUNG/OPTIK/node153.html>
79. T. M. Klapötke and A. Schulz, *Quantenmechanische Methoden in der Hauptgruppenchemie*, Spektrum, Heidelberg, 1996, p. 92.
80. P. S. Ganguli, H. A. McGee, Jr., *Inorg. Chem.*, **1972**, 12, 3071
81. R. Huisgen, & I. Ugi, *Chem. Ber.*, **1958**, 91, 531
82. R. Muller, J.D. Wallis & W. von Philipsborn, *Angew. Chem.*, **1985**, 97, 515
83. R.N. Butler, S. Collier & A.F.M. Fleming, *J. Chem. Soc. Perkin Trans. 2.*, **1996**, 801
84. R.N. Butler, A. Fox, S. Collier & L.A. Burke, *J. Chem. Soc. Perkin Trans. 2.*, **1998**, 2243
85. K.F. Ferris & R.J. Bartlett, *J. Am.Chem. Soc.*, **1992**, 114, 8302
86. R. Janoschek, *Angew.Chem. Int. Ed. Engl.*, **1993**, 37, 23

Lebenslauf

Name David Adam

D.O.B. 10/02/1962, Glasgow, Scotland

Nationality British

Education Eastbank Primary School , Shettleston, Glasgow 1967-74
Eastbank Academy, Shettleston, Glasgow 1974-78

Further Education Stow College , Glasgow 1978-81 ONC Chemistry
Glasgow Technical College, Glasgow 1981-84 HNC Chemistry
Bell College, Hamilton 1987-88 OS Maths
Bell College, Hamilton 1989-90 LRSC Chemistry
Department of Chemistry , University of Glasgow, Glasgow
Oct 1992- Feb 1995 MSc. Chemistry
Supervisors :- Prof. N.W. Isaacs & Dr. P.H McCabe
PhD, Department of Inorganic Chemistry
Ludwig-Maximilians University, Munich
Supervisor :- Prof. Dr. T.M. Klapötke
Apr. 1997 – Oct 2001

Employment Chemistry Technician, University of Glasgow, Glasgow
Sept. 1978- Feb 1997

Researcher, Department of Inorganic Chemistry
Ludwig-Maximilians University, Munich
Apr. 1997 -

